Dissertation

submitted to the

Combined Faculties for the Natural Sciences and for Mathematics

of the Ruperto-Carola University of Heidelberg, Germany

for the degree of

Doctor of Natural Sciences

Presented by

Simone Pfarr (M.Sc.)

born in Heidelberg, Germany

Oral-examination: 22.10.2018

The Role of the Medial Prefrontal Cortex in Reward Seeking:

Functional Evidence on Cellular and Molecular Mechanisms underlying Drug and Natural Reward Seeking

Referees: Prof. Dr. Rainer Spanagel

apl. Prof. Dr. Wolfgang H. Sommer

Summary

The medial prefrontal cortex (mPFC) is critically involved in cognitive flexibility and top down control of behavior. Dysfunction of this brain region is a hallmark of many psychiatric disorders including addiction. The physiological and molecular mechanisms underlying mPFC function are largely unclear. A widely accepted theory posits that distinct memories are encoded in the brain by sparsely distributed sets of neurons, so called neuronal ensembles, which has been demonstrated for reward seeking behavior. However, in the case of alcohol seeking neuronal ensembles had not been identified and it is unclear how such ensembles might differ from those involved in natural reward seeking. Furthermore, excessive alcohol use causes damage to the mPFC, especially to its ventromedial subregion, also termed infralimbic cortex (IL). Long-term alcohol-induced changes in this brain area include a deficit in metabotropic glutamate receptor subtype 2 (mGluR2). These receptors modify the signaling properties of IL neurons to their projection targets and their dysfunction within corticostriatal projections of alcohol-dependent rats is known to be associated with loss of control over alcohol seeking behavior.

Thus, this PhD thesis aims to provide insights into the organization of IL neuronal ensembles involved in alcohol and natural reward seeking and to further understand the role of an mGluR2 deficit for IL dependent control over alcohol seeking and cognitive flexibility.

In Study 1 we identify a functional neuronal ensemble in the IL involved in the control of alcohol seeking behavior, using a chemo-genetic inactivation method. In Study 2 we demonstrate that IL neuronal ensembles involved in alcohol and saccharin seeking are highly overlapping, but also contain reward specific components by using retrograde tracing techniques in combination with a novel two-reward operant task. In Study 3 we develop an advanced methodological framework for measuring neuronal ensemble activity during an operant reward seeking task using in-vivo calcium imaging. By using viral mGluR2 knockdown techniques, Study 4 and 5 establish an IL mGluR2 deficit as a common pathological mechanism for excessive alcohol seeking and impaired cognitive flexibility.

In summary, the results of this thesis provide important insights into the function and organization of neuronal ensembles involved in reward seeking. Possible changes of organization and function of neuronal ensembles in pathological conditions, like addiction, should be addressed in future studies. Furthermore an IL mGluR2 deficit is established as a common pathological mechanism for excessive alcohol seeking and impaired cognitive flexibility, thus leading to a deeper understanding of the underlying molecular mechanisms of this frequent comorbidity and providing a promising target for future medication therapies.

Zusammenfassung

Der mediale präfrontale Kortex (mPFC) ist entscheidend an der kognitiven Flexibilität und der Top-Down Kontrolle des Verhaltens beteiligt. Funktionsstörungen dieser Hirnregion sind charakteristisch für viele psychiatrische Störungen, einschließlich Suchterkrankungen. Die physiologischen und molekularen Mechanismen, die der mPFC-Funktion zugrunde liegen, sind bisher weitgehend unklar. Eine weithin akzeptierte Theorie postuliert, dass bestimmte Erinnerungen im Gehirn durch spärlich verteilte Neuronengruppen, so genannten neuronalen Ensembles, kodiert werden, was bereits für das Belohnungs- Suchverhalten demonstriert wurde. Bisher wurden jedoch noch keine solchen neuronalen Ensembles für das Alkohol Suchverhalten identifiziert und es ist unklar, wie sich diese von jenen Ensembles unterscheiden könnten, welche an dem Suchverhalten nach natürlichen Belohnungen beteiligt sind. Zusätzlich schädigt exzessiver Alkoholgebrauch den mPFC, insbesondere seine ventromediale Subregion, die auch als infralimbischer Kortex (IL) bezeichnet wird. Zu den langfristigen Alkohol-induzierten Veränderungen in dieser Gehirnregion gehört ein Defizit des metabotropen Glutamat-Rezeptor-Subtyps 2 (mGluR2). Diese Rezeptoren modifizieren die Signaleigenschaften von IL-Neuronen zu ihren Projektionszielen und deren Dysfunktion innerhalb kortikostriataler Projektionen in alkoholabhängigen Ratten ist bekanntlich mit dem Kontrollverlust über das Alkoholsuchverhalten verbunden.

Ziel dieser Dissertation ist es, Einblicke in die Organisation von neuronalen Ensembles im IL zu geben, die an der Suche nach Alkohol und natürlichen Belohnungen beteiligt sind, und die Rolle eines mGluR2 Defizits im Zusammenhang mit der IL-abhängigen Kontrolle des Alkohol Suchverhaltens und kognitiver Flexibilität besser zu verstehen.

In Studie 1 identifizieren wir mit Hilfe einer chemo-genetischen Inaktivierungsmethode ein funktionelles neuronales Ensemble im IL, das an der Kontrolle des Alkoholsuchverhaltens beteiligt ist. In Studie 2 zeigen wir mittels einer Kombination von retrograden Tracing Techniken und einem neuen operanten Verhaltensprotokoll zum abwechselnden Suchen nach zwei verschiedenen Belohnungen, dass IL-neuronale Ensembles, welche an Alkohol und Saccharin Suchverhalten beteiligt sind, stark überlappen, aber auch Belohnungsspezifische Komponenten enthalten. In Studie 3 entwickeln wir einen fortgeschrittenen methodischen Rahmen zur Aktivitätsmessung neuronaler Ensembles während eines operanten Belohnungs-Suchverhaltens unter Verwendung von in-vivo Kalzium-Bildgebung. Mittels viraler mGluR2-Knockdown-Techniken etablieren die Studien 4 und 5 ein IL mGluR2-Defizit als einen gemeinsamen pathologischen Mechanismus für übermäßiges Alkoholsuchverhalten und beeinträchtigte kognitive Flexibilität.

Zusammenfassend liefern die Ergebnisse dieser Arbeit wichtige Einblicke in die Funktion und Organisation neuronaler Ensembles, welche an der Belohnungssuche beteiligt sind. Mögliche Veränderungen der Organisation und Funktion neuronaler Ensembles bei pathologischen Konditionen, wie z.B Suchterkrankungen, sollten in zukünftigen Studien behandelt werden. Darüber hinaus haben wir ein IL mGluR2 Defizit als gemeinsamen pathologischen Mechanismus für übermäßiges Alkoholsuchverhalten und eingeschränkte kognitive Flexibilität etabliert, was zu einem tieferen Verständnis der zugrunde liegenden molekularen Mechanismen dieser häufigen Komorbidität führt und ein vielversprechendes Ziel für zukünftige medikamentöse Therapien darstellt.

Table of contents

List of Figures

List of Tables

Abbreviations

5-HT	5-hydroxytryptamine
AA	Alko alcohol preferring rat
AAV	Adeno associated virus
ACC	Anterior cingulate cortex
AMPA	α-amino-3-hydroxy-5-methyl-4-isoxazolepropionic acid
ANA	Alko alcohol non-preferring rat
ANOVA	Analysis of variance
ASST	Attentional set shifting test
AUD	Alcohol use disorder
ß-gal	ß-galactosidase
BAC	Blood alcohol concentration
BAC	Bacterial artificial chromosome
BL	Self-administration baseline
BLA	Basolateral amygdala
BNST	Bed nucleus of stria terminalis
Ca^{2+}	calcium ion
CAG	CMV early enhancer/chicken β actin promoter
CaM kinase	Calcium-calmodulin dependent kinase
CamKII	Calcium-calmodulin dependent kinase II
CaMPARI	Calcium Modulated Photoactivatable Ratiometric Integrator
CD	Compound discrimination task
CeA	Central amygdala
CIE	Chronic intermittent exposure
CMOS	Complementary metal-oxide-semiconductor
CREB	cAMP response element-binding protein

DA	Dopamine
DSM-V	Diagnostic and Statistical Manual of Mental Disorders, 5th ed.
EDS	Extradimensional set shift task
EGFP	Enhanced green fluorescent protein
ERK	Extracellular signal-regulated kinase
EtOH	Ethanol
EXT	Extinction
EYFP	Enhanced yellow fluorescent protein
FISH	Fluorescent in-situ hybridization
GABA	Gamma-Aminobutyric acid
GAD67	Glutamic acid decarboxylase 67
GECI	Genetically encoded calcium indicator
GRIN	Gradient refractive index (lens)
Grm2	Glutamate metabotropic receptor 2
HAD	High alcohol drinking rats
IDS	Intradimensional set shift task
IEG	Immediate early gene
iGluR	Ionotropic glutamate receptor
IL	Infralimbic cortex
LAD	Low alcohol drinking rats
LED	Light-emitting diode
MAPK	Mitogen-activated protein kinases
mGluR2	Metabotropic glutamate receptor 2
mPFC	Medial prefrontal cortex
mSP	Marchigian Sardinian alcohol-preferring rat
Nac	Nucleus accumbens
nACh	Nicotinic acetylcholine receptor

NeuN	Neuronal nuclei (protein marker)
NMDA	N-methyl-D-aspartate
NP-rat	Indiana alcohol non-preferring rat
OFC	Orbitofrontal cortex
PD	Post-dependent
PR	Progressive ratio
P-rat	Indiana alcohol preferring rat
PL	Prelimbic cortex
PVN	Paraventricular nucleus
RE	Reinstatement
RISC	RNA-induced silencing complex
ROI	Region of interest
SA	Self-administration
Sac	Saccharin
SD	Simple discrimination task
SEM	Standard error of the mean
shRNA	Short hairpin RNA
SNP	Single nucleotide polymorphism
sP	Sardinian alcohol preferring rat
STD	Standard deviation
TTX	Tetrodotoxin
VTA	Ventral tegmental area
WCST	Wisconsin Card Sorting Task
Z-VAD-FMK	N-benzyloxycarbonyl-Val-Ala-Asp-fluoromethyl ketone

List of publications

Losing Control: Excessive Alcohol Seeking after Selective Inactivation of Cue-Responsive Neurons in the Infralimbic Cortex.

Pfarr S*, Meinhardt MW*, Klee ML, Hansson AC, Vengeliene V, Schönig K, Bartsch D, Hope BT, Spanagel R*, Sommer WH*. J Neurosci. 2015; 35(30):10750 – 10761 (*equal contribution)

Reprogramming of mPFC transcriptome and function in alcohol dependence.

Heilig M, Barbier E, Johnstone AL, Tapocik J, Meinhardt MW, **Pfarr S**, Wahlestedt C, Sommer WH. Genes Brain Behav. 2017; 16(1): 86–100

Choice for drug or natural reward engages largely overlapping neuronal ensembles in the infralimbic prefrontal cortex

Pfarr S, Schaaf L, Reinert JK, Paul E, Herrmannsdörfer F, Roßmanith M, Kuner T, Hansson AC, Spanagel R, Körber C*, Sommer WH* J Neurosci. 2018; Apr 4;38(14):3507-3519 (*equal contribution)

1. Introduction

Reward seeking is a basic principle for satisfying our needs and desires. "*Rewards are things that have positive effects on behavior, attitude, relationships, etc., or in technical jargon, stimuli that reinforce behavior*." (Ikemoto and Bonci, 2014). Furthermore rewards can be defined as *"an induced state that subsequently leads to conditioned approach behavior*." (Ikemoto and Bonci, 2014). Rewards can be subdivided into natural rewards like food, water and sex, and drug rewards including alcohol. The underlying system of both natural and drug reward reinforcement is the mesolimbic dopamine system. It is generally assumed that drug seeking and drug intake are novel features of human behavior and drugs of abuse are thought to hijack incentive mechanisms, involved in natural reward seeking (Nesse and Berridge, 1997). However, another theory considers the fact, that mammals have been ingesting drugs and alcohol over the course of millions of years as part of their natural behavior repertoire (Dudley, 2000; Sullivan and Hagen, 2002). Therefore alcohol seeking can be considered a part of our normal behavioral repertoire (Spanagel, 2009). Both, seeking for drugs and natural rewards, seem to engage similar reward circuitries in the brain. However, given the highly different consequences of natural and drug reward seeking, this thesis is aimed to provide an insight into the neuronal encoding of natural and drug reward seeking. Furthermore the molecular mechanisms underlying alcohol seeking behavior will be examined.

1.1 Reward seeking behavior and its relevance in alcohol addiction

All mammals engage in certain activities to obtain natural rewards, because these rewards produce a feeling of pleasure, which in turn increases the probability of the individual to repeat this activity in order to experience pleasure again (McClure et al., 2004). From an evolutionary point of view, appropriate responding to natural rewards is important for survival, reproduction and fitness (Kelley and Berridge, 2002). Also today, reward seeking behavior is a fundamental part of our everyday life, because the feeling of pleasure generated by rewards is essential for our normal sense of well-being (Berridge and Kringelbach, 2008). In addition to natural rewards, also drugs of abuse like alcohol can produce these positive mood states (Kelley and Berridge, 2002; Spanagel, 2009).

Introduction

Alcohol is one of the most commonly used substances, constituting 5.9% of deaths worldwide (World Health Organization, 2014). Although most individuals successfully control their alcohol intake, the government of Germany reported that 21,4% of the current population consume potentially harmful amounts of alcohol (>12g ethanol per day for women and >24g ethanol per day for men), (Die Drogenbeauftragte der Bundesregierung). From the total German population of 3,38 Mio adults, 1.61 Mio abuse alcohol and 1.77 Mio are alcohol dependent (DHS Jahrbuch Sucht, 2018). Alcohol use disorders are characterized by chronic abstinence and relapse cycles, loss of control over alcohol intake, craving and the emergence of a negative emotional state or motivational withdrawal symptom (Koob and Volkow, 2010). Repeated cycles of abstinence and relapse can lead to the transition from controlled alcohol use to heavy alcohol use. This can result in an early dependence state, during which neutral environmental stimuli become associated with the pleasurable effects of alcohol. The early dependence state can be followed by the late dependence state, which is characterized by a low mood, high anxiety and sensitivity to stress. In the late dependence state the motivation for alcohol consumption is mainly driven by negative reinforcement in addition to the positive reinforcement, meaning that alcohol is consumed to counteract negative emotional states. The late dependence state is characterized by persistent neuroadaptations, which develop during the progression of alcohol dependence over time (Heilig and Koob, 2007; Meinhardt and Sommer, 2015). The Diagnostic and Statistical Manual of Mental Disorders, 5th ed. (DSM-V) (American Psychiatric Association, 2013) lists 11 clinical diagnostic criteria for alcohol use disorders. The presence of at least two of these symptoms indicate an alcohol use disorder (AUD). The presence of two to three symptoms indicates a mild grade of AUD. Four to five symptoms indicate a moderate grade and more than six symptoms indicate a severe grade of AUD.

Individuals engage in voluntary and controlled alcohol consumption due to its reinforcing properties and hedonic effects, also called drug "liking". Reward "liking" is a distinct process from reward "wanting", describing the incentive motivation or desire, which drives approach behavior to rewards or promotes reward consumption (Berridge et al., 2009). Under healthy conditions an individual "wants" the drug because it "likes" the drug. However, under pathological conditions the controlled alcohol consumption can develop into habitual and ultimately compulsive alcohol seeking (Everitt et al., 2008; Koob and Volkow, 2010). This process is characterized by a strong increase of "wanting" and a simultaneous decrease of "liking" (Figure 1) (Robinson and Berridge, 1993; Berridge et al., 2009) and occurs during the

transition from positive reinforcement to negative reinforcement as a motivation for alcohol consumption (Figure 1) (Heilig and Koob, 2007; Koob and Volkow, 2010).

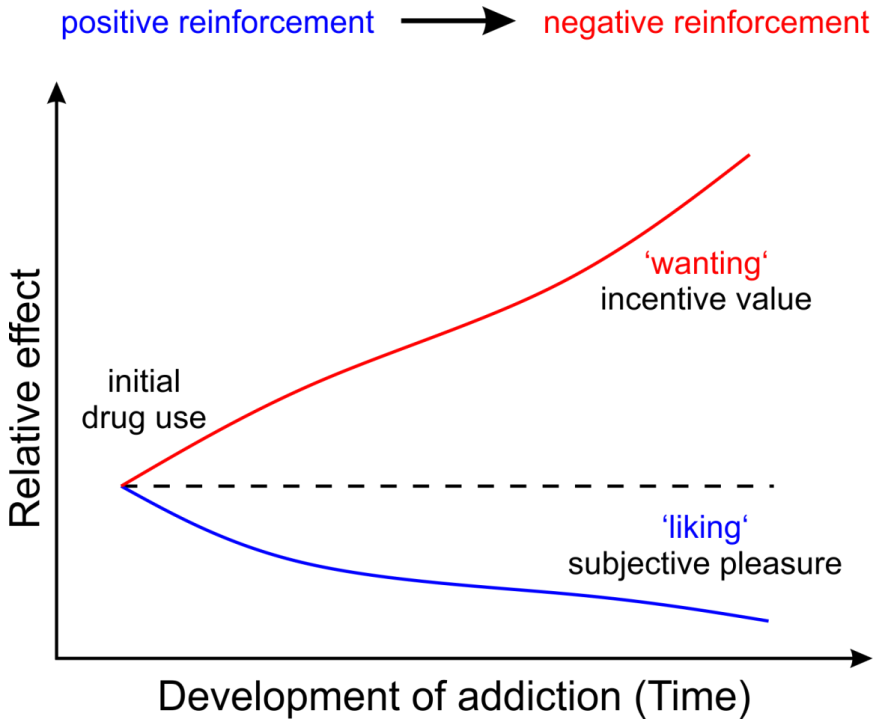

Figure 1: Schematic representation of the incentive sensitization model of addiction. Initially subjects both 'like' and 'want' the drug. During the development from controlled to compulsive drug use the incentive value of the drug increases over time, independent of the subjective feeling of pleasure or 'liking'. This mechanism occurs in parallel to the transition from positive reinforcement to negative reinforcement as the motivation to take the drug. Figure adapted from (Robinson and Berridge, 1993; Berridge et al., 2009).

In addition to the promotion of reward seeking, positive reinforcing properties of rewards also attribute positive motivational value to previously neutral stimuli or environmental contexts, which is called associative learning (Di Chiara, 1999). Following associative learning, these so called conditioned cues predict their associated rewards and thereby trigger the motivational "wanting" response to obtain the reward (Berridge et al., 2009). Through associative learning the drug-associated cues can acquire incentive-motivational properties (See, 2002). Repeated drug intoxication cycles can further strengthen the incentive salience of the conditioned cues and promote compulsive drug seeking behavior (Flagel et al., 2009).

1.2 Brain reward circuitry

In 1954 Olds and Milner identified the brain reward system in the rat. This groundbreaking work led to the discovery of many brain areas involved in mediating the reinforcing effects of alcohol and other drugs of abuse. Specifically the midbrain dopamine (DA) system has been identified as a neurochemical substrate underlying reinforcement (Wise and Rompre, 1989; Wise, 2004; Schultz, 2007; Spanagel, 2009). Midbrain A10 DA neurons project from the ventral tegmental area (VTA) to the limbic system, especially the nucleus accumbens (NAc) shell and the medial prefrontal cortex (mPFC) (Fuxe, 1965; German and Manaye, 1993). It has been shown that alcohol increases extracellular dopamine levels in the NAc due to a decrease in GABAergic feedback projections from the NAc to the VTA, leading to a disinhibition of A10 DA neurons (Figure 2A) (Kalivas, 1993; Kohl et al., 1998; Spanagel and Weiss, 1999; Lüscher and Ungless, 2006). In addition to the GABAergic feedback system, the midbrain DA system is also regulated by the glutamate system (Lüscher and Ungless, 2006; Gass and Olive, 2008). The VTA receives glutamatergic input from the mPFC, the bed nucleus of stria terminalis (BNST), the laterodorsal tegmental nucleus and the lateral hypothalamus (Figure 2C) (Omelchenko and Sesack, 2007). Also the NAc receives glutamatergic input from mPFC, the hippocampus, the amygdala and the paraventricular nucleus of the hypothalamus (Figure 2B) (Blaha et al., 1997; Howland et al., 2002; Parsons et al., 2007). Glutamate release from these projections can act directly on ionotropic glutamate receptors in the NAc shell and facilitate dopamine release.

Both drug as well as natural rewards lead to an increase in synaptic dopamine levels in the above described mesocorticolimbic system. This similarity in activation indicates a common neuroanatomical pathway (Di Chiara and Imperato, 1988; Wise and Rompre, 1989). A neuroimaging study in rats supports this theory, because voluntary consumption of a sweet saccharin solution and alcohol produced highly similar activation maps in manganese-enhanced magnetic resonance imaging in the mesocorticolimbic and nigrostriatal system (Dudek et al., 2015). A meta-analysis of 176 human cue-reactivity studies also revealed highly overlapping neuronal substrates especially in the brain reward system underlying craving for natural and drug rewards (Noori et al., 2016). These findings strengthen the theory, that drug rewards “hijack” the brain’s natural reward pathway (Gardner, 2011).

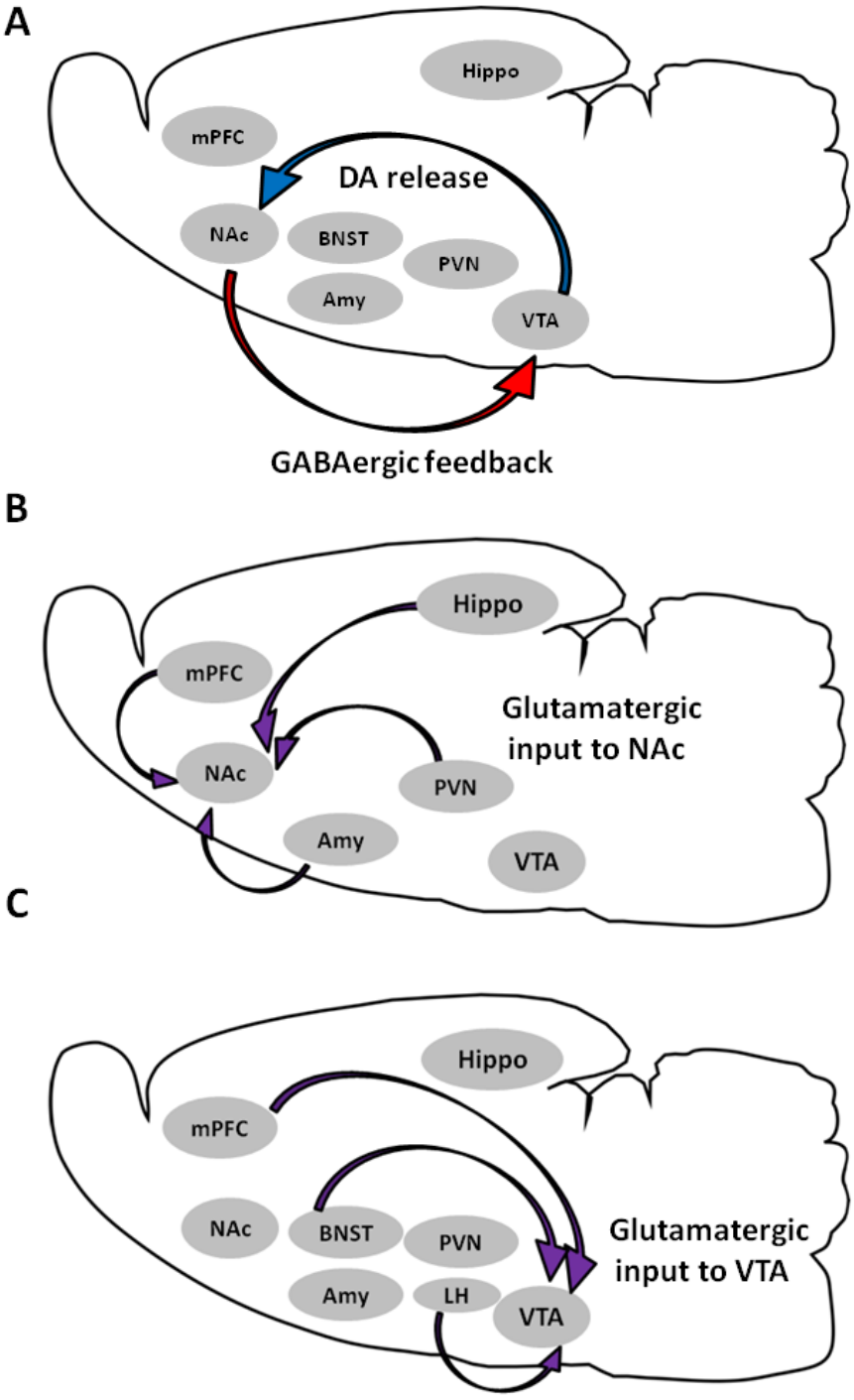

Figure 2: Projections in the mesocorticolimbic system. A) A10 dopamine (DA) neurons project from the ventral tegmental area (VTA) to the nucleus accumbens (NAc). Alcohol-induced dopamine release in the NAc is further increased by a negative GABAergic feedback loop from the NAc to the VTA. Alcohol decreases GABAergic activity, thereby disinhibiting the A10 DA neurons in the VTA. **B)** The nucleus accumbens (NAc) receives glutamatergic input from the medial prefrontal cortex (mPFC), the hippocampus (Hippo), the paraventricular nucleus (PVN) and the amygdala (Amy). **C)** The ventral tegmental area (VTA) receives glutamatergic input from the mPFC, the bed nucleus of stria terminalis (BNST), and the lateral hypothalamus (LH).

1.3 Glutamate receptors in the brain

Glutamate is the most important excitatory neurotransmitter in the brain and a crucial component for the induction of synaptic plasticity, learning, memory and cognition (McEntee and Crook, 1993; Zhou, 2014). Excessive elevated extracellular glutamate levels were found to trigger the pathophysiology of several neurological diseases like traumatic brain injury and stroke (Maragakis and Rothstein, 2001; Lau and Tymianski, 2010), which is why a tight regulation of the glutamate neurotransmitter system is crucial for normal brain function.

Several types of glutamate receptors were identified in the brain. The following ionotropic glutamate receptors (iGluRs) mediate fast excitatory glutamate transmission: N-methyl-d-aspartate (NMDA) receptor (Bonaccorso et al., 2011; Gonda, 2012), α-amino-3-hydroxy-5-methyl-4-isoxazole propionic acid (AMPA) receptor (Rogawski, 2013) and kainate receptors (Lerma and Marques, 2013). Slow, modulatory glutamate transmission is mediated by the class of metabotropic glutamate receptors (mGluRs), which are G-protein coupled receptors (Olive, 2009).

The class of mGluRs is comprised of eight subtypes of seven transmembrane domain G-protein coupled receptors, with differences in cellular localization, pharmacological and intracellular signaling characteristics (Pin and Duvoisin, 1995; Conn and Pin, 1997). The mGluR group I family consists of mGluR1 and mGluR5 and is predominantly postsynaptically localized. The mGluR group II family includes mGluR2 and mGluR3. The mGluR group III family consists of mGluR4, mGluR6, mGluR7 and mGluR8 (Schoepp and Conn, 1993; Schoepp, 2001; Olive, 2009). mGluR2 is predominantly presynaptically localized, but was also found in postsynaptic elements. However, mGluR3 was found to be predominantly localized in postsynaptic elements, which demonstrates a clearly distinct expression pattern of both group II mGluRs (Tamaru et al., 2001). Group I mGluRs are coupled to the Gαq class of G-proteins, which leads to the activation of several phospholipases and hydrolysis of phosphoinositide (PI). This in turn leads to the formation of inositol triphosphate (IP3) and diacylglycerol (DAG), which can release calcium (Ca^{2+}) from intracellular internal stores (Conn and Pin, 1997; Hermans and Challiss, 2001). Both group II and group III mGluRs are coupled to the Gαi class of G-proteins and are negatively coupled to adenylyl cyclase (AC), which leads to a reduction of intracellular cyclic adenosine

monophosphate (cAMP). Group II and III mGluRs, specifically mGluR2 and mGluR3 are thought to function as autoinhibitory receptors mediating the suppression of excessive glutamate release from the presynaptic terminal (Schoepp, 2001), thereby protecting neurons against excitotoxicity (Buisson and Choi, 1995). However, given the distinct cellular localization patterns, each mGluR is thought to have a unique function in regulating glutamatergic neurotransmission.

Glutamate transmission has been reported to mediate natural rewards (Pitchers et al., 2012; Mietlicki-Baase et al., 2013), as well as drug rewards (D'Souza, 2015). Alcohol for example has acute effects on the glutamate system involving inhibition of postsynaptic glutamate transmission (Lovinger et al., 1989; Nie et al., 1993; Carta et al., 2003) and inhibition of presynaptic mechanisms mediating glutamate release (Hendricson et al., 2003; Ziskind-Conhaim et al., 2003; Hendricson et al., 2004). Conversely, chronic alcohol exposure was shown to result in an upregulation of AMPA (Netzeband et al., 1999) and NMDA receptor signaling (Hu and Ticku, 1995), as well as altered metabotropic glutamate receptor function (Gass and Olive, 2008; Meinhardt et al., 2013; Goodwani et al., 2017), which may result in an overexcitable state of the central nervous system (Hermann et al., 2012). A transitional "hyperglutamatergic state" has been reported during acute and prolonged alcohol withdrawal, which is associated with alcohol craving and relapse (Spanagel et al., 2004). This hyperglutamatergic state can be attenuated by the drug acamprosate, which interacts with NMDA and mGluR5 receptors and restores the balance between excitatory and inhibitory neurotransmission (Spanagel and Zieglgänsberger, 1997; Spanagel and Kiefer, 2008).

These long lasting changes in glutamate transmission after chronic alcohol exposure are likely due to synaptic plasticity mechanisms (Kroener et al., 2012; Zorumski et al., 2014).

1.3.1 Group II mGluRs in addiction

In the rodent brain the highest levels of mGluR2/3 receptors can be found in the olfactory bulb and the hippocampus, moderate levels can be found in the dorsal striatum, nucleus accumbens, amygdala, anterior thalamic nuclei, the cerebral cortex and cerebellum. Low levels were detected in the pallidum, colliculi, the ventral midbrain and the hypothalamus (Shigemoto et al., 1997; Olive, 2009). Therefore mGluR2/3 are expressed in brain areas

involved in the rewarding properties of alcohol and are a potential research target for alcohol use disorders (Moussawi and Kalivas, 2010). mGluR2/3 have been shown to be involved in neuropsychiatric diseases like Alzheimer's disease, Parkinson's disease, anxiety, depression, schizophrenia and addiction (Niswender and Conn, 2010). The mGlu2/3 receptor agonist LY379268 was shown to suppress alcohol self-administration as well as cue-induced and stress-induced reinstatement of alcohol seeking in rats (Bäckström and Hyytiä, 2005; Zhao et al., 2006). An escalation of alcohol intake was also observed in a genetic mGluR2 knockout rat model, compared to control rats (Zhou et al., 2013). In addition a previous study from our lab found a downregulation of mGluR2 mRNA specifically in the infralimbic (IL) cortex after chronic intermittent alcohol exposure in the so called postdependent rat model (Meinhardt et al., 2013). This mGluR2 deficit in the IL - NAc shell projection lead to excessive cue-induced alcohol seeking behavior in rats, which was normalized after a viral restoration of mGluR2 expression in the IL. Thus, mGluR2 seems to play an important role in alcohol seeking behavior and could be a potential treatment target for alcohol use disorders.

1.4 Rodent animal models of reward seeking and drug addiction

An animal model is not a perfect replication of a complex clinical condition, but rather models aspects of a complex neuropsychiatric disorder (Denayer et al., 2014). In order to validate different animal models, a validity scoring system has been developed (Sams-Dodd, 2006). The most commonly used system evaluates the validity of an animal model based on three criteria (McKinney and Bunney, 1969; Willner et al., 1992; Sams-Dodd, 1999): face, construct and predictive validity. Face validity indicates if the animal model "looks like" the clinical condition, e.g. similar physical symptoms. Construct validity defines that the underlying disease mechanism is the same in the animal model and in the clinical condition. Predictive validity defines that the responses to drug treatment and other manipulations are similar compared to the clinical condition.

1.4.1 Post-dependent animal model

In the post-dependent model of alcoholism, a dependence-like state is induced in wildtype rats by repeated cycles of intoxication and withdrawal from alcohol. Chronic intermittent exposure (CIE) to alcohol vapor (Figure 3A) is a reliable model for anatomical, behavioral and biochemical features of alcohol addiction, providing construct, face and predictive validity (Rimondini et al., 2002; Sommer et al., 2008; Meinhardt and Sommer, 2015). Amongst other molecular and cellular changes, this procedure specifically induces a downregulation of mGluR2 in the infralimbic cortex, which makes it a promising model to study alcohol consumption and alcohol seeking behavior (Meinhardt et al., 2013). A key characteristic of this animal model is the high blood alcohol concentration (BAC) between 150 - 300 mg/dl or 1.2 - 2.4 ‰ (Figure 3B) after a 14h exposure cycle (Gilpin et al., 2009; Meinhardt et al., 2013; Meinhardt and Sommer, 2015). The post-dependent (PD) state is induced by repeated intoxication and withdrawal cycles for 8 weeks and is characterized by excessive, voluntary alcohol seeking behavior, increased alcohol intake, as well as tolerance to alcohol, increased sensitivity to stress and the presence of withdrawal signs (Figure 3C) (Sommer et al., 2008; Meinhardt and Sommer, 2015). Although the alcohol administration in this model is passive and not voluntary, the following DSM5.0 criteria are fulfilled (American Psychiatric Association, 2013): tolerance to alcohol, withdrawal symptoms, loss of control over alcohol seeking and excessive voluntary alcohol consumption (Meinhardt and Sommer, 2015). Furthermore, this model has very good predictive and construct validity, because pathological changes in the brain resemble the changes observed in alcoholic patients. Furthermore, several pharmacological substances used for relapse prevention in human alcoholics are also effective in reducing voluntary alcohol consumption in PD rats. The PD model does not have face validity, because alcohol administration is not based on a voluntary basis, but forced by the experimenter (Meinhardt and Sommer, 2015). Nevertheless, PD rats are an excellent model for long-term changes in the brain after chronic alcohol exposure.

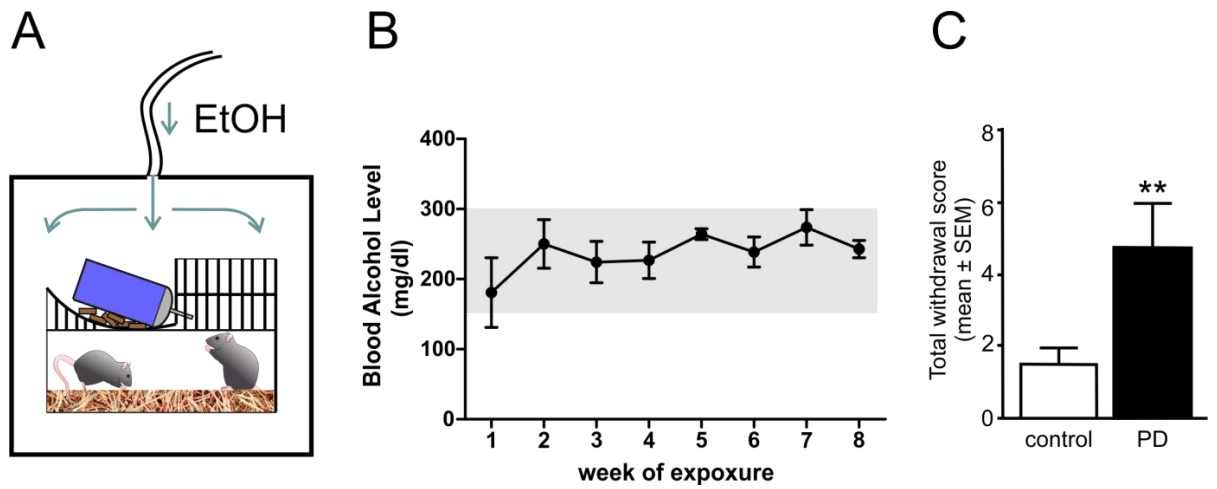

Figure 3: Post-dependent animal model. A) Schematic of vapor exposure procedure The animals are housed in groups of four in their homecages and exposed to EtOH vapor or air. The animals undergo 8 weeks of repeated cycles of chronic intermittent EtOH (CIE) or air exposure for 14h per day and 7 days a week. **B)** Blood alcohol concentrations (BAC) reach a stable level between 150 - 300mg/dl after each 14h CIE cycle. **C)** Total somatic withdrawal scores, 8 hours after the last CIE or air cycle. Total withdrawal scores are the sum of the following withdrawal signs: tail rigidity, ventro-medial limb retraction, irritability to touch (vocalization), abnormal gait and body tremors.

1.4.2 Genetically selected alcohol preferring rat lines

Alcohol preferring as well as non-preferring rat lines were generated by genetic selection and breeding of animals with high alcohol preference and animals with low alcohol preference. Several alcohol preferring and non-preferring rat lines have been generated so far. The most commonly used lines are: the finish Alko alcohol (AA) and Alko non-alcohol (ANA) preferring rats (Eriksson, 1969), the high-alcohol drinking (HAD) and low-alcohol drinking (LAD) rats (Li et al., 1993), the Sardinian preferring (sP) (Colombo, 1997), the Marchigian Sardinian (msP) rats (Ciccocioppo et al., 1998) and the Indiana alcohol preferring (P) and non-preferring (NP) rats (Lumeng et al., 1977). In the framework of this thesis, the Indiana P and NP rats were used. Indiana P and NP rats were generated by selective breeding from a wild type Wistar rat colony (Figure 4). P rats are characterized by a voluntary daily alcohol consumption of more than 5g/kg. NP rats are characterized by a voluntary daily alcohol consumption of less than 1g/kg.

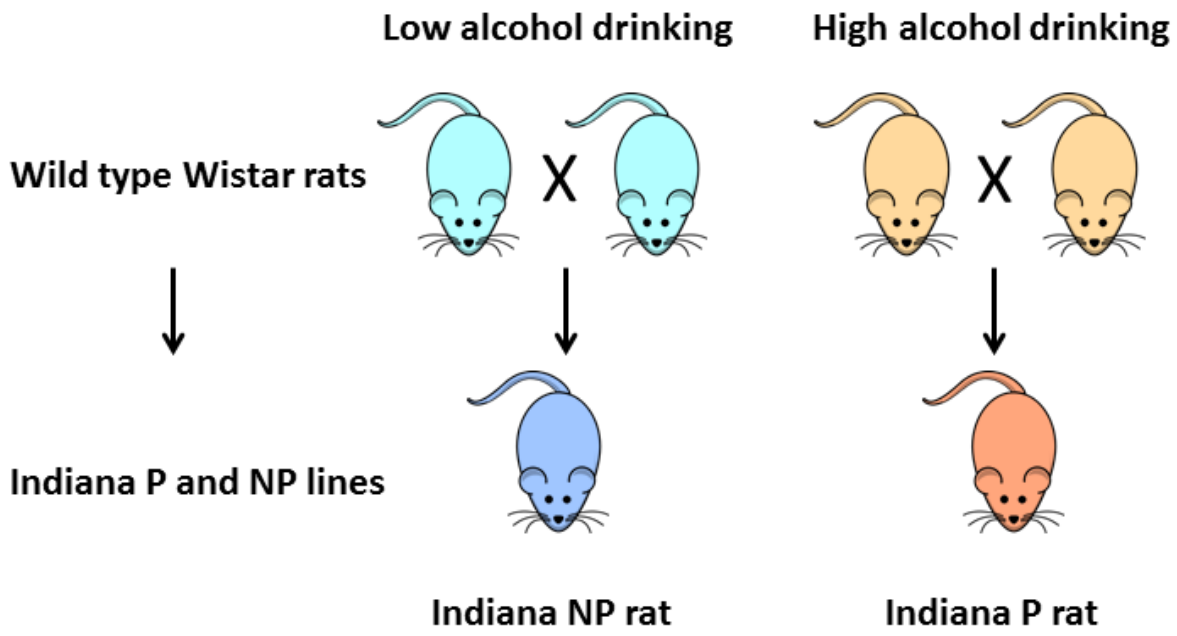

Figure 4: Generation of Indiana NP and P rats. Indiana alcohol preferring (P) rats and non-preferring (NP) rats were generated at the Indiana University Alcohol Research Center. The animals were generated by inbreeding low alcohol drinking Wistar rats to generate the NP line and high drinking Wistar rats to generate the P line.

Indiana P rats reach high blood alcohol concentrations (BACs) of 50 - 200mg/dl under 24h voluntary drinking (Rodd-Henricks et al., 2001; Bell et al., 2006) or limited access conditions (Murphy et al., 1986). Furthermore Indiana P rats are homozygous for a premature stop codon in the Glutamate metabotropic receptor 2 (Grm2) coding sequence (Zhou et al., 2013). This premature stop codon is generated by a single nucleotide polymorphism (SNP) in the Grm2 coding sequence changing the codon TGC for cysteine into TGA (stop codon) (Figure 5). As a result, a truncated version of the metabotropic glutamate receptor 2 (mGluR2) protein is translated, consisting of a partial ligand binding domain and none of the transmembrane domains. The resulting protein fragment is not functional, leading to a "knock-out" of mGluR2 in Indiana P rats. The Grm2 coding sequence and mGluR2 expression in NP rats is not affected. This genetic model for alcoholism has predictive, face and construct validity (Ciccocioppo, 2013).

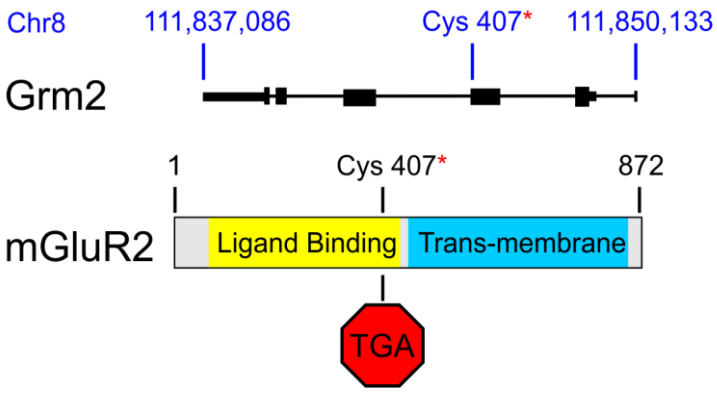

Figure 5: Premature stop-codon in Grm2 coding sequence of Indiana P rats. Schematic representation of genomic location of premature stop-codon in Indiana P rats. Due to a point mutation the sequence TGC encoding cysteine is replaced by the stop codon TGA. The stop codon, present in P-rats leads to a truncated, non-functional mGlur2 protein, consisting of a partial ligand binding domain, but none of the transmembrane domains. Adapted from (Zhou et al., 2013).

1.4.3 Operant reinstatement of drug-seeking model

The most frequently used and reliable procedure to study reward seeking behavior in rats is the reinstatement model (Shaham et al., 2003; Spanagel, 2003; Bossert et al., 2013). This operant conditioning model is an example for associative learning. The animals need to discriminate between two contingencies: responding at one lever, paired with a reward-associated stimulus will lead to a reward delivery and responding at another lever, not paired with a reward-associated stimulus will not lead to reward delivery (Sanchis-Segura and Spanagel, 2006; Martin-Fardon and Weiss, 2013). Under these conditions, animals are trained to self-administer natural rewards or drug rewards until a stable baseline response rate is reached. Following this, the animals undergo extinction training which leads to a decrease in responding due to the absence of drug- or reward predictive cues and the reward itself. For the final reinstatement test lever responding can be reinstated by administration of a small quantity of the drug or reward, so called drug priming (de Wit and Stewart, 1981), by the presentation of previously conditioned cues and stimuli (Figure 6) (Katner et al., 1999) or by exposure to stressors (Lê et al., 1998).

This model has excellent face validity to the clinical relapse condition, because craving and relapse in abstinent alcoholics can be also triggered by the re-exposure to the drug (de Wit, 1996), exposure to drug associated cues or contexts (O'Brien et al., 1992) or the exposure to stressors (Sinha et al., 2011). Furthermore, drug consumption and drug seeking occur on a

voluntary basis and are not experimenter controlled, which is another aspect of face validity. The reinstatement model has also predictive validity in the case of heroin, alcohol, and nicotine: naltrexone, acamprosate, buprenorphine, methadone, or varenicline are used as anti-relapse treatment in humans and were also shown to decrease drug priming or cue-induced reinstatement in rats (Bossert et al., 2013). The construct validity has not been demonstrated yet, because the drug-free state in the animal model occurs due to different reasons compared to the human condition. Furthermore, the contingencies involved in drug-priming and cue-induced reinstatement are not the same as in the clinical condition (Epstein et al., 2006). Also stress-induced reinstatement is mostly induced by footshock (Kupferschmidt et al., 2011) or the administration of pharmacological stressors (Lê et al., 2005), which does not represent the human condition.

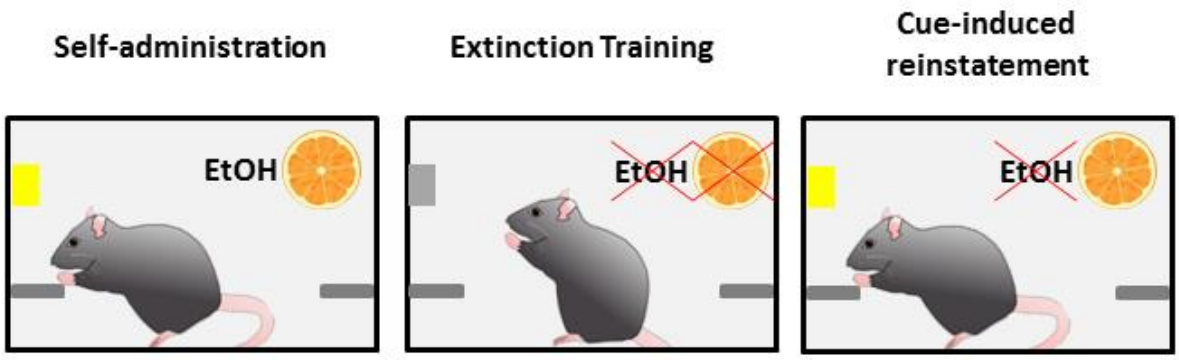

Figure 6: Schemtatic representation of cue-induced reinstatement of alcohol seeking model. The operant chamber is equipped with one response lever at each side and a blinking light stimulus located above each lever. The animals are trained to self-administer an ethanol solution by responding at the left lever. The ethanol reward is paired with activation of the left blinking light stimulus and the continuous presence of an orange odor as a contextual cue. Following self-administration and cue-conditioning, the animals undergo extinction training. No contextual orange odor cue and no blinking light stimulus are presented. Responses at the left lever do not result in ethanol reward delivery anymore. After extinction training, the animals are tested on their cue-induced reinstatement of alcohol seeking performance. The contextual orange odor cue and the blinking light stimulus after left lever responses are presented again. However, lever responses do not result in ethanol reward delivery.

1.4.4 Evaluation of the reinforcing properties of rewards

For the above described self-administration and reinstatement procedures often a fixed ratio (FR) schedule is used, meaning the reward is delivered as soon as a pre-defined number of responses is reached. To assess the reinforcing potential of rewards and the animal's motivation to obtain the reward a progressive ratio (PR) schedule can be applied. During this

test, an increasing number of responses has to be made in order to obtain the reward (Hodos, 1961). The most commonly measured variable during a PR schedule is the "breaking point" (BP). The BP is defined as the highest completed ratio of responses during the operant session and presumably reflects the maximum effort the animal is willing to make in order to obtain a single portion of the reward. Therefore the BP is often used as a measure of an animal's motivation to obtain a reward and can be used to evaluate the reinforcing properties of different substances (Richardson and Roberts, 1996; Sanchis-Segura and Spanagel, 2006).

1.5 The medial prefrontal cortex

1.5.1 Top-down control over behavior

The medial prefrontal cortex (mPFC) is a central part of the brain reward circuitry and is generally involved in higher cognitive abilities including self-control, regulation of emotion, motivation, working memory, decision making attention and cognitive flexibility (Heidbreder and Groenewegen, 2003; Goldstein and Volkow, 2011). It is furthermore involved in bottom-up processes driven by the amygdala in emotional and motivational behavior as well as top-down or executive control over goal directed behavior (Quirk and Beer, 2006). Goals are defined as desired states that an individual wants to achieve, for example a specific reward. In order to obtain the reward, an individual has to perform a certain activity, which is called goal-directed behavior (Buschman and Miller, 2014). Top-down control over behavior describes the use of previously acquired knowledge to plan and decide for appropriate actions in order to achieve a goal. It is hypothesized that goal-directed behavior is controlled by two complimentary systems: The basal ganglia structures (the ventral striatum, including the nucleus accumbens, and the dorsal striatum), which are known to be involved in reward conditioning and habit formation (Di Chiara and Imperato, 1988; Wise, 1996; Goldstein and Volkow, 2011), are thought to be involved in the rapid learning of simple and fixed goal-directed behaviors (Buschman and Miller, 2014). The second system is based on the mPFC, which is involved in the learning of complex, abstract or long-term goal-directed behavior (Buschman and Miller, 2014). Therefore the mPFC is a critical structure for the acquisition and execution of reward seeking behavior. The mPFC also plays a crucial role in alcohol use disorders, as alcohol-associated stimuli were shown to induce robust activation in prefrontal

and limbic regions (Schacht et al., 2013). Activation of these brain areas was also found in abstinent alcoholics, which subsequently relapsed (Grüsser et al., 2004).

1.5.2 Functional distinction of medial prefrontal subregions in rodents

After a long period of controversial discussions it is now accepted that rats have a functional prefrontal cortex, which is divided into several subregions and is functionally comparable to the medial, orbital and dorsolateral areas of the primate prefrontal cortex (Uylings et al., 2003). Similar to the human prefrontal cortex, also the rat prefrontal cortex has been shown to be involved in working memory, attention, behavioral flexibility, decision making, response initiation, autonomic control and emotion (Heidbreder and Groenewegen, 2003).

Along the dorsal-ventral axis the rat medial prefrontal cortex can be subdivided into the anterior cingulate cortex (ACC), the prelimbic cortex (PL) and the infralimbic cortex (IL). The rat IL is thought to be a homologue to the Brodmann's area 25 and the PL a homologue to Brodmann's area 32 in primates (Gabbott et al., 2003) and humans (Quirk and Beer, 2006). The dorsal part of the mPFC comprised of the dorsal ACC and the dorsal PL is particularly involved in the temporal shifting of behavioral strategies. The ventral part of the mPFC comprised of the ventral PL and the IL is involved in behavioral flexibility and processing of spatial cue information (Heidbreder and Groenewegen, 2003). Furthermore the PL was found to be important for voluntary goal-directed behavior, whereas the IL was found to be involved in habit formation (Killcross and Coutureau, 2003). An important function of the medial prefrontal cortex is both to drive behavior, but also to suppress inappropriate responses (Miller and Cohen, 2001; Dalley et al., 2004; Euston et al., 2012). A functional dichotomy between the PL and the IL has been postulated for fear memory and addiction (Peters et al., 2009). The PL was found to drive a behavioral sequence, while the IL is involved in behavioral suppression. However, there is growing evidence, that such a simple functional dichotomy cannot be generalized for reward seeking behavior, as promoting and suppressing neuronal correlates can be found in both the PL and IL (Bossert et al., 2011; Moorman and Aston-Jones, 2015; Moorman et al., 2015). Also in a previous study from our lab specifically the IL was found to be damaged by chronic alcohol intake and was found to be involved in the control over alcohol seeking behavior (Meinhardt et al., 2013).

1.5.3 Anatomical distinction of medial prefrontal subregions

There are clear anatomical differences between the different medial prefrontal subregions. The medial prefrontal cortex is a highly interconnected structure, which receives from and sends extensive projections to a variety of different brain areas. Already the IL subregion of the mPFC is known to have more than 60 projection targets (Hurley et al., 1991; Vertes, 2004; Noori et al., 2017).

1.5.3.1 Cortico-cortical connections of the mPFC

There are strong interconnections of the ventral and dorsal subregions of the mPFC between both hemispheres. There are also strong interconnections between the infralimbic and prelimbic cortices within the same hemisphere. However, the connection of the IL with the contralateral PL seems to be rather weak compared to the unilateral IL - PL projection (Vertes, 2004). The dorsal areas (ACC and dorsal PL) are strongly connected with the sensory and motor cortices while the ventral subregions (ventral PL and IL) are strongly connected with the association cortex and limbic system (Heidbreder and Groenewegen, 2003).

1.5.3.2 Efferent mPFC projections

The IL projects to the PL, the orbitofrontal cortex (OFC) and also to the ACC (Room et al., 1985). Furthermore the agranular insular cortex, the piriform cortex, the entorhinal and perirhinal areas are IL projection targets (Hurley et al., 1991). The IL was also found to project to the lateral septum, the BNST, the medial and lateral preoptic nuclei, substantia innominata, endopiriform nuclei of the basal forebrain and the nucleus accumbens. Furthermore the IL innervates the medial, basomedial, central and cortical nuclei of the amygdala; the dorsomedial, lateral and perifornical, posterior and supramammillary nuclei of the hypothalamus, the VTA; and the parabranchial and solitary nuclei of the brainstem (Vertes, 2004) (Figure 7A).

The PL projects to the IL and ACC and less pronounced to the premotor area F2 and caudal cingulate areas. The PL also projects to the agranular insular cortex, and perirhinal as well as entorhinal areas. The ventral part of the PL strongly innervates the piriform cortex (Datiche and Cattarelli, 1996). Furthermore the PL projects to the claustrum, the nucleus accumbens, olfactory tubercle, the paraventricular, mediodorsal and reuniens nuclei of the thalamus, the central nucleus and the basolateral amygdala, the VTA, as well as the dorsal and median raphe nuclei of the brainstem (Vertes, 2004) (Figure 7B).

Despite these overall similarities in afferent projection patterns, there are also differences between IL and PL projection patterns. For instance, the IL was shown to strongly innervate the shell of the NAc, whereas the PL was found to project mainly to the core of the NAc (Sesack et al., 1989; Brog et al., 1993; Voorn et al., 2004). Furthermore the PL was shown to innervate mainly the basal amygdala (Vertes, 2004; Gabbott et al., 2005), whereas the IL projects to the lateral division of the central amygdala and the intercalated cells (ITC) (McDonald et al., 1996; Berretta et al., 2005). These differences in projection targets are associated with the differential control of the IL and PL of drug seeking behavior and fear conditioning. The PL – basal amygdala projection was shown to be involved in the conditioned fear expression (Herry et al., 2008), whereas the IL – ITC projection is thought to be involved in conditioned fear extinction (Peters et al., 2009). Furthermore the PL – NAc core projection was found to promote cocaine and heroin seeking behavior in rats (McFarland et al., 2003; LaLumiere and Kalivas, 2008). Converseley, the IL – NAc shell projection was found to be involved in the extinction of cocaine seeking behavior in rats (Peters et al., 2008a).

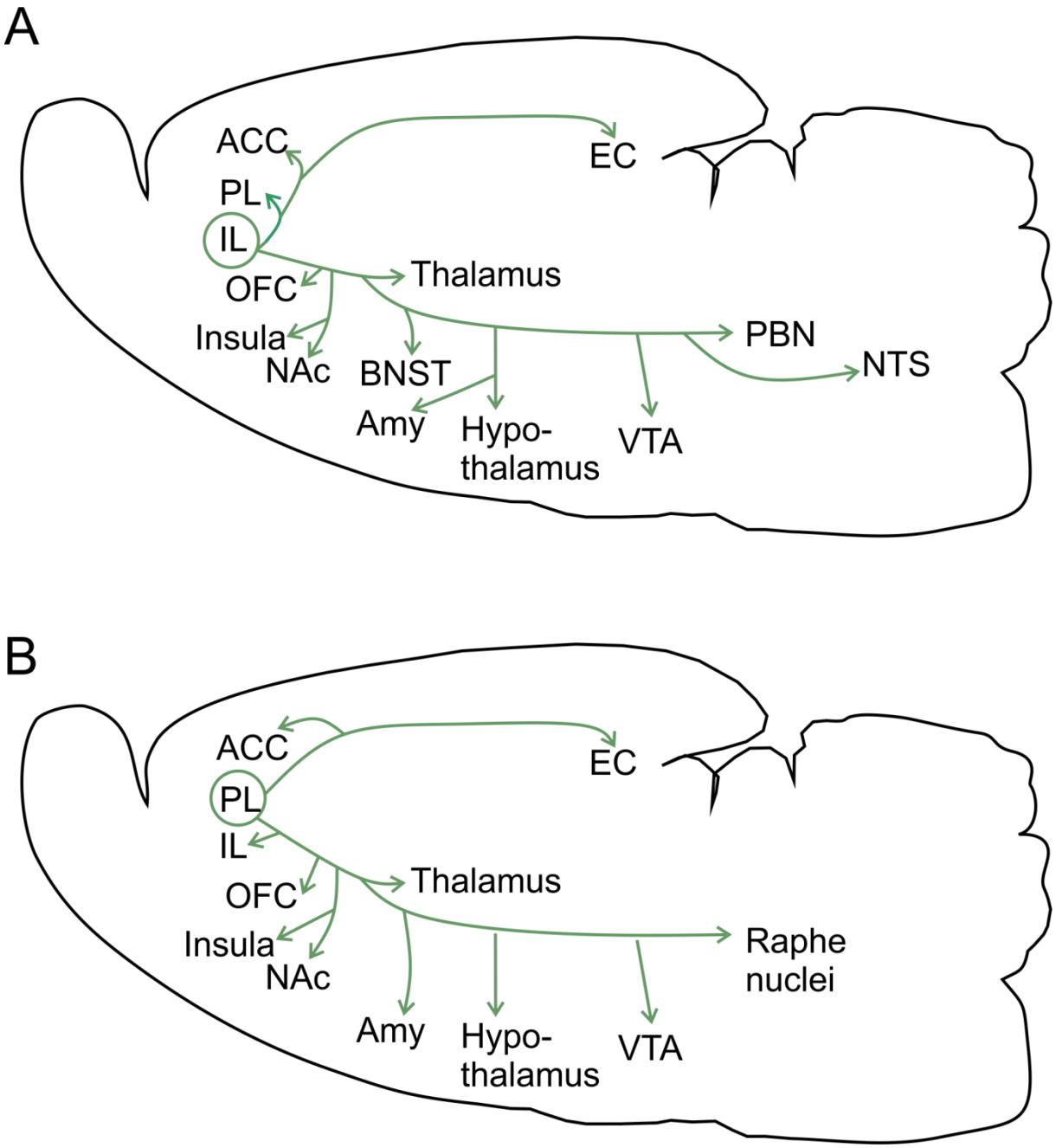

Figure 7: Efferent projections of infralimbic and prelimbic cortices. A) Afferent projections of the infralimbic cortex (IL). **B)** Afferent projections of the prelimbic cortex (PL). Projection targets: anterior cingulate cortex (ACC), orbitofrontal cortex (OFC), insular cortex (insula), nucleus accumbens (NAc), amygdala (Amy), bed nucleus of stria terminalis (BNST), thalamus, hypothalamus, ventral tegmental area (VTA), raphe nuclei, parabrachial nuclei (PBN) and nucleus of solitary tract (NTS).

1.5.3.3 Afferent PFC projections

The IL and ventral PL are strongly innervated by the piriform cortex (Datiche and Cattarelli, 1996), the perirhinal and ventral agranular insular areas (Van Eden et al., 1992). The dorsal parts of the PL and the ACC are innervated by the secondary visual, the posterior agranular insular and retrosplenial cortex. Rostral parts of the ACC receive projections from the fronto-parietal motor cortex, the somatosensory and temporal association cortex, as well as the posterior agranular insular cortex (Heidbreder and Groenewegen, 2003).

1.5.4 Laminar structure of the mPFC

Within the cortex cytoarchitectonically distinct subregions exist, which are organized in layers. Most cortical areas contain six defined layers with characteristic functional and anatomical features. Layer I (Lamina molecularis) consists mainly of dendritic and axonal fibers and is a major target of "feedback" connections between cortical areas (Douglas and Martin, 2004). This layer does not contain pyramidal neurons and generally contains very few cell bodies (Trepel, 2017). The cortical layers II (Lamina granularis externa) and III (Lamina pyramidalis externa) are important for inter-laminar as well as cortico-cortical connections and contain mainly smaller pyramidal neurons (Trepel, 2017). Afferent projections typically integrate into Layer IV (Lamina granularis interna), which is rich in stellate neurons. The deep layers V (Lamina pyradmidalis interna) and VI (Lamina multiformis) project to subcortical areas and contain mainly pyramidal neurons (Douglas and Martin, 2004; Trepel, 2017). Cortical circuit function has been extensively studied in sensory cortices, which revealed that thalamic input into layer IV is transferred to the layers II and III. In layer II and III the thalamic information is integrated with information from other cortical areas and forwarded through the output layer V to subcortical structures. In addition layer V neurons relay the signal also to layer VI neurons, which send a feedback to the thalamus (van Aerde and Feldmeyer, 2015) (Figure 8A).

The rodent mPFC belongs to the agranular cortex type, because it is lacking the afferent input layer IV, which makes cortical circuit organization and function less clear (Uylings et al., 2003; Shepherd, 2009). It has been demonstrated that both superficial and deep layers of the rodent mPFC receive afferent projections from cortical as well as subcortical regions and

project to other limbic structures (Gabbott et al., 2005; Riga et al., 2014). In comparison with the somatosensory cortex, the mPFC layer V cells receive a stronger input from layer I and VI cells, and less from layer III cells. Compared to the somatosensory cortex, the mPFC layer III is thinner and layer V thicker (Figure 8B). There are also differences in local vs. long-range inputs into layer V between the somatosensory cortex and the mPFC. The majority of layer V inputs in the somatosensory cortex originate from other cells in the ipsilateral cortex. Conversely, only a minority of layer V inputs in the mPFC originated from other ipsilateral cells. The majority of mPFC layer V inputs are long-range inputs, originating from the agranular insula, thalamic nuclei, contralateral mPFC regions, motor areas, hippocampus and basolateral amygdala. This indicates that the mPFC integrates information from very diverse brain areas, as opposed to the strict circuits in the somatosensory cortex (DeNardo et al., 2015). The different cortical layers can be identified by the presence of specific neuronal subtypes and distinct gene expression patterns, which enables a clear discrimination between the layers not only on the cellular but also on the molecular level (Molyneaux et al., 2007). A clear differentiation between different cortex layers is especially important in the agranular mPFC, because the lack of the granular layer IV makes a visual discrimination based on nuclear coutnerstainings challenging.

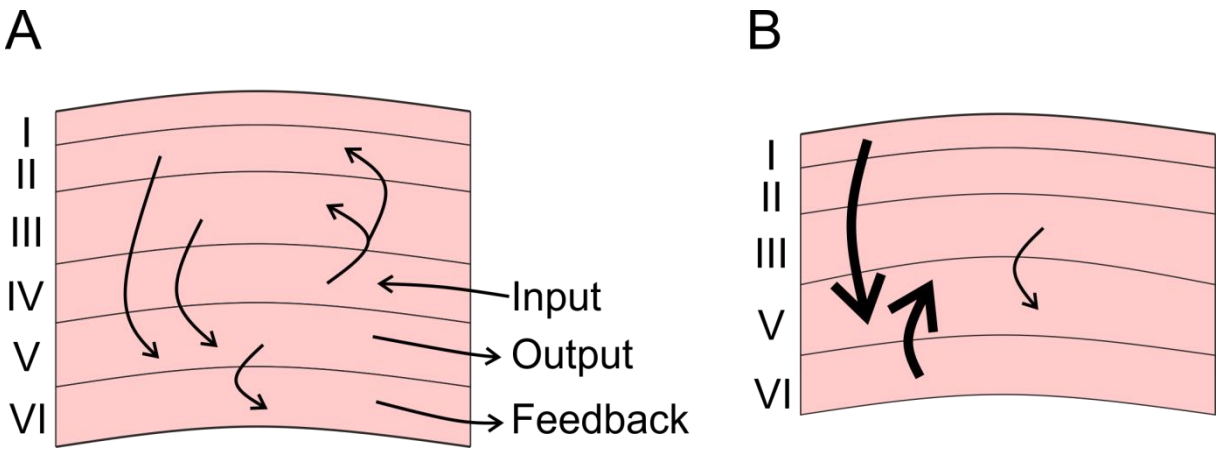

Figure 8: Comparison of layer organization between the somatosensory and the medial prefrontal cortex. A) The somatosensory cortex belongs to the neocortex and consists of six layers. Afferent input (e.g. from the thalamus) in layer IV is relayed to layer II and layer III, where the signal is integrated with other cortical areas. Information is then transferred through layer V to subcortical structures. Furthermore, the signal is also transferred from layer V to layer VI, which then sends a feedback to the source of the original signal (e.g. thalamus). **B)** The mPFC belongs to the agranular cortex type and consists of five layers, lacking the output layer IV. The mPFC lacks a clear information processing structure, as both the deep layers (V and VI) as well as the superficial layers (II and III) receive afferent inputs and are the source of efferent projections to cortical and sub-cortical brain regions. In comparison with the somatosensory cortex, the mPFC layer V is thicker and the mPFC layer III is thinner. Furthermore the mPFC layer V receives strong input from layer I and layer VI, but only weak input from layer III, as compared to the somatosensory cortex.

1.6 Behavioral assessment of executive functions

The medial prefrontal cortex (mPFC) is involved in top-down control over behavior and executive functions, including working memory, attention, cognitive flexibility and impulse control (Heidbreder and Groenewegen, 2003; Wood and Grafman, 2003; Logue and Gould, 2014). Executive functions are often subdivided into three major classes: 1.) mental set shifting, 2.) updating and monitoring of information and 3.) inhibition of prepotent responses (Miyake et al., 2000). Sets are defined as a 'tendency', 'disposition' or 'readiness' and are involved in 'facilitation', 'selection', 'determination' or 'guidance' of activity (Gibson, 1941). Attentional sets are considered as hypothetical "'stores', that maintain the reward-predicting aspects of a stimulus, and the contents of an attentional set must be updated when new dimensions become relevant" (Tait et al., 2014).

Executive dysfunctions have been found in several neuropsychiatric diseases including schizophrenia (Chan et al., 2004), autism (Hill, 2004) and alcohol use disorders (Brion et al., 2017). Several tests exist to examine executive functioning in humans, including the Wisconsin Card Sorting Task (WCST) (Berg, 1948), the Tower of Hanoi (TOH) (Simon, 1975) and the Tower of London (TOL) (Shallice, 1982) tasks and random number generation (RNG) (Ginsburg and Karpiuk, 1994). The WCST was found to be strongly related to attentional set shifting, the Tower tasks (TOH and TOL) were found to be predominantly related to inhibition of prepotent responses and the RNG task was found to be involved in inhibition of prepotent responses as well as updating and monitoring of information (Miyake et al., 2000).

In humans, alcohol use disorders are characterized by impaired cognitive functions (Brion et al., 2017). Deficits in inhibition of prepotent responses have been demonstrated using a variety of psychological tests (Garland et al., 2012; Courtney et al., 2013). In addition heavy drinkers and alcoholics were found to be impaired in shifting abilities, as demonstrated by the WCST (Sullivan et al., 1993; Wicks et al., 2001; Oscar-Berman et al., 2009; Houston et al., 2014) or Stroop task (Saraswat et al., 2006). In addition alcoholic patients were found to be impaired in the intradimensional-extradimensional set shift task (Trick et al., 2014).

1.6.1 Rodent attentional set shifting task

The rodent attentional set shifting task (ASST) was adapted from the WCST by Birrell and Brown (2000) and is used to measure cognitive flexibility and set shifting. Successful performance in this test requires rule learning, recognition of rule changes, suppression of inappropriate responses and attention. In general, formation of an attentional set occurs when an animal has to classify or discriminate complex stimuli. Attentional set formation leads to a focus on the relevant stimulus and the suppression of responses at the irrelevant stimulus (Birrell and Brown, 2000). The most frequently used ASST for rats is the digging task (Birrell and Brown, 2000; Nikiforuk et al., 2010; Klugmann et al., 2011). Other forms of rodent ASST are T-maze based (Kroener et al., 2012), cross-maze based (Stefani et al., 2003) or are performed in operant chambers (Brady and Floresco, 2015; Scheggia and Papaleo, 2016). The advantages of operant or maze-based ASST protocols are the easy implementation and simple analysis. In the case of operant ASST, the operant responses are usually automatically counted. Analysis of the T- and cross-maze tasks can be done using video tracking. On the other hand, the digging task requires more equipment and cannot be analyzed in an automated way. However, rats aquire the digging task very fast, because it is similar to their natural foraging behavior (Tait et al., 2014).

In the digging task, the animals have to collect a food reward from a pot, containing scented digging material. Based on the current rule of the task, reward availability is either indicated by the olfactory dimension (odor) or the tactile dimension (digging material). After acquisition of a simple discrimination task, reward contingencies can be reversed in the reversal stage of the ASST. The animals are furthermore required to apply a learned rule on a different set of stimuli, which is taking place during the intradimensional set shift (IDS). For the extradimensional set shift (EDS), the animals have to shift their attention from one stimulus dimension (e.g. digging material) to the other dimension (e.g. odor).

The medial prefrontal cortex (mPFC) was found to be critically involved in the EDS, as mPFC lesions induced impaired EDS performance in rats in a digging task (Birrell and Brown, 2000). In mice it was shown that chronic intermittent alcohol exposure alters mPFC plasticity and impairs EDS performance in a T-maze task (Kroener et al., 2012). In the

framework of this thesis, an ASST digging task will be used to study the molecular mechanisms of alcohol-induced ASST impairments in rats.

1.7 Neuronal ensembles in reward seeking and addiction

In 1949 D.O. Hebb described the theory of functional 'cell assemblies' (Hebb, 1949), forming the basis for a new field of neuroscience research. According to Hebb's theory, memories are encoded in specific sub-populations of cells, which are synchronously activated upon memory recall (Schwindel and McNaughton, 2011; Holtmaat and Caroni, 2016). A functional neuronal ensemble is characterized by coordinated spatiotemporal activity patterns and reliable re-activation during a specific behavioral task (Mayford, 2014; Sompolinsky, 2014; Tonegawa et al., 2015; Holtmaat and Caroni, 2016). Which cells are parts of a neuronal ensemble during a certain behavior task also depends on activity patterns of afferent inputs, meaning neuronal ensembles can be located in several different brain areas (Cruz et al., 2013; Cruz et al., 2015). Neuronal ensembles are thought to be dynamic, which means they are formed and changed throughout the learning of a certain behavioral response (Holtmaat and Caroni, 2016). Furthermore one and the same neuron can be part of several neuronal ensembles involved in different behavioral responses, neuronal ensembles can be spread throughout the brain and can co-exist in several brain areas, and neuronal ensembles encoding different behavioral responses can intermingle in the same brain area (Hebb, 1949; Schwindel and McNaughton, 2011; Cruz et al., 2013; Cruz et al., 2015; Holtmaat and Caroni, 2016).

Classical lesion studies or site-specific inactivation experiments were frequently performed in order to identify brain regions involved in learning and memory (e.g. de Bruin et al., 1994; Flavell and Lee, 2012; Hart and Izquierdo, 2017). In the context of addiction and reward-seeking behavior, site-specific pharmacological inactivation of the IL revealed a critical role of the IL in extinction of cocaine self-administration (LaLumiere et al., 2010). Furthermore Peters and colleagues (2009) proposed a functional dichotomy of the IL and PL subdivisions of the mPFC in drug seeking behavior. The PL subdivision was found to promote drug-seeking behavior, as site-specific inactivation of the PL using the sodium channel blocker tetrodotoxin (TTX) was found to impair cue-induced reinstatement of cocaine seeking in rats (McLaughlin and See, 2003). The IL subdivision of the mPFC was found to be involved in

the suppression of drug-seeking behavior, as site-specific inactivation of the IL using the $GABA_A$- and $GABA_B$-receptor agonists muscimol and baclofen induced reinstatement of cocaine seeking during extinction training (Peters et al., 2008a).

Consistent with the 'cell assemblies' theory of D.O. Hebb (1949) several neuronal ensembles, involved in drug-and reward-seeking have been identified in the mPFC using the Daun02 inactivation method (Koya et al., 2009; Koya et al., 2016). This method enables the specific inactivation of previously activated neurons in cFos-LacZ transgenic rats. A functional neuronal ensemble in the IL was found to promote context-induced heroin seeking (Bossert et al., 2011). Consistent with the results for context-induced heroin seeking, an IL ensemble was found to be involved in the promotion of food seeking behavior (Warren et al., 2016). However, other studies using non-selective inactivation techniques found an inhibitory role of the IL in cocaine seeking behavior (Peters et al., 2008a; LaLumiere et al., 2012), which suggests a possible co-existence of several functional neuronal ensembles in one brain area (Figure 9). In 2011 Schwindel and McNaughton described that several neuronal ensembles encoding learned associations can co-exist in one brain area and also other studies indicated a co-existence of functionally distinct neuronal ensembles specifically within the IL (Cruz et al., 2015; Suto et al., 2016; Warren et al., 2016).

Within the mesocorticolimbic system several neuronal ensembles have been identified. In the medial prefrontal cortex (mPFC) neuronal ensembles involved in glucose and saccharin seeking (Suto et al., 2016), food reward (Warren et al., 2016) and heroin seeking (Bossert et al., 2011) have been identified. In the nucleus accumbens (NAc) neuronal ensembles involved in cocaine seeking were found (Koya et al., 2009; Cruz et al., 2014). In the central amygdala (CeA) a functional neuronal ensemble involved in excessive alcohol drinking was found (de Guglielmo et al., 2016). Neuronal ensembles involved in fear learning (Grewe et al., 2017) have been identified in the baslolateral amygdala (BLA). In the ventral tegmental area (VTA) neuronal ensembles, involved in appetitive spatial learning tasks were found to communicate with hippocampus ensembles (Gomperts et al., 2015). Neuronal ensembles are not only intermingled in the same brain area, but are thought to be highly interconnected throughout the mesocorticolimbic reward system (Figure 10) (Cruz et al., 2013).

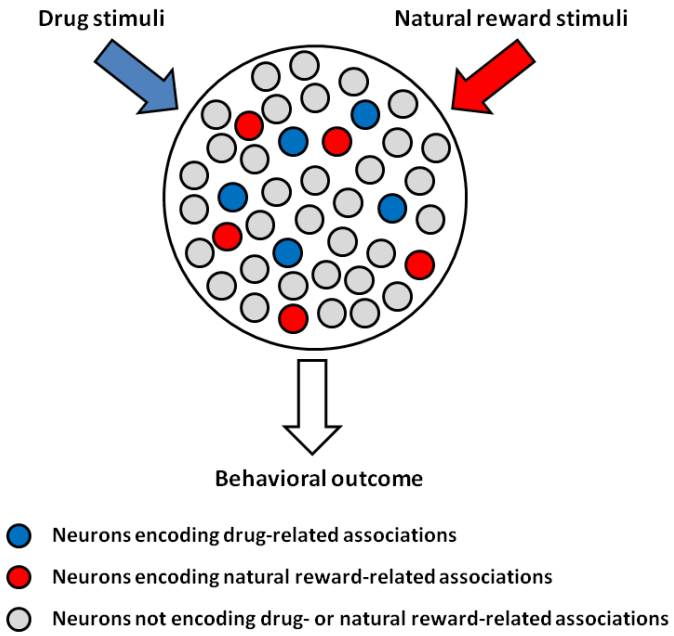

Figure 9: Schematic representation of two neuronal ensembles coexisting in the same brain area. Neuronal ensembles can be activated by drug-related stimuli (blue circles) and natural reward-related stimuli (red circles). Both ensembles can co-exist in the same brain area. Adapted from (Cruz et al., 2015).

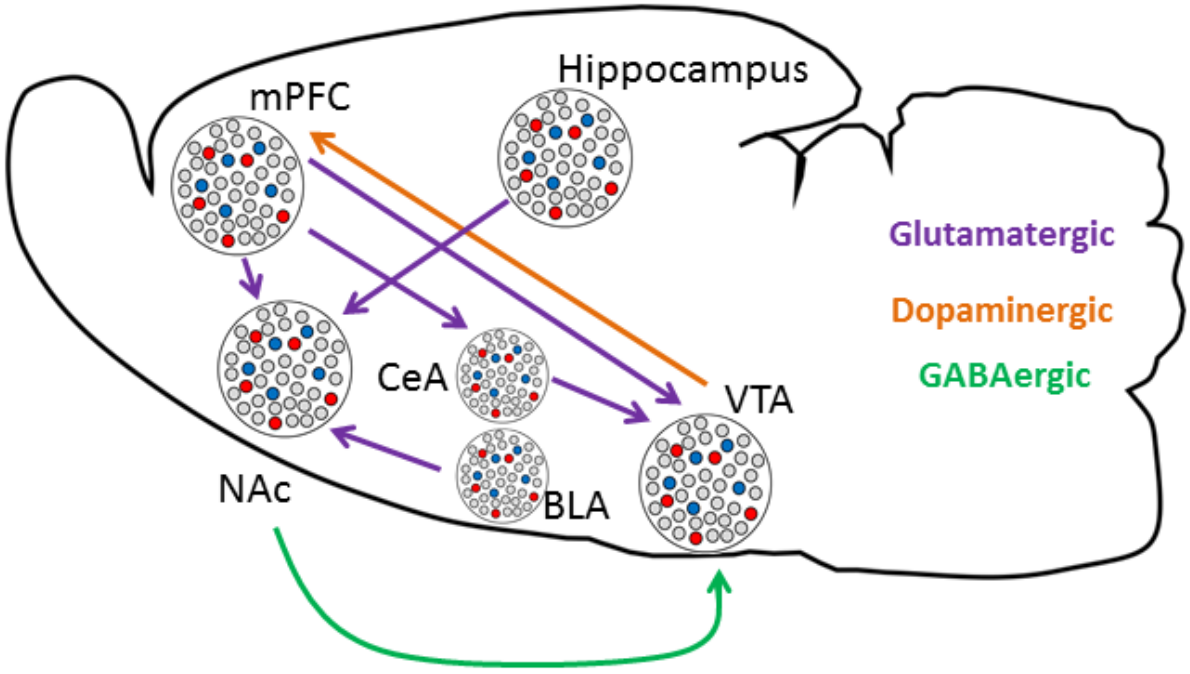

Figure 10 Neuronal ensembles in the mesocorticolimbic system. Several interconnected ensembles have been identified in the mesocorticolimbic system including the medial prefrontal cortex (mPFC), nucleus accumbens (NAc), central (CeA) and basolateral (BLA) amygdala, the ventral tegmental area (VTA) and the hippocampus. The different brain areas of the mesocorticolimbic system are highly interconnected by glutamatergic (purple), dopaminergic (orange) and GABAergic (green) projections. Adapted from (Cruz et al., 2013).

1.8 Immediate early genes

The so called immediate early genes (IEGs) represent a specific group of genes, which respond rapidly to a variety of extrinsic regulatory signals (Fowler et al., 2011). The IEG family is thought to consist of about a few hundred genes, most of which are involved in the regulation of the cell cycle and cellular growth (Greenberg and Ziff, 1984). Although there are differences in induction kinetics, typically expression of IEGs is fast and of transient nature. IEG expression requires no additional protein synthesis and is not influenced by translational inhibitors. IEGs are short genes (~19kb) and have fewer exons compared to other genes, but a high abundance of TATA boxes and CpG islands. Promoter regions of IEGs contain binding sites for certain transcription factors like: serum-response factor (SRF), nuclear factor kappa B (NF-kB) and cyclic AMP response element-binding protein (CREB) (Bahrami and Drablos, 2016). Despite these similarities, IEGs have different activators, are involved in different upstream regulatory pathways and have different expression patterns (Beckmann and Wilce, 1997; Herdegen and Leah, 1998; O'Donovan et al., 1999). Especially the IEGs cFos, Egr-1 and Arc are rapidly induced in activated neurons and are suitable markers for the detection of neuronal ensembles (Morgan and Curran, 1991; Herdegen and Leah, 1998; Cohen and Greenberg, 2008; Cruz et al., 2015).

Arc (activity-regulated cytoskeleton-associated protein, also: arg3.1) is a frequently used IEG for the detection of neuronal activity and the identification of neuronal ensembles. Arc is regulated by neuronal activity and basal expression is driven by natural synaptic activity (Lyford et al., 1995). Activity-dependent morphological restructuring of existing synapses was shown to be driven by Arc expression, which indicates a role of Arc in plasticity during development and in adult animals (Dobbing and Smart, 1974; Greenough et al., 1985). Furthermore, Arc expression was shown to be crucial for the formation of long term memory (Plath et al., 2006). A unique property of Arc is its synaptic localization. Upon induction Arc mRNA is first detected in the nucleus and subsequently exported into the cytoplasm and translocated into the dendritic compartment (Wallace et al., 1998; Guzowski et al., 1999).

Egr-1 (also known as zif 268, NGF1-A or Krox 24) is another IEG frequently used to map neuronal ensembles and is a transcription factor, containing a zinc-finger motif (Wang and McGinty, 1996). Increased egr-1 mRNA levels can be detected after induction of long term

potentiation (LTP), which indicates a role in synaptic plasticity (Cole et al., 1989). Interestingly following synaptic activation egr-1 binds to the Arc promoter, facilitating Arc transcription (Li et al., 2005). Furthermore egr-1 is involved in the control of complex transcriptional processes involved in synaptic reorganization on multiple levels (Duclot and Kabbaj, 2017).

cFos is the most frequently used IEG for activity mapping and ensemble detection, especially in addiction research (Cruz et al., 2015). cFos expression was found to be associated with neuronal plasticity and learning and memory (Kaczmarek, 1993). Together with the proto-oncogene c-Jun, cFos forms the activator protein-1 (AP-1) complex, which is a transcription factor complex that binds to the TPA (12-O-tetradecanoylphorbol 13-acetate) response element (TRE) in the promoter region of several AP-1 inducible genes (Angel and Karin, 1991). The molecular mechanisms underlying cFos promoter activation have been intensively studied. The serum response element (SRE) and the calcium response element (CaRE) are the most important regulatory elements, responsible for cFos gene expression. cFos transcription in the adult rat brain is primarily mediated by calcium-dependent activation of the extracellular signal-regulated kinases (ERK)/ mitogen-activated protein kinases (MAPK) pathway (Bading et al., 1997; Cohen and Greenberg, 2008). Activation of the ERK/MAPK pathway is achieved by strong neuronal activity, which leads to calcium influx though activated N-methyl-D-aspartate (NMDA) receptors and L-type voltage sensitive calcium channels (VSCCs). Elevated intracellular calcium levels can then activate Ras-GRP, which in turn leads to activation of the Ras/Raf kinase pathway, which results in ERK phosphorylation (Agell et al., 2002; Cahill et al., 2014). Phosphorylated ERK is subsequently translocated to the nucleus and leads to phosphorylation and activation of the transcription factors CREB via the ribosomal S6 kinase (RSK) and Elk-1. Both transcription factors can then bind to the SRE and CaRE elements in the cFos promoter region and drive cFos gene expression (Morgan and Curran, 1991; Chen et al., 1992; Cohen and Greenberg, 2008) (Figure 11). However, there are several alternative cFos activation pathways distinct form ERK/MAPK (Cruz et al., 2015).

Different cFos mRNA isoforms and the translated protein have characteristic expression kinetics *in-vivo*. It has been shown that the peak expression of the unspliced cFos mRNA transcript can be clearly separated from the expression peak of the spliced mRNA and the cFos protein. Unspliced cFos mRNA peaks as early as 5 minutes after induction, whereas the spliced mRNA species peaks around 30 minutes after induction (Jurado et al., 2007; Lin et al.,

2011). Expression of the cFos protein reaches its peak around 90 minutes after induction (Sheng and Greenberg, 1990). The distinct kinetics of spliced and unspliced mRNA isoforms were used to label two neuronal ensembles in the same animal in Study 2.

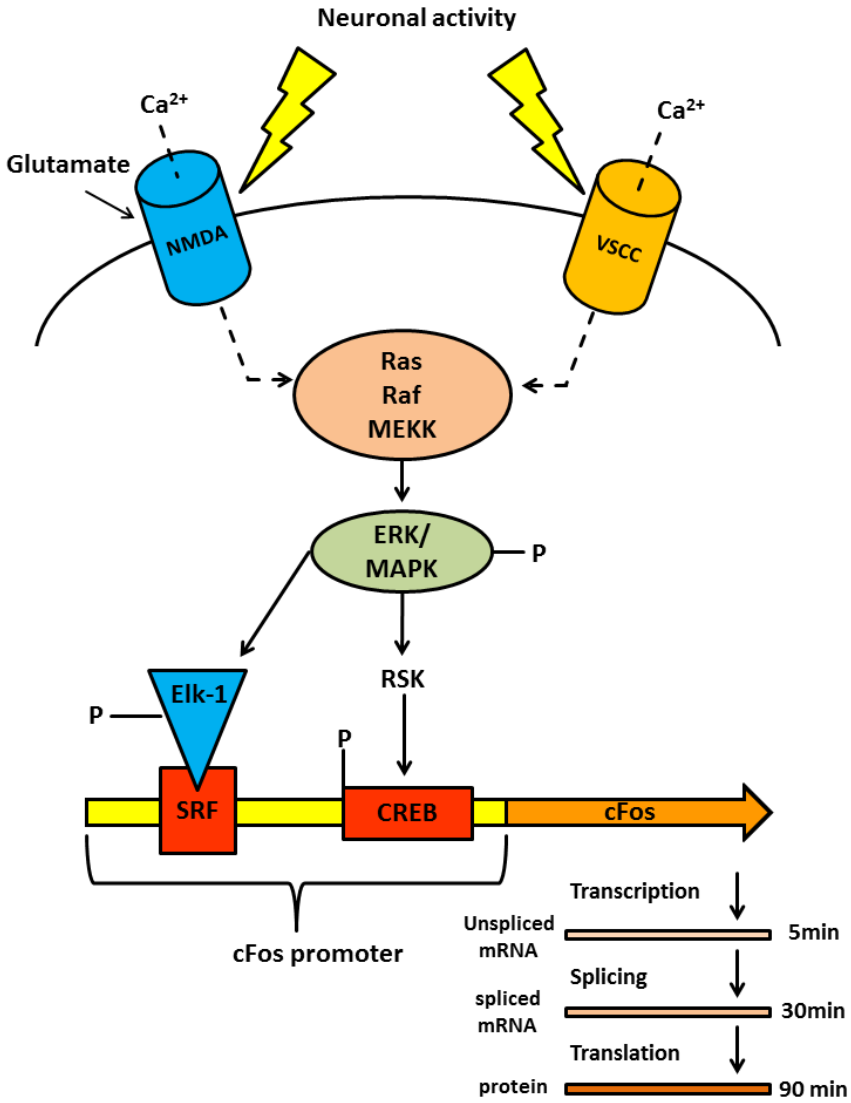

Figure 11: Mechanism of cFos induction. Schematic representation of the induction, transcription and translation of cFos mRNA and protein. Simultaneous activation of N-methyl-D-aspartate (NMDA) receptor and L-type voltage sensitive calcium channels (VSCC) leads to calcium (Ca^{2+}) influx into the cell. As a result the Ras-Raf-MEKK pathway is activated, which leads to phosphorylation of ERK/MAPK. ERK/MAPK activation triggers phosphorylation of Elk-1, which binds to the serum response factor (SRF) in the cFos promoter region. Furthermore ERK/MAPK phosphorylates CREB via ribosomal S6 kinase (RSK). Together the phosphorylated transcription factors Elk-1/SRF and CREB can induce the transcription of the downstream cFos gene. Transcription of the cFos gene results in an unspliced mRNA product, which then undergoes splicing and translation into the cFos protein. cFos is an immediate early gene (IEG), with rapid induction kinetics. Transcription of the unspliced mRNA product takes 5 minutes. 30 minutes after induction the spliced mRNA product reaches its peak expression and 90 minutes following induction the protein product reaches peak expression. Adapted from (Cruz et al., 2015).

1.9 Genetically modified animals

Both rats and mice have been proven to be valuable models in biomedical research. Although both species belong to the order of *Rodentia* (Wilson and Reeder, 2005), multiple differences on the transcriptomic, physiological and behavioral level have been reported (Ellenbroek and Youn, 2016). Between the 1970s and 1980s there was a strong increase in the use of mice in neuroscience research, which coincides with the simultaneous development of genetic manipulation methods in mice (Thomas and Capecchi, 1987). However, especially in the alcohol research field rats seem to be better suited compared to mice, because they show pronounced alcohol deprivation effects and compulsive alcohol drinking patterns, comparable to the human condition. This effect has not been observed in mice (Vengeliene et al., 2014). Furthermore differences in social interaction and impulsive behavior have been demonstrated (Ellenbroek and Youn, 2016). In the meantime genetic manipulation techniques have also been established in rats. Most available transgenic rat lines were generated by DNA microinjection into the pronuclei of fertilized oocytes using Bacterial artificial chromosomes (BAC), which results in a random integration of one or several transgene copies in the host genome of the rat (Cho et al., 2009; Schönig et al., 2012). In the framework of this thesis cFos-LacZ transgenic rats for activity-tagging of cells and a transgenic rat line, expressing the Cre-recombinase enzyme under the control of the CaM-kinase II promoter were used.

1.9.1 cFos-lacZ transgenic rats

The extensive knowledge about the induction mechanisms and expression kinetics of the cFos promoter lead to the development of several cFos-based animal models and molecular methods. The most extensively used cFos promoter-based rat model is the cFos-lacZ transgenic rat, generated by Drs. J. Morgan and T. Curran (St. Jude Children's Hospital, Memphis, TN), expressing the bacterial lacZ gene under cFos promoter control (Kasof et al., 1995). This rat model is a crucial component for the so called Daun02 inactivation method (Koya et al., 2009), which allows to selectively inactivate only cFos expressing neurons in a given brain area. The second component of the Daun02 inactivation method is the inactive prodrug Daun02, which is converted to daunorubicin by ß-galactosidase (lacZ) activity

(Farquhar et al., 2002). Daun02 has no effect on lacZ negative cells, but the conversion into the active compound daunorubicin leads to the inactivation of lacZ positive cells (Santone et al., 1986; Mortensen et al., 1992; Jantas and Lason, 2009; Engeln et al., 2016). The Daun02 inactivation method has been frequently used to identify several neuronal ensembles involved in cocaine, heroin, alcohol and food seeking (Koya et al., 2009; Bossert et al., 2011; Pfarr et al., 2015; Warren et al., 2016).

1.9.2 Cre recombination system

In order to restrict transgene expression or knockdown of genes of interest to certain neuronal cell types, transgenic Cre (cyclization recombination) recombinase driver rat lines in combination with Cre-inducible viral vectors are powerful tools and are frequently used (Weber et al., 2011; Witten et al., 2011; Schönig et al., 2012).

The Cre recombination system consists of the Cre-recombinase enzyme of the P1 bacteriophage (Sternberg et al., 1986; Sauer, 1998) and its 34-base pair (bp) consensus loxP (locus of X-over P1) sequence (Hamilton and Abremski, 1984). The loxP site consists of a 8bp core sequence flanked by two palindromic 13bp sequences. The asymmetric core sequence determines the direction of the loxP site, which determines if the sequence flanked by loxP sites ("floxed") is excised or inverted (Figure 12) (Hoess et al., 1990). The Cre-loxP inversion mechanism is commonly used for Cre-mediated viral transgene expression e.g. using the Double-floxed Inverted Orientation (DIO) system (Saunders et al., 2012). Also the excision mechanism is frequently used in transgenic animal models or viral vectors. Therefore a floxed Stop-casette, carrying a Stop-codon, is excised by Cre-recombination, which enables downstream transgene expression (Ventura et al., 2004; Weber et al., 2011).

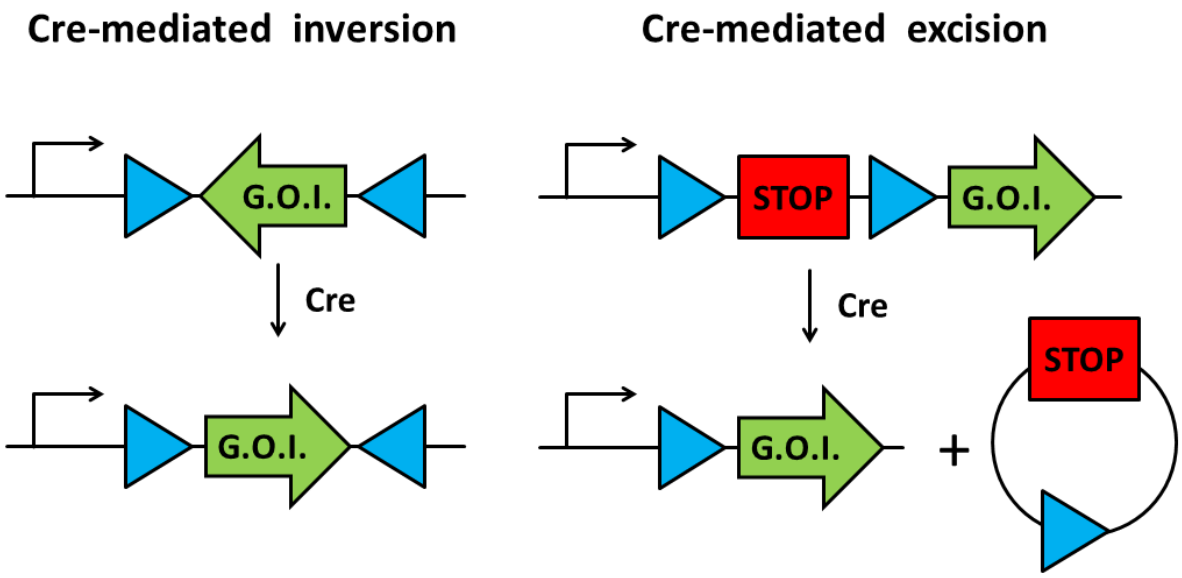

Figure 12: The Cre-loxP system. Depending on the orientation of both loxP recognition sites (blue triangles), Cre-recombinase mediates inversion or excision of the floxed (flanked by two loxP sites) sequence. In case of the frequently used DIO (Double-floxed Inverted Orientation) systems, the gene of interest (G.O.I.) is inserted in the opposite direction of the promoter (black arrow). After Cre-mediated inversion gene expression is possible. The lox-STOP system is using the excision mechanism of the Cre-loxP system. Here, a floxed STOP cassette is located upstream of the G.O.I. After Cre-mediated excision of the floxed STOP-casette, gene expression is possible.

For conditional transgene expression, the tamoxifen inducible Cre-ERT2 has been developed (Feil et al., 1997; Indra et al., 1999). The Cre-ERT2 recombinase is a fusion protein, containing the ligand binding domain of the human estrogen receptor. Cre-ERT2 recombinases can be activated by a synthetic estrogen receptor ligand called tamoxifen (4-hydroxytamoxifen). However, acute tamoxifen treatment has been shown to alter and influence learning behavior in mice (Chen et al., 2002b, a) and has also been shown to have long lasting effects on sexual behavior in adult rats (Csaba and Karabelyos, 2001).

To overcome these negative effects of tamoxifen treatment on behavior, a constitutive tamoxifen-independent Cre-expression system can be used, if no precise time control of transgene expression is required.

1.10 Calcium imaging microendoscopy

With methods like IEG in-situ hybridization (ISH), IEG immunohistochemistry (IHC) or the Daun02 inactivation method, previously activated neurons can only be analyzed post-mortem. The mentioned post-mortem methods have only a poor temporal resolution, which does not allow studying spatial and temporal patterns of neuronal ensemble activity during a certain behavior. In-vivo electrophysiology provides a good temporal resolution of cellular activity but lacks spatial resolution. Therefore, the most appropriate method to detect both spatial and temporal activity patterns is in-vivo calcium imaging (Table 1). Repeated ensemble detection under different behavioral conditions is another advantage of in-vivo calcium imaging over terminal post-mortem methods.

Table 1: Comparison of neuronal ensemble detection methods. Comparison of immediate early gene in-situ hybridization (IEG ISH), immediate early gene immunohistochemistry (IEG IHC), the Daun02 inactivation method, in-vivo electrophysiology and in-vivo calcium imaging. (-) = criterion not fullfilled, (+) = criterion fullfilled, (++) = very good, (+++) = excellent.

Method	In-vivo	Detection of multiple ensembles	Temporal resolution	Spatial resolution
IEG ISH	-	+	+	+++
IEG IHC	-	-	+	+++
Daun02	+	-	+	++
In-vivo e-phys	+	+	+++	+
In-vivo Ca^{2+} imaging	+	+	++	+++

Influx of calcium (Ca^{2+}) ions into the intracellular space induces a large variety of downstream processes in almost every cell type in biological organisms (Berridge et al., 2000). In neurons, an increase in intracellular Ca^{2+} has been reliably shown to regulate immediate early gene (IEG) expression (Figure 11) involved in activity-dependent

restructuring of synapses, regulation of dendritic complexity, synaptic strength, growth factor signaling and memory consolidation (Hagenston and Bading, 2011). Activity-dependent increases in intracellular Ca^{2+} can activate two signaling pathways: the MAP kinase/extracellular signal-regulated kinase (ERK1/2) cascade (Figure 11) and the calcium/calmodulin (CaM) dependent protein kinase pathway (Hardingham et al., 2001). Both pathways result in CREB transcription factor activation and subsequently induce IEG expression. Therefore the influx of Ca^{2+} ions can be used to measure neuronal activity.

1.10.1 Calcium indicators

The two most frequently used classes of calcium indicators are the chemical small molecule calcium indicators and the genetically encoded calcium indicator (GECI) proteins (Grienberger and Konnerth, 2012). Small molecule calcium indicators are chemically engineered fluorophores, which undergo molecular conformational changes upon Ca^{2+} binding, leading to changes in fluorescence intensity (Paredes et al., 2008). For ex-vivo applications chemical calcium indicators (e.g fura-2, fluo and Oregon Green BAPTA) have several advantages compared to GECIs. Chemical indicators cover a broad range of Ca^{2+} affinities, which enables individual adjustments to the respective experimental condition. Furthermore no viral transduction or transfection into the target cells is necessary as membrane-permeable chemical calcium indicators can simply be loaded to the target cells (Takahashi et al., 1999). A disadvantage of chemical calcium indicators is the frequently observed compartmentalization of the indicators to certain parts of the cell, and the clearance of the membrane-permeable indicator during the imaging experiment (Paredes et al., 2008).

GECIs are the most suitable calcium indicators for in-vivo experiments where cell-type specific loading with the calcium indicator (Zariwala et al., 2012) or a specific subcellular localization of the indicator (Mao et al., 2008) is necesary. Furthermore, GECIs enable chronic calcium imaging experiments, because they are not cleared from the target cell but constantly expressed (Huber et al., 2012). There are two major classes of GECIs: those based on Förster resonance energy transfer (FRET) or single fluorophore indicators like the GCaMP family. FRETs consist of two fluorophores and are based on a non-radiative energy transfer between the excited donor fluorophore and an acceptor fluorophore (Jares-Erijman and Jovin, 2003).

Introduction

The GCaMP family is the most frequently used type of single fluorophore GECIs. GCaMPs consist of a circularly permuted enhanced green fluorescent protein (cpEGFP), flanked by the calcium-binding protein calmodulin (CaM) and the M13 domain of a myosin light chain kinase (Nakai et al., 2001). Upon Ca^{2+} binding, the CaM domain undergoes a conformational change and binds to the M13 domain, resulting in an increase in fluorescence intensity (Figure 13) (Nakai et al., 2001; Tian et al., 2009).

Several versions of GCaMP proteins have been developed in the past by mutagenesis of the interface between the cpEGFP and the CaM domain (Akerboom et al., 2012; Chen et al., 2013). The GCaMP6 family is widely used for in-vivo calcium imaging and consists of the following versions: GCaMP6s (slow kinetics), GCaMP6m (medium kinetics) and GCaMP6f (fast kinetics). Generally, the versions with slow kinetics have a higher sensitivity as compared to the versions with fast kinetics (Chen et al., 2013). GCaMP6s produces 10-fold larger signals as compared to GCaMP3 and threefold higher calcium-affinity as compared to GCaMP5G. The intensity of emitted fluorescence of calcium-saturated GCaMP6s is 27% brighter as compared to EGFP. GCaMP6f is one of the fastest GECIs for cytoplasmic calcium imaging in neurons, with similar sensitivity as Oregon Green BAPTA-1-AM (Chen et al., 2013). In the framework of this thesis, the fast version of GCaMP6 was used for in-vivo calcium imaging experiments in freely moving rats.

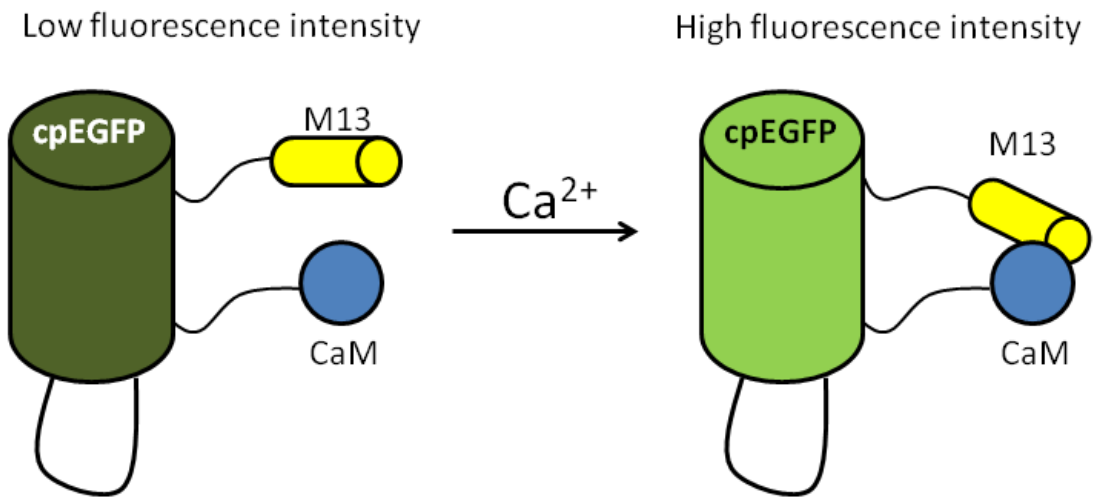

Figure 13: Schematic representation of GCaMP function. The genetically encoded calcium indicator GCaMP was generated by a circularly permutated (cp) EGFP, fused to a calmodulin domain (CaM) and the M13 domain of a myosin light chain kinase. Upon calcium binding the CaM domain undergoes a conformational change and binds to the M13 domain, resulting in an increased fluorescence intensity compared to baseline levels.

1.10.2 Microendoscopy system for in-vivo calcium imaging in freely moving rats

For ex-vivo calcium imaging experiments in cultured neurons or acute brain sections, conventional epifluorescence, confocal or two-photon microscope applications are used. Early methods used for in-vivo calcium imaging required a head-fixation of the animal, which is not compatible with most rodent behavior tasks (Nimmerjahn et al., 2009). In order to perform bulk in-vivo calcium imaging experiments in awake and freely moving rodents, the fiber photometry method can be used (Cui et al., 2013; Gunaydin et al., 2014). For fiber photometry, optical fibers are used to detect bulk calcium signals from GECI labelled cells. However, this approach does not provide single cell resolution.

For in-vivo calcium imaging experiments in freely moving rodents with single cell resolution, the miniscope microendoscopy technique has been developed. The miniscope microendoscopy techniques enable the simultaneous recording of hundreds of neurons. Chronic and repeated recordings of the same field of view can be performed (Ghosh et al., 2011; Ziv et al., 2013; Jennings and Stuber, 2014). All available miniscope systems (Inscopix nVista system, UCLA open source miniscope etc.) have similar underlying construction principles. A fully equipped, small and light-weight miniature epifluorescence microscope with a mass of ~2g can be directly mounted on the animal's head. The miniature epifluorescence microscope consists of a small light-emitting diode (LED) providing the excitation light source. The excitation light beam derived from the LED is collected by a half ball lens and guided through an excitation filter and a dichroic mirror into an objective lens. The emitted light from the calcium sensor is guided through the emission filter, the dichroic mirror and an achromatic lens onto a complementary metal-oxide-semiconductor (CMOS) image sensor (Figure 14A).

For in-vivo calcium imaging of deep brain areas, a gradient refractive index (GRIN) lens can be implanted into the brain, reaching the GECI expressing target cells in the target brain area. The Miniscope can then be mounted onto the animal's head using an implanted baseplate as an anchoring mechanism, ensuring the same field of view during repeated imaging sessions. Excitation and emission light will then be guided through the GRIN relay lens, enabling in-vivo calcium imaging of deep brain areas with single cell resolution (Figure 14B) (Ghosh et al., 2011; Ziv et al., 2013; Jennings and Stuber, 2014; Cai et al., 2016). In the framework of

this thesis, the open source UCLA (University of California) miniscope version was used (www.miniscope.org).

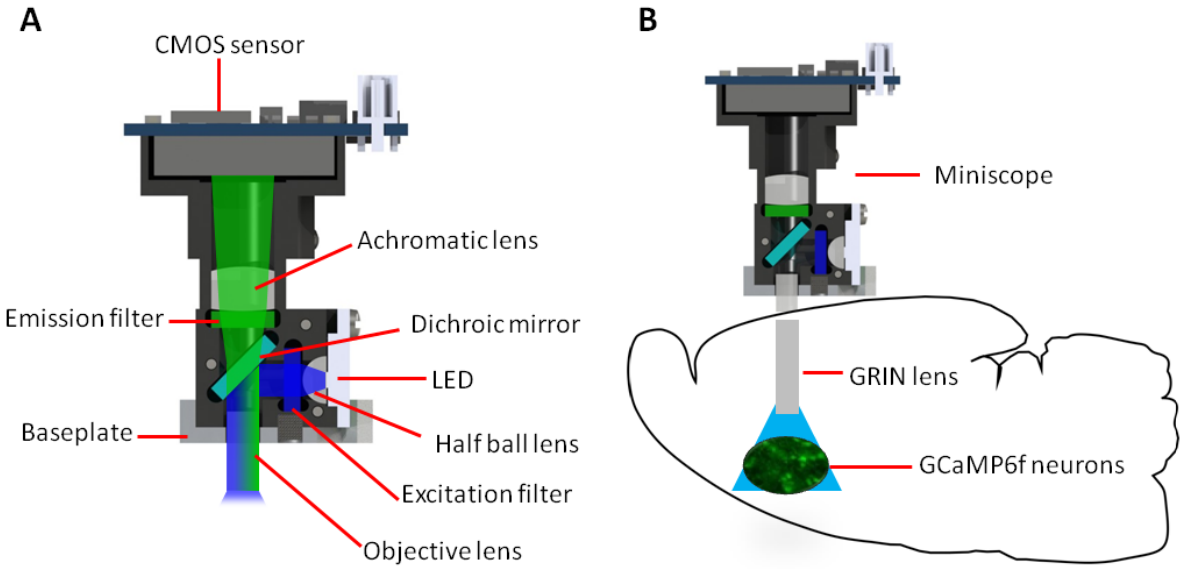

Figure 14: In-vivo calcium imaging using microendoscopy. A) Schematic representation of a head-mountable miniature epifluorescence microscope. Excitation light is generated by a LED and guided into an objective lens through a half ball lens, an excitation filter and a dichroic mirror. Emission light from the calcium indicator is guided though the objective lens, the dichroic mirror, the emission filter and an achromatic lens onto the CMOS image sensor. A baseplate can be fixed on the animal head and serves to anchor the miniature microscope during recordings. Image adapted from www.miniscope.org. **B)** Schematic representation of a miniature epifluorescence microscope mounted onto an animal's head using a baseplate. A gradient index (GRIN) lens is implanted into the brain. Calcium imaging of cell bodies located below the lens can be performed using this configuration.

1.11 Hypothesis and aims

The molecular and cellular mechanisms underlying natural reward and alcohol seeking behavior are not well understood, which importantly contributes to the lack of effective medication for addictive disorders. The medial prefrontal cortex (mPFC) exerts top-down control over reward seeking behavior and executive functions, and alcohol-induced reductions in metabotropic glutamate receptor 2 levels in the infralimbic (IL) part of the mPFC were found to be involved in the control of alcohol seeking behavior. Furthermore, several studies recently identified functional neuronal ensembles in the IL involved in natural and drug reward-seeking. However, the existence of such a neuronal ensemble has not yet been established for alcohol seeking. Thus the following hypotheses will be tested in the framework of this thesis:

Hypothesis 1:

We hypothesize, that neuronal ensembles in the infralimbic cortex participate in the control of alcohol seeking behavior. Furthermore we will test the hypothesis that neuronal ensembles involved in natural reward and drug reward seeking are overlapping in the infralimbic cortex.

Hypothesis 2:

Given the previously observed mGluR2 deficit in thse IL of alcohol dependent subjects, we hypothesize, that a knockdown of this gene in the IL will induce excessive alcohol seeking behavior, as well as impairments in executive functioning.

1.12 Specific aims

To identify cellular and molecular mechanisms in the infralimbic cortex, involved in the control of reward seeking behavior and cognitive flexibility.

Specific Aim 1: To characterize the function and spatial organization of infralimbic neuronal ensembles involved in drug reward and natural reward seeking

Specific Aim 2: To establish the link of IL mGluR2 expression levels in alcohol-seeking behavior and cognitive flexibility

1.13 List of Studies

Study 1: Identification of an infralimbic neuronal ensemble involved in alcohol seeking behavior (Aim 1)

Study 2: Characterization of infralimbic neuronal ensembles involved in alcohol and saccharin seeking behavior (Aim 1)

Study 3: In-vivo calcium imaging of IL neuronal ensembles involved in an operant reward seeking task (Aim 1)

Study 4: The influence of infralimbic mGluR2 expression levels on alcohol seeking behavior (Aim 2)

Study 5: The influence of infralimbic mGluR2 expression levels on cognitive flexibility (Aim 2)

2. Materials and Methods

2.1 Animals

Male **cFos-lacZ** transgenic rats (Kasof et al., 1995; Koya et al., 2009), carrying a cFos-lacZ fusion protein (Schilling et al., 1991) (Figure 15A) and wild type litter mates, bred on a Sprague Dawley genetic background at the Central Institute of Mental Health (CIMH) of Mannheim (Germany), initially weighing 250 - 300g were used for Daun02 inactivation experiments in Study 1. Founder animals were kindly provided by Dr. Bruce T. Hope from the National Institute on Drug Abuse, Baltimore, USA. Breeding of the animals was performed by Valentina Vengeliene and Sabrina Koch at the CIMH.

Male **CAG-lacZ** transgenic rats (Weber et al., 2011) (Figure 15B) bred on a Sprague Dawley genetic background at the Central Institute of Mental Health of Mannheim (Germany), initially weighing 250 - 300g were used for Daun02 inactivation experiments in Study 1. The animals were generated and provided by Dr. Kai Schönig and Prof. Dusan Bartsch from the department of Molecular Biology at the Central Institute of Mental Health of Mannheim.

Male **Wistar rats** (Charles River Germany) initially weighing 250 - 300g were used for the ethanol and saccharin seeking behavior, the retrograde tracing and the double cFos fluorescent in-situ hybridization experiments of Study 2 and in-vivo calcium imaging experiments in Study 3. Furthermore male Wistar rats were used in Study 4 to test the effect of a general mGluR2 knockdown on alcohol seeking behavior. In Study 5 male Wistar rats were used to perform attentional set shift experiments after chronic intermittent alcohol exposure and for the general mGluR2 knockdown experiment.

Male **Indiana alcohol preferring (P) and non-preferring (NP) rats** (Lumeng et al., 1977) were obtained from the Animal Production Core facility at the Indiana Alcohol Research Center, Indiana University, USA. The animals had an initial weight of 250 - 300g and were used for attentional set shift experiments in Study 5.

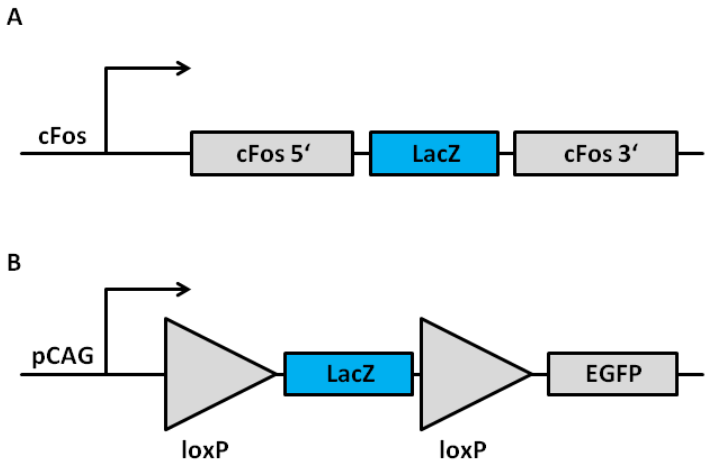

Figure 15: Schematic representation of cFos-LacZ and CAG-LacZ transgenes. A) A fusion protein of cFos and lacZ is expressed under control of the cFos promoter. The LacZ gene contains a stop codon, preventing expression of the C-terminal negative regulatory elements of the cFos coding sequence. Thus endogenous cFos expression is not affected. **B)** The CAG-LacZ transgenic rat line is a double reporter line. Without Cre-recombination LacZ expression is driven by the pCAG promoter. In the presence of Cre recombinase, the floxed LacZ gene would be excised and EGFP expression would be driven by the pCAG promoter.

Male **CamKII-Cre transgenic rats** (Figure 16), bred on a Sprague-Dawley genetic background were used for CamKII-targeted mGluR2 knockdown experiments in Study 4 and Study 5. These animals are characterized by a constitutive expression of Cre-recombinase under the control of the CamKII promoter. The animals had an initial weight of 250 - 300g and were generated using a random integration BAC-approach (Casanova et al., 2001; Schönig et al., 2012) and provided by Dr. Kai Schönig and Prof. Dusan Bartsch from the department of Molecular Biology at the Central Institute of Mental Health of Mannheim (Germany).

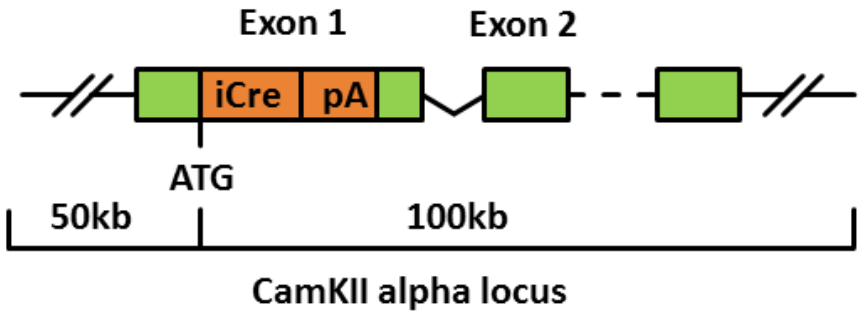

Figure 16: BAC construct for neuronal specific Cre-expression in trasngenic rats. A CamKII-Cre bacterial artificial chromosome was used to generate a transgenic rat based on a Sprague-Dawley background, expressing Cre-recombinase constitutively under control of the CamKII promoter. Transgenic CamKII-Cre rats were generated and provided by Dr. Kai Schönig and Prof. Dusan Bartsch based on (Casanova et al., 2001).

All animals were housed in groups of 4 or in pairs (Study 3) under a reversed 12h light-dark cycle (lights on at 6am) for alcohol and saccharin operant experiments and under a normal 12h light dark cycle (lights off at 6am) for attentional set shift experiments. CAG-LacZ rats and cFos-LacZ rats as well as wild type littermates from Study 1 were single housed after guide cannula implantation. Generally rat chow and water were available *ad libitum* with the following exceptions: 18h water deprivation during the first three days of operant conditioning for saccharin or ethanol and food restriction during attentional set shift experiments. All animal experiments including behavior experiments and surgical procedures were performed in the animal facility of the Central Institute of Mental Health in Mannheim. Operant behavior experiments and chronic intermittent alcohol vapor exposure was performed during the dark phase for 5 days per week. Attentional set shifting task experiments were conducted in the light phase for 5 days per week. Animal experiments were conducted in accordance with the European Union guidelines for the care and use of laboratory animals and were approved by the local animal care committee (Regierungspräsidium Karlsruhe, Karlsruhe,Germany).

2.2 General experimental designs

2.2.1 Study 1: Identification of an infralimbic neuronal ensemble involved in alcohol seeking behavior

For neuronal ensemble inactivation (Experiment 1), male cFos-LacZ rats were trained on an operant alcohol self-administration task, followed by extinction training and guide cannula implantation into the infralimbic cortex (IL). Next, the animals were tested on their cue-induced reinstatement performance, followed by Daun02 infusions through the guide cannula. Following this, the animals were again tested on their cue-induced reinstatement performance after Daun02 inactivation.

The above described experiment was repeated with male CAG-LacZ rats (Experiment 2), for a general inactivation of the IL and with wild type littermates (Experiment 3) of the cFos-LacZ rats in order to control for unspecific effects of Daun02 on operant alcohol seeking behavior.

For Experiment 4, male cFos-LacZ rats were trained on an operant alcohol seeking task, followed by extinction training and guide cannula implantation into the prelimbic cortex (PL). Next, the animals were tested on their cue-induced reinstatement performance, followed by Daun02 infusions through the guide cannula. Following this, the animals were again tested on their cue-induced reinstatement performance after Daun02 inactivation (Figure 17).

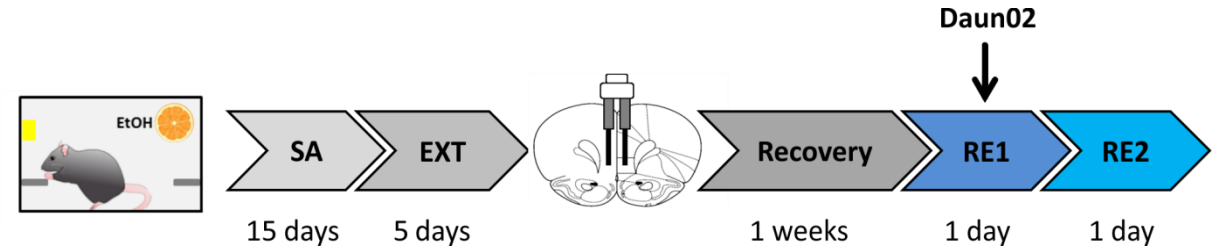

Figure 17: Experimental timeline for Daun02 inactivation experiments (Study 1). The animals were first trained to self-administer a 10% EtOH solution for 3 weeks. Next the animals underwent extinction training, followed by guide cannula implantation to target the infralimbic (IL) cortex. After 1 week of recovery, the animals were tested in a cue-induced reinstatement (RE1) of alcohol seeking. 90 minutes after RE1, the animals received Daun02 or vehicle infusions into the IL through the guide cannula. After three days, the animals were again tested on their cue-induced reinstatement (RE2) performance.

2.2.2 Study 2: Characterization of infralimbic neuronal ensembles involved in alcohol and saccharin seeking behavior

First, the behavioral protocol for a two-reward operant seeking task was established and validated using male Wistar rats. The animals were trained to self-administer a 10% ethanol solution or a sweet saccharin solution. Each reward was paired with a different set of visual and olfactory cues. During the self-administration (SA) training, the animals' motivation for each reward was tested by breakpoint analysis under a progressive ratio (PR) schedule. After reaching a stable baseline, the animals underwent extinction training followed by counterbalanced cue-induced reinstatement sessions for each reward (Figure 18A).

In a second experiment the previously established two-reward operant task was used to identify potential differences in infralimbic cortex (IL) ensemble size for EtOH and saccharin, and to identify potential differences in projection targets of these activated neurons. Therefore a second batch of Wistar rats was trained on the previously established behavior task. After the first counterbalanced cue-induced reinstatement sessions for both rewards, the animals received unilateral retrograde tracer injections into the IL, prelimbic cortex (PL), nucleus accumbens (NAc) and ventral tegmental area (VTA). After 5 days of recovery, the animals underwent either cue-induced reinstatement for EtOH or saccharin and were perfused in order to perform cFos immunohistochemistry and co-localization analysis with the respective retrograde tracer signal in the IL (Figure 18B).

A third batch of Wistar rats was trained on the previously described task, in order to identify EtOH and saccharin cue-responsive neurons in the IL of the same animal. After self-administration training, progressive ratio test, extinction and the first counterbalanced cue-induced reinstatement sessions for both rewards the animals underwent additional two cue-induced reinstatement sessions of 5 minutes length, separated by 30 mins. These animals were decapitated immediately after the final cue-induced reinstatement session and used for double cFos fluorescent *in-situ* hybridization for co-localization analysis of EtOH and saccharin cue-responsive neurons in the IL (Figure 18C).

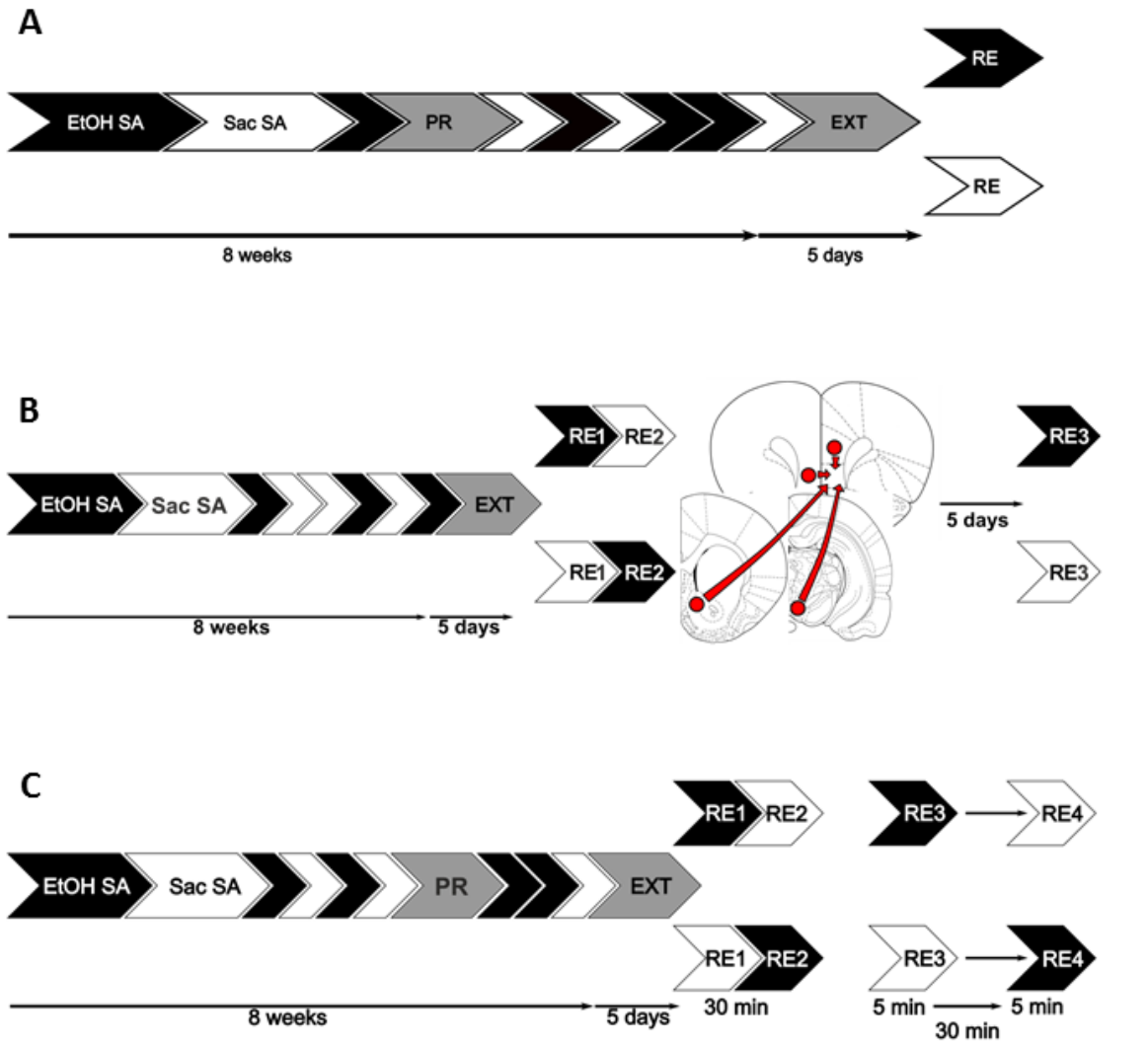

Figure 18: Experimental timelines for behavioral experiments in Study 2. A) Set-up of two-reward operant conditioning task. Timeline for ethanol (EtOH) and saccharin self-administration (SA), progressive ratio test (PR), extinction training (EXT) and counterbalanced cue-induced reinstatement (RE) of ethanol and saccharin seeking. **B)** Timeline for behavioral experiments to determine the size and projection targets of IL neuronal ensembles involved in EtOH (white) and saccharin (black) seeking. Experimental timeline for self-administration (SA), extinction (EXT), counterbalanced cue-induced reinstatement (RE1+2) of ethanol and saccharin seeking, followed by retrograde tracer injections and the final cue-induced reinstatement for either ethanol or saccharin (RE3). **C)** Timeline for behavioral experiments to identify IL ensembles involved in ethanol or saccharin seeking in the same animal. Experimental timeline for ethanol and saccharin self-administration (SA), extinction (EXT), and counterbalanced cued reinstatement sessions (RE1+2) and a final session (RE3+4) for activation of ethanol and saccharin ensembles in the same animal.

2.2.3 Study 3: In-vivo calcium imaging of IL neuronal ensembles involved in an operant reward seeking task

First, 8 week old Wistar rats were allowed to habituate to the animal facility for one week. Next, the animals received GCaMP6f AAV injections into the right hemisphere of the IL, followed by GRIN lens implantation. The animals were allowed to recover from surgery for one week, followed by operant self-administration training. After three weeks of operant self-administration training, baseplates were secured to the animals' impants for in-vivo calcium imaging experiments. Next, the animals were habituated to the miniscope mounting procedure, followed by self-administration sessions combined with simultaneous calcium-imaging. After reaching a stable self-administration baseline, the animals underwent extinction training combined with in-vivo calcium imaging recordings. After reaching the extinction criterion of <10% of baseline activity, the animals were tested on their cue-induced reinstatement performance, with simultaneous calcium-imaging (Figure 19).

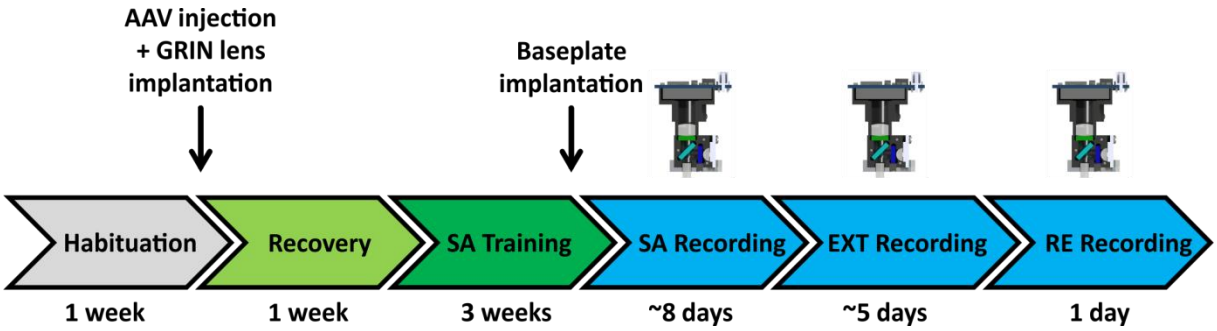

Figure 19: Experimental timeline for in-vivo calcium imaging experiments (Study 3). After 1 week of habituation the animals received GCaMP6f AAV injections into the right hemisphere of the IL, followed by GRIN lens implantation. After 1 week of recovery, the animals were trained to self-administer (SA) a 0.2% saccharin solution for 3 weeks. Next, a baseplate was fixed to the GRIN lens implant, enabling recording of self-administration, extinction (EXT) and cue-induced reinstatement (RE) operant sessions.

2.2.4 Study 4: The influence of infralimbic mGluR2 expression levels on alcohol seeking behavior

First, male Wistar rats were trained to self-administer (SA) and associate a 10% ethanol solution with a specific set of visual and olfactory cues. Next, all animals underwent extinction (EXT) training. Following extinction training the animals received bilateral

injections of either a general mGluR2 knockdown AAV into the IL, or a control AAV. After a recovery period of 4 weeks, the animals were tested for their cue-induced reinstatement of alcohol seeking (Figure 20A).

In a second experiment, a batch of male CamKII-Cre transgenic rats was also trained to self-administer a 10% EtOH solution and underwent extinction training, as well as a cue-induced reinstatement session (RE1) prior to the AAV injection. Next, the animals received either a floxed mGluR2 knockdown AAV for cell-type specific knockdown or a control AAV. After a recovery period of 4 weeks, the animals were again tested for their cue-induced reinstatement (RE2) of alcohol seeking. (Figure 20B).

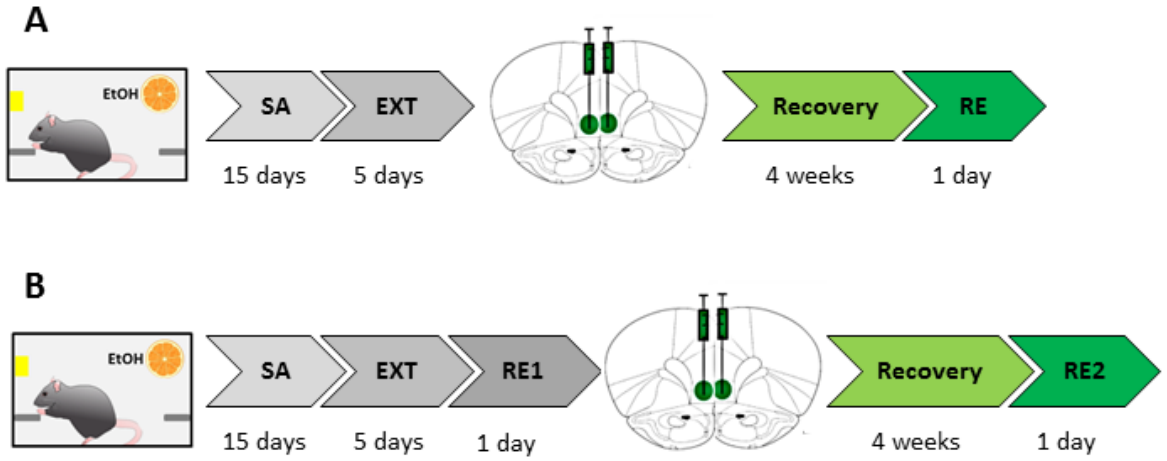

Figure 20: Timelines for behavioral experiments in Study 4. A) Experimental timeline for general mGluR2 knockdown experiment. 15 days of operant alcohol self-administration (SA) were followed by 5 days of extinction (EXT) training. After extinction the animals received bilateral control or knockdown AAV injections. Following a recovery period of 4 weeks, the animals were tested on their cue-induced reinstatement (RE) performance. **B)** Experimental timeline for CamKII-Cre targeted mGluR2 knockdown. 15 days of operant alcohol self-administration (SA) were followed by 5 days of extinction (EXT) training and one cue-induced reinstatement of alcohol seeking session (RE1). Next, the animals received bilateral control or knockdown AAV injections. Following a recovery period of 4 weeks, the animals were again tested on their cue-induced reinstatement (RE2) performance.

2.2.5 Study 5: The influence of infralimbic mGluR2 expression levels on cognitive flexibility

A batch of Indiana alcohol preferring (P) and non-preferring (NP) rats was tested on their ASST performance. Furthermore the Wistar rats and CamKII-Cre rats from Study 4, injected

with a general and Cre-inducible mGluR2 knockdown AAV respectively, were also tested on their ASST performance as part of Study 5.

2.3 Behavioral procedures

2.3.1 Operant chamber experiments

2.3.1.1 Operant self-administration apparatus

Standard operant chambers (Med Associates, Fairfax, VT, USA), enclosed in sound attenuating cubicles were used for operant conditioning and reward-seeking experiments in Study 1. Each chamber was equipped with a retractable response lever on each side panel, as well as a yellow stimulus light and a liquid receptacle on each side panel. Responses at the appropriate lever (active lever) activated a syringe pump, which lead to reward delivery (~30µl liquid reward) into the liquid receptacle next to the lever and cue-light activation above the respective lever. Recording of lever responses, fluid delivery and cue-light activation was controlled by an IBM-compatible computer.

2.3.1.2 Operant alcohol self-administration and cue conditioning

Study 1:

Daily 30 minutes self-administration sessions were performed 3 hours after beginning of the dark phase of the 12h dark/light cycle. The animals were trained to self-administer a 10% (v/v) alcohol solution under a fixed ratio 1 (FR1) schedule using a saccharin fading procedure adapted from (Tolliver et al., 1988). During the first three days of self-administration training, the animals were kept water deprived for 20h per day, to motivate them to search for the liquid reward (Tabbara et al., 2016). During the next three days, the animals underwent the same procedure without water deprivation. Following acquisition of saccharin-reinforced responding, rats were trained to self-administer ethanol. In the next three sessions, responses at the left lever resulted in the delivery of 5% (v/v) ethanol plus 0.2% saccharin solution.

Responses at the right lever were recorded but had no programmed consequences. For the following sessions the concentration of ethanol was increased first to 8% and then to 10% (v/v), and the concentration of saccharin was decreased until saccharin was completely eliminated from the ethanol solution. Next, the animals were trained to associate a set of visual and olfactory cues with the availability of the alcohol reward, which is a well established method for alcohol self-administration (Ciccocioppo et al., 2002; Ciccocioppo et al., 2003; Meinhardt et al., 2013). An orange odor (orange oleum aurantii dulcis g420, Caelo, Hilden, Germany) served as an olfactory contextual stimulus for ethanol and was generated by application of six drops of orange oil onto the bedding material in the operant chamber before the start of each session. As a discrete, visual stimulus a 5 s blinking light was used, which was activated after a response at the active lever (left lever) and was therefore directly connected to alcohol availability. The 5 s period served as a "time out", during which responses were recorded, but did not lead to reward delivery. After completion of 10 cue-conditioning sessions with both the olfactory and visual cues, the animals were ranked based on their self-administration baseline performance (mean performance over the last six training sessions) and equally divided into two groups.

Study 2:

First, all animals were trained to self-administer a 10% (v/v) ethanol (EtOH) reward in daily 30min operant sessions, without prior sucrose- (Tolliver et al., 1988) or saccharin (Meinhardt et al., 2013; Pfarr et al., 2015) fading procedures. Two natural odors were used as contextual, olfactory cues for ethanol (orange oleum aurantii dulcis g420, Caelo, Hilden, Germany) and saccharin (lemon grass oil w861, Caelo, Hilden, Germany). The animals underwent nine self-administration sessions for the ethanol reward, during which only the active lever was presented. Following this also the inactive lever was introduced during the next four training sessions. Thereafter the same procedure was repeated for the saccharin-reward (Figure 18A, B, C). The concentration of the saccharin solution was adjusted to match the response rate for the 10% EtOH solution. The saccharin concentration for experiment 1 (Figure 18A) was 0.04% (w/v), for experiment 2 (Figure 18B) was 0.08% (w/v) and for experiment 3 (Figure 18C) was 0.025% (w/v). After acquisition of EtOH and saccharin self-administration, the animals underwent eight randomized concurrent self-administration (SA) sessions for each

reward, to obtain a stable baseline for each reward. The baseline was calculated as the mean over the last three SA sessions for each reward.

Study 3:

After AAV injection and GRIN lens implantation, the animals were trained to self-administer a 0.2% saccharin solution. The animals were trained in standard operant chambers (Med Associates, Fairfax, VT, USA). Active lever presses (right lever) activated the cue-light located above the right lever for 5 sec. However, there was no contextual odor cue presented. The animals underwent self-administration training for three weeks. After the baseplate surgery, the animals underwent further self-administration sessions in combination with miniscope calcium imaging recordings, using operant chambers with large liquid receptacle entry ports (CT-ENV-202M-S-6.0, Med Associates, Fairfax, VT, USA).

Study 4:

Operant EtOH self-administration was performed as described in Study 1. However, no saccharin fading procedure was used.

2.3.1.3 Progressive ratio test

After acquisition of self-administration for each reward, the animals from Study 2 were tested for their motivation to obtain each reward using a progressive ratio (PR) schedule (Figure 18A + C). Each animal underwent two 30min counterbalanced PR sessions, to test its' motivation to obtain each reward. During the PR test, the animals had to make an increasing number of lever presses during one trial (step size 2: 1, 2, 4, 6, 8, 10, 12, 14…) in order to obtain one drop (~30µl) of reward solution (Hodos, 1961). If an animal stopped responding for more than 2 minutes, the respective trial was aborted. The highest completed ratio of lever presses during the 30min PR session was used to calculate the breakpoint (Richardson and Roberts, 1996).

2.3.1.4 Extinction training

Study 1:

The animals underwent 30 minute extinction sessions for four days in a row. The animals reached the extinction criterion of <10 active lever presses or <25% of baseline activity at the previously active lever per session. During extinction sessions, both response levers were presented, without presentation of the contextual or visual conditioned cues. Responses at the previously active lever activated the syringe pump but did not result in reward delivery or presentation of the discrete CS (blinking light). After the last extinction session, all animals underwent guide cannulation surgery.

Study 2 - 4:

The animals underwent daily 30min extinction sessions for both rewards. Extinction training was performed for five days, which was sufficient to reach the extinction criterion of < 10% of baseline activity at the active lever per session.

2.3.1.5 Cue-induced reinstatement of alcohol seeking

Study 1:

During the 30 minute cue-induced reinstatement sessions, the animals were presented with the olfactory orange odor cue. Active lever presses activated the visual blinking light stimulus, however active lever presses did not lead to reward delivery. Ninety minutes after the beginning of the first cue-induced reinstatement session, the animals received their respective microinfusions (Daun02 or vehicle) through the implanted guide cannulae targeting the infralimbic cortex (Experiments 1-3) or prelimbic cortex (Experiment 4). Two animals from Experiment 1 were killed to perform X-gal immunohistochemistry after the second cue-induced reinstatement session. The remaining animals from Experiment 1 were subjected to repeated cue-induced reinstatement sessions, a well established procedure for alcohol reinstatement tests (Ciccocioppo et al., 2006; Cannella et al., 2009). Between repeated cue-induced reinstatement sessions no extinction sessions were performed.

Study 2:

In all three experiments from Study 2 the animals underwent counterbalanced cue-induced reinstatement sessions for each reward (Figure 18A, B and C). Next, the animals underwent further cue-induced reinstatement sessions, without further training or extinction sessions. The last counterbalanced cue-induced reinstatement sessions of experiment 3 were only 5 min long and separated by 30min (Figure 18C).

Study 3:

During 30min cue-induced reinstatement sessions, only the light cue was presented.

Study 4:

Cue-induced reinstatement as described under Study 1

2.3.1.6 Stress-induced reinstatement of alcohol seeking

A footshock protocol adapted from (Liu and Weiss, 2002) was used for stress-induced reinstatement of alcohol seeking in Study 1. Footshocks were delivered in a different kind of operant chamber (Imetronic, Pessac, France), environmentally distinct from the training and reinstatement operant chambers (Med Associates). After the last cue-induced reinstatement session, the animals underwent 5 days of extinction training. Prior to each extinction session, the animals were habituated to the Imetronic operant chambers for 10 minutes without the presentation of cues or response levers. After 10 minutes of habituation the animals were moved to the Med Associated operant chambers for extinction training (as described above). On the day of stress-induced reinstatement, the animals were placed in the Imetronic operant chambers for 10 minutes and received variable intermittent footshocks according to the schedule published by Liu and Weiss (2002). Footshock settings were 0.5 mA, 0.5 ms duration, 40 s mean inter shock interval with a range from 10 to 70 s. The shock was delivered through a scrambler to the stainless steel grid floor of the Imetronic chambers. After

the 10 minute variable intermittent footshock procedure the animals were immediately moved to the Med Associates operant chambers. For the stress-induced reinstatement test, the same settings as for extinction training were used, meaning no cue presentation and no reward delivery.

2.3.2 Attentional set shifting task (Study 5)

2.3.2.1 Test apparatus

The test apparatus was made of dark grey PVC consisting of a small compartment (20 cm x 40cm x 40 cm) adjacent to the test compartment (40 cm x 50 cm x 40 cm). The two compartments were separated by a sliding door (width 20 cm). Two small ceramic bowls (diameter 7 cm, depth 4 cm) were positioned into the test compartment 16 cm apart from each other, separated by a divider. The two bowls were filled with different digging materials and/or were differently scented. A casein pellet (Bio Serve Dustless Precision Pellets, Bilaney, Kent, UK) served as a reward and was deeply buried in one of the bowls. Rats were trained to dig in the bowl to retrieve the reward. The presence or absence of the reward pellet in the digging bowl was indicated by either an olfactory (odor) or a visual-tactile cue (shape and tactile quality of digging medium) (Klugmann et al., 2011).

2.3.2.2 Habituation procedure

Animals were familiarized with the food reward, the ceramic bowl and the different digging materials in their home cage prior to testing. During 1-2 nights prior to the test, the pots were filled with home cage bedding and several casein pellets were presented at the top of the bedding as well as deeply buried within the bedding. The pots were rebaited regularly and left in the home cage overnight. In the following night the digging media used for the pretraining period, simple and compound discrimination tasks were baited and equally placed in the home cage. On the second day of habituation two familiar animals were placed into the test apparatus and were allowed to explore it freely for 15 min. On the third day of habituation each rat was placed into the test apparatus individually for another 15min habituation period.

During the entire habituation and testing period the animals were maintained on approximately 90% of their body weight (12g/rat/day). Food restriction started one week prior to testing.

2.3.2.3 Attentional set shifting test procedure

The testing procedure was adapted from (Birrell and Brown, 2000; Klugmann et al., 2011). After habituation all animals underwent a pretraining schedule. Therefore the animals had to retrieve the reward from empty pots and subsequently from pots filled with digging medium. First, the reward was placed on top of the digging medium and was subsequently buried deeper into the medium in further trials. Each trial within the pretraining schedule was repeated until the reward was retrieved. The rats had to retrieve the pellet five times within two minutes followed by four pellet retrievals within one minute. As soon as the rat retrieved the reward pellet or the trial time expired, the animal was placed back into the starting area. The pots were rebaited during the inter-trial-interval (ITI, 30s). During this time the rat had to wait inside the starting area until the sliding door was lifted for the next trial. The digging medium from the pretraining was not used again in the further testing procedure.

Eight common spices and media were used for all discrimination tasks, which are listed in Table 2. The digging media were intermixed with powdered casein pellets to avoid olfactory detection of the pellet in the bowl. In all testing sessions a criterion of six consecutive correct trials was used for successful learning (trials to criterion).

Table 2: Examples of odor-medium pairs used for ASST

Digging medium	Digging medium	Odor 1	Odor 2
Seramis			
Colored silica sand	Hamster bedding	Cumin	Capsicum
Beech chipping	Rough stones	Nutmeg	Basil
Straw pellets	Pine bark	Thyme	Dill
Cork granules	Black silica sand	Rosemary	Curcuma

During the ASST the animals were tested in the following sub tasks:

Simple Discrimination (SD):

Two bowls containing different media but scented with the same odor were presented to each rat. The visual/tactile stimulus indicated the position of the reward (Medium 1 (M1)).

Compound Discrimination (CD):

For the compound discrimination an additional odor was introduced and used together with the two previously used media and the previously used odor. The previously baited digging medium used during SD (M1) also indicated the location of the reward during CD, independent from the presented odors.

Compound Discrimination reversal (CDrev):

The previously learned rule was reversed. The previously baited medium is not baited, but the second medium instead (M2).

Compound Discrimination repetition (CDrep): A repetition test of CDrev.

Intradimensional shift (IDS):

Introduction of a new set of complex stimuli. The animals had to discriminate the baited from the unbaited bowl by using the same perceptual dimension (digging medium) as in the previous testing.

Intradimensional shift 2 (IDS2): Repetition of IDS with new sets of stimuli.

Extradimensional shift (EDS):

A new set of stimuli was introduced. However, now the previously irrelevant dimension predicted the reward. Therefore not the type of digging material predicted the reward but the odor was relevant to obtain the pellet.

If an animal stopped responding for several trials during a test session it was returned to the homecage for up to 1h before resuming the test again. In this case, the sum of the number of trials was taken for analysis.

2.4 Surgical procedures

2.4.1 Guide cannula implantation

The animals from Study 1 were anesthetized with isoflurane and fixed in a stereotaxic frame (David Kopf Instruments, Tujunga, CA, USA). A single double-barreled guide cannula (22 gauge; Plastics One) was implanted using the following stereotaxic coordinates anterior-posterior (AP): +3.2 mm, (medial-lateral) ML: ±0.5 mm for each cannula and dorsal-ventral (DV): −2.8 relative to bregma and midline as illustrated in Figure 21 (Paxinos and Watson, 1998). Obturators were fixed to the guide cannula throughout the experiment. Following surgery, the animals were kept single housed to prevent possible damage to the cannula implant. The animals were allowed to recover for 7 days before further behavioral testing.

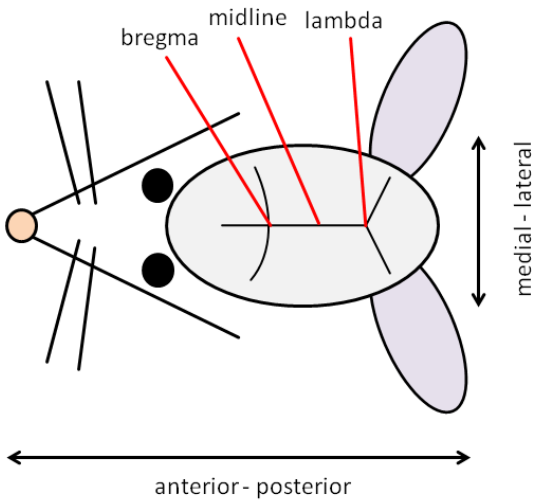

Figure 21: Schematic representation of bregma, midline and the lambda coordinate on the rat skull.

2.4.1.1 Guide cannula microinfusions

Double-barreled injector needles (28 gauge, Plastics One) were connected to polyethylene tubing, attached to a Hamilton syringe, fitted into a syringe infusion pump (PHD 2000, Harvard Apparatus, Holliston, USA). The injector needles extended 3 mm beyond the end of the cannula to target the infralimbic cortex (IL) and 1.2 mm beyond the end of the cannula to target the prelimbic cortex (PL). Ninety minutes after the start of the first cue-induced

reinstatement session, half of the animals received 2µg Daun02 infusions (volume: 0.5µl), per hemisphere and the other half of the animals received vehicle infusions (5% DMSO and 5% Tween 80 in 1X PBS). Infusion speed was 0.25µl/min (Koya et al., 2009) and injector needles were kept in place for an additional 1 minute before the animals were placed back into their homecages for three days.

2.4.2 Stereotaxic injections

In Study 1, three CAG-lacZ rats were injected with 2 µg Daun02 in the IL of one hemisphere and 2 µg Daun02 + 80 ng of the pan caspase inhibitor *N*-benzyloxycarbonyl-Val-Ala-Asp-fluoromethyl ketone (Z-VAD-FMK Promega, Mannheim, Germany; solved in 1× PBS containing 2% DMSO) in the other hemisphere. Another three CAG-lacZ rats were injected with Daun02 vehicle in the IL of one hemisphere and vehicle for both drugs in the other hemisphere. Rats were anesthetized, placed into a Kopf stereotaxic frame, and 1µl of the respective solutions was injected, using the coordinates: AP: + 3.2 mm, ML: ± 0.6 mm, DV: −5.2 relative to bregma and midline (Paxinos and Watson, 1998).

The Wistar rats from experiment 2 (Study 2) received unilateral stereotaxic injections with the retrograde cholera toxin B (CTB) tracer coupled to fluorescent Alexa488 and Alexa647 dyes (Thermo Fisher, Darmstadt, Germany). The animals were anesthetized with isoflurane and fixed in a stereotaxic frame (David Kopf Instruments, Tujunga, CA, USA). Approximately 1µl of CTB solution (1mg/ml in PBS) was injected into the IL using glass micropipettes (BLAUBRAND® intraMARK, Brand, Wertheim, Germany). The injection coordinates were determined using the Paxinos and Watson rat brain atlas and calculated from the bregma and midline: prelimbic cortex (PL): anterior-posterior (AP): +3mm, medial-lateral (ML): ±0.5mm, dorsal-ventral (DV): – 4mm; infralimbic cortex (IL): AP: +3mm, ML: ±0.5mm, DV: -5.5mm; nucleus accumbens (NAc): AP: +1.6mm, ML: ± 0.9mm, DV: -7.5mm; ventral tegmental area (VTA): AP: -5.3mm, ML: ± 0.8mm, DV: -9.5mm. The animals quickly recovered from anesthesia and were further kept in groups of 4 for 5 days, before further behavioral testing.

The Wistar rats from experiment 1 (Study 4) received bilateral IL injections of either 0.5µl general knockdown AAV or universal control AAV. The injection coordinates were

determined using the Paxinos and Watson rat brain atlas and calculated from the bregma and midline: anterior-posterior: +2.9, medial-lateral: ±0.5, dorsal-ventral: -5.1. After the surgery, the animals were kept in groups of four and allowed to recover from surgery for 4 weeks, before further behavioral testing.

2.4.3 Stereotaxic AAV injection and GRIN lens implantation (Study 3)

A batch of eight week old male Wistar rats (n=8) received unilateral IL injections of AAV1.Syn.GCaMP6f.WPRE.SV40 (AV-1-PV2822, U Penn Vector Core, Pennsylvania, USA). The animals were anesthetized with isoflurane and fixed in a stereotaxic frame (David Kopf Instruments, Tujunga, CA, USA). Approximately 1µl of a 1:20 AAV dilution was injected into the IL of the right hemisphere using glass micropipettes (BLAUBRAND® intraMARK, Brand, Wertheim, Germany). Next, three self-tapping stainless steel bone screws (Fine Science Tools, Heidelberg, Germany) were fixed to the skull. A modified linear actuator (Luigs & Neumann, Ratingen, Germany; modified by Ivo Sonntag from the Institute of Anatomy and Cell Biology at Heidelberg University) was controlled by Pronterface 3D software (Printrun, created by Kliment Yanev) and used for slow insertion (~ 300 µm/min) of an optic glass fiber (127µm diameter) into the brain. This step served to create a path for the GRIN lens implantation. Next, the GRIN lens (1.0 mm diameter, ~9.0 mm length, 1050-002177, Insopix, Palo Alto, CA, USA) was slowly inserted using the linear actuator. When fully inserted into the target position, the lens was secured to the skull using Surgibond tissue adhesive (190740, Praxisdienst, Longuich, Germany). Next, the skull surface was pre-treated with the OptiBond™ FL Kit (Kerr, Orange, CA, USA) according to the manufacturer's instructions, in order to improve adhesion of the implant to the skull. After preparation of the skull surface a stable implant was created by surrounding the GRIN lens with black dental cement (Contemporary Ortho-Jet™, black, Lang Dental, Wheeling, USA).

The injection coordinates were determined using the Paxinos and Watson rat brain atlas and calculated as distance in mm from bregma and midline: anterior-posterior: +3.0, medial-lateral: ±0.5, dorsal-ventral: -5.0. The priming glass fiber and the GRIN lens were inserted to the following coordinates: +3.0, medial-lateral: ±0.5, dorsal-ventral: -4.7. After the surgery,

the animals were housed in pairs and allowed to recover from surgery for 1 week, before behavioral training.

2.4.4 Baseplate surgery (Study 3)

The baseplate serves as an anchor for the miniscope and therefore has to be permanently secured to the skull above the GRIN lens implant. Therefore, the previously implanted GRIN lens had to be exposed and cleaned using lens paper and acetone. Next, the baseplate was fixed to a miniscope. Both were fixed to a stereotactic arm using a gripper tool (Insopix, Palo Alto, CA, USA). Then, the excitation LED and imaging settings of the miniscope were adjusted using the UCLA Miniscope control software (Cai et al., 2016). After correct positioning of the miniscope above the implanted GRIN lens, when GCaMP6f expressing cells were clearly visible and in focus, the baseplate was permanently fixed to the GRIN implant using a mixture of black dental cement powder (Contemporary Ortho-Jet™, black, Lang Dental, Wheeling, USA) and super glue. Next, the miniscope was removed from the implanted baseplate and a baseplate cover was fixed to the baseplate to protect the exposed GRIN lens from dust or other physical damage.

2.4.5 Transcardial perfusion

Study 1: Ninety minutes after the beginning of the last cue-induced reinstatement, at the timepoint of highest cFos expression (Sheng and Greenberg, 1990), rats were deeply anesthetized with isoflurane and transcardially perfused with 100 ml of 1× PBS followed by 200 ml of fixative solution (phosphate buffer, containing 4% paraformaldehyde and 14% saturated picric acid). Brains were collected and postfixed for 24 h at 4°C in fixative solution. Postfixation for X-gal staining was for 1.5 h at room temperature.

Study 2 + 4: 90 minutes after the beginning of the last cue-induced reinstatement session, the animals were transcardially perfused with 100ml 1xPBS (137 mm NaCl, 2.7 mm KCl, 8 mm Na_2HPO_4, 1.46 mm KH2PO_4, pH 7.4), containing 10000 units of Heparin sodium/L. Next, the animals were perfused with 50ml of 4% paraformaldehyde (PFA) in 1xPBS solution (pH 7.4).

The brains were removed and postfixed in 4%PFA in 1xPBS over night at 4°C. The brains were washed in 1xPBS before further processing of brain tissue.

Study 3: The animals were perfused as described in Study 2. The perfused animals were decapitated and the head containing the implant was postfixed in 4% PFA in 1xPBS for two weeks at 4°C. After two weeks, the brains were removed and stored in 1xPBS until further processing.

2.5 Immunohistochemical procedures

2.5.1 X-Gal immunohistochemistry

For X-gal immunohistochemistry in Study 1, 55 µm coronal sections were cut using a vibrating blade microtome (Leica Microsystems). Brain sections were incubated in freshly prepared X-gal reagent (0.6 mg/ml in 1× PBS plus 5 mm $K_4Fe(CN)_6$, 5 mm $K_3Fe(CN)_6$, and 2 mm $MgCl_2$) at 37°C for ~10 minutes. The reaction was stopped by washing the sections with 1× PBS, brain sections were mounted on Super Frost Plus microscope slides (Thermo Fisher) using Immu-Mount (Fischer Scientific) and were investigated using a stereo microscope (Carl Zeiss). For quantification, the number of positively stained nuclei was determined using the cell-counter analysis macro of ImageJ covering an area of 1 mm^2 within the IL.

2.5.2 Fluorescent double labeling immunohistochemistry and image analysis

Study 1: 40-µm-thick coronal sections were cut, collected in 1× PBS, washed three times in 1× TBS and then incubated in blocking solution (7.5% donkey serum, 2.5% BSA in 1× TBS with 0.2% Triton X-100) for 1h at room temperature (RT). For cFos/NeuN double-labeling sections were incubated with the anti-cFos antibody (c-Fos (9F6) mAb no. 2250, Cell Signaling Technology, rabbit, 1:500) and the anti-NeuN-Cy3-conjugated primary antibody (clone A60, Cy3 conjugate, MAB377C3, Millipore, mouse, 1:500) in blocking solution over night at 4°C. The sections were then washed three times in 1× TBS and incubated for 1h at RT in 1× TBS with 0.2% Triton X-100 (TBS-Tx) containing the secondary antibody

AlexaFluor 488-labeled donkey anti-rabbit (A-21206, Invitrogen, 1:200 dilution). For cFos/CaMKII and Fos/GAD67 double-labeling sections were incubated for 24 h at 4°C with the anti-cFos antibody (rabbit, 1:500 dilution) and either anti-CaMKII (6G9 MA1-048, Pierce Biotechnology, mouse, 1:500) or anti-GAD67 (1G10.2 MAB5406, Millipore, mouse, 1:1000) antibody in blocking solution, then washed three times in 1× TBS and incubated for 1 h in TBS-Tx containing a mixture of secondary antibodies (AlexaFluor 488-labeled donkey anti-rabbit, 1:200, and AlexaFluor 555-labeled donkey anti-mouse, 1:200, A-31570, Invitrogen). For cFos/β-gal double-labeling anti-cFos antibody (rabbit, 1:500) and anti-β-gal antibody (ab9361, Abcam, chicken, 1:10,000) in blocking solution were used. Secondary antibody solution contained AlexaFluor 488-labeled donkey anti-rabbit (1:200) and Cy3-labeled donkey anti-chicken (703-165-155, Jackson ImmunoResearch, 1:1000). Following staining all sections were washed three times in 1× TBS and mounted as described above.

Slides were investigated using a Leica TCS SP confocal imaging system attached to a DM IRE2 microscope using a HCX PL APO 63× oil planchromat lens with a NA 1.40 (Leica, Mannheim, Germany). Z-stacks were acquired with sections taken every 0.99 µm. All images were saved as Tiff files. For quantification, three Z-stacks were acquired per hemisphere from IL or PL of eight rats. The number of all NeuN stained cells and the number of cFos and NeuN colocalized cells was counted using the cell counter analysis macro of ImageJ. The ratio of colocalization was calculated for each animal and the mean ± SEM for the eight animals was calculated. For quantification of cFos + GAD67 or CaMKII colocalization, the number of all cFos stained cells and the number of the cFos and GAD67 or CaMKII colocalized cells was counted and the ratio of colocalization was determined as described above.

Study 2: 70µm thick brain sections were prepared from the perfused and fixed brains from experiment 2 (Figure 18B) using a vibratome (VT1000S, Leica, Wetzlar, Germany). Sections were stained using the above described protocol for cFos (Alexa 568) and NeuN (Alexa 405).

NeuN and cFos stained mPFC sections (see 2.3.3 Immunohistochemistry procedures) were examined by confocal microscopy using a Leica TCS SP5 microscope (Leica Microsystems, Wetzlar, Germany) equipped with a 63x HCX PL APO (1.45 NA) objective. Four image stacks were acquired at random positions in the IL of each hemisphere (image resolution: 512 x 512 pixels; voxel size: 0.459 x 0.459 x 2.519 µm; image dimensions: x,y = 234.32 µm, z = 2. 52 µm). Three slices were examined per animal.

Image analysis was performed in a semi-automated way. A custom-written Matlab (MATLAB, RRID:SCR_001622 Mathworks, Natick, MA, USA) procedure was generated and provided by Dr. Frank Herrmannsdörfer from the Institute of Anatomy and Cell Biology at Heidelberg University. This procedure was used to determine the number of objects recorded in each imaging channel (NeuN, cFos, two tracer signals) and the number of objects positive for cFos. All channels were first smoothed by a 2D Gaussian filter (sigma = 3 pixels, 1 pixel = 0.459 µm) before the intensities of all channels were binarized. The threshold for the binarization was chosen such that 95% of the NeuN signal and the 98% of the cFos signal and of both tracer signals were defined as background pixels. Thresholds were calculated for each frame individually to correct for decreasing intensities in deep tissue layers. The NeuN signal was eroded by removing two pixels from the edge of the signal. A connected components analysis with a connectivity of 26 was performed for each channel. Connected components that did not reach a certain size (500 voxels for NeuN and cFos, 750 voxels for tracer channels) were excluded from analysis as they are likely to not represent true signals. The center of mass of each connected component in each channel was determined. Co-localization between cFos signals and objects in the other three channels was assigned by close proximity analysis (range: 10 µm) based on the centers of mass. The results of the co-localization analysis were confirmed by manual inspection.

Study 4: In order to characterize cells expressing the Cre-inducible mGluR2 knockdown AAV, three CamKII-Cre rats received bilateral injections of the knockdown AAV into the IL as described above. Four weeks after virus injection rats were perfused and postfixed as described above. 60µm coronal sections were cut using a vibrating blade microtome (Leica Microsystems) and collected in 1x PBS. Immuno-labeling for either NeuN, GAD67 or CamKII were performed as described above using Alexa-555 secondary antibodies. Two brain sections containing the mPFC were analyzed per animal. Three image stacks per hemisphere were recorded in random positions in the IL using a Leica TCS SP confocal imaging system attached to a DM IRE2 microscope using a HCX PL APO 63× oil planchromat lens with a NA 1.40 (Leica, Mannheim, Germany). Co-localization quantification of eYFP with the respective neuronal marker was performed manual using the cell counter macro in ImageJ (Fiji, RRID:SCR_002285).

2.5.3 Fluorojade B immunohistochemistry

For Fluorojade B staining in Study 1 rats were perfused as described above and the brains were postfixed in the fixative for 24 h at 4°C, dehydrated in 1× PBS/10% sucrose solution for 3 days and flash frozen at −80°C. A standard Fluorojade B staining protocol was used (Schmued and Hopkins, 2000). Briefly, sections were dried for 30 minutes at 50°C. The sections were then incubated in a solution containing 1% sodium hydroxide (NaOH) and 80% EtOH for 5 minutes, followed by 2 min incubation in 70% EtOH. Next, the sections were washed in aqua dest. and incubated in 0.06% potassium permanganate for 10 minutes. After another washing step with aqua dest. the sections were incubated in 0,001% Fluorojade B und 0.1% acetic acid for 30 minutes. After three washing steps with aqua dest. the sections were dried at 50°C for 10 minutes, cleared by immersion in xylene for 1 min and coverslipped with Eukitt quick-hardening mounting medium (Sigma-Aldrich).

Images of Fluorojade B-labeled sections were acquired using a Zeiss Axioskop 2 plus microscope with a 2.5× lens. Image analysis was performed using ImageJ. First, the images were transformed into an 8-bit gray scale image. Then a region-of-interest (ROI) was defined for the mPFC in each image, followed by the measurement of the integrated density of each ROI.

2.5.4 Injection site mapping

Brain sections containing the brain area of interest were mounted on microscope slides (Super Frost Plus, Thermo Fisher) using Immu-Mount (Fischer Scientific) and validated using a Zeiss Axioskop 2 plus microscope with a 2.5× lens.

2.5.5 Fluorescent *in-situ* hybridization (FISH)

Study 2:

In order to detect both, IL neuronal ensembles involved in EtOH and saccharin seeking, we used a double cFos fluorescent *in-situ* hybridization (FISH) approach. Therefore we made use

of the different temporal profiles of nascent (unspliced) and mature (spliced) cFos mRNA species. After a certain stimulus, cFos mRNA is rapidly induced within 5 mins (unspliced mRNA), but quickly undergoes splicing (spliced mRNA) (Jurado et al., 2007), which peaks around 30mins after the stimulus presentation (Lin et al., 2011). These specific time courses were used in the cue-induced reinstatement design of experiment 3 (Study 2). The cue-responsive neurons from the first cue-induced reinstatement session can be detected using spliced cFos mRNA and the second session can be detected using unspliced cFos mRNA (Figure 18C).

For double cFos FISH, the animals were decapitated 5min after the final cue-induced reinstatement session. The brains were quickly removed, snap frozen in isopentane (-50°C) and stored at -80°C until further processing. Next, 20µm brain sections were cut using a cryostat and thaw-mounted onto Super Frost Plus slides (Thermo Fisher, Darmstadt, Germany). Mounted sections were stored at -80°C in sealed boxes until FISH processing.

FISH experiments were performed using the RNAscope Multiplex Fluorescent Reagent Kit (Advanced Cell Diagnostics, Newark, USA; Probes Rn-Fos-O1-C2, Rn-Fos-Intron1-C3, Rn-Bcl11b and Rn-Rgs8-C3) according to the manufacturer's instructions for fresh frozen tissue (Wang et al., 2012). The Rn-Fos-o1-C2 and Rn-Fos-Intron1-C3 probes were used to detect spliced and unspliced cFos mRNA, respectively. Rn-Bcl11b and RnRgs8-C3 were used to detect the cortical layers 5/6 and 2/3, respectively.

Briefly, the slides were transferred from -80°C into sterile 4%PFA in 1xPBS at 4°C for 15min. The slides were rinsed 3 times in sterile 1xPBS and dehydrated in 50%, 70% and two times 100% EtOH. Next, the slides were dried at room temperature (RT) and sections were surrounded with a physical barrier using a hydrophobic barrier pen (ImmEdge^{TM} Hydrophobic Barrier Pen, Vector Laboratories). The sections were then pretreated with protease IV solution (PN 322340, ACD) for 15min at RT. After two 1XPBS washing steps the sections were incubated in 1x target probe solutions for 2h at 40°C using the HybEZ Hybridization Oven (ACD). Following two washing steps using 1xRNAscope® Wash Buffer the sections were incubated in preamplifier and amplifier solutions: AMP1 (30min, 40°C), AMP2 (15min, 40°C), AMP3 (30min, 40°C). The sections were then hybridized to fluorescently labeled probes using the AMP AltB solution, which labels C1 with Atto 550, C2 with Alexa 488 and C3 with Atto 647. Two washing steps using 1xRNAscope® Wash Buffer were performed

between each amplification step. Finally the sections were incubated in DAPI solution for 30sec and coverslipped with Shandon™ Immu-Mount™ (Thermo Scientific™).

Brain sections containing the mPFC were examined by confocal microscopy. Three images were acquired at random positions in the IL of each brain slice. Two slices were examined per animal. For layer specific cFos expression, three images were then taken per layer in each brain slice.

Data was analyzed for co-localization of FISH signals in both fluorescent channels using the cell counter macro of ImageJ (Fiji, RRID:SCR_002285). Specificity of FISH signal was verified by co-localization with DAPI. In case of double labeling for spliced and unspliced cFos mRNA, the scattered signal pattern prevented semi-automated analysis. This dataset was manually analyzed as follows: first, the fraction of DAPI-positive cells expressing spliced cFos was calculated for each animal. Then, expression of unspliced cFos mRNA was measured as mean gray value per cell, based on manually determined regions of interest using ImageJ. To discriminate basal from activity induced expression of unspliced cFos, gray values were ranked and the fraction of cells showing the highest unspliced cFos mRNA expression, identical to the fraction of spliced cFos mRNA, were used for co-localization analysis.

Study 4:

In order to quantify the knockdown efficiency of the Cre-inducible mGluR2 knockdown AAV on mRNA level, three male CamKII-Cre rats were injected with the control AAV expressing shUnc and three rats were injected with the mGluR2 knockdown AAV. Four weeks after AAV injection the animals were rapidly decapitated. Brains were removed, frozen in isopentane (-50°C) and kept at -80°C until further processing. Brain slices of 20 µm thickness were cut on a cryostat and thaw-mounted onto Super Frost Plus slides (Thermo Fisher, Darmstadt, Germany). FISH analysis was performed using the RNAscope Multiplex Fluorescent Reagent Kit (Advanced Cell Diagnostics, Newark, USA; Probes Rn-Grm2 and EYFP-C2) according to the manufacturer's instructions (freshly frozen tissue).

Brain sections containing the mPFC were examined by confocal microscopy using a Leica TCS SP5 microscope (Leica Microsystems, Wetzlar, Germany) equipped with a 63x HCX PL APO (1.45 NA) objective. Three images were acquired at random positions in the IL of each hemisphere. Two brain slices were examined per animal.

Co-localization of mGluR2 and EYFP signals were analyzed using the cell counter macro in ImageJ. Specificity of FISH signal was verified by co-localization with DAPI. Next, the mean grey value of mGluR2 signals were determined by manually drawing ROIs containing the perinuclear mGluR2 signals of each cell. For control as well as knockdown AAV injected animals the mGluR2 mean grey value ratio was calculated: $\frac{mGluR2^{+}\ EYFP^{+}}{mGluR2^{+}\ EYFP^{-}} = mGluR2\ ratio.$

2.6 Western blot (Study 4):

Protein levels of mGluR2 were examined within the NAc Shell of male CamKII-Cre rats, injected either with the control shUnc AAV or the Cre-inducible knockdown AAV into the IL as illustrated in Figure 22 (n=8/group).

NAc Shell brain tissue was micropunched as previously described (Meinhardt et al., 2013). Brain tissue was transferred to a lysis buffer: 100mM Tris HCl pH 8 and 20mM EDTA containing cOmplete mini protease inhibitor (Roche Diagnostics, Mannheim, Germany). Ultrasonic lysis was performed using an ultrasonic device (Branson Sonifier 250, Danbury, CT, USA). Protein concentrations were analyzed using BioRad Protein Assay (Bio-Rad Laboratories, Munich, Germany) and visualized using a microplate spectrophotometer (PowerWave XS, BioTek Instruments, Bad Friedrichshall, Germany).

Next, samples were mixed with Laemmli 2x buffer (4% sodium dodecyl sulfate, 10% β-mercaptoethanol, 0,004% bromphenol blue and 0,125 Tris-HCl pH 6.8). An amount of ~10 µg of total protein as well as 5µl of pre-stained protein ladder (Chameleon® Duo Li-Cor, Lincoln, NE, USA) was loaded and separated on Novex™ WedgeWell™ 4-12% Tris-Glycine Gels using 1x Tris Glycine SDS Running Buffer (Invitrogen, Carlsbad, CA, USA). Proteins were then transferred to nitrocellulose membranes (Protran BA85, Cat no. 10401196, GE Healthcare Life Sciences Whatman™) in a blotting chamber (X Cell II™ Blot Module, Invitrogen) using Novex™ Tris-Glycine Transfer buffer (invitrogen). Membranes were then incubated in Odyssey® Blocking Buffer in PBS (Li-Cor) for 1h at room temperature (RT) and probed with mouse anti-metabotropic glutamate receptor 2 antibody (1:1000, mG2Na-s, ab15672, Abcam, MA, USA) and rabbit anti-beta actin (1:3000, #4970, Cell Signaling Technology, Danvers, MA, USA) diluted in Odyssey® Blocking Buffer in PBS for 2 days at 4°C. Blots were then washed with 1x PBS followed by 1x PBS-T (containing 0.5%

Tween20). Next, blots were incubated for 2h at RT in secondary antibody solution containing IRDye 800 CW Donkey Anti-Mouse IgG (1:1000, LI-COR®, 926-32212) and IRDye 680LT Donkey Anti-Rabbit IgG (1:1000, LI-COR®, 926-68023) in Odyssey® Blocking Buffer/PBS, followed by washing steps with 1x PBS, 1xPBS-T and aqua bidest. Signals were detected using an ODYSSEY® CLx234 (LI-COR®, Lincoln, NE, USA) fluorescent imaging system. The signal was quantified using Image Studio™ 235 software (LI-COR®, Lincoln, NE, USA) by calculating the ratio of mGluR2 signal normalized to ß-actin.

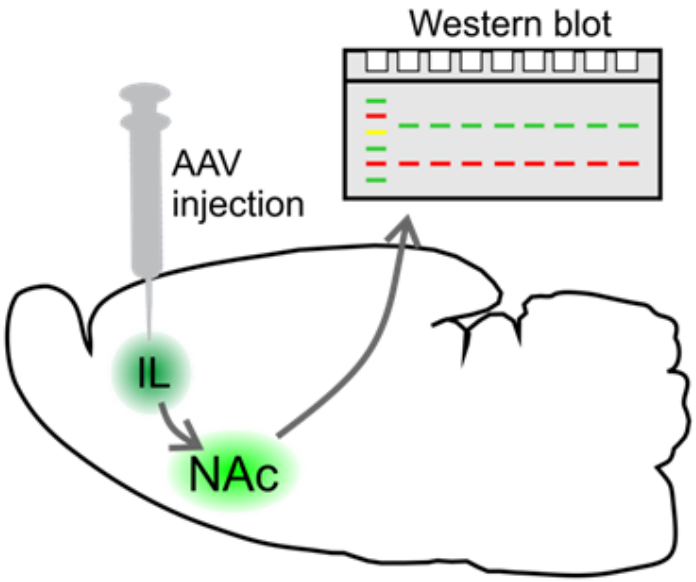

Figure 22: Schematic representation of Western blot procedure. The animals received bilateral injection of either the control (shUnc) or Cre-inducible mGluR2 knockdown AAV into the IL. Tissue for western blot analysis of mGluR2 protein levels was micropunched from the nucleus accumbens (NAc), which is a major projection target of the IL

2.7 TaqMan quantitative realtime PCR

2.7.1 Genotyping for Grm2 Cys407* mutation (Study 4)

Tissue for Grm2 cys407* genotyping was obtained from the animals by tail biopsy. Genomic DNA was isolated using the NucleoSpin® 8 / 96 Tissue kit (Macherey – Nagel, Düren, Germany) according to the manufacturer's protocol. The Grm2 cys407* SNP (c.1221C>A, p.Cys407*) was detected by a custom TaqMan® SNP Genotyping Assay (Assay ID: AHGJ96C, Applied Biosystems, Carlsbad, USA, Table 3) on an ABI QuantStudio 7 Flex RT-

PCR system with QuantStudio™ Real-Time PCR software (20 µl reaction volume containing 10 ng genomic DNA, 55 cycles of 95 °C for 15 sec and 57 °C for 30 sec). Only homozygous wild type allele carriers were used for further experiments.

Table 3: TaqMan Assay information for Grm2 Cys407* genotyping.

TaqMan Assay ID	**AHGJ96C**
Forward primer	TGCCCTCTGTCCCAACAC
Reverse primer	GCGGCGCCCATTGAC
Wildtype allele reporter (VIC)	TAGCATCGCAGAGGTG
Mutant allele reporter (FAM)	CATAGCATCTCAGAGGTG

2.7.2 TaqMan PCR validation of cFos mRNA time course (Study 2)

In order to validate the time course of spliced and unspliced cFos mRNA expression reported by Lin et al. (2011), we trained nine Wistar rats on a standard operant alcohol-seeking protocol (described in 2.3.1.2). Three animals were decapitated without previous behavioral testing. Three animals were decapitated immediately after a 5min cue-induced reinstatement of alcohol seeking session. And three animals were decapitated 30 minutes after a 5 min cue-induced reinstatement of alcohol seeking session. Following decapitation, the brains were quickly removed, snap frozen in isopentane (-50°C) and stored at -80°C until further processing. Next, 120µm thick sections were cut using a cryostat. The IL area was extracted from the sections using a micropunch and the samples were stored at -80°C until RNA isolation.

The total RNA was extracted from the micropunched tissue using 1ml of TRIzol® Reagent (Invitrogen) and isolated using the RNeasy Kit (Qiagen, Hilden, Germany) according to the manufacturer's protocol. The total RNA was transcribed into cDNA using the SuperScript™ VILO™ cDNA Synthesis Kit (Therma Fisher). 200ng of total RNA were transcribed into cDNA. 2µl of a 1:5 dilution of the cDNA product were used in a 20µl TaqMan reaction mix for gene expression analysis.

The spliced cFos cDNA (Rn.103750) was detected by a TaqMan® Gene Expression Assay (Assay ID: Rn02396759_m1; Applied Biosystems, Carlsbad, USA). The unspliced cFos cDNA was detected by a customized TaqMan® Gene Expression Assay (Assay ID: APCE4TY, Applied Biosystems, Carlsbad, USA, Table 4) on an ABI QuantStudio 7 Flex RT-PCR system with QuantStudio™ Real-Time PCR software (20 µl reaction volume containing 2µl cDNA solution, 40 cycles of 95 °C for 15 sec and 60 °C for 1 min).

Quantification of the TaqMan gene expression assay was done using the ΔΔCT method (Livak and Schmittgen, 2001). Expression data for spliced and unspliced cFos of the cue-induced reinstatement groups (killed immediately or after 30 minutes) were normalized to the no-behavior (control) group. Therefore the mean ΔCT for the three untreated samples was calculated. The ΔΔCT for each treatment sample was calculated by subtracting the mean value of the control group from each ΔCT value of the sample group. Data are expressed as fold change to control by calculating $\Delta\Delta CT^2$.

Table 4: TaqMan Assay information for customized unspliced cFos mRNA gene expression assay.

TaqMan Assay ID	**APCE4TY**
Probe sequence (VIC)	AGACTCCGGAGCAGCGCCTGCGT
Forward primer	CGGTGTGTAAGGCAGTTTCATTGATAA
Reverse primer	TTCAGCATCACTCGCTCGAAAG

2.8 AAV Plasmid cloning

2.8.1 Generation of a general mGluR2 knockdown shRNA AAV plasmid

We used a commercial siRNA sequence (siRNA ID: s127825, Silencer® Select Pre-Designed, Ambion, Thermo Fisher) to construct a shRNA targeting mGuR2 in the rat. In order to generate an AAV plasmid expressing a shRNA against rat mGluR2, we first generated the shRNA by annealing the following oligo nucleotide strands:

5’-3’ forward primer:

P-GATCCAAAAGCTACAACATCTTCACCTATTCAAGAGATAGGTGAAGATGTTGT
AGCTTTTTTTCCAAA

3’-5’ reverse primer:

GTTTTCGATGTTGTAGAAGTGGATAAGTTCTCTATCCACTTCTACAACATCGAAAA
AAAGGTTTTCGA-P

Oligo annealing was done using the following protocol:

- 2µl forward primer
- 2µl reverse primer
- 5µl nuclease-free water (AM9938 Ambion, Thermo Fischer)
- 1µl New England Biolabs 2 buffer (NEB, USA)
  10µl total volume

First nuclease-free water and both oligo strands were heated up to 95°C for 5 min. Next NEB buffer 2 was added and the mixture was again heated up to 95°C for 5 min. Next, the mixture was incubated at room temperature for 10 minutes resulting in the following double stranded shRNA sequence (Figure 23, Table 5):

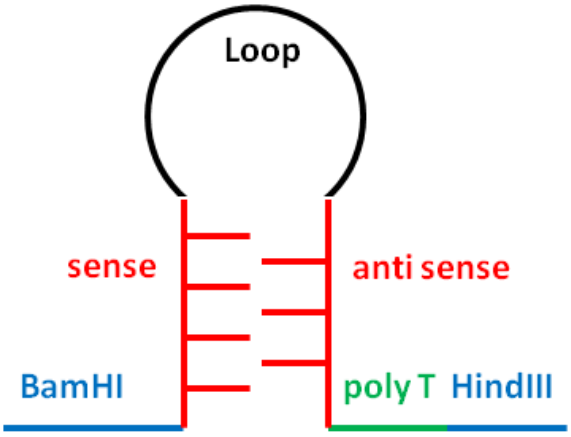

Figure 23: Schematic representation of mGluR2 shRNA. The shRNA consists of a sense and antisense strand, connected by a loop sequence. A poly T termination sequence is located downstream of the antisense strand. The shRNA sequence is flanked by a BamHI and HindIII restriction site for cloning into the target vector backbone.

Table 5: Nucleic acid sequences of mGluR2 shRNA features.

Feature	Sequence
BamHI	**GGATCC AAAA**
shRNA sense strand	**GCTACAACATCTTCACCTA**
Loop sequence	**TTCAAGAGA**
shRNA anti sense strand	**TAGGTGAAGATGTTGTAGC**
Poly T termination sequence	**TTTTTTTCCAA**
HindIII	**AAGCTT**

For AAV-mediated expression of the shRNA, we cloned the shRNA sequence into the following backbone provided by Hilmar Bading, Department of Neurobiology, University of Heidelberg: U6-shUnc-CamkII-eGFP (Figure 24) (Mauceri et al., 2015). Using the BamHI and HindIII restriction sites, the universal control shRNA (shUnc) was replaced by the mGluR2 knockdown shRNA. The resulting AAV plasmid was purified, sequenced, tested in cell culture, and finally used for AAV production.

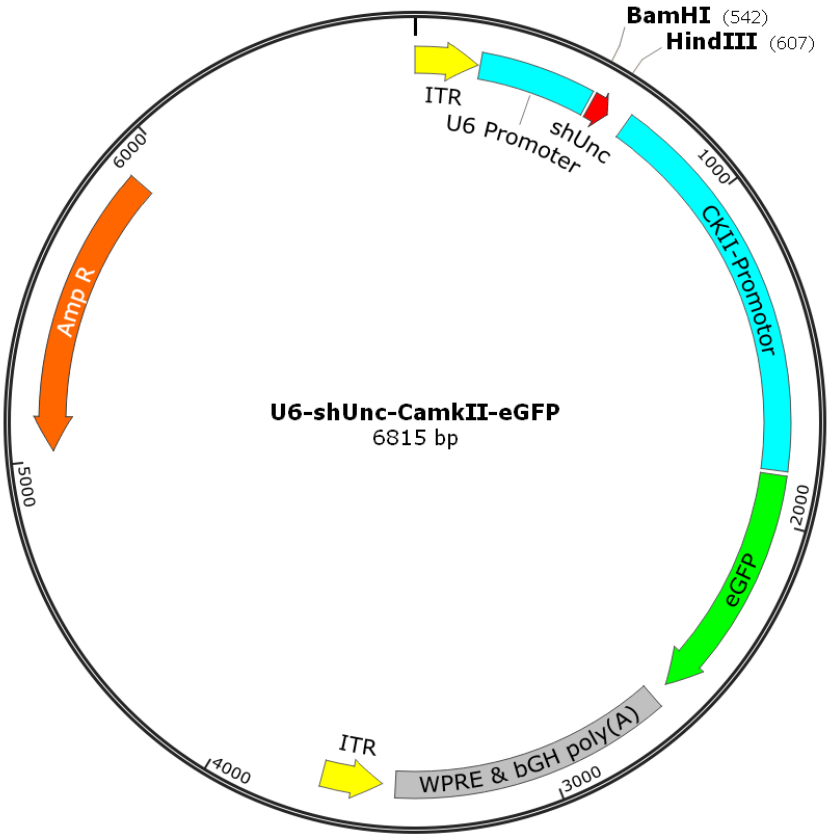

Figure 24: Circular plasmid for AAV-mediated shRNA expression. The plasmid contains an ampicillin resistance gene (Amp R) for antibiotic-based bacterial colony selection. Expression of the universal control shRNA (shUnc) is driven by the U6 Promoter. eGFP marker gene expression is driven by the CamKinaseII promoter (CKII-promoter). eGFP expression was enhanced by the Woodchuck Hepatitis Virus Posttranscriptional Regulatory Element (WPRE) and a bovine growth hormone (bGH) poly (A) sequence. The shRNA and eGFP expression casette is flanked by two inverted terminal repeats (ITR), for transfer into an AAV vector. This plasmid was kindly provided by Hilmar Bading (Mauceri et al., 2015).

2.8.2 Generation of a Cre-inducible mGluR2 knockdown shRNA AAV plasmid

In order to generate a Cre-inducible version of the above mentioned mGluR2 knockdown AAV, we cloned a construct based on the double-floxed inverted orientation technique (Schnütgen et al., 2003; Saunders et al., 2012). To prevent Cre-independent unspecific shRNA expression, both the sense and antisense sequences were separated from each other as can be seen in Figure 25. Only after Cre-recombination, the floxed sequence flips and a functional shRNA sequence is expressed under control of U6 promoter and eYFP is expressed under control of EF1α promoter. The fragment containing the split shRNA sequence and the eYFP sequence was cloned into a pMK-RQ_U6_COIN vector (obtained from GeneArt,

Thermo Fisher). This vector was generated by Ana Gallego-Roman as part of her Master Thesis under the joint supervision of Kai Schönig (Institute of Molecular Biology, CIMH) and myself (Gallego-Roman, 2016).

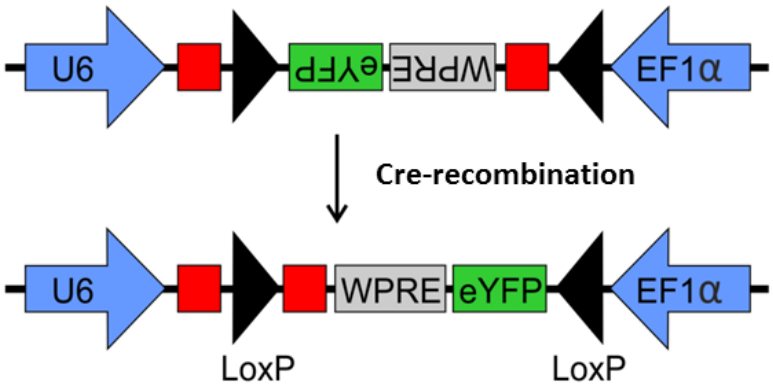

Figure 25: Schematic representation of Cre-inducible mGluR2 shRNA expression cassette. The shRNA was split in the middle and inserted into opposite directions into the floxed cassette. The reporter gene eYFP was also inverted and inserted opposite of the EF1α promoter. Without Cre-recombination no shRNA and no eYFP expression are possible. After Cre recombination shRNA expression is driven by U6 promoter and eYFP expression is driven by EF1α.

2.9 Cell culture

2.9.1 AAV production

A standard protocol was used for AAV production (Xiao et al., 1999; Hauck et al., 2003). Briefly HEK293 cells were transfected with 3 helper plasmids (pFdelta6, pRV1 and pH21) and the respective shRNA containing AAV plasmid by calcium phosphate precipitation. 60 hours after transfection cells were harvested and purified using heparin columns.

The general mGluR2 knockdown AAV and the shUNC AAV were produced in the Institute for Psychopharmacology at the Central Institute for Mental Health, Mannheim. The Cre-inducible mGluR2 shRNA AAV was produced and kindly provided by the research group of Thomas Kuner from the Institute of Anatomy and Cell Biology at Heidelberg University.

2.9.2 Dual luciferase assay

In order to quantify the knockdown efficiency of the Cre-inducible mGluR2 knockdown AAV a dual luciferase assay was performed. To induce the Cre-mediated switch of the floxed mGluR2 knockdown cassette, the plasmid was transformed into EL350 E.coli cells (Liu et al., 2003). For quantification of mGluR2 knockdown efficiency, the mGluR2 target sequence was inserted into a pMIR-REPORT miRNA Expression Reporter Vector System (Thermo Fisher, Waltham, MA, USA). Both the control AAV construct (shUnc) and the recombined mGluR2 knockdown AAV construct were each co-transfected with the pMIR-REPORT vector (containing the mGluR2 knockdown target site and Firefly luciferase) and pSV40-Renilla containing Renilla luciferase for normalization into HeLa cell cells (jetPRIME™, Polyplus transfection, Illkirch, France). Three technical replicates were performed for each plasmid. Transfected HeLa cells were incubated for 48h at 37 °C and 5% CO2 in Dulbecco´s Modified Eagle Medium (DMEM) + GlutaMax-I (Invitrogen) supplemented with 10% fetal calf serum (FCS) (Invitrogen) and 1% Streptomycin/Penicillin (Invitrogen). After 48h cells were washed with 1x PBS and placed on ice. PBS was replaced with 1x Passive lysis buffer (Promega) and cells were harvested using cell scrapers (VWR). The cell suspension was transferred into a pre-cooled Eppendorf tube and centrifuged for 5min at 4°C at 13200rpm. 10µl of each lysate were then analyzed using VICTOR 1420 Multilabel Counter (PerkinElmer, Hamburg, Germany) with automatic LAR II (Firefly luciferase) and Stop & Glo Reagent (Renilla luciferase) injection. All Firefly luciferase signals were normalized to Renilla luciferase signals.

2.10 In-vivo Calcium Imaging

2.10.1 Set-up for in-vivo calcium imaging recordings

Operant behavior for in-vivo calcium imaging recordings was performed in extra tall operant chambers (ENV-007, Med Associates, Fairfax, VT, USA), equipped with large liquid receptacle ports and switchable liquid dipper cups for reward delivery (CT-ENV-202M-S-6.0, Med Associates, Fairfax, VT, USA). TTL outputs from the operant chamber were generated by a SuperPort Output Module (DIG-726TTL –G). An Arduino board was used to deliver the

output signals from the operant chamber to a laptop (Lenovo Ideapad 510-15ISK), for synchronization with the calcium imaging data.

Calcium imaging data were recorded using self-assembled open source epifluorescence mini-microscopes (UCLA Microscopes) (Cai et al., 2016). Digital imaging data was sent from the CMOS imaging sensor to data acquisition (DAQ) board over a lightweight, highly flexible cable. Data was then transmitted over super speed USB (USB 3.0) to the laptop running the Miniscope Data Acquisition Software (miniscope.org). Images were acquired with 20 frames per second and maximum gain (64) and saved as uncompressed avi files to the local hard drive. Simultaneously, time stamps of all elements of the cue-conditioned operant self-administration paradigm were acquired on separate streams (cue presentation, lever pressing, time spending at the liquid receptacle) using Bonsai software (http://www.open-ephys.org/bonsai/) (Lopes et al., 2015). The Med Associates operant chamber was controlled using the MedPC IV software (Med Associates, Fairfax, VT, USA).

2.11 Statistical analysis

Study 1:

Data are expressed as mean ± SEM. Behavioral data were analyzed using two-way ANOVA with repeated measures, followed by Newman–Keuls post hoc tests, where appropriate, using the program Statistica 10 (StatSoft). Alpha level for significant effects was set to 0.05. The dependent measures and the factors used in the statistical analyses are described in Results. The X-gal staining was analyzed by two-tailed t test. Fluorojade-B data were analyzed by one-way ANOVA.

Study 2:

Data are presented as mean ± SEM. Behavioral data was analyzed using two-tailed paired t-test or two-way repeated measures ANOVA followed by Newman-Keul's post hoc test, where appropriate (Statistica 10, RRID:SCR_015627, Statsoft, Hamburg, Germany). Animals were excluded from analysis if they either failed to discriminate the active and inactive lever during self-administration or they did not show significant (> 15 lever presses in 30 min) reinstatement behavior in response to either of the cues. Immunohistochemistry and FISH

data were analyzed by two-tailed unpaired t-test and two-way ANOVA and TaqMan data were analyzed by unpaired one-tailed t-test using GraphPad Prism 5 (Graphpad Prism, RRID:SCR_002798, La Jolla, CA, USA). The alpha level for significant effects was set to 0.05. The dependent measures and the factors used in the statistical analyses are described in Table 6, Table 7 and Table 9 in the Results part. In case of co-localization of spliced and unspliced cFos mRNA, statistical significance of co-localization was tested by shuffle test using custom written IGOR macros (100.000 repetitions, RRID:SCR_000325, Wavemetrics, Lake Oswego, OR), performed and provided by Janine K Reinert from the Institute of Anatomy and Cell Biology at Heidelberg University. Therefore, the thresholded signal of unspliced cFos (see above) and the signal of mature cFos were binarized and analyzed for co-localization.

Study 3:

Behavioral data are expressed as mean ± SEM. Preprocessing of calcium imaging data was done with customized code in combination with available repositories (https://github.com/zhoupc/CNMF_E) both coded in MATLAB. Initial preprocessing of the data includes correction of movement artefacts by aligning all the recorded frames with the average of all recorded frames. Detection of neurons and their activity was done by a constrained nonnegative matrix factorization (CNMF-E) delivering spatiotemporal features of each neuron: spatial coordinate of each ROI (neuron) and calcium signal as a function of time. Data was then analyzed using custom made MATLAB routines.

Study 4:

Data are expressed as mean ± SEM. Behavioral data were analyzed using one-way or repeated measures ANOVA using the program Statistica 10 (Statsoft; RRID:SCR_015627). Unpaired t-tests for mGluR2 knockdown quantification were analyzed using GraphPad Prism 5 (Graphpad Prism, RRID:SCR_002798, La Jolla, CA, USA). Alpha level for significant effects was set to 0.05. Detailed statistics and dependent measures for the operant alcohol-seeking experiments can be found in Table 10 and Table 11.

Study 5:

Data are expressed as mean ± SEM. Behavioral data were analyzed using one-way ANOVA. Overall statistical significance was analyzed by repeated measures ANOVA or MANOVA using the program Statistica 10 (Statsoft; RRID:SCR_015627).

3. Results

3.1 Study 1: Identification of an infralimbic neuronal ensemble involved in alcohol seeking behavior

This study contains experiments published in the *Journal of Neuroscience* with the title "Losing Control: Excessive Alcohol Seeking after Selective Inactivation of Cue-Responsive Neurons in the Infralimbic Cortex", as well as additional experiments characterizing an infralimbic neuronal ensemble involved in alcohol seeking and further characterizing the mechanism of action of the Daun02 inactivation method.

3.1.1 Introduction

The medial prefrontal cortex (mPFC) is involved in top-down control over behavior in humans and rodents and controls whether or not to engage in excessive alcohol drinking (Heidbreder and Groenewegen, 2003; Wood and Grafman, 2003). A previous study from our lab found that the infralimbic cortex (IL) exerts inhibitory control over alcohol seeking behavior in rats (Meinhardt et al., 2013). This inhibitory function is severely impaired after a history of chronic intermittent alcohol exposure in rats. However, the pathophysiological mechanisms underlying this impaired IL control function are still poorly understood. Alcohol seeking behavior is a prototypical example of associative learning, which is thought to be represented in distinct neuronal ensembles (Hebb, 1949). Several neuronal ensembles have been identified in the IL, involved in drug and natural reward seeking (Bossert et al., 2011; Cruz et al., 2015; Suto et al., 2016; Warren et al., 2016). Furthermore it has been reported, that the prelimbic cortex (PL) and the IL have opposing effects on drug seeking behavior (Peters et al., 2008a; Peters et al., 2008b; Peters et al., 2009).

In order to identify IL and PL neuronal ensembles and their effect on alcohol seeking behavior, we used the Daun02 inactivation method (Koya et al., 2009; Koya et al., 2016). The Daun02 inactivation method is based on the inactive prodrug Daun02, which gets converted into the active form by ß-galactosidase activity, encoded by the bacterial LacZ transgene. In order to test the effect of IL and PL ensemble ablation on alcohol seeking behavior, the

Daun02 inactivation method was used in cFos-LacZ rats (Kasof et al., 1995; Farquhar et al., 2002), which express LacZ only in activated neurons. To compare this effect with an IL lesion, the Daun02 inactivation method was used in the IL of CAG-LacZ rats, which constitutively express LacZ in all cells (Weber et al., 2011). In order to test for unspecific drug effects of Daun02, IL Daun02 infusions were performed in wild type littermates of the cFos-LacZ rats, which do not express LacZ. Characterization of the ensemble size and containing cell types was done using double fluorescent immunohistochemistry for cFos and the cell type markers NeuN, GAD67 and CamKII. In order to further examine the mechanism of action of Daun02 we used the Fluorojade B neurodegeneration staining method, to identify apoptotic neurons.

The guide cannula implantation into the cFos-LacZ rats targeting the IL was performed by Marcus Meinhardt at the Institute of Psychopharmacology, Central Institute of Mental Health, Mannheim. The operant conditioning and perfusion of the IL cFos-LacZ batch was performed by me as part of my Master Thesis under the supervision of Dr. Wolfgang Sommer (Pfarr, 2013). The guide cannula implantations into the CAG-LacZ rats and the wild type littermates of the cFos-LacZ rats were performed by Manuela Klee at the Institute of Psychopharmacology, Central Institute of Mental Health, Mannheim. Operant conditioning training for the CAG-LacZ rats and the wild type rats was performed by Jana Zell under my supervision at the Institute of Psychopharmacology, Central Institute of Mental Health, Mannheim.

3.1.2 Results

3.1.2.1 Daun02 permanently inactivates neurons via induction of neurodegeneration

Although the Daun02 method was used to inactivate and study various neuronal ensembles in several brain areas (Koya et al., 2009; Bossert et al., 2011; Cruz et al., 2013; Cruz et al., 2014), the mechanism of action of Daun02 inactivation of LacZ expressing cells was still unclear (Bashir and Banks, 2017). One possible mechanism of action is temporal silencing of neurons by inhibition of calcium channels, which would lead to reduced excitability (Santone et al., 1986; Engeln et al., 2016). Another possible mechanism of action is permanent

inactivation of LacZ expressing neurons by induction of apoptosis (Mortensen et al., 1992; Jantas and Lason, 2009). In order to identify the mechanism of action of Daun02 we used a new transgenic rat line, the CAG-LacZ line, which constitutively expresses LacZ (Weber et al., 2011). Injection of Daun02 into this rat leads to non-selective inactivation of the entire brain area. To test the apoptosis hypothesis, we injected CAG-LacZ rats with 2µg Daun02, 2µg Daun02 + 80ng Z-VAD-FMK or vehicle alone into the mPFC. Z-VAD-FMK is a general caspase inhibitor with anti-apoptotic properties (Hara et al., 1997). Three days after injection, the animals were killed, transcardially perfused and mPFC brain sections were stained with Fluorojade B to detect degenerated neurons (Schmued and Hopkins, 2000). We found that Daun02 injection induced massive neurodegeneration, which was almost completely prevented by Z-VAD-FMK ($F_{(1,18)}$ = 54.8, $p < 0.001$; Figure 26). These results show that Daun02 inactivation of β-gal-expressing neurons involves apoptotic mechanisms. Therefore Daun02 inactivation is a permanent method.

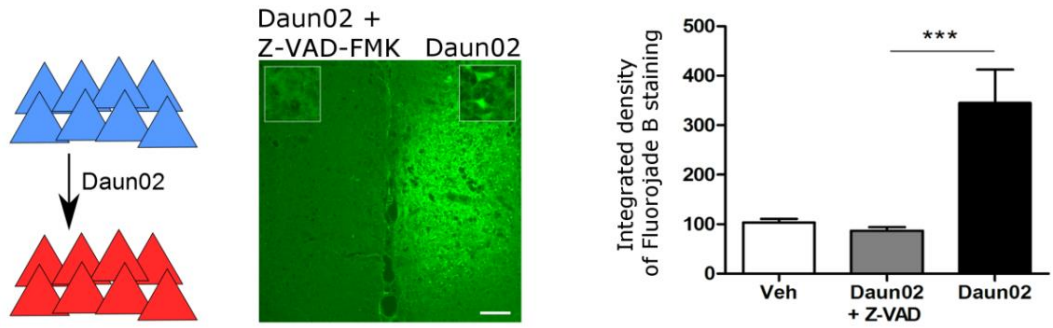

Figure 26: Characterization of Daun02 inactivation in pCAG-lacZ rats. Representative image of Daun02 and Daun02 + Z-VAD-FMK injections into the mPFC of pCAG-lacZ rats. Scale bar, 300µm. Green fluorescence represents Fluorojade-B signal, labeling neurodegeneration. Massive neurodegeneration was induced by Daun02 injections, whereas there was less neurodegeneration at the Daun02 + Z-VAD-FMK injection site. Integrated density measurement of Fluorojade-B signal in mPFC (mean ± SEM, n = 30 sections/group) revealed that the combination of Daun02 + Z-VAD-FMK significantly reduced neurodegeneration. ***$p < 0.001$. For detailed statistics, see Results. Adapted from (Pfarr et al., 2015).

3.1.2.2 Selective, but not non-selective Daun02 inactivation of the IL induces excessive alcohol seeking behavior

In order to investigate the role of IL neuronal ensembles in cue-induced alcohol seeking behavior, we used cFos-LacZ and CAG-LacZ rats for specific and non-specific Daun02 inactivation. Following acquisition of alcohol self-administration and cue-conditioning, the

two cohorts of rats were ranked based on their baseline response rate at the active lever and assigned into separate prospective Daun02 and control groups (cFos-lacZ: n = 10 vs11, $F_{(1,19)}$ = 1.214, n.s.; pCAG-lacZ: n = 7/group, $F_{(1,11)}$ = 0.618, n.s.). Next, all rats underwent extinction training resulting in <10 responses at the active lever, followed by guide cannula implantation to target the IL, and tested after 1 week of recovery for cue-induced reinstatement (RE1), which served to activate cue-responsive neurons. All cFos-lacZ and pCAG-lacZ animals showed a significant increase in responding between the last extinction session and cue-induced reinstatement of alcohol seeking (RE1) (two-way repeated-measures ANOVA; cFos-lacZ rats: main effect of sessions, $F_{(1,19)}$ = 14.8, p = 0.001; of prospective group assignment, $F_{(1,19)}$ = 0.1, n.s., and interaction, $F_{(1,19)}$ = 0.04, n.s.; Newman–Keul's *post hoc* test extinction vs RE1 $p < 0.001$ for both groups; pCAG-lacZ rats: session, $F_{(1,11)}$ = 55.3, p < 0.001; group, $F_{(1,11)}$ = 0.3, n.s., and interaction, $F_{(1,11)}$ = 0.06, n.s.; *post hoc* test for both groups $p < 0.05$; Figure 27A+B). Ninety minutes after the beginning of the first reinstatement session (RE1), all animals received their respective vehicle or Daun02 microinjections (Figure 27C+D show respective cannula placements). The animals were then returned to their home cages for 3 d before being tested on a second cue-induced reinstatement (RE2). Selective inactivation of IL cue-responsive neurons by Daun02 in cFos-lacZ rats caused a significant increase in alcohol-seeking responses in the Daun02 group, but not in the control group (Figure 27A). Two-way repeated-measures ANOVA confirmed a significant main effect of the sessions ($F_{(1,19)}$ = 18.2, p < 0.001) and a significant interaction ($F_{(1,19)}$ = 10.05, p < 0.01), but no significant effect of treatment ($F_{(1,19)}$ = 3.71, p = 0.069). The *post hoc* test revealed a significant difference between RE1 versus RE2 for the Daun02 group (p < 0.001) but not for the control group (p > 0.05; Figure 27A). Interestingly, nonselective inactivation of IL neurons in CAG-lacZ rats had no significant effect on alcohol-seeking behavior (two-way repeated-measures ANOVA: effect of session, $F_{(1,1)}$ = 2.2, n.s.; treatment, $F_{(1,11)}$ = 0.003, n.s.; and interaction, $F_{(1,11)}$ = 0.272, n.s.; Figure 27B). Inactive lever presses and cannula placements are illustrated in Figure 27C for cFos-LacZ and Figure 27D for CAG-LacZ rats. Thus, only task-specific inactivation of cue-responsive neurons leads to excessive alcohol seeking in a cue-induced reinstatement paradigm, whereas a nonspecific lesion did not affect alcohol seeking. Consequently, the resulting deficits from a global lesion of the IL can either be rapidly compensated by other brain regions or opposing processes within the IL could result in a zero net effect.

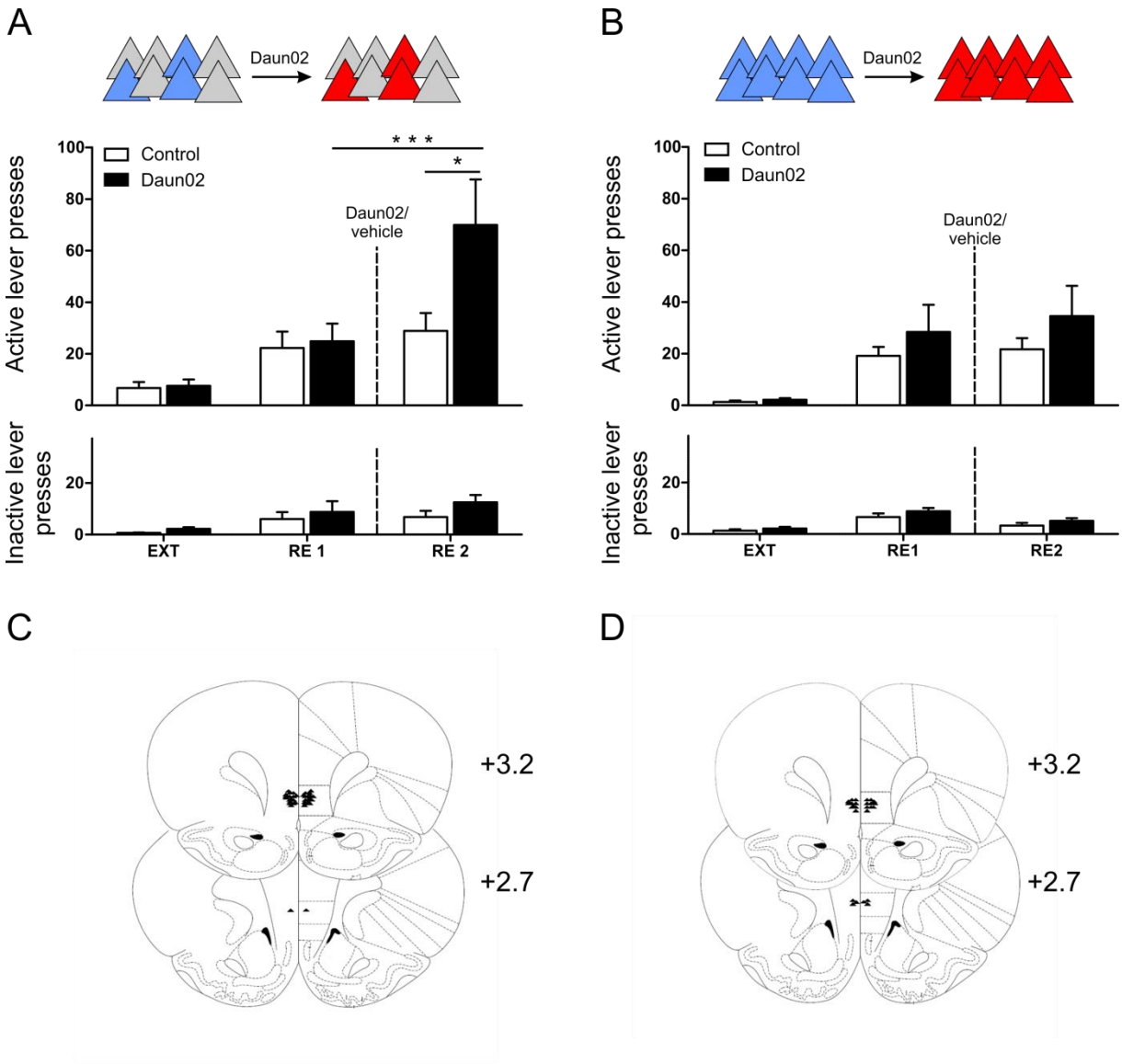

Figure 27: Effect of infralimbic Daun02 inactivation on alcohol-seeking behavior. Responses at the active and inactive lever (mean + SEM) are shown for extinction (EXT) as well as reinstatement before (RE1) and after (RE2) Daun02 injection. Grey triangles represent LacZ negative cells. Blue triangles represent LacZ expressing cells and red triangles represent inactivated cells. **A)** Daun02 microinjection into the IL of cFos-lacZ rats after RE1 resulted in a significant increase in alcohol seeking in RE2 (n = 10–11/group). There were no significant differences in inactive lever presses between the groups. **B)** Nonselective IL inactivation by Daun02 in pCAG-lacZ rats (n = 7/group) had no effect on reinstatement behavior. **C)** Injection site mapping of cFos-LacZ rats. **D)** Injection site mapping of CAG-LacZ rats. Approximate locations of the 28 gauge injection-cannula tips are indicated by small black triangles. Cannula placements were verified within the infralimbic cortex from +3.2 to +2.7 anterior to bregma (Paxinos and Watson, 1998). *p < 0.05; ***p < 0.001. For detailed statistics, see Results. Figure adapted from (Pfarr et al., 2015).

Using double fluorescent immunohistochemistry we showed that cue-induced reinstatement of alcohol seeking induces both cFos and LacZ expression in the mPFC of cFos-LacZ rats

(Figure 28A). In order to validate the Daun02 inactivation of cue-responsive neurons, we used two cFos-LacZ animals per group for X-gal immunohistochemistry after the second cue-induced reinstatement (RE2). Daun02 microinjections into the IL after the first cue-induced reinstatement (RE1) caused a significant decrease of β-gal-positive cells in the second reinstatement compared with the vehicle injected group ($t = 5.23$, $p < 0.01$; Figure 28B).

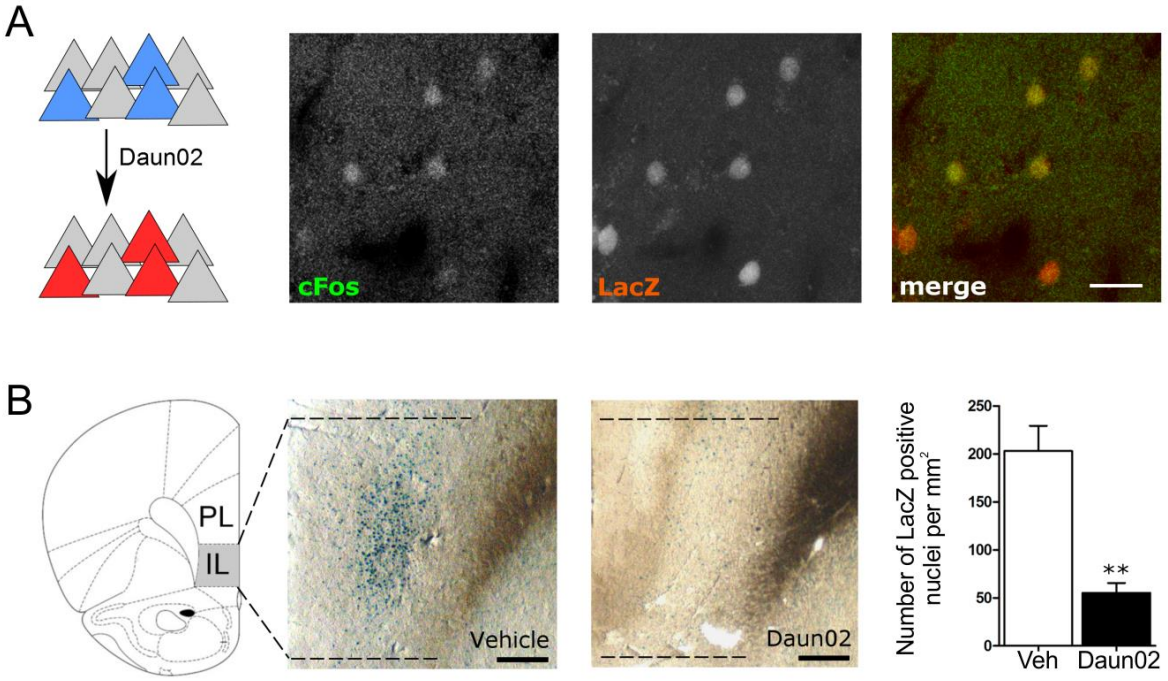

Figure 28: Activity-dependent Daun02 inactivation in cFos-lacZ rats. A) Exposure to alcohol-associated cues results in coexpression of cFos and lacZ in cFos-lacZ rats. Scale bar, 20µm. **B)** Representative X-Gal staining of lacZ-positive cells in the IL region of cFos-lacZ rats after RE2. Scale bar, 300µm. Drawing of coronal section adapted from Paxinos and Watson (1998). Quantification of LacZ-positive nuclei after RE2 showed a significant reduction in cFos-lacZ rats after Daun02 treatment compared with vehicle. **p < 0.01. Figure taken from (Pfarr et al., 2015).

3.1.2.3 Effect of IL Daun02 inactivation in cFos-LacZ rats is permanent

In previous studies the Daun02 effect was only followed up for 3 days after inactivation (Koya et al., 2009; Bossert et al., 2011). Due to our previous finding, that Daun02 induces apoptosis in neurons, we hypothesized that the effect of Daun02 on alcohol seeking behavior should be long lasting. Therefore the remaining cFos-LacZ rats were tested on two additional cue-induced reinstatement tests (RE3 and RE4, days 7 and 14 post-Daun02 infusion). As

expected, there were no differences in alcohol-seeking behavior between sessions RE2 and RE4 (two-way repeated-measures ANOVA: effect of treatment, $F_{(1,15)} = 5.41$, $p < 0.05$; session, $F_{(2,30)} = 0.01$, n.s.; and interaction, $F_{(2,30)} = 0.29$, n.s.; Figure 29). Thus, the behavioral effects of Daun02 lesions last at least for 2 weeks.

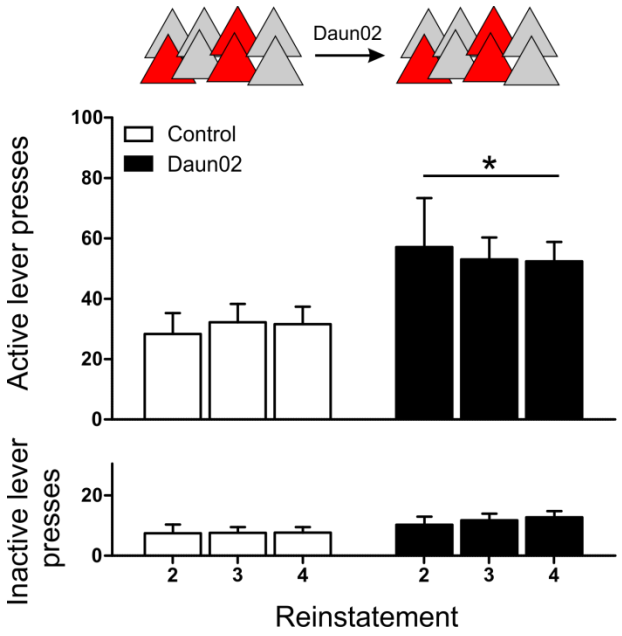

Figure 29: Permanent increase in alcohol seeking after IL Daun02 inactivation in cFos-LacZ rats. The increase in alcohol seeking in the cFos-lacZ rats after Daun02 treatment persists for at least 2 weeks (RE 2 same as in Figure 27A), RE3 at 7, and RE4 at 14 days after RE1 (n = 8–9/group). There was no significant difference between the groups in inactive lever presses. Data is expressed as mean ± SEM. *p < 0.05. Figure adapted from (Pfarr et al., 2015).

3.1.2.4 Neuronal circuits for cue- and stress-induced reinstatement of alcohol seeking differ in the IL

Apart from the exposure to alcohol conditioned cues, a reinstatement of alcohol seeking can be also elicited by exposure to stress (Lê et al., 1998; Liu and Weiss, 2002; Martin-Fardon and Weiss, 2013). The IL is known to integrate information from various brain areas including those that process emotional states. Therefore we asked, whether the previously inactivated ensemble, involved in cue-induced reinstatement of alcohol seeking would be also involved in the processing of stress-induced reinstatement of alcohol seeking. To do so, the

cFos-LacZ animals from the previous experiment were exposed to 10 min of intermittent footshocks before the beginning of the reinstatement session. The baseline responses from the previous experiment were 30.8 ± 6.2 for the control and 32.5 ± 4.9 for the Daun02 group. Both the control and the Daun02 group significantly increased their active lever presses in the stress-induced reinstatement compared with their extinction performance, however, there was no significant difference between the groups (two-way repeated-measures ANOVA: main effect of the sessions, $F_{(1,11)} = 31.57$, $p < 0.001$; treatment, $F_{(1,11)} = 0.51$, n.s.; and interaction, $F_{(1,11)} = 0.33$, n.s.; Newman–Keul's *post hoc* test: $p < 0.05$ extinction vs reinstatement session for both groups; Figure 30). Thus, the response to stress involves different neuronal substrates than the ones processing specific alcohol associated cues.

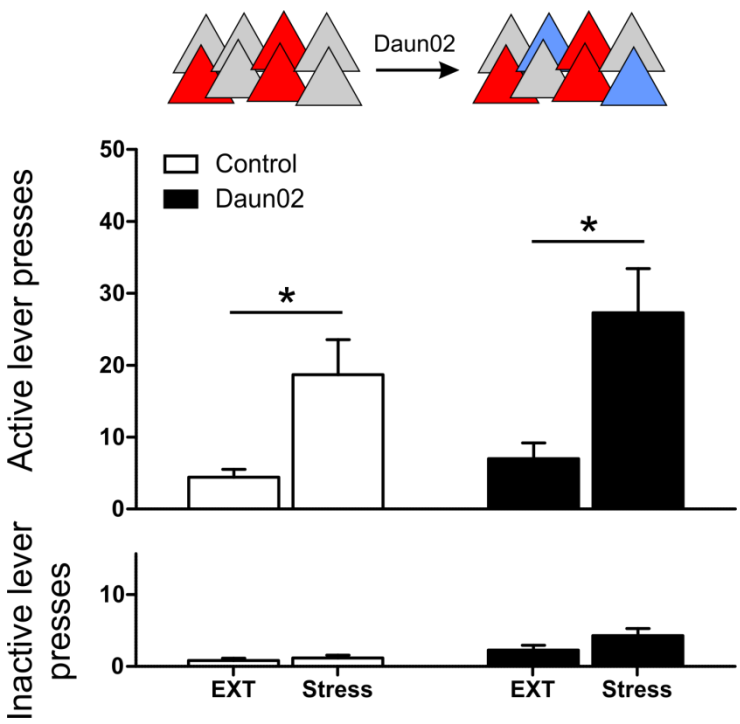

Figure 30: Cue-responsive neurons in the IL are not involved in stress-induced reinstatement of alcohol seeking. There was no significant difference between the groups in active lever presses and inactive lever presses in a footshock stress-induced reinstatement session. *p < 0.05. For detailed statistics see Results. Figure adapted from (Pfarr et al., 2015).

3.1.2.5 Cue-responsive neurons involved in alcohol seeking are not involved in alcohol self-administration

Because the same set of olfactory and visual cues was used in alcohol self-administration and cue-induced reinstatement sessions, we tested both groups of animals from the previous experiments again on their alcohol self-administration performance. During five consecutive alcohol self-administrations sessions, there was no significant difference in active lever responses between the groups (Figure 31). Repeated measures ANOVA analysis of the alcohol self-administration data with the treatment group as a between group factor and the five self-administration sessions as within group factors revealed no significant effects of treatment [$F_{1,15} = 0.498$, $p > 0.05$], time points (self-administration sessions 1-5) [$F_{1,15} = 2.293$, $p > 0.05$] or the interaction between treatment and the time points [$F_{1,15} = 0.737$, $p > 0.05$].

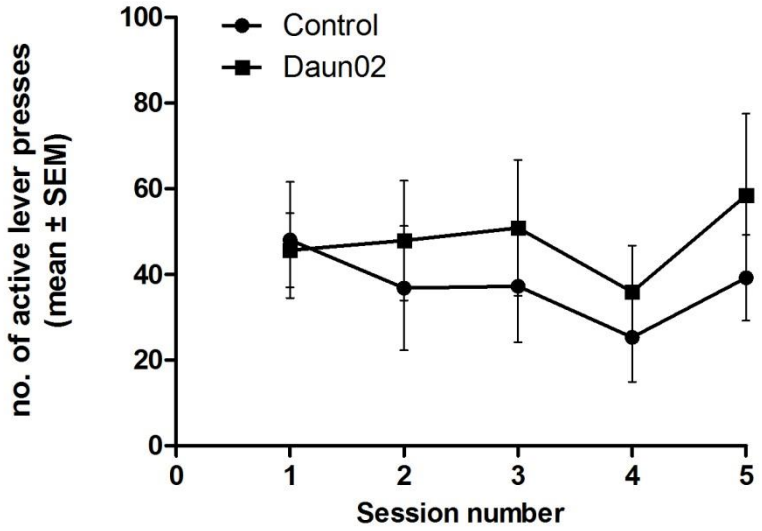

Figure 31: Neurons involved in the control of cue-induced reinstatement are not involved in self-administration. Mean ± SEM responses at the active lever are shown. Responses of the Control group (circles , n = 9) are compared to the Daun02 treated group (squares, n = 8). There was no significant difference between the groups.

3.1.2.6 Daun02 does not have unspecific side effects on behavior

To test for potential unspecific treatment effects, a group of wild-type littermates (n = 8) of cFos-lacZ rats, which do not express LacZ, underwent the reinstatement procedure as described before. As expected, neither vehicle injection into the IL after RE1 nor Daun02 after RE2 resulted in a significant change in lever pressing (baseline and extinction responding: 118.3 ± 15.6 and 7.8 ± 1.2, respectively, one-way repeated-measures ANOVA; $F_{(2,14)}$ = 0.41, n.s.; Figure 32). Therefore we confirm, that Daun02 is an inactive prodrug, which does not induce unspecific side effects on animal behavior in the absence of ß-galactosidase activity.

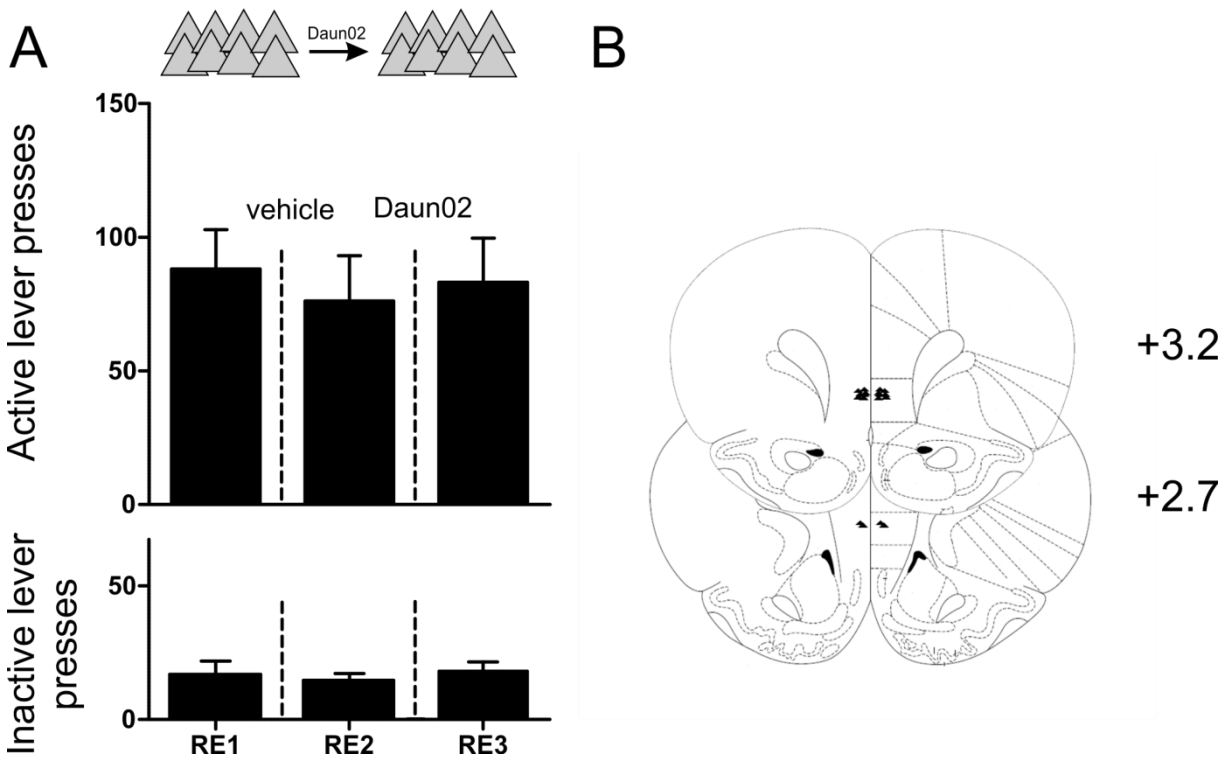

Figure 32: No unspecific effect of Daun02 on behavior. A) There was no significant difference in active and inactive lever presses in wild type littermates of cFos-LacZ rats (n=8) after IL vehicle or IL Daun02 injections. **B)** Cannula placements were verified within the infralimbic cortex from +3.2 to +2.7 anterior to bregma (Paxinos and Watson, 1998). Figure adapted from (Pfarr et al., 2015).

3.1.2.7 Selective inactivation of prelimbic neuronal ensembles have no effect on alcohol seeking behavior

The prelimbic cortex (PL) was found to be functionally distinct from the IL in behavioral control (Heidbreder and Groenewegen, 2003) and was previously found to have an opposing effect on cocaine seeking as compared to the IL (Peters et al., 2009). Apart from cocaine seeking, the PL was previously found to be involved in the expression of context-induced reinstatement of alcohol seeking (Willcocks and McNally, 2013). Therefore we next studied the role of neuronal ensembles in the PL on alcohol seeking behavior.

A separate cohort of cFos-lacZ rats was trained to self-administer alcohol and implanted with guide cannulae as described above. There were no differences in alcohol self-administration behavior between the prospective Daun02 and control groups (n = 7 vs 8, $F_{(1,13)} = 0.16$, n.s.). There was also no difference between the groups in their cue-induced reinstatement performance after extinction (two-way repeated-measures ANOVA: main effect of the sessions, $F_{(1,13)} = 79.14$, $p < 0.001$; treatment, $F_{(1,13)} = 0.09$, n.s; and interaction, $F_{(1,13)} = 0.2$, n.s.; *post hoc* test $p < 0.001$ extinction vs reinstatement for both groups; Figure 33). Daun02 treatment did not alter cue-induced reinstatement performance in the second test (RE2) (two-way repeated-measures ANOVA: main effect of treatment, $F_{(1,13)} = 0.63$, n.s.; session, $F_{(1,13)} = 1.89$, n.s.). There was a significant interaction effect ($F_{(1,13)} = 8.99$, $p < 0.05$) due to a decrease in responding in the control (*post hoc* test RE1 vs RE2, $p < 0.05$), but not in the Daun02 treated group. A Fluorojade B staining was performed with mPFC sections injected with Daun02 into the PL, to confirm degradation of neurons. Figure 34 shows fluorescent Fluorojade B signal, which labels apoptotic neurons in the PL of the cFos-LacZ animals. It can be also seen, that the signal is less dense as compared to the Daun02 injections into the constitutive CAG-LacZ line.

Because our previous experiment in wild-type littermates of the cFos-LacZ rats showed no indication for unspecific drug effects and because of the induction of apoptosis in the PL after Daun02 injection, we interpret the overall outcome of the PL experiment as a lack of treatment effect. This result sets alcohol apart from other drugs like cocaine or heroin which show a different involvement IL and PL in the seeking response (Fuchs et al., 2005; Peters et al., 2009; Bossert et al., 2011; Willcocks and McNally, 2013).

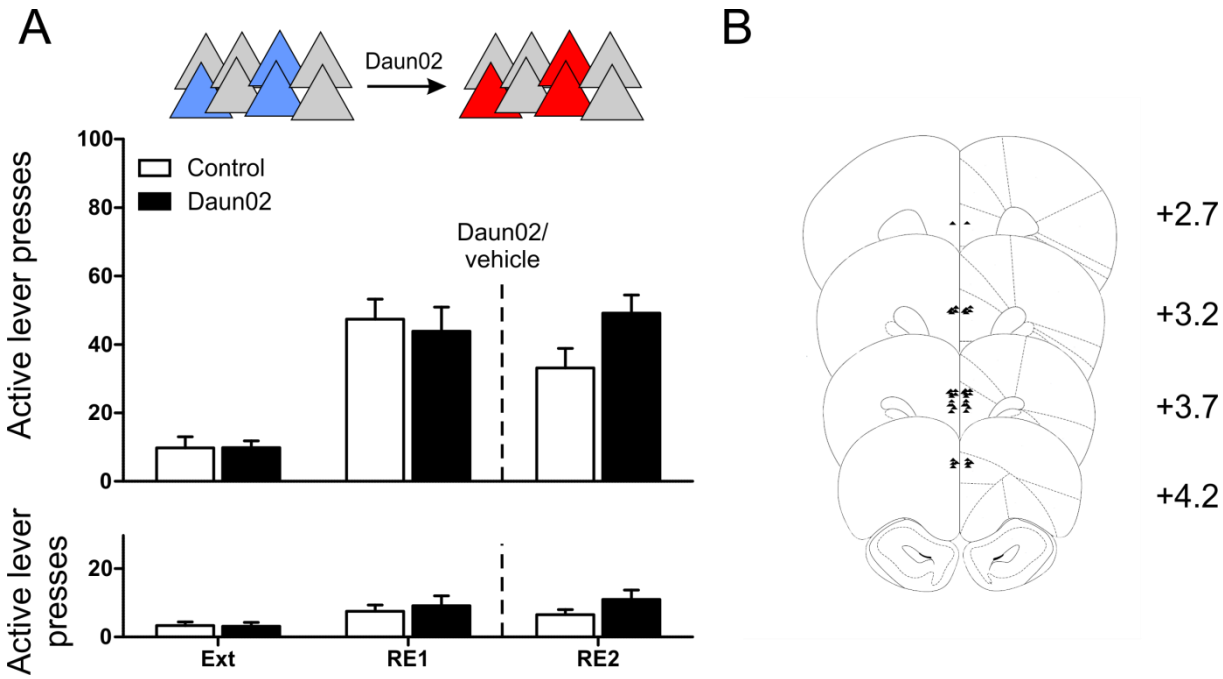

Figure 33: No effect of selective inactivation of PL ensembles on alcohol seeking. A) Daun02 microinjection into PL of cFos-lacZ rats after RE1 had no effect on active lever presses in RE2. There was no difference in inactive lever presses between the groups in extinction (EXT), RE1 or RE2. **B)** Cannula placements were verified within the infralimbic cortex from +4.2 to +2.7 anterior to bregma (Paxinos and Watson, 1998). Figure adapted from (Pfarr et al., 2015).

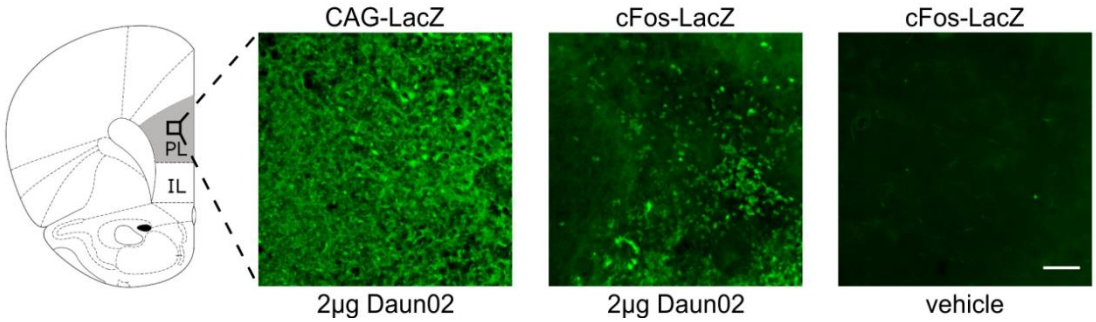

Figure 34: Neurodegeneration induced by Daun02 in CAG-LacZ and cFos-LacZ rats. Representative images of Flurojade-B stainings are shown for cFos-LacZ rats after cue-induced reinstatement and for CAG-LacZ rats. 2 µg Daun02 injections into the PL of CAG-LacZ rats induced massive neurodegeneration. Daun02 infusions into cFos-lacZ rats after cue-induced reinstatement caused less, therefore specific neurodegeneration. Vehicle injections into cFos-lacZ rats caused no neurodegeneration. Scale bar, 25 µm. Figure adapted from (Pfarr et al., 2015).

3.1.2.8 Cell types participating in IL neuronal ensemble

To further characterize the cue responsive neurons in the mPFC, eight cFos-lacZ rats were killed 90 min after a cue-induced reinstatement session and brain sections were double-stained for cFos and cell-type-specific markers (NeuN, GAD67 or CamKinaseII as pan-neuronal, GABAergic and glutamatergic projection neuron markers, respectively; Figure 35A). Co-localization analysis demonstrated that both in the IL and PL regions somewhat >10% of all neurons are cFos-positive, and more than two-thirds of those belong to the glutamatergic class (Figure 35B). In line with similar studies (Bossert et al., 2011; Cruz et al., 2014), cue responsive neuronal ensembles are formed by a small but substantial number of neurons in a given brain region.

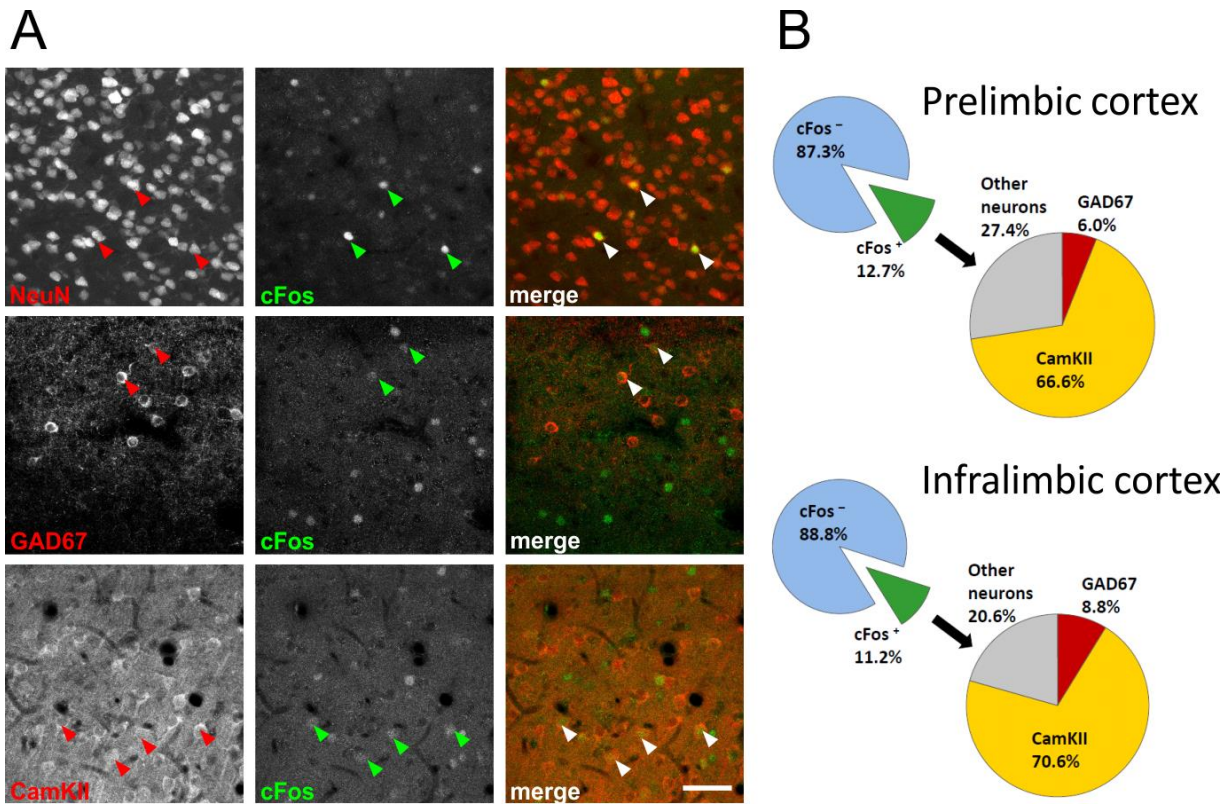

Figure 35: Characterization of cue-responsive neurons in the prelimbic and infralimbic cortex of cFos-lacZ rats after cue-induced reinstatement of alcohol seeking. A) Representative images of cFos and NeuN (top row), cFos and GAD67 (middle row), cFos and CaMKII (bottom row) double-labeling are shown. Scale bar, 50 µm. Arrows indicate colocalization. **B)** Quantification of double-labelings of the PL neurons, 12.7% were cFos-positive; 6% of the cFos-positive neurons were GAD 67-positive, and 66.6% of all cFos-positive neurons were CaMKII-positive; 11.2% of all IL neurons were cFos-positive; 8.8% of the cFos-positive neurons were GAD67-positive, and 70.6% of the cFos-positive neurons were CaMKII-positive. Figure taken from (Pfarr et al., 2015).

3.1.3 Summary

In Study 1, we identified an inhibitory neuronal ensemble in the IL of cFos-LacZ transgenic rats, which is involved in the control over alcohol seeking behavior. Pharmacogenetic ablation of this ensemble using the Daun02 inactivation technique resulted in excessive cue-induced alcohol seeking behavior. The identified neuronal ensemble consisted of ~11% if IL neurons, the majority belonging to the glutamatergic projection neuron class and only a minority belonging to the class of inhibitory interneurons. After further characterization of the identified IL neuronal ensemble, we found that neuronal substrates for cue-induced and stress-induced reinstatement of alcohol seeking behavior differ in the IL, as the animals only showed excessive alcohol seeking behavior in a cue-induced, but not stress-induced reinstatement of alcohol seeking behavior. Furthermore, the identified ensemble, involved in cue-induced reinstatement of alcohol seeking was not involved in alcohol self-administration. Opposed to a selective inactivation of neuronal ensembles, a general inactivation of the IL, using the constitutive CAG-LacZ line had no effect on alcohol seeking behavior.

Although the cFos response in the PL after cue-induced reinstatement of alcohol seeking was comparable to the cFos response in the IL, there was no effect of Daun02 inactivation in the PL of cFos-LacZ rats on alcohol seeking behavior. Using CAG-LacZ rats, we furthermore clearly identified the induction of apoptosis as the underlying mechanism of action of the Daun02 inactivation method.

3.2 Study 2: Characterization of infralimbic neuronal ensembles involved in alcohol and saccharin seeking behavior

This study contains experiments published in the *Journal of Neuroscience* with the title "Choice for drug or natural reward engages largely overlapping neuronal ensembles in the infralimbic prefrontal cortex", as well as additional experiments characterizing neuronal ensembles involved in alcohol and saccharin seeking.

3.2.1 Introduction

In Study 1, we identified a functional neuronal ensemble in the infralimbic cortex (IL), involved in the control of cue-induced alcohol seeking behavior (Pfarr, 2013; Pfarr et al., 2015). Other IL ensembles have been identified for context- or cue-induced seeking of other drugs or natural rewards (Bossert et al., 2011; Cruz et al., 2015; Suto et al., 2016; Warren et al., 2016). Although there is evidence, that several neuronal ensembles could co-exist in the same brain area (Schwindel and McNaughton, 2011), comparisons between several studies are difficult because of differences in experimental setup or batch- and strain differences of the animals used. Therefore we first established a two-reward operant conditioning model for the concurrent self-administration of ethanol as a drug and saccharin as a natural reward. First, we tested for differences in projection target areas of activated neurons upon cue-induced alcohol or saccharin seeking, using a combination of retrograde tracing and cFos immunohistochemistry. In order to answer the question, if both ensembles in the IL are distinct, overlapping or partially overlapping, we used the two-reward operant conditioning protocol in combination with double cFos fluorescent in-situ hybridization (FISH). This technique enabled us to specifically label cue-responsive neurons for alcohol and saccharin within the same animal.

The set-up of the two-reward operant conditioning model was done in collaboration with Elisabeth Paul at the Institute of Psychopharmacology at the Central Institute of Mental Health, Mannheim. Immunohistochemistry, image acquisition and analysis of the retrograde tracer experiment were done by Marion Schmitt and Christoph Körber from the Institute of Anatomy and Cell Biology at Heidelberg University. Operant training of the animals for FISH experiments and analysis of FISH experiments was done by Laura Schaaf at the Central

Institute of Mental Health as part of her Master Thesis under my supervision (Schaaf, 2017). The bootstrap analysis of the double cFos FISH data was performed by Janine K Reinert from the Institute of Anatomy and Cell Biology at Heidelberg University.

3.2.2 Results

3.2.2.1 Set-up of two-reward operant conditioning protocol

In order to set-up the two-reward operant conditioning task for concurrent self-administration of ethanol and saccharin solutions, 16 male Wistar rats were trained to self-administer a 10% (v/v) ethanol solution. Following this, the animals were trained to self-administer a 0.04% (w/v) saccharin solution. The saccharin solution was adjusted to reach a similar lever response ratio as compared to 10% ethanol. This was necessary in order to prevent potential neuronal ensemble biases caused by motor activity effects, because typically Wistar rats respond more than 200 times per session under these conditions. Following acquisition of ethanol and saccharin self-administration, the animals underwent a random training sessions for ethanol or saccharin self-administration until a stable baseline (BL) for each reward was reached. Two counterbalanced progressive ratio (PR) sessions were performed between the random baseline sessions, to test for the animals' motivation to self-administer each reward. After reaching a stable self-administration baseline for each reward, the animals underwent five extinction (EXT) sessions, followed by a cue-induced reinstatement (RE) session for either ethanol or saccharin. Three animals were excluded from analysis, because they failed to reach the criterion for successful reinstatement (>15 lever presses per session).

As can be seen in Figure 36A and Table 6, there were no significant differences in active lever presses in baseline and extinction training. After five days of extinction all animals reached the criterion of < 10% lever presses of the respective baseline responding for each reward. There was a significant increase in active lever responding in cue-induced reinstatement for each reward. However the animals responded significantly more at the active lever for ethanol seeking compared to saccharin, indicating that 10% ethanol is more rewarding under reinstatement conditions, compared to 0.04% saccharin. This is consistent with the PR test, where the animals had a significantly higher breakpoint for ethanol compared to saccharin ($t=-4.38$, $p=0.0009$, $n=13$, two-tailed paired t-test, Figure 36C).

Inactive lever responses are illustrated in Figure 36B and the respective detailed statistics are displayed in Table 6. There was a significant difference in baseline and cue-induced reinstatement responding for the ethanol and saccharin reward. There was no significant difference between inactive lever presses during extinction for both rewards. Independent of the presented reward, all animals responded more often at the active than at the respective inactive lever (Figure 36, Table 6), which demonstrates that the animals successfully acquired the behavioral contingencies and are able to discriminate between the two rewards and the associated cues.

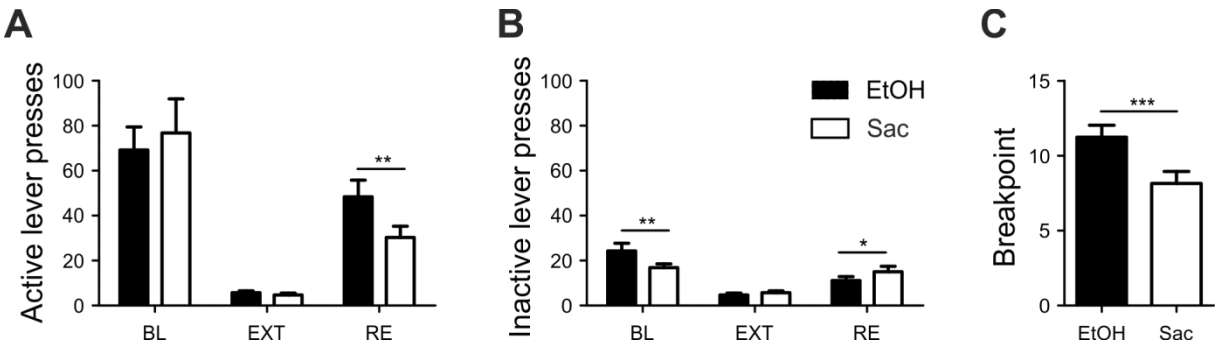

Figure 36: Set-up of two reward operant conditioning task. A) Active lever presses during baseline self-administration (BL), extinction (EXT) and cue-indued reinstatement (RE) of ethanol (black bars) and saccharin (white bars). **B)** Inactive lever presses forBL, EXT and RE. **C)** Progressive ratio test: *$p < 0.05$; **$p < 0.01$; ***$p < 0.001$. For detailed statistics, see Table 6. Figure taken from (Pfarr et al., 2018).

Table 6: Statistics for set-up of two reward operant conditioning task. Results for repeated measures ANOVA and Newman-Keuls post hoc test are shown. Comparison between active and inactive lever was done using two-tailed paired t-test. Abbreviations: DF = degrees of freedom, F = F-value, p = p-value, t = t-value, BL = self-administration baseline, EXT = extinction, RE = cue-induced reinstatement, Sac = saccharin, EtOH = ethanol

Lever	Repeated measures ANOVA					Newman-Keuls post hoc test					t-test (comparison active/ inactive)	
	Test	DF	Effect	F	p	Within group comparison			Between reward comparison			
						reward	Test	p	Test	p	Test	p
active	BL, EXT	1, 24	**reward**	0.136	0.716						**EtOH**	
			Test-session	53.099	0.0001	**EtOH**	BL, EXT	0.0002	BL	0.559	BL	0.0002
			interaction	0.214	0.648	**Sac**	BL, EXT	0.0002	EXT	0.939	EXT	0.273
	EXT, RE	1, 24	**reward**	4.194	0.052							
			Test-session	61.623	0.0001	**EtOH**	EXT, RE	0.0001			RE	0.0001
			interaction	3.851	0.061	**Sac**	EXT, RE	0.001	RE	0.007		
inactive	BL, EXT	1, 24	**reward**	3.242	0.084						**Saccharin**	
			Test-session	51.616	0.0001	**EtOH**	BL, EXT	0.0001	BL	0.01	BL	0.0012
			interaction	3.873	0.06	**Sac**	BL, EXT	0.001	EXT	0.72	EXT	0.273
	EXT, RE	1, 24	**reward**	1.544	0.225							
			Test-session	43.587	0.0001	**EtOH**	EXT, RE	0.002			RE	0.0012
			interaction	1.419	0.245	**Sac**	EXT, RE	0.0001	RE	0.1		

3.2.2.2 Analysis of IL neuronal ensemble size for ethanol and saccharin reward

In order to determine the size of the neuronal ensembles activated during cue-induced reinstatement of saccharin or ethanol seeking, a second batch of 32 Wistar rats was trained on the newly established two-reward operant conditioning paradigm and ranked based on their cue-induced reinstatement performance, followed by stereotaxic retrograde tracer injections into the contralateral IL, prelimbic cortex (PL), nucleus accumbens (NAc) and ventral tegmental area (VTA). Five days after tracer injections, the animals underwent either an additional cue-induced reinstatement of 10% ethanol or 0.08% saccharin seeking, followed by perfusion 90min after the start of the reinstatement session. Four animals had to be excluded from analysis, because they failed to reach reinstatement criterion (>15 active lever responses in 30 min). Active and inactive lever responses for baseline (BL), extinction (EXT) and the first counterbalanced cue-induced reinstatement sessions for ethanol and saccharin (RE1+2) are shown in Figure 37A. Detailed statistics are shown in Table 7. There were no significant differences in active lever presses for both rewards in BL and EXT. Consistent with the previous Wistar batch (Figure 36A), the animals made significantly more active lever

responses in the cue-induced reinstatement (RE1+2) for ethanol, compared to saccharin (Figure 37A), however the animals made significantly more responses at the active compared to the respective inactive lever in all stages of the operant conditioning paradigm (Table 7). There were no significant differences in inactive lever responding for ethanol or saccharin in BL, EXT and RE1+2. After stereotaxic tracer injection, the difference in active lever responses for cue-induced reinstatement of ethanol and saccharin (RE3) seeking still persisted (Figure 37B). Also in RE3, there was no significant difference in inactive lever responses for each reward and the animals made significantly more responses at the respective active compared to the inactive lever (Figure 37B), demonstrating that the animals successfully learned the task and are able to discriminate between the rewards and associated cues. 90 minutes after the final cue-induced reinstatement for either ethanol or saccharin, the animals were perfusion and brains were processed for cFos and NeuN immunohistochemistry, detecting activated neurons and the total neuronal population, respectively (Figure 37C). Quantification of activated neurons revealed no difference in the activated neuronal population after saccharin or ethanol cue-induced reinstatement (saccharin: 15.32% ± 0.63%, ethanol: 14.9% ± 0.58%, $p = 0.63$, $n = 14$/reward; Figure 37D). Thus, IL neuronal ensembles involved in ethanol and saccharin seeking are of similar size.

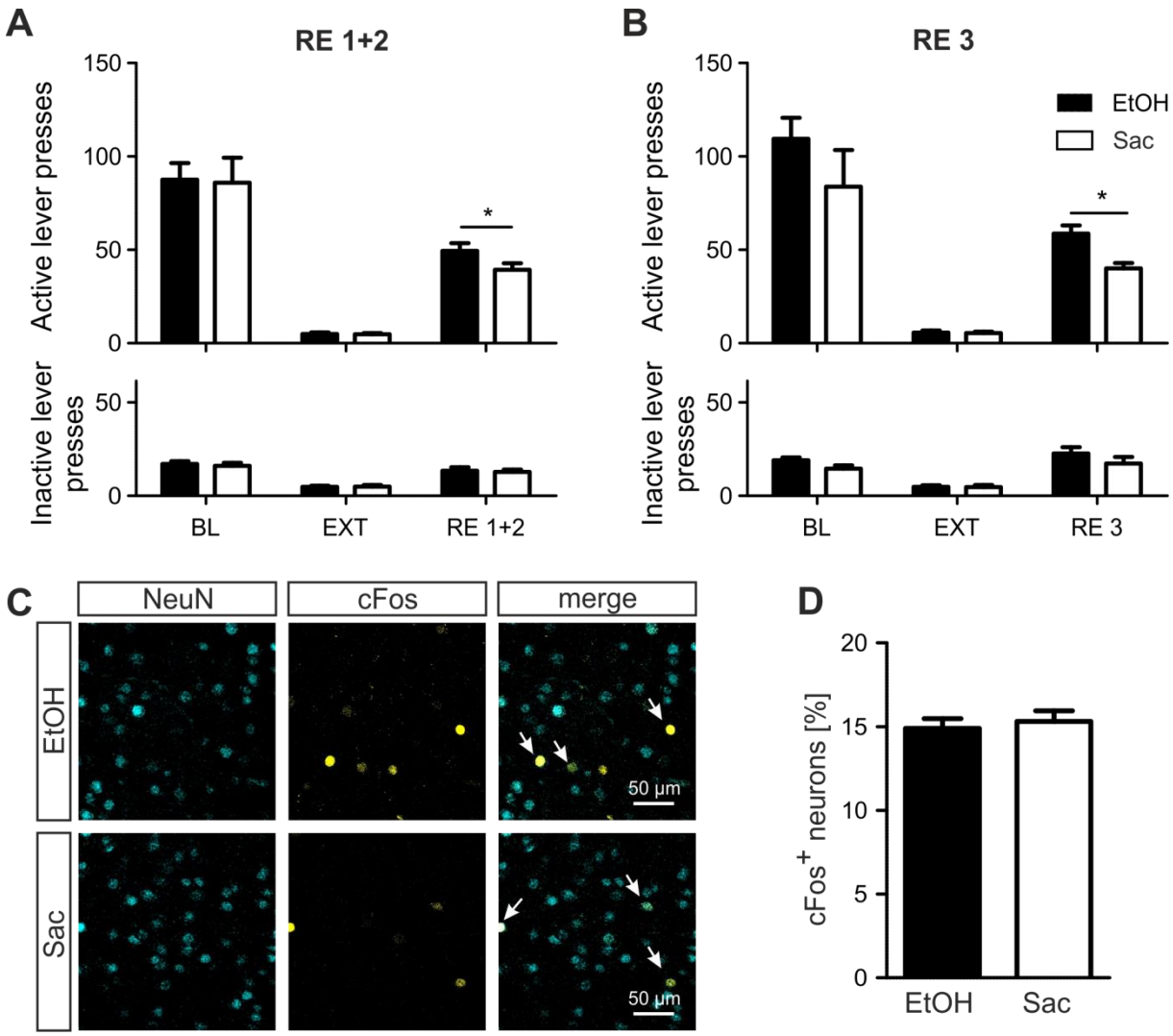

Figure 37: Neuronal ensembles involved in ethanol and saccharin seeking are of similar size. A, B) Active and inactive lever presses for ethanol and saccharin self-administration baseline (BL), extinction (EXT) and cue-induced reinstatement (RE) (B: RE1+2, C: RE3). **C)** Representative images of NeuN and cFos immuno double-labelling in the IL after ethanol and saccharin reinstatement (RE3). Arrows indicate co-localization. Kindly provided by Christoph Körber. **D)** Quantification of cFos and NeuN double labeled neurons in the IL, provided by Christoph Körber. Results are expressed as the fraction of double-labelled neurons (Data presented as mean ± SEM). *p < 0.05. For detailed statistics, see Table 7. Figure taken from (Pfarr et al., 2018).

Table 7: Statistics for two-reward conditioning of Wistar batch 2. Results for repeated measures ANOVA and Newman-Keuls post hoc test are shown. Comparison between active and inactive lever was done using two-tailed paired t-test. Abbreviations: DF = degrees of freedom, F = F-value, p = p-value, t = t-value, BL = self-administration baseline, EXT = extinction, RE = cue-induced reinstatement, Sac = saccharin, EtOH = ethanol

Lever	Repeated measures ANOVA					Newman-Keuls post hoc test					t-test (comparison active/ inactive)	
	Test	DF	Effect	F	P	Within group comparison			Between group comparison			
						reward	Test	p	Test	p	Test	p
Active RE 1+2	BL, EXT	1, 54	**reward**	0.01	0.917						**EtOH**	
			Test-session	107.94	0.0001	**EtOH**	BL, EXT	0.0001	BL	0.89	BL	0.0001
			Interaction	0.008	0.928	**Sac**	BL, EXT	0.0001	EXT	0.99	EXT	0.889
	EXT, RE 1+2	1, 54	**reward**	3.468	0.068							
			Test-session	205.14	0.0001	**EtOH**	EXT, RE1+2	0.0001			RE 1+2	0.0001
			interaction	3.246	0.077	**Sac**	EXT, RE1+2	0.0001	RE 1+2	0.01		
Inactive RE 1+2	BL, EXT	1, 54	**reward**	0.098	0.755						**Saccharin**	
			Test-session	159.09	0.0001	**EtOH**	BL, EXT	0.0002	BL	0.54	BL	0.0001
			interaction	0.422	0.518	**Sac**	BL, EXT	0.0001	EXT	0.93	EXT	0.889
	EXT, RE 1+2	1, 54	**reward**	0.029	0.865							
			Test-session	41.168	0.0001	**EtOH**	EXT, RE1+2	0.0002			RE 1+2	0.0001
			interaction	0.078	0.78	**Sac**	EXT, RE1+2	0.0002	RE 1+2	0.75		
active RE 3	BL, EXT	1, 26	**reward**	1.226	0.278						**EtOH**	
			Test-session	68.683	0.0001	**EtOH**	BL, EXT	0.0001	BL	0.12	BL	0.0001
			interaction	1.334	0.259	**Sac**	BL, EXT	0.0002	EXT	0.99	EXT	0.586
	EXT, RE3	1, 26	**reward**	9.576	0.005							
			Test-session	315.38	0.0001	**EtOH**	EXT, RE3	0.0001			RE3	0.0001
			interaction	13.967	0.0009	**Sac**	EXT, RE3	0.0001	RE3	0.0001		
inactive RE 3	BL, EXT	1 ,26	**reward**	2.367	0.136						**Saccharin**	
			Test-session	107.27	0.0001	**EtOH**	BL, EXT	0.0001	BL	0.02	BL	0.0026
			interaction	3.275	0.082	**Sac**	BL, EXT	0.0001	EXT	0.91	EXT	0.586
	EXT, RE3	1, 26	**reward**	1.16	0.291							
			Test-session	37.699	0.0001	**EtOH**	EXT, RE3	0.0002			RE3	0.0003
			interaction	1.101	0.304	**Sac**	EXT, RE3	0.004	RE3	0.14		

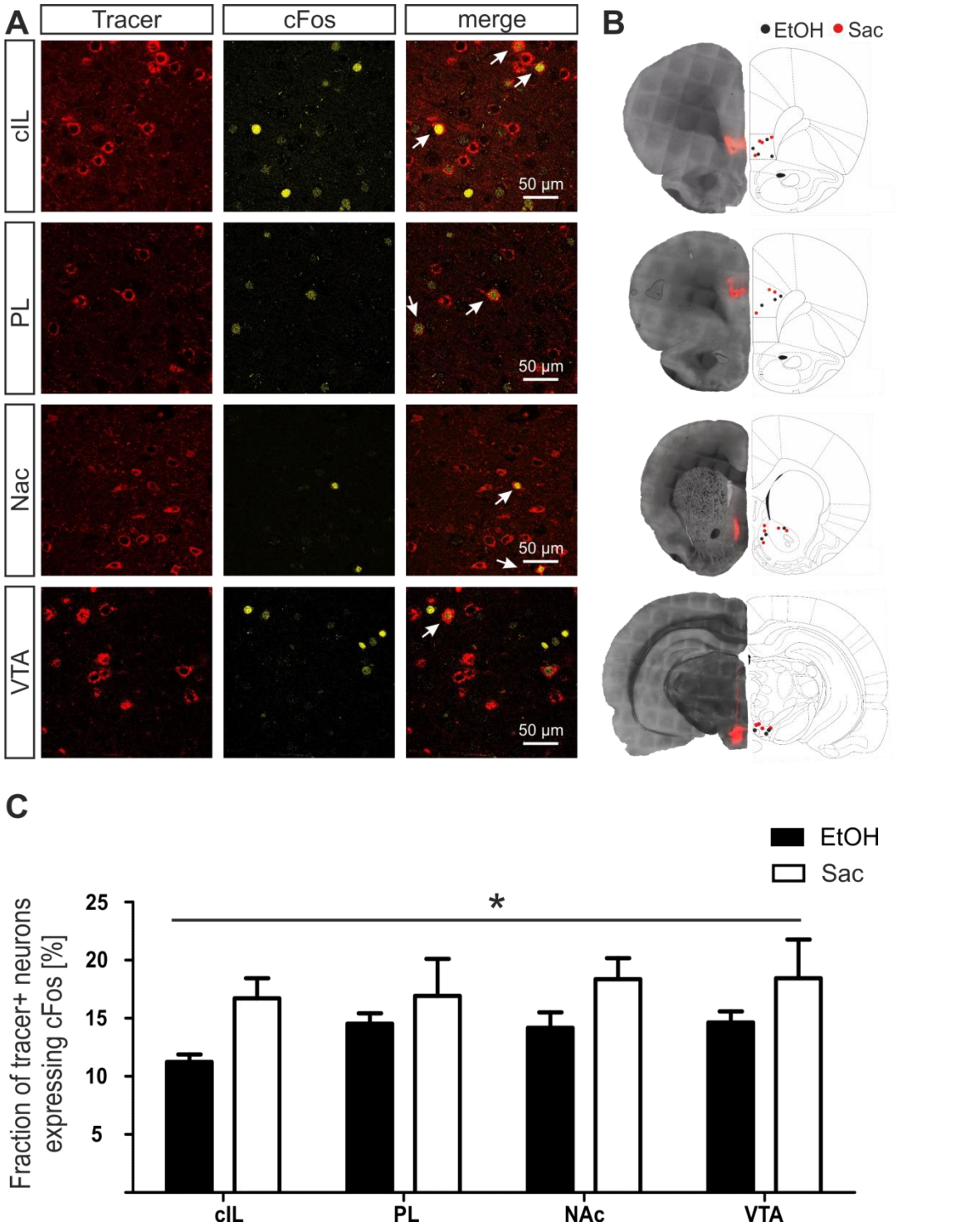

Figure 38: Activated IL projections during ethanol and saccharin seeking behavior. A) Representative images of retrograde tracer signals and cFos immunolabeling in the IL. From top to bottom colocalization of cFos with retrograde tracer signals from contralateral IL (cIL), ipsilateral prelimbic cortex (PL), nucleus accumbens (Nac) and ventral tegmental area (VTA). Arrows indicate co-localization. **B)** Injection placements are represented by black circles for ethanol and red circles for the saccharin group. Injection sites were verified in contralateral IL and PL+3.0mm anterior to bregma, Nac +1,6mm anterior to bregma and VTA -5.3 posterior to bregma, Adapted from (Paxinos and Watson, 1998). **C)** Quantification of the fraction of cFos positive tracer neurons (mean ± SEM) of activated IL projections during ethanol and saccharin seeking *$p < 0.05$. Figure taken from (Pfarr et al., 2018).

3.2.2.3 Analysis of projection targets of ethanol and saccharin cue-responsive neurons

In Study 3.1, we found that the majority of cue-responsive neurons involved in cue-induced reinstatement of ethanol seeking belong to the class of glutamatergic projection neurons (Pfarr et al., 2015). Even though the size of neuronal ensembles involved in ethanol and saccharin seeking is highly similar, we performed retrograde tracer injections into known projection targets of the IL (Figure 38B). Co-localization of retrograde tracer signals with the neuronal activity marker cFos revealed an overall significant difference in activated projections for ethanol compared to saccharin. Taking together all tracer injections from contralateral IL (cIL), prelimbic cortex (PL), nucleus accumbens (Nac) and ventral tegmental area (VTA), there was significantly more co-localization of IL cFos with the tracer signals in the saccharin group compared to the ethanol group (2-way ANOVA for reward x target: reward effect $F_{[1,27]}$ = 6.69, p=0.018; region effect $F_{[1,27]}$= 0.57, p=0.64; interaction $F_{[1,27]}$= 0.16, p=0.92; Figure 38A+C). Given, that there was no difference in the size of each IL ensemble (Figure 37D), our results indicate that ethanol cue-responsive neurons might engage a wider long-range network compared to saccharin cue-responsive neurons.

3.2.2.4 Analysis of ethanol and saccharin cue-responsive neurons in the IL using double cFos FISH

The previous experiments revealed that the IL ethanol and saccharin ensembles are of similar size and seem to engage different neuronal networks as indicated by differences in co-localization wit retrograde tracer signals from the contralateral IL, prelimbic cortex, nucleus accumbens and ventral tegmental area (Figure 38). In order to answer the question, if the respective ensembles are distinct, overlapping or partly overlapping it is necessary to activate and label both populations in the same animal. Therefore we combined our two-reward operant model with double cFos-fluorescent in-situ hybridization. 24 Wistar rats were trained on the two-reward operant protocol using 10% ethanol and 0.025% saccharin solution, including counterbalanced progressive ratio (PR) tests for each reward. Following extinction (EXT) training and counterbalanced cue-induced reinstatement sessions (RE1+2) for each reward, the animals were ranked based on their reinstatement performance and split into two groups. In the final reinstatement session, each animal underwent two 5min cue-induced reinstatement sessions for each reward, separated by a break of 30mins (RE3+4), followed by

decapitation immediately after the last 5min reinstatement session. The final reinstatement sessions were performed in a counterbalanced design, meaning half of the animals underwent cue-induced reinstatement of ethanol seeking first followed by cue-induced reinstatement of saccharin seeking and vice versa.

The time course for RE3 and RE4 was adapted from the cat-FISH experiments of Lin et al. (2011) in order to induce the spliced cFos mRNA species for RE3 and unspliced cFos mRNA species, labeling neurons activated during RE4. Both mRNA species can then be detected by double cFos fluorescent in-situ hybridization (FISH) using specific probes for spliced cFos mRNA and against intron1, which is present in the unspliced cFos mRNA isoform. This time course was also confirmed by a preliminary experiment, using mRNA extracted from IL tissue punches of six Wistar rats, which underwent a 5min cue-induced reinstatement session for ethanol seeking. Three animals were decapitated immediately after the 5min reinstatement session (RE), which should mainly induce unspliced cFos mRNA. Three animals were decapitated 30 minutes after the 5min reinstatement session (RE + 30min), which should mainly induce spliced cFos mRNA. Quantification of mRNA levels was done by quantitative TaqMan PCR, using probes for spliced cFos mRNA and intron1 of the unspliced cFos mRNA (Figure 40, Table 8). There was significantly more unspliced cFos mRNA after RE, compared to RE + 30min as confirmed by unpaired one-tailed t-test ($t_{1,4}$ = 2.27, p = 0.04, n=3/group, normalized to baseline cFos expression of control animals, Figure 40A). There was significantly more spliced cFos mRNA in the RE + 30min group compared to RE (unpaired one-tailed t-test: $t_{1,4}$ = 5.94, p = 0.002, n=3/group, normalized to baseline cFos expression of control animals, Figure 40A).

The lever responses from all animals before the final cue-induced reinstatement sessions are displayed in Figure 39A and full statistics are listed in Table 9. There were no significant differences in active lever presses for each reward in BL and EXT. Consistent with the previous experiments, the animals made significantly more active lever presses in cue-induced reinstatement of ethanol seeking compared to saccharin (RE1+2). There were no significant differences in inactive lever responses for each reward in BL, EXT and RE1+2. Consistent with the first experiment (Figure 36C) the animals had a significantly higher breakpoint for ethanol compared to saccharin ($t_{1,46}$=3.122, p=0.0031, two-tailed, paired t-test Figure 39B).

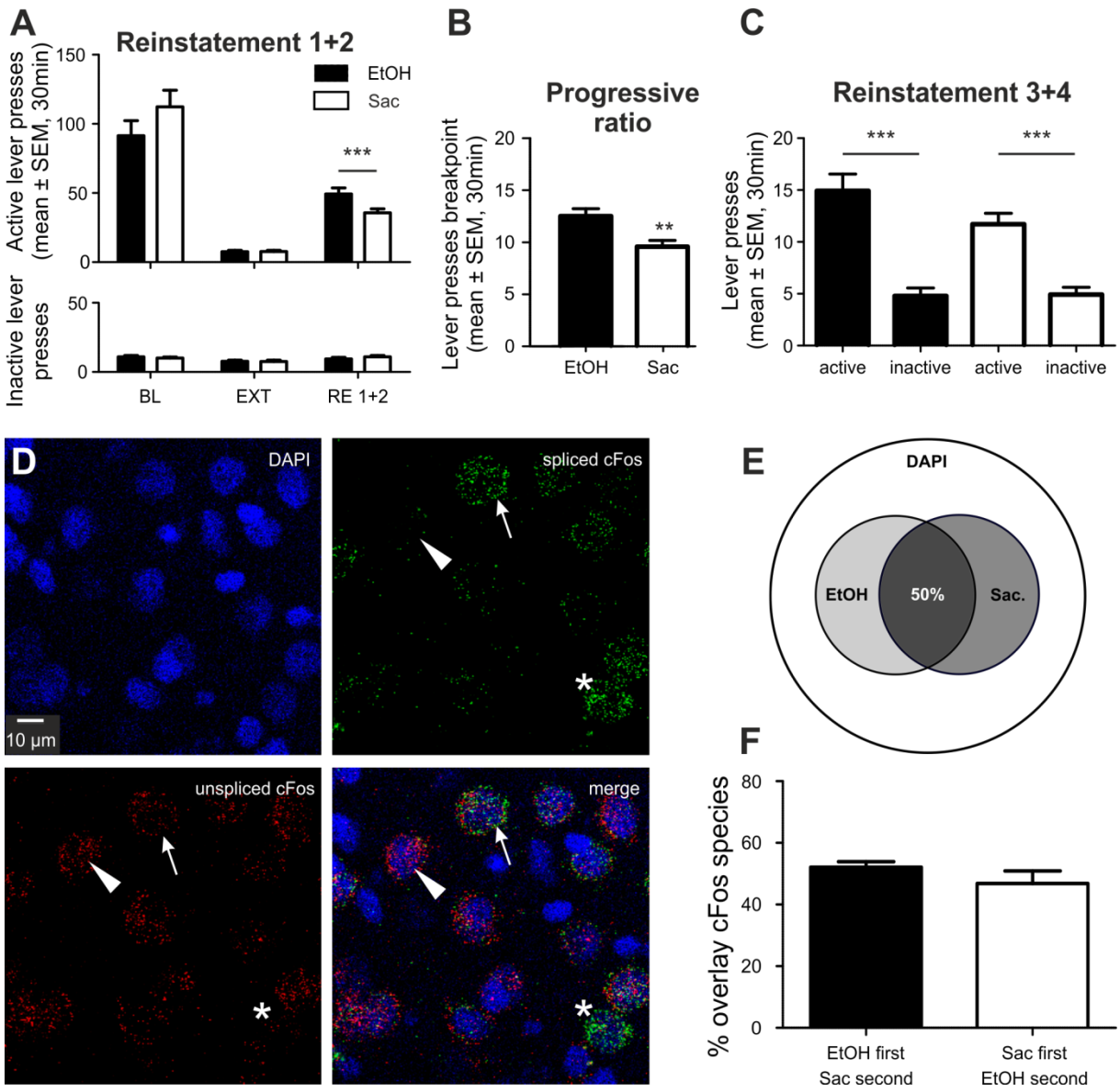

Figure 39: Double cFos FISH of IL ethanol and saccharin ensembles. A) Active and inactive lever presses (mean ± SEM) for ethanol and saccharin self-administration baseline (BL), EXT and RE1+2. **B)** Breakpoint analysis for the ethanol and saccharin rewards. **C)** Lever presses (mean ± SEM) for EtOH and saccharin in RE3+4. **D)** Representative images of double cFos in-situ hybridization for DAPI counterstaining, spliced and unspliced cFos. Arrows indicate a double positive cell, triangles indicate a single positive cell for unspliced Fos and asterisks indicate a single positive cell for spliced Fos only. **E)** Venn diagram indicating the size of saccharin and ethanol ensembles in relation to total cell number (DAPI). **F)** Quantification of overlay between both ensembles (mean ± SEM). *p < 0.05; **p < 0.01; ***p < 0.001. For detailed statistics, see Results and Table 9. Figure taken from (Pfarr et al., 2018).

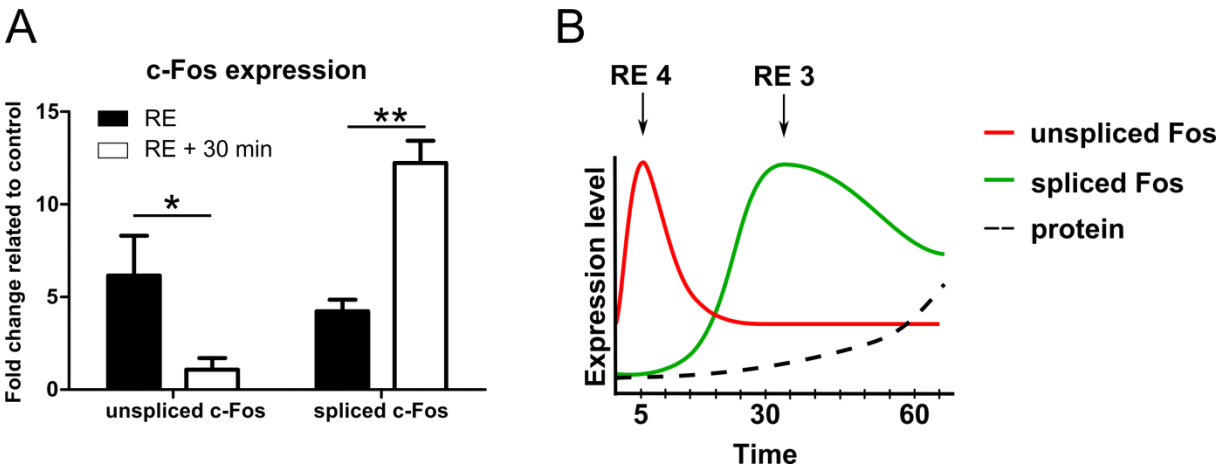

Figure 40: Expression time course of unspliced and spliced cFos isoforms. A) TaqMan analysis of unspliced and spliced cFos expression levels immediately after 5min cue-induced reinstatement (black bars, RE) or 30 minutes after a 5 min cue-induced reinstatement of ethanol seeking session (white bars, RE + 30min). Data are expressed as mean ± SEM fold change to control (animals undergoing no reinstatement test). **B)** Scheme of expression time courses of spliced and unspliced cFos mRNA isoforms as well as the cFos protein relative to activity controlled induction. Arrows indicate the chosen time-points for RE3 and RE4. Time courses are based on TaqMan results and (Lin et al., 2011). *p < 0.05; **p < 0.01. For ΔCT, ΔΔCT and fold change values see Table 8.

Table 8: ΔCT, ΔΔCT and fold change results for cFos TaqMan Assay.

Sample	Spliced ΔCT	Spliced ΔΔCT	Spliced fold change	Unspliced ΔCT	Unpliced ΔΔCT	Unspliced fold change
Control 1	8,16			12,09		
Control 2	8,19			16,89		
Control 3	8,07			12,80		
RE 1	5,92	-2,22	4,91	10,74	-3,18	10,12
RE 2	5,95	-2,19	4,79	12,27	-1,65	2,74
RE 3	6,41	-1,73	2,99	11,56	-2,37	5,60
RE + 25min 1	5,00	-3,14	9,84	14,52	0,60	0,36
RE + 25min 2	4,47	-3,67	13,48	13,19	-0,74	0,54
RE + 25min 3	4,48	-3,66	13,38	12,39	-1,53	2,34

Table 9: Behavioral statistics for double cFos FISH experiment. Results for repeated measures ANOVA and Newman-Keuls post hoc test are shown. Comparison between active and inactive lever was done using two-tailed paired t-test. Abbreviations: DF = degrees of freedom, F = F-value, p = p-value, t = t-value, BL = self-administration baseline, EXT = extinction, RE = cue-induced reinstatement, Sac = saccharin, EtOH = ethanol.

Lever	Repeated measures ANOVA					Newman-Keuls post hoc test					t-test (comparison active/ inactive)	
	Test	DF	Effect	F-value	P-value	Within group comparison			Between group comparison			
						reward	Test	p-value	Test	p-value	Test	p-value
active	BL, EXT	1,46	**reward**	1.547	0.219						**EtOH**	
			Test-session	146.81	0.0001	**EtOH**	BL, EXT	0.0001	BL	0.07	BL	0.0001
			interaction	1.771	0.189	**Sac**	BL, EXT	0.0001	EXT	0.99	EXT	0.949
	EXT, RE 1+2	1,46	**reward**	5.551	0.023							
			Test-session	176.80	0.0001	**EtOH**	EXT, RE1+2	0.0002			RE1+2	0.0001
			interaction	6.788	0.012	**Sac**	EXT, RE1+2	0.0001	RE	0.0009		
inactive	BL, EXT	1,46	**reward**	0.219	0.642						**Saccharin**	
			Test-session	16.127	0.0002	**EtOH**	BL, EXT	0.006	BL	0.48	BL	0.0001
			interaction	0.336	0.565	**Sac**	BL, EXT	0.049	EXT	0.95	EXT	0.949
	EXT, RE 1+2	1,46	**reward**	0.394	0.533							
			Test-session	7.285	0.009	**EtOH**	EXT, RE1+2	0.195			RE1+2	0.0001
			interaction	0.707	0.405	**Sac**	EXT, RE1+2	0.073	RE	0.31		

In order to specifically label the cell population activated during ethanol and saccharin seeking behavior, all animals underwent counterbalanced 5min cue-induced reinstatement sessions for each reward, separated by 30min (RE3+4). 14 animals successfully reinstated under these conditions and were included in the analysis. For each reward there was a significant difference in responses at the respective active and inactive lever (Two-tailed paired t-tests: EtOH: $t_{1,13} = 8.33$, $p = 0.0001$; saccharin: : $t_{1,13} = 7.01$, $p = 0.0001$; Figure 39C). The order of the rewards in RE3+4 did not influence the lever responses (EtOH first vs EtOH second: $t_{1,12} = 0.74$, $p = 0.48$; saccharin first vs. saccharin second: $t_{1,12} = 0.07$, $p = 0.95$; unpaired two-tailed t-tests), so responses from both groups were pooled for analysis.

All animals were decapitated immediately after RE4 and the brains were processed for double cFos FISH. Representative images of double cFos FISH are shown in Figure 39D. There were no significant differences in spliced cFos expression after ethanol or saccharin cue-induced reinstatement (25±1% vs. 23±2%, respectively; $t_{1,12}$=0.715, p=0.488, two-tailed, unpaired t-test). There was also no significant difference in unspliced cFos expression after ethanol or saccharin cue-induced reinstatement (49±2% vs. 51±2%, respectively; $t_{1,12}$=0.44, p=0.67,

two-tailed, unpaired t-test). Co-localization analysis revealed an overlap of 50% of both ensembles, regardless of the order of the rewards presented ($t_{1,12}$=1.190, p=0.257, unpaired two-tailed t-test, Figure 39E+F).

Bootstrap analysis of the double cFos FISH data confirmed, that the experimentally obtained distributions of cells expressing either both, one or none of the investigated cFos mRNA species are significantly different from a random sampled population. This confirms that our results are highly non-random and that the order of the reward in RE3 and RE4 does no influence the results (Figure 41).

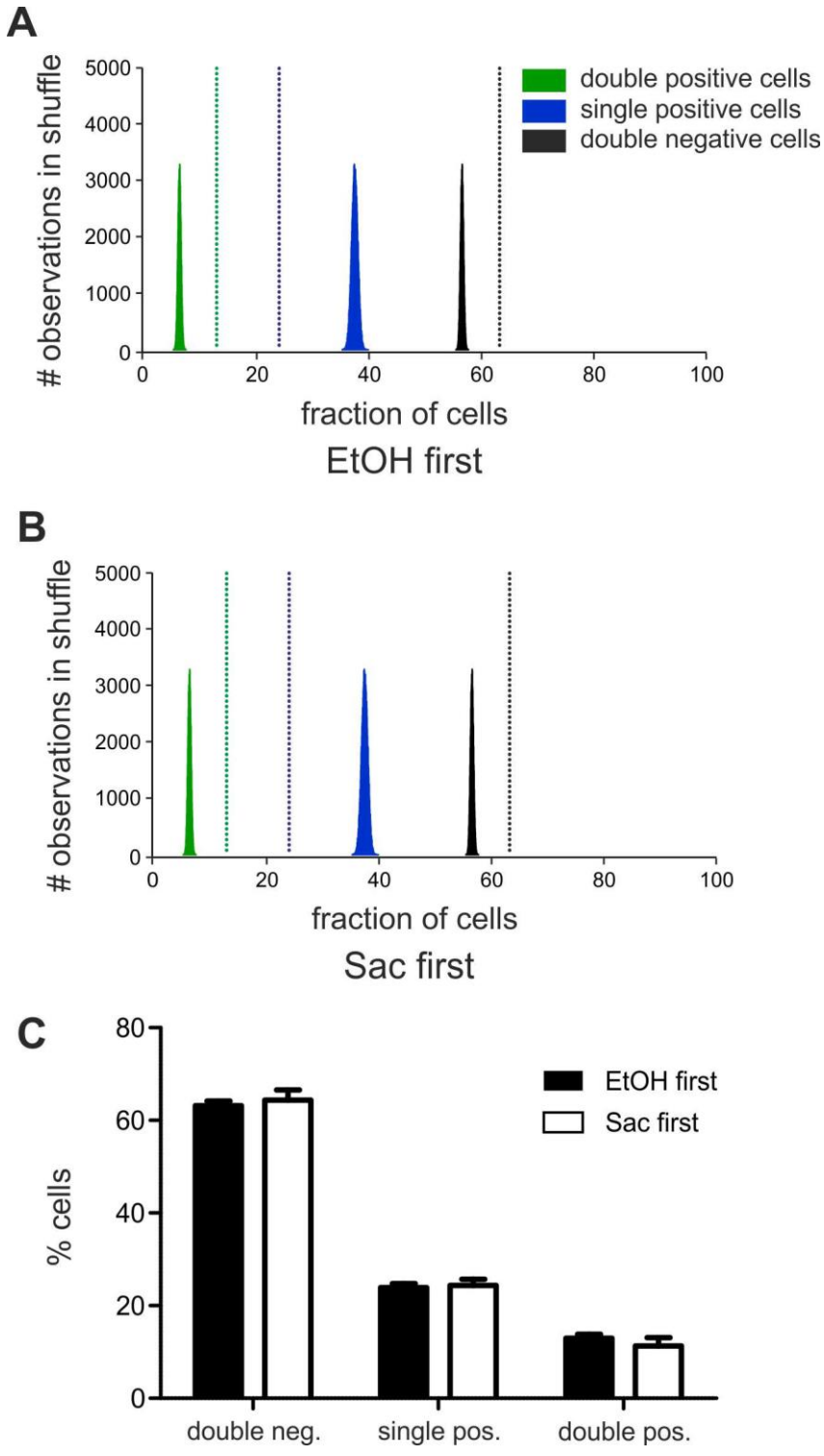

Figure 41: Bootstrap analysis of double cFos FISH. Bootstrap analysis confirms that neuronal IL ensembles activated by cue-induced reinstatement and detected by FISH against different Fos mRNA species are highly non-random, independent of the order of cues presented for reinstatement. **A, B)** Histograms of random distributions of cells expressing one, both or none of the Fos mRNA obtained by 100,000 shuffles. The vertical, dashed lines mark the fractions of cells experimentally determined. **C)** Quantification of cells expressing one, both or none of the Fos mRNA species, according to the reward reinstated first. Kindly provided by Janine K Reinert. Figure taken from (Pfarr et al., 2018).

3.2.2.5 Analysis of layer distribution of cue-responsive neurons involved in ethanol and saccharin seeking

In order to analyze, if there are differences in the cortical layer distribution of IL cFos activated by saccharin or ethanol conditioned cues, we performed FISH using a probe against spliced cFos and either RGS8 as a layer 2/3 marker or Bcl11b as a layer 5/6 marker (Figure 42 + Figure 43). Analysis was performed with seven animals, which underwent cue-induced reinstatement of ethanol seeking in RE3 and seven animals, which underwent saccharin reinstatement in RE3. There was no significant difference in the number of saccharin and ethanol cue-induced cFos in layer 2/3 (unpaired two-tailed t-test: $t_{1,12}$=0.24, p=0.81, Figure 42C). There was also no significant difference in cFos induced by either reward in layer 5/6 (unpaired two-tailed t-test: $t_{1,12}$=0.19, p=0.85, Figure 43C).

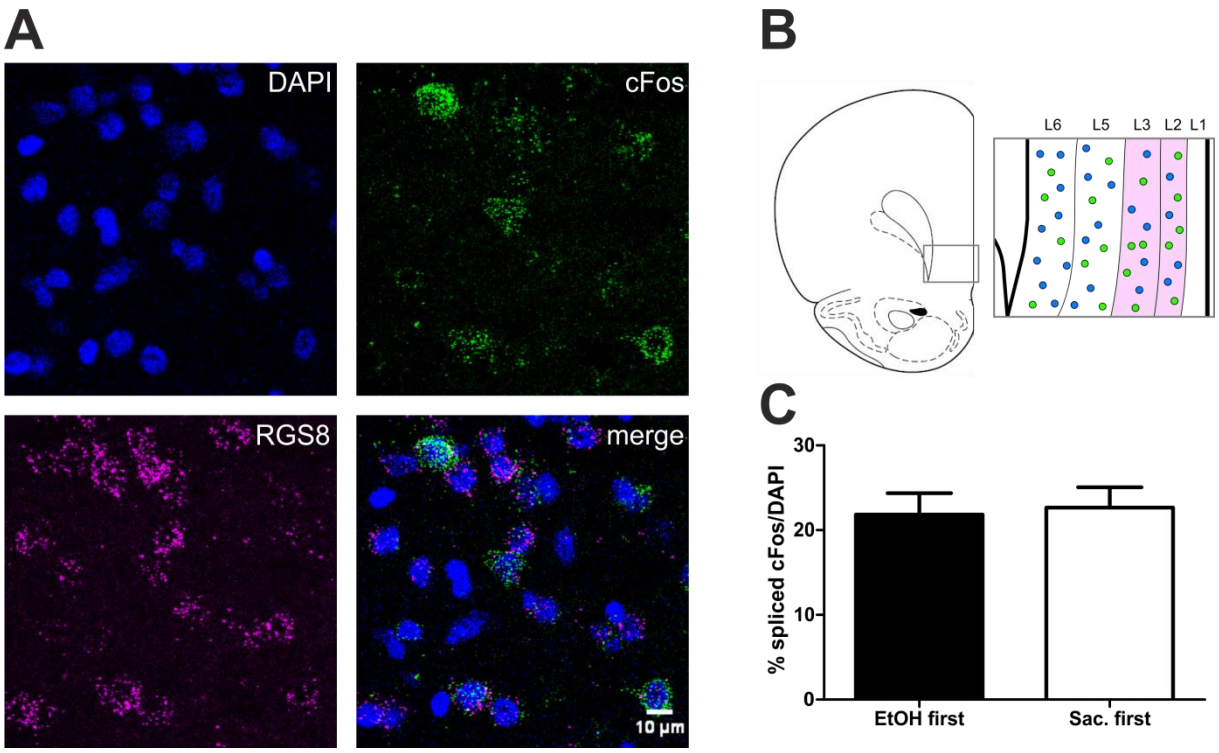

Figure 42: Layer 2/3 distribution of Fos mRNA expression. A) Representative images of fluorescent in-situ hybridization for spliced Fos mRNA (green), layer 2/3 marker RGS8 (magenta) and DAPI (blue). Expression of the layer marker was used to confirm image acquisition within the correct layer of the IL. **B)** Schematic of laminar structure of the IL. The analyzed region (layer 2/3) is highlighted in magenta. **C)** Quantification of the ratio of spliced Fos expressing cells in layer 2/3 of the IL. Figure adapted from (Pfarr et al., 2018).

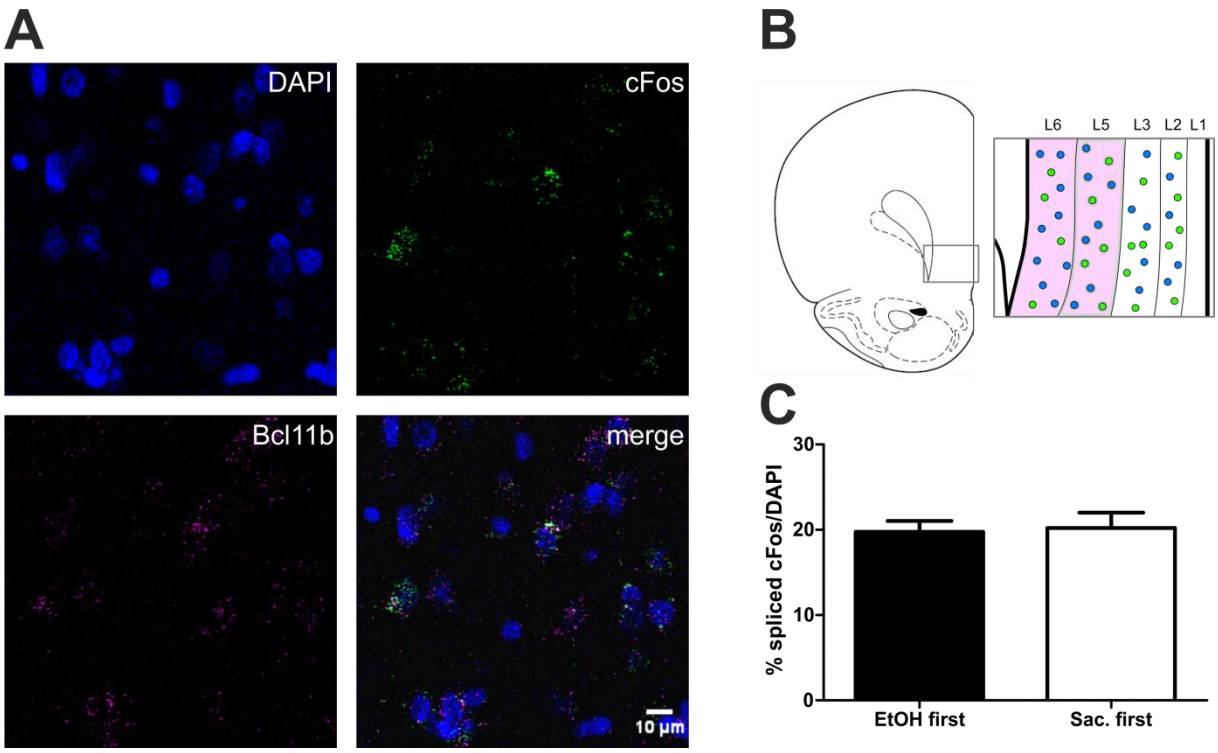

Figure 43: Layer 5/6 distribution of Fos mRNA expression. A) Representative images of fluorescent in-situ hybridization for spliced Fos mRNA (green), the layer 5/6 marker Bcl11b (magenta) and DAPI (blue). **B)** Schematic of laminar structure of the IL. The analyzed region (layer 5/6) is highlighted in magenta. **C)** Quantification of the ratio of spliced Fos expressing cells in layer 5/6 of the IL. Figure adapted from (Pfarr et al., 2018).

3.2.3 Summary

In the framework of this study we established a novel two-reward operant training protocol for the concurrent self-administration, extinction and cue-induced reinstatement of two different rewards. Using cFos immunohistochemistry, we identified infralimbic (IL) neuronal ensembles involved in ethanol and saccharin seeking of similar size (~15% of total neurons). Retrograde tracing of contralateral IL, prelimbic cortex, nucleus accumbens and ventral tegmental area projections originating from the IL revealed a significant difference in projections activated after ethanol or saccharin cue-induced reinstatement. Using the two-reward operant conditioning protocol in combination with fluorescent in-situ hybridization, we specifically labeled ethanol and saccharin activated ensembles in the same animal, using probes detecting intronic (unspliced) and spliced cFos. Together the data from Study 1 show that IL neuronal ensembles activated by ethanol and saccharin conditioned cues are of similar size with differences in projection targets. Furthermore both ensembles are highly overlapping (~50%) and comprise of a general (overlapping) and a specific (non-overlapping) component.

3.3 Study 3: In-vivo calcium imaging of IL neuronal ensembles involved in an operant reward seeking task

3.3.1 Introduction

In Study 1 (Pfarr et al., 2015) and Study 2 (Pfarr et al., 2018) of this thesis, we identified IL neuronal ensembles involved in alcohol and saccharin seeking. We found that both ensembles are highly overlapping, but also contain a reward specific component. However, we used *post mortem* cFos immunohistochemistry or cFos *in-situ* hybridization methods, which is why the temporal resolution of neuronal activity during the 30min operant task remains unknown.

In-vivo calcium imaging methods with head-fixed animals are frequently used to record neuronal ensemble activity in the mPFC (Low et al., 2014; Kondo et al., 2017; Otis et al., 2017; Tian et al., 2018). However, a head-fixed setup clearly limits the possible behavioral tasks, as the animals' movements are restricted. For live recordings of neuronal activity in the mPFC during a behavior task in freely moving animals, in-vivo electrophysiology is often used (Hajos et al., 2003; Ji and Neugebauer, 2012). Although this method provides excellent temporal resolution of neuronal activity patterns, the information about spatial distribution is very limited. In-vivo calcium imaging using the miniscope system enables live calcium imaging of deep brain regions in freely moving animals. So far, this method has been only successfully used in mice (Ghosh et al., 2011; Resendez and Stuber, 2014; Jennings et al., 2015; Cai et al., 2016; Gulati et al., 2017).

In order to obtain a deeper understanding about the role of the mPFC in reward seeking behavior, we setup *in-vivo* calcium imaging in freely moving rats combined with a saccharin reward seeking task. Recordings were done during self-administration, extinction and cue-induced reinstatement of saccharin seeking behavior using the UCLA open source miniscope version (www.miniscope.org).

The set-up of the surgery protocol was done in collaboration with Ivo Sonntag from the Institute of Anatomy and Cell Biology at Heidelberg University. Pre-training of the animals for operant saccharin self-administration was done with the help of several students during their internship at our lab (Laura Schaaf, Rebecca Hoffmann, Katja Lingelbach, Nicole Weigelt, Arian Hach, and Valentina Neukel) under my supervision. Operant sessions combined with *in-vivo* calcium imaging were performed in collaboration with Janet Barroso-

Flores, Ivo Sonntag, Valentina Neukel and Arian Hach. Data were analyzed and kindly provided by Janet Barroso-Flores and Ivo Sonntag. Histological analysis of GRIN lens placement and AAV injection site was done by Ivo Sonntag.

3.3.2 Results

In order to perform in-vivo calcium imaging recordings during an operant saccharin seeking task, several batches of male Wistar rats (n = 70) were trained and underwent surgery. However, in this thesis the results of only one batch will be presented, because data analysis for the remaining animals has not yet been completed. A batch of seven wild type Wistar rats received unilateral stereotaxic injections with a GCaMP6f AAV, followed by the implantation of a GRIN lens (9mm x 1mm) into the infralimbic cortex in the right brain hemisphere (Figure 44A). After one week of recovery, the animals were trained to self-administer a 0.2% saccharin solution in standard operant chambers for three weeks (Figure 44B). Next, a baseplate was secured at the GRIN lens implant, which served to anchor the miniscope for in-vivo calcium imaging recordings. In general only ~25% of all animals could be successfully used for in-vivo calcium imaging experiments. Reasons for the high drop-out rate of ~75% were misalignments of the GRIN lens and the AAV injection site, no clear field of view even though the GRIN lens and AAV injections were correctly placed or losses of the GRIN lens headmount during the long-term imaging and operant behavior sessions. In-vivo calcium imaging recordings were performed during five saccharin self-administration (SA) sessions, followed by four extinction (EXT) sessions and two cue-induced reinstatement (RE) sessions (Figure 45A). In this thesis calcium imaging data from one animal will be shown, because data analysis of the remaining animals is not yet completed.

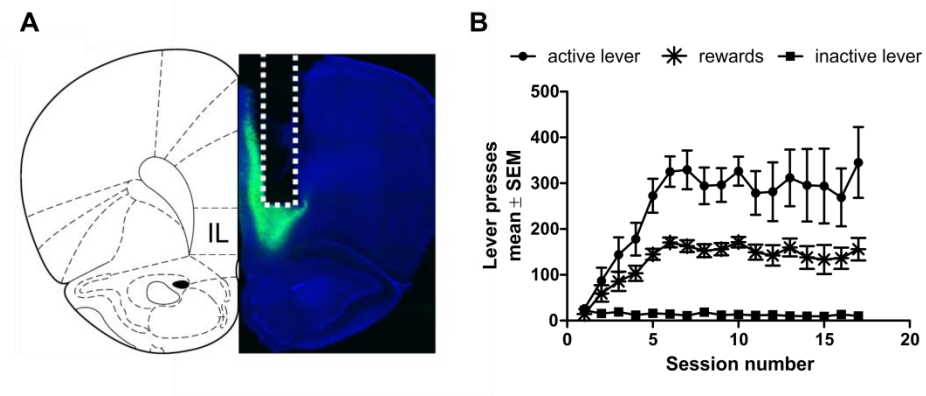

Figure 44: GRIN lens placement and pretraining for saccharin self-administration. A) Placement of GRIN lens in the infralimbic cortex. Left image: illustration of anatomical boundaries adapted from (Paxinos and Watson, 1998). Right image: DAPI (blue) and GCaMP6f (green) merge image. Dashed white lines indicate the placement of the GRIN lens. **B)** Active and inactive lever presses as well as the amount of delivered rewards are shown for the saccharin self-administration pretraining of Wistar rats (n=7).

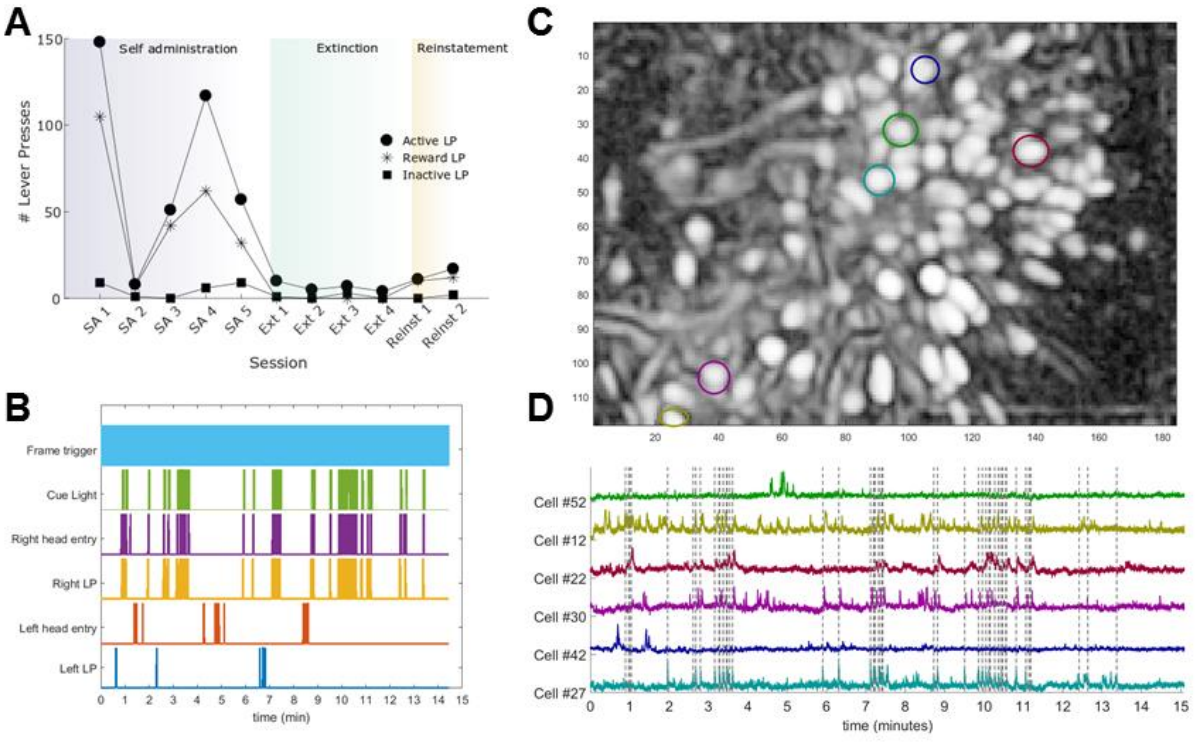

Figure 45: In-vivo calcium imaging recordings from one rat. A) Operant behavior during 30 min in-vivo calcium imaging sessions. Active lever presses, the number of delivered rewards and inactive lever presses are shown for the five self-administration (SA), four extinction (EXT) and two cue-induced reinstatement (RE) sessions for one animal. **B)** Synchronization of operant behavior in- and outputs with calcium imaging recordings. Only 15min of the 30min operant session are displayed. The frame trigger (light blue) serves to synchronize the calcium imaging video with the cue-light activation (green), the head entry into the right (rewarded) liquid receptacle port (purple), the right (active) lever press (orange), the head entry into the left liquid receptacle port (not rewarded, red) and the left (inactive) lever presses (blue). **C)** Correlation spatial map containing all active neurons in an operant session. **D)** Calcium transients recorded during 15 min opertant session and extracted from selected neurons marked in the spatial map.

Up to ~100 neurons were simultanously recorded in each operant-recording session from the same animal (Figure 45C). Activity traces for each cell were extracted and synchronized with behavior data (Figure 45B + D). To determine if the overall activity was reward related, calcium traces of all active neurons were aligned around the active lever response (5 seconds before and after the onset of the lever press) (Figure 46A), averaged across all rewarded lever presses (Figure 46B) and compared with the overall activity of the same active neurons across all inactive lever presses (Figure 46C). Mean activity of the same neurons, within the same behavioral session, showed different activity patterns if the lever press was rewarded or not, indicating a reward related main activity.

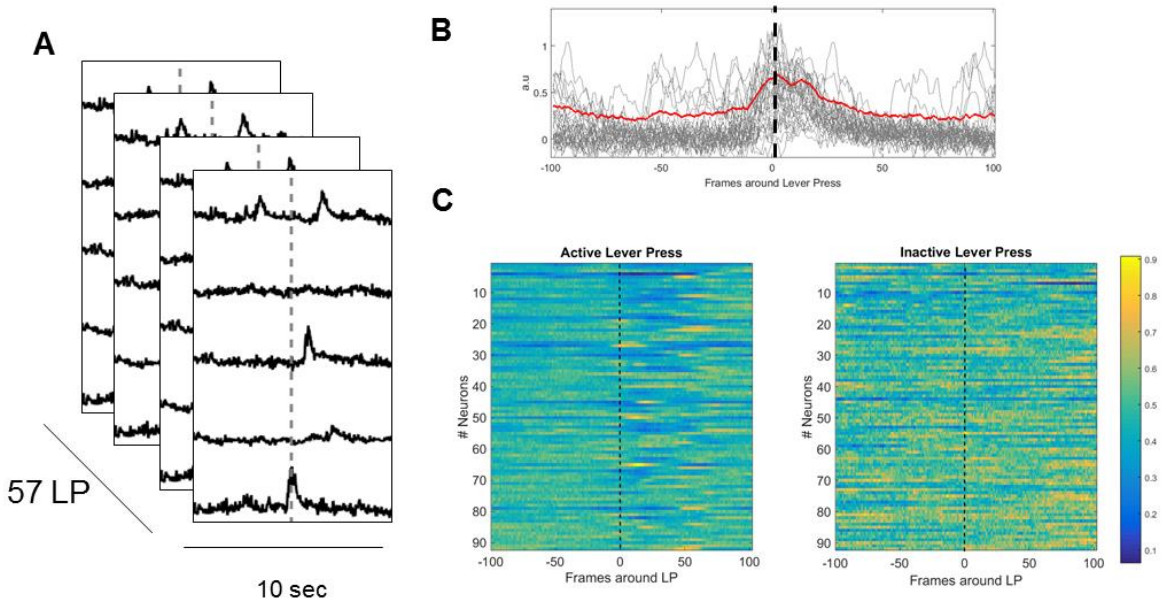

Figure 46: Overall neuronal activity around active or inactive lever presses. A) Activity of all neurons around the lever press (+/- 5 sec or +/- 100 frames; recording at 20Hz). **B)** Individual activity of a neuron around each lever press (LP) (gray) and the mean activity across all lever presses (red). **C)** Heatmap of activity of all active neurons across all lever presses (active lever (57 LPs) vs inactive lever (9 LPs)).

A preliminary analysis includes a simple classifier based on the sign of the first derivative of the main activity of each neuron around the lever press event (± 15 frames) (Figure 48A). The mode of the slope of the activity histogram is slightly negative, meaning that the main activity of most neurons is decreasing at the onset of the active lever press (Figure 48B). Neurons displaying steeper slope values (mean ± STD) were selected and the main activity displayed as separate activity heatmaps. These heatmaps have been generated for all stages of the cue-conditioned operant paradigm: self-administration, extinction and reinstatement showing

different structures of neuronal activity (Figure 47A). Interestingly for each condition (self-administration, extinction and cue-induced reinstatement), two groups of neurons were detected. One group decreased their activity around the lever press event (Figure 47C), while the other group clearly increased their activity (Figure 47B). Furthermore, the overall number of detected activated neurons during the self-administration and cue-induced reinstatement session was highly similar, while the number of activated neurons was clearly increased during extinction sessions (Figure 47D).

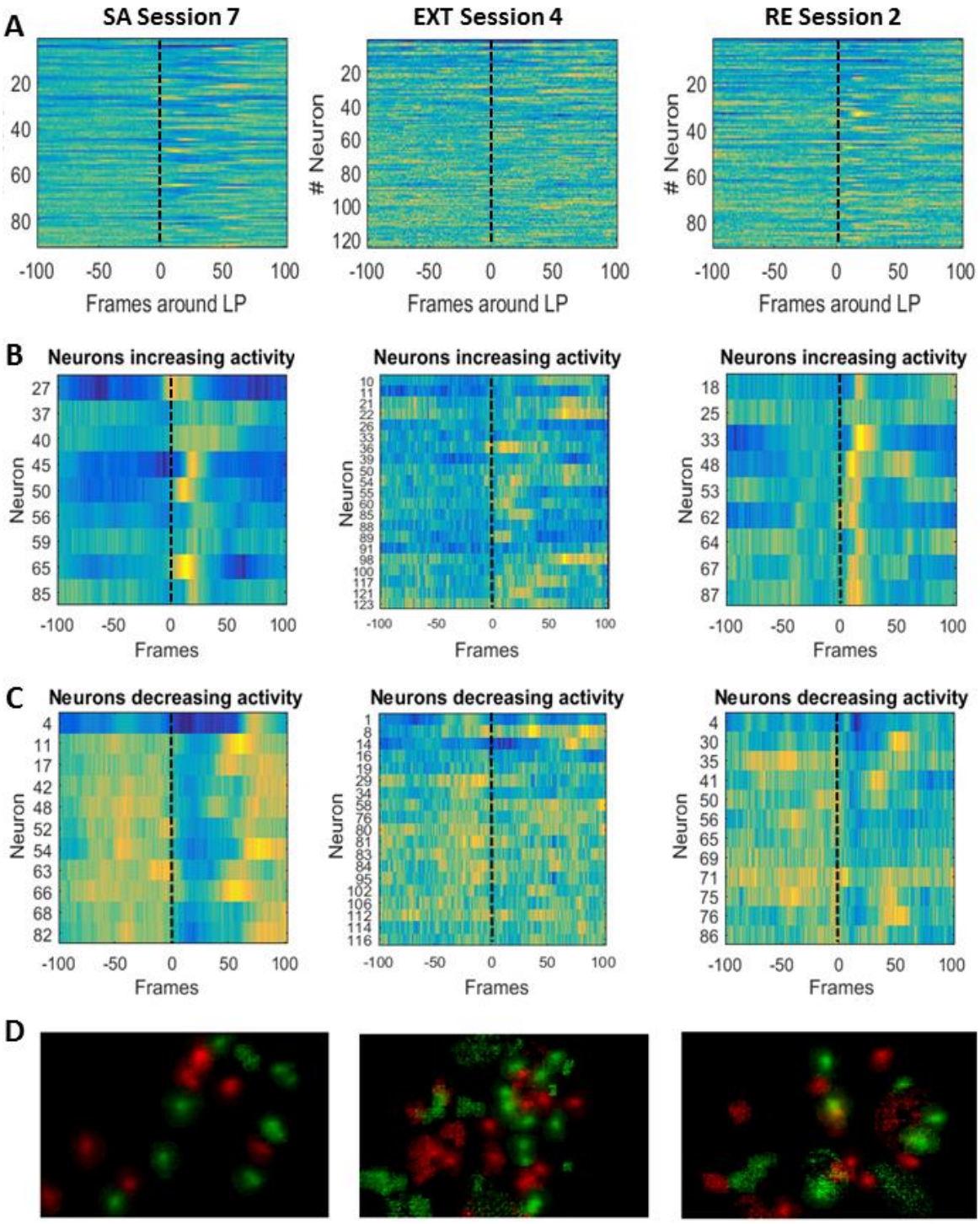

Figure 47: Neuronal activity heatmaps and space maps around rewarded lever press events. **A)** Activity heatmaps of all active neurons across all rewarded lever presses in different operant sessions: self-administration session 7 (SA), extinction session 4 (EXT), cue-induced reinstatement of saccharin seeking session 2 (RE). **B)** Individual heatmaps for neurons increasing their activity around the lever press event (from left to right: SA, EXT and RE). **C)** Individual heatmaps for neurons decreasing their activity around the lever press event (from left to right: SA, EXT and RE). Dashed lines represent the timepoint of the lever press. Each heatmap illustrates the activity 5sec before and after (100 frames before and after) the lever press. **D)** Spatial maps illustrating the location of neurons increasing (green) or decreasing (red) their activity around the lever press event (from left to right. SA, EXT and RE).

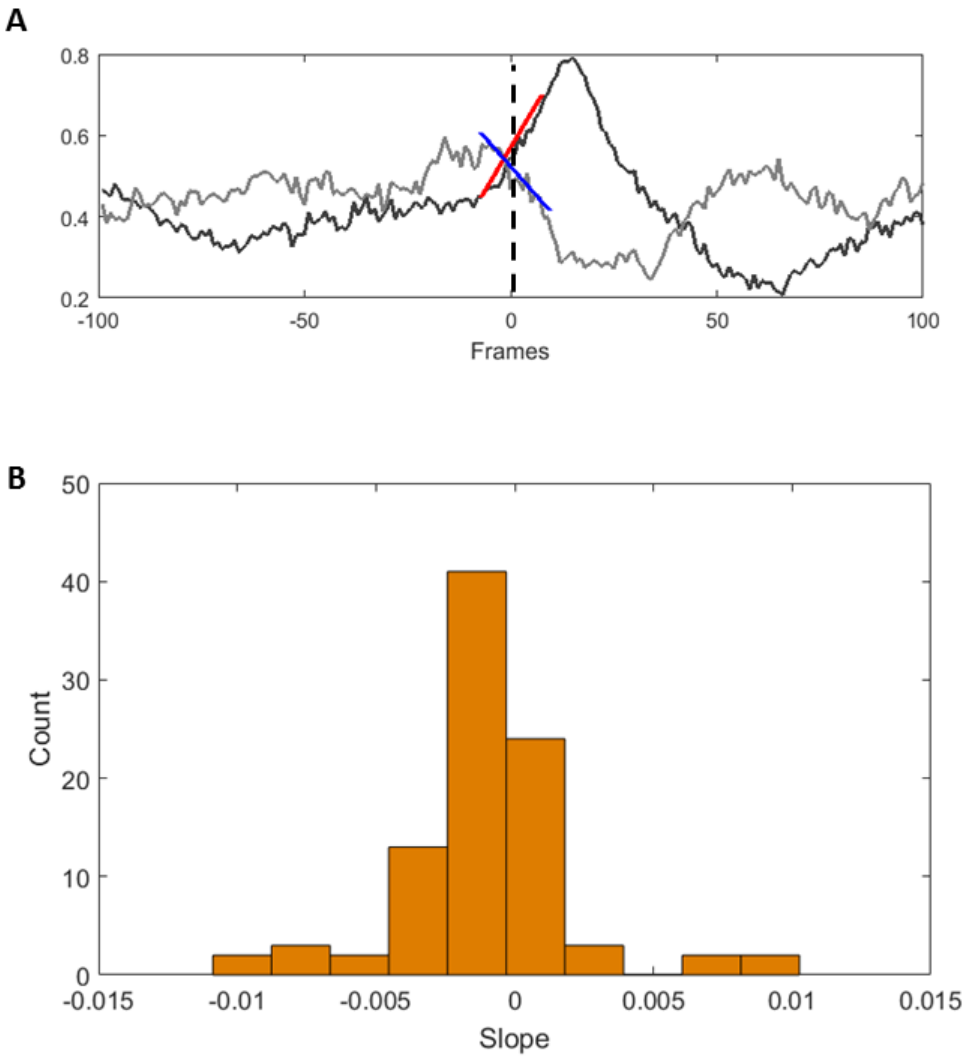

Figure 48: Classification of neurons with increasing or decreasing activity. A) Mean activity of representative neurons showing an increase (red slope) or a decrease (blue slope) in average activity around the lever press event (dashed line). **B)** Histogram of slopes of all neurons in a recording session.

3.3.3 Summary

In Study 3, we setup an in-vivo calcium imaging protocol using the UCLA miniscope system in freely moving adult rats. Furthermore, we combined in-vivo calcium imaging with an operant saccharin seeking task and established synchronization of the calcium imaging data with all in- and outputs from the operant box: active and inactive lever presses, cue-light activation and reward consumption based on head entry detection. By generating activity heatmaps of all active lever presses during a 30 min operant session, we identified two

populations of neurons each comprising about 10-13% of the total population of recorded neurons. One subpopulation is characterized by an increase in activity, while the second subpopulation is characterized by a decrease in activity around the lever press event. Thus, this method enables analysis of neuronal activity during specific parts of operant saccharin seeking behavior with relatively high temporal and spatial resolution. Both, increases and decreases in activity can be analyzed using this method, which will provide important information about activity patterns underlying complex behavior tasks like operant reward seeking.

3.4 Study 4: The influence of infralimbic mGluR2 expression levels on alcohol seeking behavior

3.4.1 Introduction

A previous study from our lab revealed a link between infralimbic (IL) metabotropic glutamate receptor 2 (mGluR2) expression and alcohol seeking behavior in postdependent (PD) Wistar rats (Meinhardt et al., 2013). PD rats were found to have reduced IL mGluR2 mRNA expression levels after chronic intermittent alcohol vapor exposure and a period of prolonged abstinence. This reduction in IL mGluR2 mRNA was associated with an increase in alcohol seeking behavior. After lentiviral restoration of mGluR2 mRNA levels in the IL of PD rats, alcohol seeking was normalized to control level. A similar link between mGluR2 expression and alcohol seeking behavior was found in the Indiana alcohol preferring (P) and non-preferring (NP) rat lines (Ciccocioppo et al., 2001). The Indiana P rat carries a point mutation in the mGluR2 coding sequence, which prevents functional mGluR2 expression (Zhou et al., 2013). In line with the previous findings, pharmacological blockade using the mGluR2/3 antagonist LY341495 resulted in an escalation of alcohol self-administration in Wistar rats (Zhou et al., 2013) and mGluR2/3 agonist LY379268 treatment reduced alcohol seeking behavior in rats (Bäckström and Hyytiä, 2005). The above mentioned findings suggest a role of mGluR2 expression levels and function in alcohol seeking behavior. While these studies provide evidence that the IL mGluR2 deficit is necessary for excessive alcohol seeking, it remains unclear if an IL mGluR2 deficit would be sufficient to induced this phenotype. Therefore, we constructed an adeno-associated virus (AAV) expressing a short hairpin (sh)RNA against mGluR2 mRNA. We used this AAV to specifically knockdown mGluR2 in the IL of wild type Wistar rats to directly test the effect of reduced IL mGluR2 expression levels on operant conditioned alcohol seeking.

Cloning of the Cre-inducible mGluR2 knockdown AAV was done by Ana Gallego-Roman as part of her Master Thesis under the joint supervision of Kai Schönig (Institute of Molecular Biology, CIMH) and myself (Gallego-Roman, 2016). Production of the AAV was performed by the research group of Thomas Kuner at the Institute of Anatomy and Cell Biology at Heidelberg University. Operant training of Wistar rats was done in collaboration with Jana Zell at the Central Institute of Mental Health. Operant training of Cam-iCre animals and mGluR2 western blots were done by Rebecca Hoffmann at the Central Institute of Mental

Health as part of her Master Thesis under my supervision (Hoffmann, 2017). Analysis of mGluR2 in-situ hybridization was done by Konstantin Wagner under my supervision.

3.4.2 Results

3.4.2.1 In-vitro and in-vivo validation of mGluR2 knockdown AAVs

In order to validate the efficiency of the mGluR2 knockdown AAVs, dual luciferase assays were performed with the *in-vitro* recombined Cre-dependent AAV (Figure 49D) and a standard mGluR2 shRNA AAV (general knockdown, Figure 49B). As both knockdown AAV versions contained the same shRNA sequence, one target-firefly luciferase construct was generated as a knockdown target for both versions. Each knockdown AAV version or a control AAV were co-transfected with the target-firefly luciferase plasmid and a renilla luciferase plasmid, which served as a loading control. The general mGluR2 knockdown construct significantly reduced firefly luciferase activity to ~30% compared to control AAV (two-tailed t-test: $t_{(1,4)} = 37.99$, $p = 0.0001$, Figure 49A). The Cre-inducible mGluR2 knockdown construct reduced firefly luciferase activity to ~27% compared to control AAV (two-tailed t-test: $t_{(1,4)} = 3.255$, $p = 0.03$; Figure 49C).

To test the knockdown efficiency of the Cre-inducible knockdown AAV version *in-vivo*, three CamKII-Cre rats were injected with the knockdown AAV and three animals with the control AAV (Figure 50A). After four weeks of virus expression mRNA levels of mGluR2 were analyzed using fluorescent in-situ hybridization (Figure 50B). Compared to the control AAV, the knockdown AAV significantly reduced mGluR2 mRNA levels to ~60% (Two-tailed t-test: $t_{(1,2)} = 16.8$, $p = 0.004$; Figure 50C).

To test the knockdown efficiency of the Cre-inducible knockdown AAV *in-vivo* on the protein level, western blots (Figure 51B) for mGluR2 and ß-actin were performed on NAc shell samples (Figure 51A) from CamKII-Cre rats from the operant alcohol seeking experiment (see Study 4) and attentional set shift experiment (see Study 5) (n=8/group). Compared to control AAV, the knockdown AAV significantly reduced mGluR2 protein levels to ~26% (One-tailed t-test: $t_{(1,14)} = 1.84$, $p = 0.04$; Figure 51C).

Thus, the chosen shRNA sequence produces a significant downregulation of mGluR2 mRNA and protein. The knockdown efficiency was validated in-vitro using a dual-luciferase assay as well as in-vivo using RNAscope FISH and western blot.

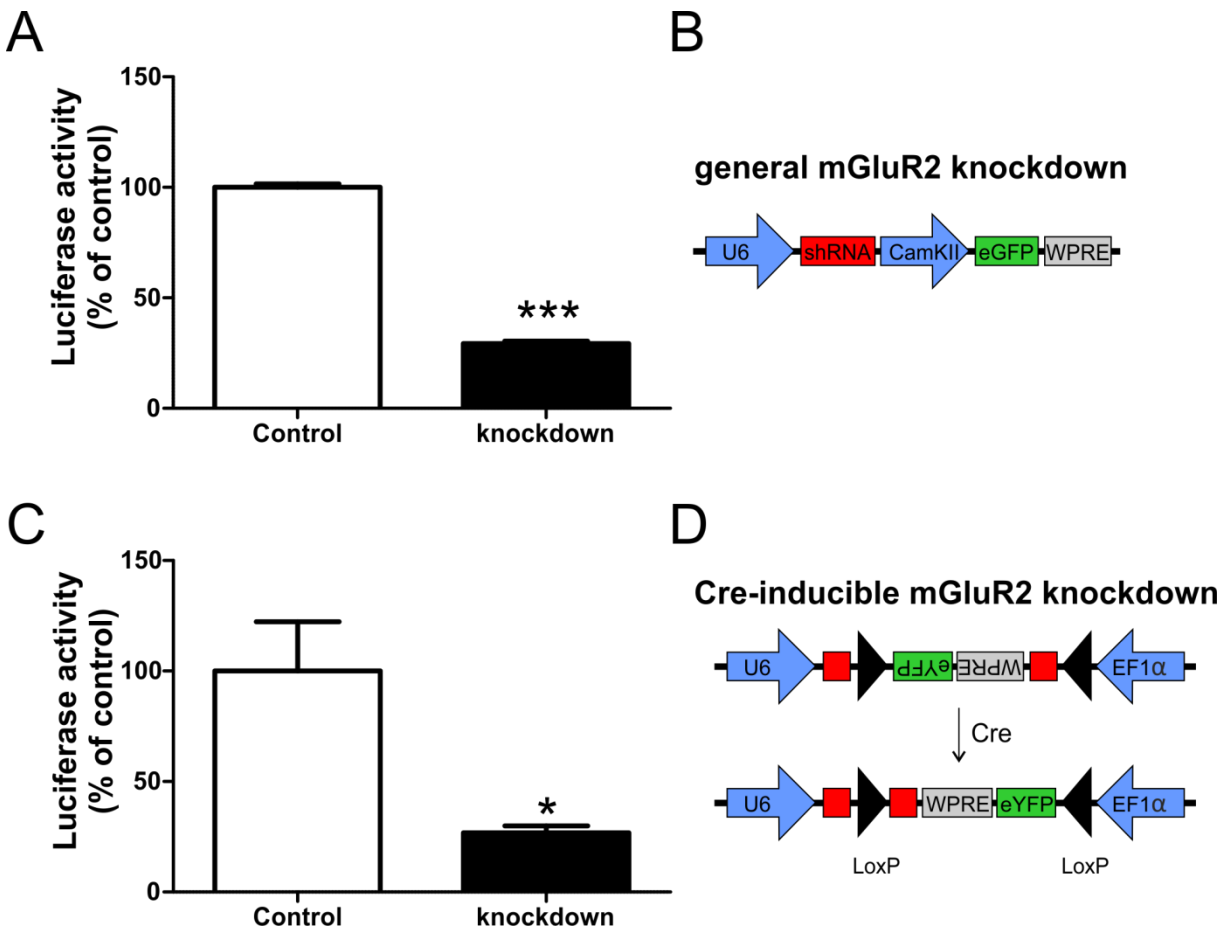

Figure 49: In-vitro validation of mGluR2 knockdown AAVs. A) Dual luciferase assay of control AAV (white bar) and general mGluR2 knockdown AAV (black bar). There was a significant downregulation of mGluR2 reporter luciferase activity when co-transfected with the knockdown AAV compared to control AAV. **B)** Schematic representation of general mGluR2 knockdown AAV construct. The shRNA targeting mGluR2 mRNA is expressed under the control of a U6 promoter. EGFP expression is driven by CamKII promoter. **C)** Dual luciferase assay of control AAV (white bar) and Cre-inducible mGluR2 knockdown AAV (black bar). There was a significant downregulation of mGluR2 reporter luciferase activity when co-transfected with the knockdown AAV compared to control AAV. **D)** Schematic representation of AAV construct. The shRNA was split in the middle and inserted into opposite directions into the floxed cassette. The reporter gene eYFP was also inverted and inserted opposite of the EF1α promoter. Without Cre-recombination no shRNA and no eYFP expression are possible. After Cre recombination shRNA expression is driven by U6 promoter and eYFP expression is driven by EF1α. *p<0.05, ***p<0.001

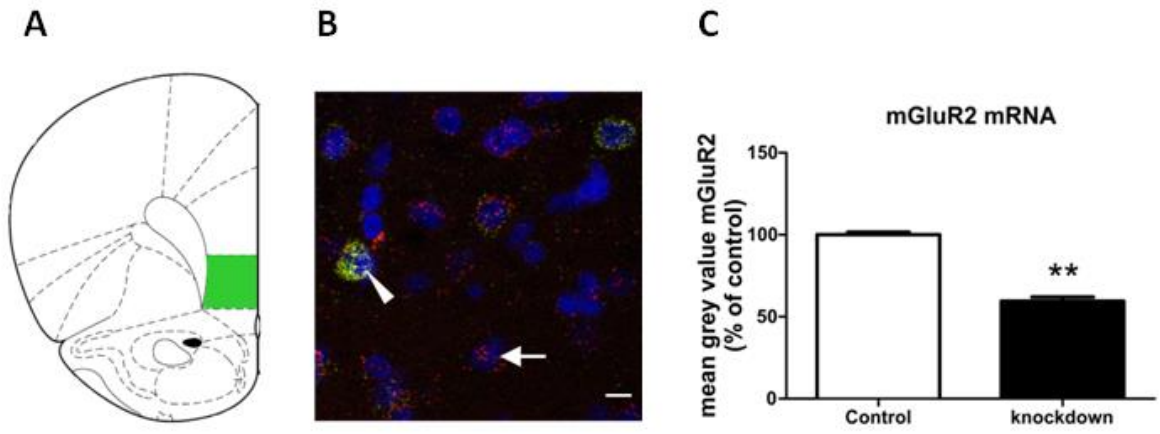

Figure 50: Knockdown efficiency of Cre-inducible shRNA AAV on mRNA level. A) Schematic representation of Cre-inducible mGluR2 knockdown AAV expressing eYFP in the IL adapted from (Paxinos and Watson, 1998). **B)** Representative image of eYFP and mGluR2 fluorescent in-situ hybridization of CamKII-Cre rats injected with Cre-inducible mGluR2 knockdown AAV. Arrow indicates a single cell for mGluR2. Triangle indicates a double positive cell expressing eYFP and mGluR2. Scale bar: 10µm. **C)** Quantification of Cre-inducible knockdown efficiency on mRNA level using fluorescent in-situ hybridization in CamkII-Cre rats. There was a significant reduction of mGluR2 mRNA transcripts in animals injected with the knockdown AAV (black bar) compared to control AAV (white bar). **p<0.01

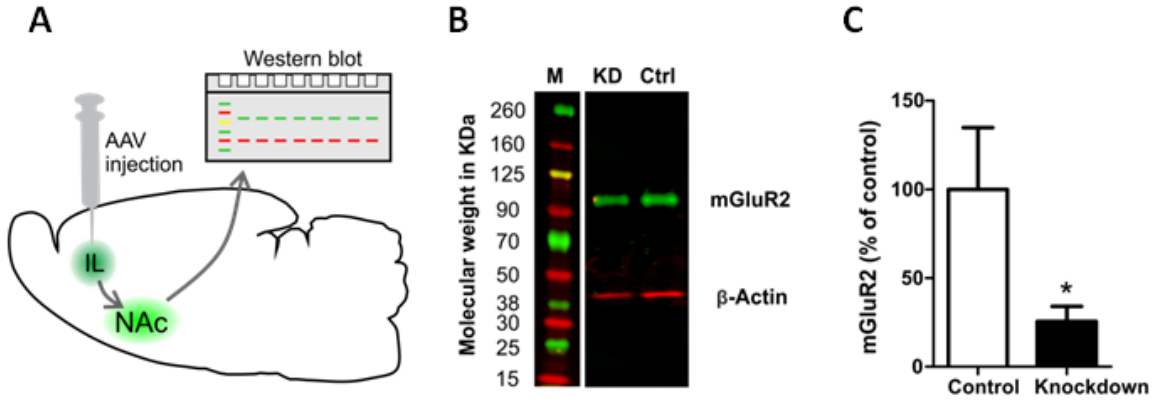

Figure 51: Knockdown efficiency of Cre-inducible shRNA AAV on mRNA level. A) Schematic representation of AAV injection into the IL and projection to the nucleus accumbens (NAc). Knockdown of mGluR2 protein level was determined by western blot using NAc tissue punches. **B)** Representative Western blot for mGluR2 and ß-actin in micropunched NAc shell tissue of CamKII-Cre rats after Cre-inducible knockdown AAV (KD) or control AAV (Ctrl) injection. M = Marker. **C)** Quantification of mGluR2 protein levels in NAc shell of CamKII-Cre rats after injection of control (white bar) or Cre-inducible knockdown AAV (Black bar). There was a significant downregulation of mGluR2 protein in IL after knockdown AAV injection. *p<0.05

3.4.2.2 Effect of a general mGluR2 knockdown in the IL on alcohol seeking behavior

In order to test the effect of a general mGluR2 knockdown in the IL on alcohol seeking behavior, 20 wild type Wistar rats were trained to self-administer a 10% ethanol solution followed by extinction training. After extinction training the animals were ranked based on their baseline performance (last three self-administration sessions) and equally divided into two groups. The animals either received bilateral control AAV injections (n=10) or mGluR2 knockdown AAV injections (n=10) into the IL (Figure 52C). After a 4 week recovery period the animals were then tested on their cue-induced alcohol seeking behavior.

Table 10: Statistics for operant alcohol seeking behavior for general IL mGluR2 knockdown experiment. Results for repeated measures ANOVA and Newman-Keuls post hoc test are shown. Comparison between active and inactive lever was done using two-tailed paired t-test. Abbreviations: DF = degrees of freedom, F = F-value, p = p-value, KD = knockdown, BL = self-administration baseline, EXT = extinction, RE = cue-induced reinstatement

Lever	Repeated measures ANOVA					Newman-Keuls post hoc test					t-test (comparison active/ inactive)	
	Test	DF	Effect	F	p	Within group comparison			Between group comparison			
						group	Test	p	Test	p	Test	p
active	BL, EXT	1,18	**group**	0.002	0.97						**control**	
			Test-session	33.75	0.0001	**control**	BL, EXT	0.003	BL	0.93	BL	0.002
			interaction	0.0077	0.93	**KD**	BL, EXT	0.0008	EXT	0.97	EXT	0.0002
	EXT, RE	1,18	**group**	0.007	0.94							
			Test-session	132.65	0.0001	**control**	EXT, RE	0.0002			RE	0.0001
			interaction	0.0003	0.99	**KD**	EXT, RE	0.0002	RE	0.97		
inactive	BL, EXT	1,18	**group**	2.49	0.13						**KD**	
			Test-session	14.73	0.001	**control**	BL, EXT	0.02	BL	0.3	BL	0.002
			interaction	0.19	0.67	**KD**	BL, EXT	0.07	EXT	0.13	EXT	0.009
	EXT, RE	1,18	**group**	3.99	0.06							
			Test-session	70.64	0.0001	**control**	EXT, RE	0.0002			RE	0.0001
			interaction	0.004	0.95	**KD**	EXT, RE	0.0002	RE	0.14		

There were no significant differences between the prospective experimental groups during in alcohol self-administration baseline (BL) and extinction (EXT). Four weeks after AAV injection there was also no difference in cue-induced reinstatement of alcohol seeking (RE) between the groups (Figure 52A, Table 10). There was also no difference in RE performance when data was normalized to BL responding (within control group BL – RE: $t_{(1,17)} = 1.45$, p =

0.16; within knockdown group BL – RE: $t_{(1,17)} = 1.54$, $p = 0.14$; between group RE: $t_{(1,17)} = 0.06$, $p = 0.95$; Figure 52B). Thus, general mGluR2 knockdown in the IL had no effect on alcohol seeking behavior.

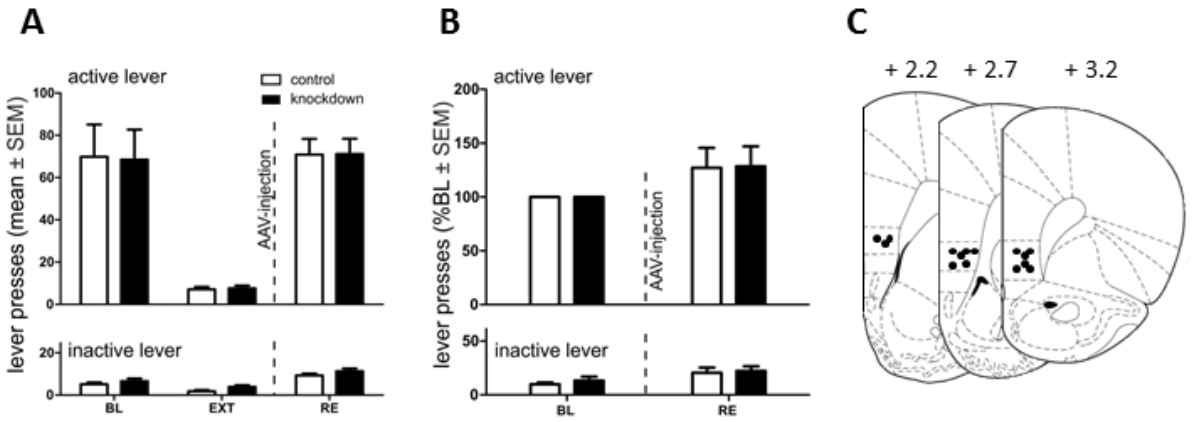

Figure 52: No effect of a general IL mGluR2 knockdown on alcohol seeking behavior. A) Active and inactive operant responses of wild type Wistar rats before and after control (white bars, n=10) and general knockdown (black bars, n=10) AAV injection. There was no significant difference between the groups in baseline (BL) and EXT responding. There was also no significant difference between the groups in RE performance after AAV injection. **B)** BL and RE responses at the active and inactive lever of general knockdown and control group, normalized to BL responses. Also after normalization to BL responding, there was no difference in cue-induced reinstatement between the groups. **C)** Injection placements of general knockdown AAV and control AAV are represented by black circles. Injection sites were verified within the IL from +3.2 to +2.2mm anterior to bregma (Paxinos and Watson, 1998).

3.4.2.3 Effect of a CamKII-targeted mGluR2 knockdown in the IL on alcohol seeking behavior

To test the effect of a neuron- specific mGluR2 knockdown in the IL on alcohol seeking behavior, a CamKII-Cre transgenic rat line in combination with a Cre-dependent mGluR2 knockdown AAV was used. 19 CamKII-Cre transgenic rats were trained to self-administer 10% ethanol solution. After reaching a stable self-administration baseline (BL) all animals underwent extinction training (EXT) and one cue-induced reinstatement session before AAV injection (RE1). The animals were ranked based on their BL and RE1 performance and equally divided into two groups. Next, the animals received bilateral control (n=9) or Cre-inducible mGluR2 knockdown AAV (n=9) injections (Figure 53C). Four weeks after AAV injection the animals were again tested on their operant alcohol seeking performance. Two control and two knockdown animals had to be excluded from analysis, because they failed to reach the criterion for successful cue-induced reinstatement of alcohol seeking (>10 lever active lever presses).

There were no significant differences between the prospective experimental groups in BL, EXT and RE1 (Figure 53A, Table 11). However, there was a significant increase in reinstatement of alcohol seeking in the knockdown group compared to the control group in RE2 ($t_{(1,11)} = 2.54$, $p = 0.03$; data normalized to RE1 performance, Figure 53B). There was also a significant difference within the knockdown group between RE1 (before AAV injection) and RE2 (after AAV injection) ($t_{(1,11)} = 3.2$, $p = 0.007$).

Thus, a neuron- specific mGluR2 knockdown in the IL of CamKII-Cre rats but not a general mGluR2 knockdown induces increased cue-induced reinstatement of alcohol seeking.

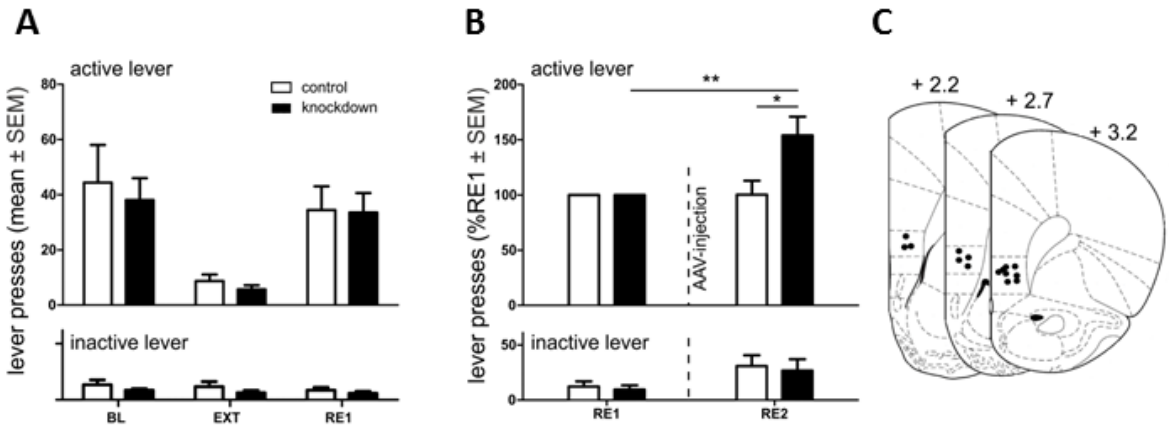

Figure 53: Escalation of alcohol seeking behavior after CamKII targeted IL mGluR2 knockdown. A) Active and inactive operant responses of CamKII-Cre rats before control (white bars, n=7) and knockdown (black bars, n=7) AAV injection. There was no significant difference between the groups in baseline (BL), extinction (EXT) and cue-induced reinstatement (RE1) responding. **B)** Performance of CamKII-Cre rats injected with control (white bars, n=7) or Cre-induced mGluR2 knockdown AV (black bars, n= 7). Data normalized to RE1 performance (before AAV injection). There was a significant difference between the groups in RE2 as well as a significant difference in the knockdown group between RE1 (before AAV injection) and RE2. **C)** Injection placements of Cre-inducible knockdown AAV and control AAV are represented by black circles. Injection sites were verified within the IL from +3.2 to +2.2mm anterior to bregma (Paxinos and Watson, 1998). *p<0.05, **p<0.01.

Table 11: Statistics for operant alcohol seeking behavior for CamKII targeted IL mGluR2 knockdown experiment. Results for repeated measures ANOVA and Newman-Keuls post hoc test are shown. Comparison between active and inactive lever was done using two-tailed paired t-test. Abbreviations: DF = degrees of freedom, F = F-value, p = p-value, KD = knockdown, BL = self-administration baseline, EXT = extinction, RE = cue-induced reinstatement

Lever	Repeated measures ANOVA					Newman-Keuls post hoc test					t-test (comparison active/ inactive)	
	Test	DF	Effect	F	p	Within group comparison			Between group comparison			
						group	Test	p	Test	p	Test	p
active	BL, EXT	1,12	**group**	0.272	0.611						**control**	
			Test-session	23.77	0.0003	**control**	BL, EXT	0.0009	BL	0.58	BL	0.023
			interaction	0.005	0.82	**KD**	BL, EXT	0.017	EXT	0.81	EXT	0.02
	EXT, RE	1,12	**group**	0.089	0.77							
			Test-session	29.88	0.0001	**control**	EXT, RE	0.008			RE	0.008
			interaction	0.048	0.048	**KD**	EXT, RE	0.005	RE	0.92		
inactive	BL, EXT	1,12	**group**	1.52	0.24						**KD**	
			Test-session	1.19	0.3	**control**	BL, EXT	0.69	BL	0.73	BL	0.005
			interaction	0.28	0.61	**KD**	BL, EXT	0.28	EXT	0.39	EXT	0.49
	EXT, RE	1,12	**group**	1.01	0.34							
			Test-session	0.17	0.34	**control**	EXT, RE	0.22			RE	0.006
			interaction	2.03	0.18	**KD**	EXT, RE	0.45	RE	0.7		

3.4.2.4 Characterization of Cam-iCre transgenic rat line

In order to characterize the Cre expression pattern of CamKII-Cre rats in the mPFC, we combined the Cre-dependent AAV-induced eYFP expression with immunolabeling for the neuronal marker NeuN, the interneuron marker GAD67 and CamKII as a marker for prefrontal projection neurons. Three CamKII-Cre rats were injected with the Cre-inducible mGluR2 knockdown AAV, expressing eYFP after Cre-recombination and three rats received control AAV injections (Figure 54A). Four weeks after the AAV injection rats were killed and brain sections were stained with TOTO-3 for nuclear counter staining and either NeuN, GAD67 or CamKII (Figure 54C). We found that ~43% of all TOTO-3 cells colocalized with eYFP expression and 52% of all neurons (NeuN) colocalized with eYFP. From all eYFP positive cells, ~88% were NeuN positive, ~64% were CamKII positive and ~11% were GAD67 positive (Figure 54B). Thus, there is no exclusive co-localization of Cre with CamKII neurons in the mPFC of CamKII-Cre rats, however the majority of Cre-expressing neurons is CamKII positive and we reach a strong neuronal restriction of the AAV expression in this rat line.

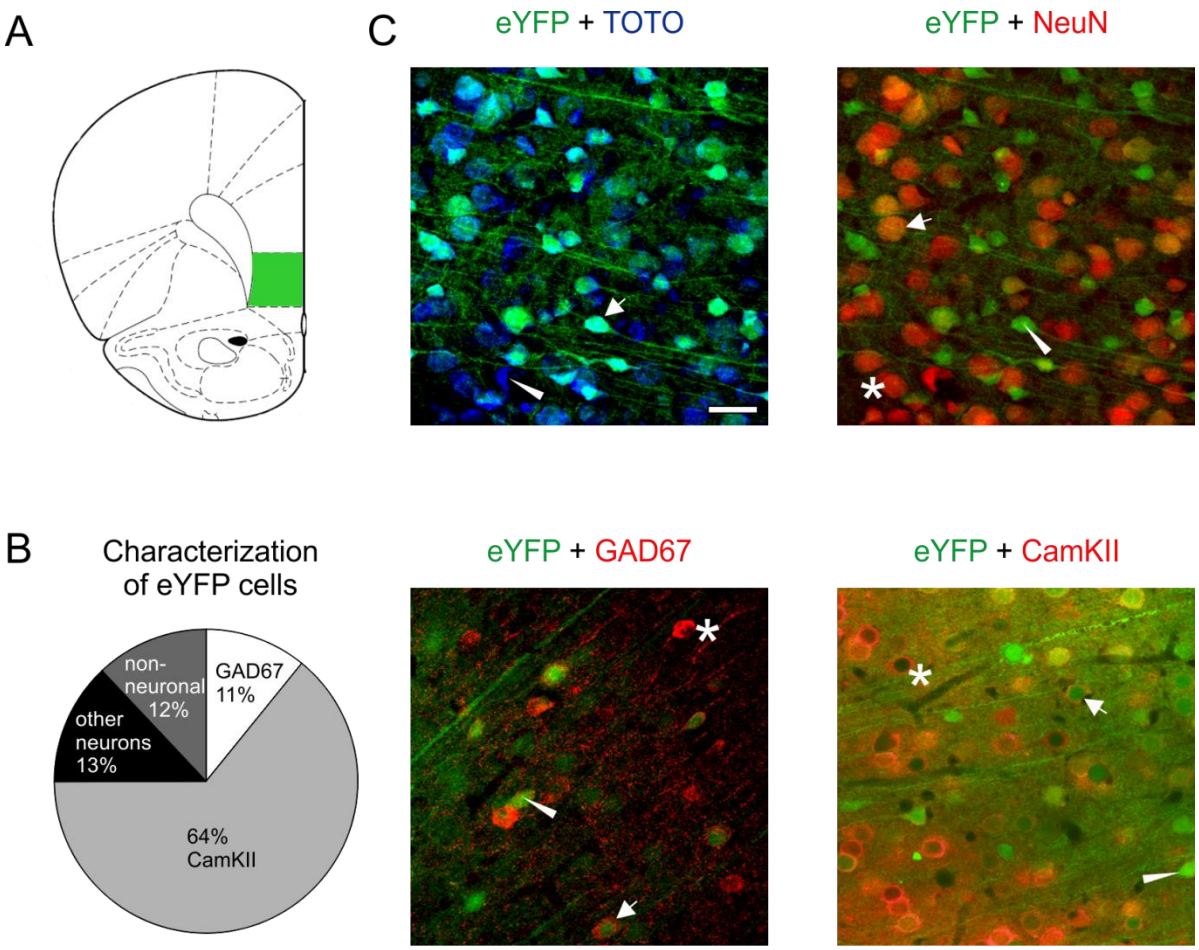

Figure 54: Characterization of Cre-expression pattern in mPFC of CamkII-Cre rats. A) Schematic representation of Cre-inducible mGluR2 knockdown AAV expressing eYFP in the IL. **B)** Pie chart illustrating the characterization of eYFP expressing cells. **C)** Representative images of eYFP co-localization with TOTO-3 (nuclear acid stain), NeuN, GAD67 and CamKII. Triangles indicate single positive eYFP expressing cells, asterisks indicate single positive cells for the respective cellular marker and arrows indicate co-localized cells. Scale bar 20µm.

3.4.3 Summary

Taken together the results described above, we generated two AAV viral vectors expressing an shRNA against mGluR2 mRNA. Both the general version and the Cre-inducible version induced an efficient downregulation of the target mRNA in a dual luciferase assay. Furthermore, we demonstrated a strong knockdown of endogenous mGluR2 mRNA and protein in the IL-NAc projection after injection of the Cre-inducible version into CamKII-Cre transgenic rats. Injection of the general mGluR2 knockdown AAV into the IL of wild type Wistar rats did not affect cue-induced reinstatement of alcohol seeking behavior. However, injection of the Cre-inducible version of the mGluR2 knockdown AAV into the IL of

CamKII-Cre rats induced an increase in alcohol seeking behavior, both compared to their cue-induced reinstatement performance before AAV injection and compared to the control group. Characterization of Cre-induced eYFP expression in the IL of CamKII-Cre rats revealed no exclusive co-localization of Cre in CamKII positive cells. However, the majority of Cre-expressing neurons is CamKII positive and the vast majority of Cre-expressing cells was neuronal. Taken together the results obtained from Study 4 show that CamKII targted, but not a general knockdown if IL mGluR2 induces excessive alcohol seeking behavior. The observed alcohol-seeking phenotype was similar compared to the postdependent rats after chronic intermittent alcohol exposure (Meinhardt et al., 2013). Therefore, we demonstrated that a mGluR2 deficit in IL projection neurons is not only necessary but also sufficient to induce the high alcohol-seeking phenotype observed after chronic intermittent alcohol exposure.

3.5 Study 5: The influence of infralimbic mGluR2 expression levels on cognitive flexibility

3.5.1 Introduction

The medial prefrontal cortex (mPFC) is critically involved in cognitive flexibility and top down control over behavior (Heidbreder and Groenewegen, 2003; Wood and Grafman, 2003). Both, in humans and animals, excessive alcohol use causes damage in the prefrontal cortex (Jernigan et al., 1991; Pfefferbaum et al., 1997; Meinhardt et al., 2013; Meinhardt and Sommer, 2015). A previous study from our lab showed that chronic intermittent alcohol exposure induced damage especially in the infralimbic (IL) subregion of the mPFC in Wistar rats (Meinhardt et al., 2013). This damage in the IL subregion was characterized by a downregulation of metabotropic glutamate receptor 2 (mGluR2) in the IL. The IL mGluR2 deficit induced a high-alcohol seeking phenotype in Wistar rats and could be rescued to control level after restoration of mGluR2 expression in the IL (Meinhardt et al., 2013). In Study 2, we demonstrated that a viral knockdown of mGluR2 in the IL of wild type Wistar rats can mimic the high-alcohol seeking phenotype, observed after chronic intermittent alcohol exposure. An open question is, if this IL mGluR2 deficit is also involved in cognitive deficits like impaired cognitive flexibility, which is frequently observed in human alcoholics (Loeber et al., 2009; Houston et al., 2014) or mice after chronic alcohol exposure (Kroener et al., 2012). A behavioral model to test executive functions and cognitive flexibility in rats is the attentional set shifting test (ASST) (Birrell and Brown, 2000; Klugmann et al., 2011), which is a rodent equivalent for the human Wisconsin Card Sorting Task (Berg, 1948).

In order to study the role of IL mGluR2 expression levels on cognitive flexibility, we used postdependent (PD) rats, Indiana alcohol preferring (P) and non-preferring (NP) rats, as well as the CamKII-Cre animals and the Wistar rats with general IL mGluR2 knockdown from Study 2, which received bilateral IL injections of a Cre-inducible mGluR2 knockdown AAV. In order to induce a ‘postdependent’ state (PD), chronic intermittent alcohol vapor exposure was used, followed by a period of prolonged abstinence (Rimondini et al., 2002; Meinhardt and Sommer, 2015). This procedure leads to high alcohol intoxication levels around 200mg/dl and induces behavioral as well as molecular changes in the brain (Hansson et al., 2008; Sommer et al., 2008; Meinhardt et al., 2013). Alcohol preferring Indiana P rats carry a stop codon in the mGlur2 coding sequence and can be considered as an mGluR2 knockout rat

(Zhou et al., 2013). The CamKII-Cre rats from Study 2, injected with an mGluR2 knockdown AAV have been already characterized in Study 4 and were tested in Study 5 on their cognitive flexibility.

Chronic intermittent alcohol vapor exposure of the wild type Wistar rats and subsequent ASST, as well as the lentiviral rescue experiment was performed by Manuela Klee (Klee, 2014) as part of her Master Thesis under the supervision of Marcus Meinhardt at the Central Institute of Mental Health.. These data are important for the interpretation of my own data and are shown with permission of the investigators. The ASST of Indiana P and NP rats was performed by Elisabeth Paul under my supervision at the Central Institute of Mental Health, Mannheim. The ASST of CamKII-Cre rats injected with Cre-inducible mGluR2 knockdown AAV was performed by Rebecca Hoffmann as part of her Master Thesis (Hoffmann, 2017).

3.5.2 Results

3.5.2.1 No impaired ASST performance in Grm2 knockout rats

Previous, unpublished experiments from our lab indicated a role of mGluR2 in ASST performance. Chronic intermittent alcohol exposure, which is known to induce an IL mGluR2 deficit, caused impairments in the most complex subtask of the ASST (IDS2 and EDS). After lentiviral restoration of mGluR2 expression in the IL in PD rats, a normal ASST performance was partially restored in the IDS2, but not in the EDS subtask (see Supplementary Information).

In order to investigate, if a global knockout of mGluR2 will lead to similar impairments in ASST performance as chronic intermittent alcohol exposure or local IL mGluR2 knockdown, we used 12 male Indiana alcohol preferring (P) rats and 14 male Indiana non-preferring (NP) rats. 2 NP rats were excluded from the experiment, because they failed to learn the early stages of ASST. As can be seen in Figure 55, there was a significant difference in SD ($F_{(1,21)}$ = 8.9, p = 0.007). However there were no significant differences in the other subtasks of the ASST (CD: $F_{(1,21)}$ = 1.49, p = 0.24; CDrev: $F_{(1,21)}$ = 0.07, p = 0.8; CDrep: $F_{(1,21)}$ = 0.74, p = 0.4; IDS: $F_{(1,21)}$ = 0.75, p = 0.4; IDS2: $F_{(1,21)}$ = 4.15, p = 0.05; EDS: $F_{(1,21)}$ = 0.0002, p = 0.99).

There was also no overall significant difference as confirmed by repeated measures ANOVA analysis ($F_{(1,21)} = 1.55$; p=0,23).

Thus, a global mGluR2 knockout does not result in cognitive impairments in the ASST.

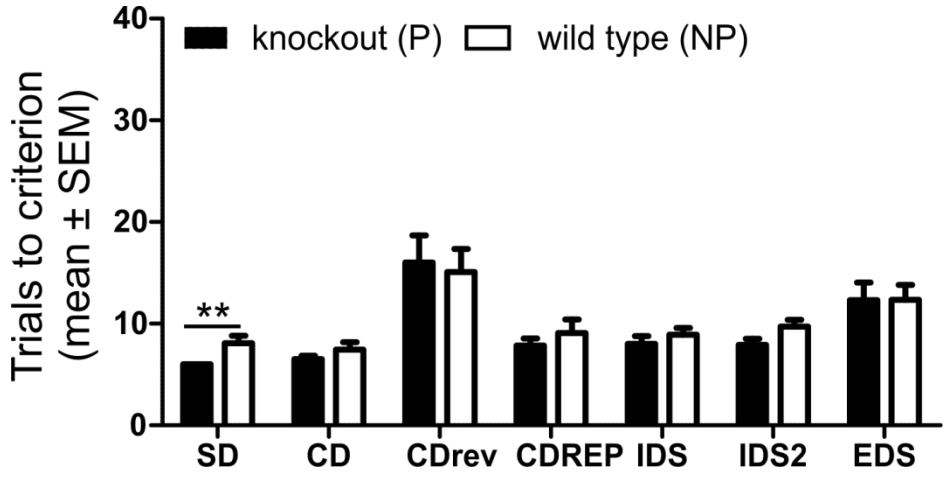

Figure 55: A whole brain knockout of mGluR2 does not influence ASST performance. There was no significant difference in ASST performance in Indiana P rats (n=12, black bars) compared to Indiana NP rats (n=12, white bars) in CD, CDrec, CDrep, IDS, IDS2 or EDS. The NP rats needed significantly more trials to criterion in the SD task. Overall there was no significant difference between the lines. SD=simple discrimination, CD=compound discrimination, CDrev=compound discrimination reversal, CDREP=repetition of CDrev, IDS=intradimensional shift, IDS2=intradimensional shift 2, EDS=extradimensional shift. **p<0.01

3.5.2.2 No effect of a general mGluR2 knockdown in the IL on ASST performance

To test, if an AAV-induced general knockdown of mGluR2 in the IL will lead to similar impairments in ASST performance as chronic intermittent alcohol exposure, we used 20 male Wistar rats. Six animals had to be excluded, because they failed to learn the early stages of the task or did not accept the food reward (final group size n=7/group). The animals were divided into two groups and received either bilateral U6-shUnc-CamkII-eGFP AAV (control) or U6-shRNA25-CamkII-eGFP AAV (Figure 56B) injections into the IL. After 4 weeks of recovery and AAV expression the animals were first tested on their operant alcohol seeking performance (see Study 4) and then tested on their ASST performance. As can be seen in Figure 56A, there was no significant difference between the groups in any of the ASST subtasks as confirmed by one-way ANOVA (SD: $F_{(1,12)} = 0.67$, p = 0.43; CD: $F_{(1,12)} = 0.0001$, p = 0.99; CDrev: $F_{(1,12)} = 0.05$, p = 0.83; CDrep: $F_{(1,12)} = 3.7$, p = 0.08; IDS: $F_{(1,12)} = 0.44$, p = 0.52; IDS2: $F_{(1,12)} = 1.23$, p = 0.29; EDS: $F_{(1,12)} = 1.27$, p = 0.28). There was also no overall

significant difference as confirmed by MANOVA analysis (Wilk's λ=0.46; $F_{(7,6)}$ = 0.99; p=0,51). Thus, a general mGluR2 knockdown in the IL is not sufficient to induce cognitive impairments in the IDS2 or EDS subtasks of the ASST.

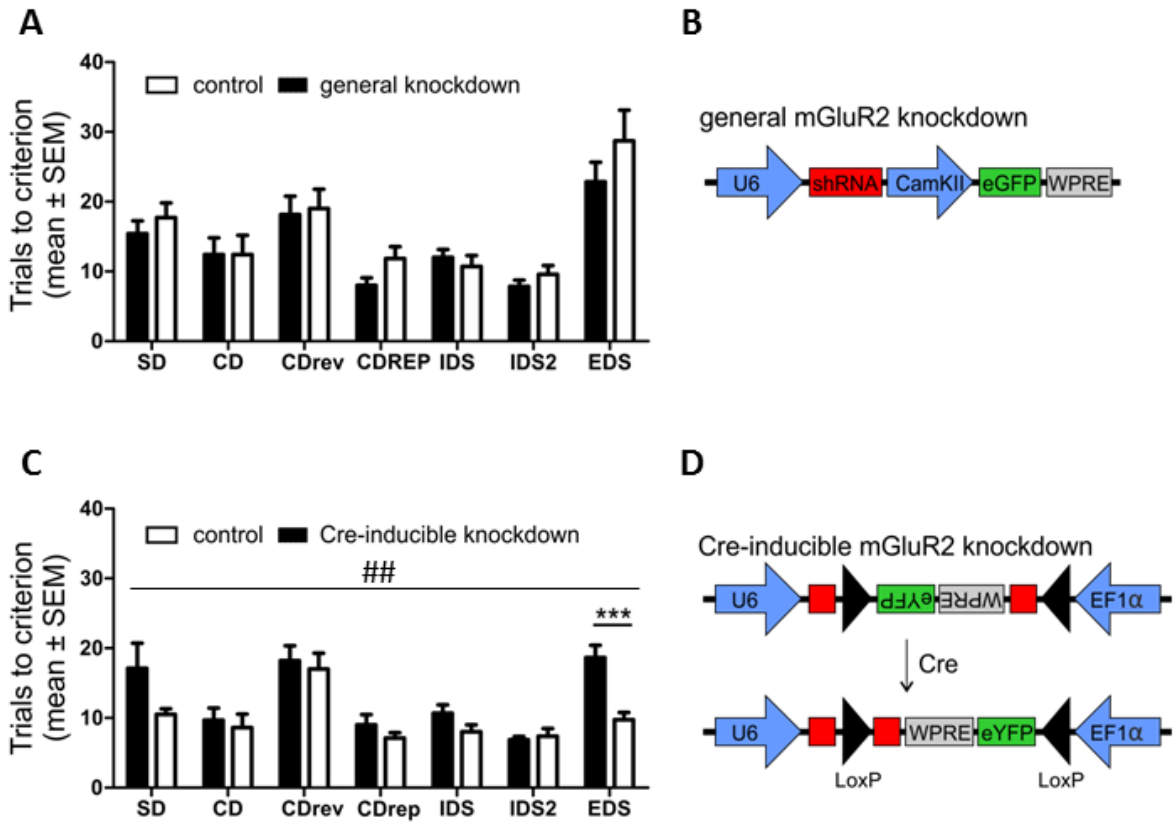

Figure 56: CamKII-targeted but not a general knockdown of IL mGluR2 affects ASST performance. A) There was no significant difference in ASST performance in animals injected with a general mGluR2 knockdown AAV or a control AAV. **B)** Schematic representation of general knockdown AAV construct. The shRNA is driver by a U6 promoter and eGFP is driven by a CamKII promoter. **C)** ASST performance of CamKII-Cre rats injected with either control AAV (n=9, white bars) or Cre-inducible knockdown AAV (n=9, black bars) into the IL. The knockdown animals needed significantly more trials to criterion in the EDS subtask and overall needed more trials to criterion as compared to control animals. **D)** Schematic representation of AAV construct. The eYFP reporter gene is expressed under control of CamKII promoter. For the Cre-inducible shRNA construct the shRNA was split in the middle and inserted into opposite directions into the floxed cassette. The reporter gene eYFP was also inverted and inserted opposite of the EF1α promoter. Without Cre-recombination no shRNA and no eYFP expression are possible. After Cre recombination shRNA expression is driven by U6 promoter and eYFP expression is driven by EF1α. ***p<0.001, Repeated measures ANOVA: ##p<0.01

3.5.2.3 Effect of CamKII-targeted IL mGluR2 knockdown on ASST performance

To test if an IL mGluR2 deficit induces the PD ASST phenotype, the 18 CamKII-Cre rats from the operant alcohol seeking experiment (see Study 4) were tested on their ASST performance (Figure 56C). One control animal had to be excluded as it showed aversive behavior when the casein pellet was presented. There were no significant differences in ASST subtasks SD – IDS2 as confirmed by one-way ANOVA (SD: $F_{(1,15)} = 2.85$, $p = 0.11$; CD: $F_{(1,15)} = 0.16$, $p = 0.69$; CDrev: $F_{(1,15)} = 0.16$, $p = 0.69$; CDrep: $F_{(1,15)} = 1.18$, $p = 0.29$; IDS: $F_{(1,15)} = 2.78$, $p = 0.12$; IDS2: $F_{(1,15)} = 0.18$, $p = 0.68$). However there was a significant difference between the groups in EDS performance as confirmed by one-way ANOVA ($F_{(1,15)} = 18.07$, $p = 0.0006$) and an overall significant difference between the control and knockdown group as confirmed by repeated measures ANOVA ($F_{(1,15)} = 9.02$, $p = 0.009$).

Thus, CamKII-Cre restricted mGluR2 knockdown in the IL leads to similar impairments in EDS performance as seen after chronic intermittent alcohol exposure.

3.5.3 Summary

Taken together the results described above, our lab previously found that a history of alcohol dependence leads to impaired executive functions and cognitive flexibility in PD rats. A significant impairment in PD rats in the IDS2 and EDS subtasks of the ASST was reported, which represent the cognitive most demanding subtasks of the ASST. Interestingly there does not seem to be a general impairment in ASST, but only impairments in the intra- and extradimensional set shift. This shows that chronic intermittent alcohol exposure does not impair ASST performance in general, but specifically the cognitive most demanding subtasks. Furthermore, we showed that a general loss of mGluR2 function in Indiana Alcohol preferring (P) rats did not affect ASST performance at all. Importantly, we showed that a CamKII-targeted, but not a general knockdown of IL mGluR2 induced impairments in the EDS subtask, similar to those seen in PD rats. Therefore, we identified an IL mGluR2 deficit in CamKII neurons as a molecular mechanism of alcohol-induced impaired cognitive flexibility.

4. Discussion

4.1 Discussion Study 1: Identification of an infralimbic neuronal ensemble involved in alcohol seeking behavior

Most research about brain areas involved in drug seeking behavior is based on classical lesion studies (Whitelaw et al., 1996; Ito et al., 2004; Lasseter et al., 2009) or non-selective pharmacological inactivation/ activation studies of whole brain regions (McFarland and Kalivas, 2001; Peters et al., 2008a; LaLumiere et al., 2010; Willcocks and McNally, 2013). However, based on a hypothesis of D.O. Hebb (1949), information is not processed by all cells in a given brain area, but by subgroups of neurons, so-called neuronal ensembles, which have been identified in several brain areas (Pennartz et al., 1994; Nicolelis et al., 1997; Buzsáki, 2004; Schwindel and McNaughton, 2011; Cruz et al., 2015). Neuronal ensembles are defined as subpopulations of neurons, which are selectively activated by certain environmental cues. Using the Daun02 inactivation method several of such neuronal ensembles have been identified in different brain areas, involved in drug and reward-seeking behavior (Koya et al., 2009; Bossert et al., 2011; Cruz et al., 2014; de Guglielmo et al., 2016; Suto et al., 2016; Warren et al., 2016). Although the Daun02 inactivation method has been frequently used, little was known about the mechanism of action of Daun02 inactivation. Daun02 is supposed to be an inactive prodrug, which gets converted into daunorubicin by ß-galactosidase (ß-gal) activity, encoded by the bacterial LacZ transgene (Koya et al., 2009). Daunorubicin was thought to inactivate cells either temporally by inhibition of calcium channels, which would lead to reduced excitability (Santone et al., 1986; Engeln et al., 2016), or permanent via the induction of apoptosis (Mortensen et al., 1992; Jantas and Lason, 2009). In order to clarify the mechanism of action of Daun02 inactivation we used a constitutive CAG-LacZ rat line and injected either Daun02 alone or Daun02 in combination with a pan-caspase inhibitor (Z-VAD-FMK). Daun02 injections into the mPFC of CAG-LacZ rats induced massive neurodegeneration, as detected by Fluorojade B staining. This neurodegeneration was almost completely prevented by simultaneous injection of Z-VAD-FMK. Therefore, we are certain, that the Daun02 concentration used in our experiments permanently inactivated neurons via the induction of apoptosis.

Using cFos-LacZ and CAG-LacZ transgenic rats, for cFos-induced and constitutive LacZ expression respectively, we found that selective cFos-dependent, but not a general ablation of IL neurons after cue-induced reinstatement of alcohol seeking induced excessive alcohol seeking in a second cue-induced reinstatement test. The lack of effect after a general ablation of IL neurons on alcohol seeking behavior confirms other findings in rats with no effect on context-induced reinstatement of alcohol seeking after reversible baclofen/muscimol inactivation of the IL (Willcocks and McNally, 2013). Although manipulations of IL activity were found to affect the seeking response for several drugs of abuse (Peters et al., 2008a; Bossert et al., 2011; LaLumiere et al., 2012), there is no evidence for a generally inhibitory or stimulatory role of this brain region. If the IL is more involved in inhibition or stimulation of a certain behavior seems to depend strongly on the drug itself, the specific cues and stimuli, or the setting and timing of the experiment (Moorman et al., 2015). In our present study we used a combination of contextual and discrete cues for reinstatement of alcohol seeking (Ciccocioppo et al., 2002; Ciccocioppo et al., 2003), which is similar to the context-induced reinstatement procedure used by (Bossert et al., 2011) for heroin seeking, but which is different from the highly discrete cues used by (LaLumiere et al., 2012) for cocaine seeking.

In addition to alcohol-associated cues also stress and alcohol itself can induce cFos expression in the mPFC and other brain areas (Morrow et al., 2000; Zhao et al., 2006; Funk et al., 2008; Hansson et al., 2008). Therefore, we tested the cFos-LacZ animals, which showed excessive alcohol seeking in the cue-induced reinstatement task, on a footshock stress-induced reinstatement of alcohol seeking task and found no elevated alcohol seeking response. Thus, we provide evidence that the neuronal correlates involved in cue-induced and stress-induced reinstatement of alcohol seeking differ in the IL. In addition, we found that the neuronal ensemble involved in cue-induced alcohol seeking is not critically involved in alcohol self-administration.

There is evidence that different mPFC subregions play opposing roles in the control of behavior. Based on findings from fear conditioning and cocaine seeking studies, a functional dichotomy of the PL and IL is proposed (Peters et al., 2009; Van den Oever et al., 2010; Gass and Chandler, 2013), because the PL seems to promote both fear expression and drug seeking, while the IL seems to suppress fear expression and drug seeking. To test, if this "PL-go/ IL-no go" model also applies to cue-induced alcohol seeking, we performed the Daun02 inactivation experiment in the PL of cFos-LacZ transgenic rats to specifically inactivate PL cue-

responsive neurons. There was no effect of neuronal ensemble inactivation in the PL on alcohol seeking behavior, although we detected a similar level of cFos activation as compared to the IL.

The above discussed findings indicate that the mPFC subregions IL and PL are differentially involved in the control of alcohol seeking behavior. However, the "PL-go/ IL-no go" model seems to be oversimplified. Furthermore, our results indicate that IL and PL control over alcohol seeking is distinct from IL and PL control over cocaine or heroin seeking.

4.1.1 Summary

The results discussed above provide new insights into the IL control over alcohol seeking behavior, as cue-induced alcohol seeking recruits a highly specific neuronal ensemble in the IL, which is not involved in stress-induced reinstatement of alcohol seeking or alcohol self-administration. Furthermore, we identified the induction of apoptosis as the underlying mechanism of action of the Daun02 inactivation method, meaning that Daun02 inactivation is permanent.

4.2 Discussion Study 2: Characterization of infralimbic neuronal ensembles involved in alcohol and saccharin seeking behavior

Recently, several neuronal ensembles in the infralimbic cortex (IL) involved in context- or cue- induced seeking of drugs or natural rewards have been identified (Bossert et al., 2011; Cruz et al., 2015; Pfarr et al., 2015; Suto et al., 2016; Warren et al., 2016). Although it is hypothesized that several neuronal ensembles could co-exist in the same brain area (Schwindel and McNaughton, 2011; Cruz et al., 2015), little is known about the organization and formation of co-existing ensembles in a given brain area. This lack of knowledge is likely due to the lack of appropriate methods to study co-existing neuronal ensembles in the same brain area and within the same subject.

Most Methods to identify and study the function and spatial organization of neuronal ensembles are immediate early gene (IEG) based. For example the Daun02 inactivation method is frequently used to inactivate a neuronal ensemble in a certain brain area (Koya et

al., 2009; Bossert et al., 2011; Cruz et al., 2013; Cruz et al., 2014; Cruz et al., 2015; de Guglielmo et al., 2016; Koya et al., 2016; Suto et al., 2016; Warren et al., 2016). However, we previously identified the induction of apoptosis as mechanism of action of Daun02 (Study 1) (Mortensen et al., 1992; Jantas and Lason, 2009; Pfarr et al., 2015), which limits its application to study only one neuronal ensemble in a certain brain area. Immunohistochemical labeling of cFos protein or cFos mRNA *in-situ* hybridization are frequently used to identify and quantify such neuronal ensembles (Dayas et al., 2007; Koya et al., 2009; Bossert et al., 2011; Cruz et al., 2014; Rubio et al., 2015; de Guglielmo et al., 2016; Suto et al., 2016; Warren et al., 2016). However, both cFos immunohistochemistry and cFos *in-situ* hybridization are *post-mortem* methods, which only allow to study one neuronal ensemble at the time. In addition to the lack of detection methods for two co-existing neuronal ensembles in one brain area, there was also a lack of an appropriate activation protocol of two ensembles in the same animal.

In Study 2 we set-up a two-reward operant conditioning task for concurrent self-administration of a sweet saccharin solution, which can be considered a natural reward (Green et al., 2015), and an ethanol solution as a drug reward. Therefore we modified a standard operant protocol for alcohol self-administration, extinction and cue-induced reinstatement, which is frequently and reliably used (Spanagel, 2000; Crombag and Shaham, 2002; Epstein et al., 2006; Sanchis-Segura and Spanagel, 2006; Martin-Fardon and Weiss, 2013; Marchant et al., 2015). If rats are allowed to choose, they will nearly always chose a high concentrated saccharin solution over most other drug rewards, including alcohol (Lenoir et al., 2007; Madsen and Ahmed, 2015). In order to achieve a similar operant response rate and preference for both, the saccharin and the ethanol reward, we first determined the response rate for the ethanol reward and then diluted the saccharin solution to reach a similar response level. By matching the behavioral performance for both rewards, we prevented unspecific effects on ensemble activity, which could be possibly induced by a high versus low response rate or differences in preference. Availability of both rewards was predicted by a combination of a contextual odor as well as a response-contingent light stimulus. Although similar cue combinations were used to predict both rewards, the animals clearly discriminated between both sets of cues and both rewards, as demonstrated by reward specific differences in breakpoint and cue-induced reinstatement tests. In the three tested Wistar rat batches, the animals had a higher breakpoint and higher cue-induced reinstatement performance for the ethanol reward, although there was no significant difference in self-administration between

both rewards. This response bias clearly shows that the animals do not simply generalize their lever response behavior, which makes this new two-reward operant conditioning model a powerful tool to study two neuronal ensembles in the same animals.

cFos immunolabeling after either cue-induced reinstatement for ethanol or saccharin seeking revealed an ensemble size of ~15% for both rewards. This ensemble size is slightly larger than the IL ensemble size involved in the control of alcohol seeking in a previous experiment (~11%) (Pfarr et al., 2015) (Study1). Other IL ensembles involved in cocaine, heroin or natural reward seeking were reported to be even smaller comprising 3-6% of neurons (Koya et al., 2009; Bossert et al., 2011; Cruz et al., 2014; Suto et al., 2016; Warren et al., 2016). The larger ensemble size detected in our operant reward seeking models compared to other ensembles reported in the literature could be explained by the complex and similar predictive cue sets. It is possible that the combined contextual and visual cues, the positive valence and the shared properties of both rewards engage a more complex neuronal network compared to studies using highly distinct predicting cues.

Using retrograde tracer injections into the contralateral IL, the prelimbic cortex, the nucleus accumbens and the ventral tegmental area, brain areas involved in the mesolimbic reward system (Arias-Carrión et al., 2010), we identified differences in projection targets of ethanol and saccharin cue-responsive neurons. Due to the small group sizes of ~3 animals per tracer region/ treatment group, there were no significant differences between the groups in a single brain area. However, there was a higher degree of overall co-localization of cFos positive neurons with all retrograde tracer signals in the saccharin cue-induced reinstatement group, compared to the ethanol group. The difference in co-localization indicates differences in the projection targets of the respective neuronal ensemble in the IL. The IL is a highly interconnected brain area with more than 60 detected projection target areas and receives inputs from more than 40 brain areas (Hurley et al., 1991; Vertes, 2004; Noori et al., 2017) and the ethanol ensemble could possibly engage a wider long range network, as compared to saccharin. For a more precise analysis, activity-dependent anterograde tracing methods should be used (Sørensen et al., 2016), as the retrograde tracing method is not suitable to investigate all 60 projection target areas of the IL.

Fluorescent *in-situ* hybridization (FISH) for cFos and layer II/III and layer V/VI specific cellular markers revealed, that there was no difference in laminar distribution of cFos positive nuclei between the EtOH and saccharin group. cFos positive cells in both reinstatement

groups were distributed throughout layers II – VI, which can be explained because the mPFC belongs to the class of the agranular cortex. In contrast to barrel cortices, the mPFC is lacking clearly defined input or output layers and both superficial and deep layers receive input from subcortical and cortical structures and project to other limbic structures (Gabbott et al., 2005; Riga et al., 2014).

The above discussed experiments gave a basic insight into the size and connectivity of the respective ensemble. In order to directly compare the size and potential overlap of both ensembles in the IL, a slightly modified cue-induced reinstatement procedure was used in combination with a double cFos FISH method. Co-localization analysis of both ensembles revealed a large overlap of ~50%. The high degree of overlap could be explained by a general motivation to obtain rewards. However, the tested rewards are highly distinct both in their sensory perception (taste and smell) and the internal states they produce and are therefore perceived as different by the animal. The obtained behavioral results in the breakpoint and cue-induced reinstatement tests support this theory. Similarly large overlapping cFos positive neuronal populations were also reported after exploration of two different environmental contexts (Cai et al., 2016).

4.2.1 Summary

Our study demonstrated that a drug reward (ethanol) and a natural reward (saccharin) engage neuronal ensembles in the IL of similar size. Furthermore, we identified differences in the downstream projection targets of the respective cue-responsive neurons. Using a double cFos FISH approach we identified the organization of two co-existing neuronal ensembles in the IL of the same animal. Each ensemble consists of a general overlapping component as well as a specific component for each reward. Thus, we provide a powerful tool to study co-existing neuronal ensembles involved in different reward seeking behaviors in the same animal. In addition we provide essential insights into the coding for different behaviors in the IL, by distinct, but overlapping neuronal ensembles.

4.3 Discussion Study 3: In-vivo calcium imaging of IL neuronal ensembles involved in an operant reward seeking task

In Study 1 (Pfarr et al., 2015) and Study 2 (Pfarr et al., 2018) of this thesis we identified infralimbic (IL) neuronal ensembles involved in drug and natural reward seeking behavior. However, in both studies cFos-based post-mortem methods were used for ensemble identification, providing a very good spatial resolution, but a limited temporal resolution. cFos expressing cells, identified in these studies could have been activated at every timepoint during the 30min operant session. This means, cells could have been activated by the general context of the operant chamber, active or inactive lever presses, rewarded or non-rewarded active lever presses, reward consumption or the activation of the cue-light. A clear separation of these events can only be achieved using in-vivo electrophysiology, light-activated manipulations or labeling methods, or in-vivo calcium imaging techniques. Although in-vivo electrophysiology provides excellent temporal resolution it does not provide a good spatial resolution. Light activated manipulation or labeling techniques like CaMPARI (Fosque et al., 2015), Cal-Light or FLARE (Lee et al., 2017; Wang et al., 2017) provide a good spatial resolution, however labeling or manipulations can only be targeted against one of the specific behavioral actions during a 30min operant session, e.g. only active lever presses or only inactive lever presses. Furthermore these techniques cannot be repeatedly used in the same individual across different behavior sessions. Although the temporal resolution is not as good as with in-vivo electrophysiology techniques, in-vivo calcium imaging provides the most powerful tool for good temporal and excellent spatial resolution of neuronal activity patterns. In contrast to light-activated labeling or manipulation techniques (e.g. CaMPARI) longitudinal in-vivo calcium imaging recordings can be repeatedly performed within the same animal. Furthermore, all behavioral responses during a complex behavior session can be recorded and analyzed. However, this method alone does not enable targeted or specific manipulation of neuronal ensembles.

A first analysis of the calcium imaging data during saccharin self-administration, extinction and cue-induced reinstatement of saccharin seeking revealed at least two sub-populations of neurons, which either increased or decreased their activity during responses at the active lever. Specifically the population which decreased the activity around the lever press event would most likely not have been identified using standard IEG-based methods. Also previous studies using single unit electrophysiological in-vivo recordings revealed that some prefrontal

neurons decrease their activity while others increase their activity during drug seeking behavior (Chang et al., 1997b; Chang et al., 1997a; Rebec and Sun, 2005; West et al., 2014). A clear limitation of single-unit recordings is the lack of the spatial component. In our approach simultaneous recordings of up to 100 neurons are possible, which will enable us to detect specific activity patterns between groups of neurons.

Despite the advantages of in-vivo calcium imaging, there are also certain limtiations and drawbacks. In our hands we found that only about ~25% of animals showed clear and usable calcium signals during the recording sessions. This low number of usable preparations was due to problems during surgery like misplacement of the GRIN lens relative to the AAV injection site or due to losses of the headmounts in some cases. Furthermore some animals did not have a clear field of view, which made recordings of calcium dynamics not possible. In addition to these problems, we found that some animals were distracted from the operant self-administration task by the miniscope cable. Although we used very thin and light weight cables we found that the animals' performance during the recording sessions dropped compared to the pre-training sessions. This effect cannot be due to the implant and the resulting brain damage itself, because the animals were already implanted during the pre-training session. Animals distracted by the Miniscope cable frequently tried to bite it, which made it necessary to constantly observe the animal. This fact makes parallel recordings of animals difficult and clearly limits the possible throughput of recordings per day.

Despite these limitations, in-vivo calcium imaging in freely moving rats provides an enormous gain of knowledge. To date, no other method provides a comparable level of spatial and temporal resolution to record neuronal activity patterns during complex behavior tasks. In contrast to in-vivo electrophysiology approaches, simultaneous recordings of >100 neurons is possible, which enables to detect complex network dynamics (Russell, 2011; Patel et al., 2015). Furthermore, using cell-type specific expression of calcium indicators, local information processing in specific microcircuits can be studied (Pinto and Dan, 2015).

In addition some of the described problems could be solved by the implementation of a wireless miniscope version (Liberti et al., 2017). Using this version, the animals will not be distracted by the cable anymore, which might increase the performance during the operant behavior task. Without the possibility of cable bites/ breaks, it could be furthermore possible to run several animals in parallel, supervised by only one experimenter.

4.3.1 Summary

In summary, we successfully setup in-vivo calcium imaging in freely moving rats using the UCLA miniscope version. In addition we managed to combine live calcium recordings with an operant reward seeking-task. Using the Bonsai software we are able to combine and synchronize all inputs and outputs from the operant chamber with the recorded calcium signals. A first analysis revealed that during saccharin self-administration, extinction training and cue-induced reinstatement of saccharin seeking some cells increase their activity, while others decrease their activity around the active lever responses. Furthermore our results indicate, that a similar number of neurons are engaged in self-administration and cue-induced reinstatement tasks, while extinction training requires a larger number of neurons.

4.4 Discussion Study 4: The influence of infralimbic mGluR2 expression levels on alcohol seeking behavior

In a previous study from our lab a link between an alcohol-induced reduction of infralimbic mGluR2 expression levels and excessive alcohol seeking behavior was found. Chronic intermittent alcohol exposure specifically reduced mGluR2 mRNA expression levels in the infralimbic cortex (IL). Lentiviral restoration of IL mGluR2 expression also reduced alcohol seeking behavior to control level (Meinhardt et al., 2013). A link between mGluR2 expression and alcohol intake has also been established using the Indiana alcohol preferring (P) and non-preferring (NP) rat lines. The P rat carries a single nucleotide polymorphism, leading to a premature stop codon in the mGluR2 coding sequence, and thereby preventing functional mGluR2 expression (Zhou et al., 2013). Indiana P rats are characterized by high voluntary alcohol intake, compared to NP rats (Murphy et al., 1986; Rodd-Henricks et al., 2001; Bell et al., 2006). Furthermore a link between mGluR2 function and alcohol seeking was found using the mGluR2 positive allosteric modulator AZD8529, which blocked cue-induced reinstatement of alcohol seeking in male Wistar rats (Augier et al., 2016). Also the mGluR2/3 agonist LY379268 prevented cue-induced reinstatement of alcohol seeking (Bäckström and Hyytiä, 2005; Kufahl et al., 2011).

The above mentioned studies implicate mGluR2 function to be is necessary for control of alcohol seeking. Furthermore these data show that an alcohol induced IL deficit of mGluR2 is necessary to induce the high alcohol seeking phenotype of the postdependent model (Meinhardt et al., 2013). However, none of these studies have demonstrated that the IL mGluR2 deficit is sufficient to induce the high alcohol-seeking phenotype, observed after chronic intermittent alcohol exposure.

In order to conclusively demonstrate causality between mGluR2 expression and the investigated phenotypes, we used a viral knockdown approach. We constructed a general mGluR2 knockdown AAV expressing a shRNA under control of the non-selective U6 promoter (Kunkel et al., 1986). We found, that a general mGluR2 knockdown in the IL did not alter cue-induced reinstatement of alcohol seeking, compared to control AAV injected animals. This finding is consistent with a mGluR2 knockdown study in the prelimbic cortex (PL), which did not change alcohol drinking behavior in rats (Ding et al., 2017). The lack of effect in the study by Ding and colleagues (2017) could be due to the chosen brain area for mGluR2 knockdown, as the study by Meinhardt and colleagues (2013) identified an alcohol-induced reduction of mGluR2 levels specifically in the IL but not in the PL. Furthermore, we showed in Study 1, that neuronal ensembles in the IL but not in the PL are critically involved in alcohol seeking (Pfarr et al., 2015). We also showed that this effect was only observed after selective inactivation of IL ensembles but not after a general lesion of the IL. Therefore, we constructed a Cre-inducible mGluR2 knockdown AAV, for targeted mGluR2 downregulation in the IL in predominantly excitatory projection neurons (Liu and Murray Karl, 2012).

A CamKII-targeted mGluR2 knockdown in the IL induced excessive alcohol seeking behavior, which was similar to the postdependent phenotype.

Taken together these results, a CamKII-targeted but not a general mGluR2 knockdown in the IL induced excessive alcohol seeking behavior. This effect is due to the cell-type restriction of the Cre-inducible AAV, as both viruses carry the same shRNA sequence and both AAV constructs produced highly comparable knockdown efficiencies in a dual luciferase assay. We further characterized the Cre-inducible AAV on mRNA and protein level. A significant downregulation of endogenous IL mRNA was detected using fluorescent *in-situ* hybridization. Furthermore a significant downregulation of mGluR2 protein in the nucleus accumbens projection was detected by western blot after IL AAV injections.

The Cre-inducible mGluR2 knockdown AAV was also used to characterize the Cre expression pattern in the transgenic CamKII-Cre rat line. We found that the CamKII-Cre rat line provides a strong neuronal localization of Cre expression. However, this transgenic line is not entirely CamKII-positive, as a minority of Cre-expression is also found in interneurons. In turn, the lack of effect of a general mGluR2 knockdown versus the excessive alcohol seeking behavior after Cre-restricted mGluR2 downregulation demonstrates the importance of a neuronal restriction of this genetic manipulation. This finding indicates that alcohol-induced mGluR2 downregulation in the IL might be specifically restricted to neuronal mGluR2 without affecting the glial mGluR2 population (Petralia et al., 1996) or the microglial mGluR2 population, which is involved in the induction of apoptosis (D'Antoni et al., 2008). While neuronal mGluRs play a role in synaptogenesis and synaptic plasticity, mGluRs located in glia cells are thought to be mainly involved in the regulation of glia function and the interaction between glia and neurons (Aronica et al., 2000).

4.4.1 Summary

Our study demonstrated that a neuronal restricted, but not a general downregulation of mGluR2 in the IL induces excessive alcohol seeking behavior, similar to the postdependent phenotype. Thus we demonstrated that a neuronal IL mGluR2 deficit is not only necessary, but also sufficient to induce the high alcohol seeking phenotype, observed after chronic intermittent alcohol exposure. Our data further indicate that the downregulation of IL mGluR2 observed in the postdependent animal model could be predominantly neuronal and not in the glia population.

4.5 Discussion Study 5: The influence of infralimbic mGluR2 expression levels on cognitive flexibility

The medial prefrontal cortex (mPFC) is involved in top-down control over behavior and executive functions, including working memory, attention, cognitive flexibility and impulse control (Heidbreder and Groenewegen, 2003; Wood and Grafman, 2003; Logue and Gould, 2014). Furthermore it is known, that excessive alcohol consumption leads to damage in the

PFC, both in humans and in animal models (Jernigan et al., 1991; Pfefferbaum et al., 1997; Meinhardt et al., 2013; Meinhardt and Sommer, 2015). In addition significant impairments in cognitive flexibility were reported in human alcoholics (Loeber et al., 2009; Houston et al., 2014).

A previous study from our lab found that excessive alcohol seeking behavior in postdependent (PD) rats after chronic intermittent ethanol (CIE) exposure is based on an alcohol-induced downregulation of mGluR2 in the infralimbic cortex (IL) of the mPFC (Meinhardt et al., 2013). In this study viral restoration of mGluR2 expression in the IL of PD rats normalized alcohol seeking behavior to control level. Therefore, we first answered the question, if CIE exposure also leads to changes in cognitive flexibility in PD rats. Using the attentional set shifting task (ASST) adapted from (Birrell and Brown, 2000; Klugmann et al., 2011), a rodent analogue of the Wisconsin Card Sorting Task using in humans (Berg, 1948). Previous experiments from our lab identified significant impairments in the intradimensional shift 2 (IDS2) and the extradimensional shift (EDS) subtasks of the ASST in PD rats, compared to controls (see Supplementary Information; Klee 2014). This finding confirms results from a study in mice, which showed cognitive impairments after CIE exposure (Kroener et al., 2012). Next, we asked if the IL mGluR2 deficit observed in PD rats is also responsible for the ASST impairments. Therefore, a lentiviral rescue experiment similar to the Meinhardt et al. (2013) study was performed (see Supplementary Information; Klee 2014). Restoration of IL mGluR2 rescued the impaired IDS2 performance in PD rats, but did not rescue the EDS deficit. The partial rescue of ASST performance after IL mGluR2 restoration could be due to additional alcohol-induced alterations in mPFC function, which are not mGluR2 dependent.

These previous data suggest the involvement of IL mGluR2 function in executive control. Furthermore, it has been reported that the mGluR2 positive allosteric modulator (PAM) LY487379 improved ASST performance in rats (Nikiforuk et al., 2010). In order to further identify the role of mGluR2 function in executive functioning, the ASST was performed with the Indiana alcohol preferring (P) and non-preferring (NP) rat lines. The Indiana P rats are homozygous knockout animals for mGluR2 (Zhou et al., 2013) but did not show any impairments in ASST performance when compared to NP rats. This finding does not support a role for mGluR2 in executive control. A possible explanation for the normal cognitive performance of P rat could be a possible compensatory mechanism of mGluR3. Both mGluR2

and mGluR3 are autoinhibitory metabotropic glutamate receptors (Niswender and Conn, 2010; De Filippis et al., 2015). Compensatory mechanisms of mGluR3 taking over mGluR2 function could be the underlying mechanism in the Indiana P rat, as these rats are born without functional mGluR2 receptors (Rodd et al., 2006; Augier et al., 2016). In addition, unspecific phenotype changes caused by tightly-linked loci flanking the deleted gene are frequently observed in knockout animals (Eisener-Dorman et al., 2009), which however is unlikely in the case of the Indiana P rat, as this rat has only one point mutation in the Grm2 gene. In order to circumvent possible compensatory mechanisms of mGluR3, which is known to play an important role in working memory and PFC-dependent cognitive tasks (Walker et al., 2015; Caprioli et al., 2018; Hernandez et al., 2018), we tested the effect of local mGluR2 knockdown in the IL on ASST performance. First, we investigated the general mGluR2 knockdown animals from Study 4 on their ASST performance and found that there was no impairment in any of the ASST subtasks. Next, we tested if a CamKII-targeted IL mGluR2 knockdown had an effect on cognitive flexibility. Therefore we tested the CamKII-Cre rats from Study 4, injected with a Cre-inducible mGluR2 shRNA AAV on their ASST performance. We found, that the knockdown group was significantly impaired in the EDS subtask and showed an overall impaired performance throughout the ASST procedure.

Although the PD rats and CamKII-Cre rats injected with a Cre-inducible mGluR2 knockdown AAV into the IL showed an overall impairment throughout the ASST procedure, the most pronounced impairments were seen in IDS2 and EDS in PD rats and EDS in CamKII-Cre rats. These subtasks represent the cognitive most demanding subtasks of the ASST, because in IDS2 a completely new and unknown set of media and odors is introduced and during the EDS the animals have to shift their attention to the previously irrelevant dimension and have to ignore the previously relevant dimension. There were no significant differences between the groups in the compound discrimination (CD) and the reversal of compound discrimination (CDrev). This confirms findings from a study in mice, which showed a facilitation in pairwise visual discrimination and reversal learning and clearly no impairment in a touchscreen based task after chronic alcohol exposure (DePoy et al., 2013). The CDrev performance has been shown to be critically dependent on orbitofrontal cortex (OFC) function (McAlonan and Brown, 2003). The lack of impairment in CDrev in the PD rats may be explained by the fact that chronic intermittent alcohol exposure mainly affects the IL subregion of the mPFC, but not the OFC (Meinhardt et al., 2013). Furthermore it has been reported, that mPFC lesions

specifically impaired the EDS subtasks of the ASST but not the early compound discrimination or reversal stages (Birrell and Brown, 2000).

4.5.1 Summary

Taken together, we established a role of IL mGluR2 in executive functions and cognitive flexibility. After chronic intermittent alcohol exposure, PD rats are clearly impaired in the IDS2 and EDS subtasks, which represent the cognitive most demanding subtasks of the ASST. Lentiviral restoration of mGluR2 expression in the IL of PD rats improved IDS2 performance, but not EDS performance. Therefore, the impairments seen after chronic intermittent alcohol exposure were only partially rescued by mGluR2 overexpression, which could be explained by additional alcohol-induced alterations in the brain independent of IL mGluR2 downregulation. A CamKII targeted knockdown of IL mGluR2 also induced an impairment in the EDS subtask, similar to the EDS impairment seen after chronic intermittent alcohol exposure. Consequently, our data indicate a critical role of IL mGluR2 expression and function on executive functions and cognitive flexibility. Although an IL mGluR2 deficit is not the only molecular mechanism underlying cognitive impairments after chronic intermittent alcohol exposure, we clearly established a critical role of IL mGluR2 expression levels and normal cognitive function and flexibility.

4.6 General discussion

4.6.1 Detection of neuronal ensembles

In summary, this thesis provides conclusive evidence for the important role of neuronal ensembles in the control of reward seeking behavior. Study 1 identified a functional neuronal ensemble in the infralimbic cortex (IL), which serves to control alcohol seeking behavior. Activity-dependent and targeted ablation of this ensemble induced excessive alcohol seeking, demonstrating the inhibitory function of this IL ensemble. Furthermore Study 1 showed, that a general, non-selective lesion of the IL had no effect on alcohol seeking behavior, which is consistent with findings after non-selective reversible inactivation of the IL (Willcocks and

McNally, 2013). This negative finding after the classical lesion experiment could be explained by opposing processes in the IL, possiblly resulting in a zero-net effect. Such opposing mechanisms in the IL have already been demonstrated in a recent study showing bidirectional modulation of a learned behavior by functionally distinct IL neuronal ensembles (Suto et al., 2016). The above discussed findings highlight the importance of appropriate methods and techniques for a certain scientifc question. We show that classical lesion studies or non-selective inactivation studies, especially ones with negative outcome (Saksida et al., 2006; Willcocks and McNally, 2013), have to be carefully interpreted, as it is possible that a similar zero net effect was generated as in Study 1 of this thesis. In Study 2 we demonstrated, using a novel two-reward concurrent operant self-administration task, that both seeking for natural rewards and drug rewards are encoded in the IL by co-existing neuronal ensembles. These results confirm previous hypotheses and findings of co-existing and intermingled neuronal ensembles within the same brain area (Hebb, 1949; Schwindel and McNaughton, 2011; Cruz et al., 2015; Suto et al., 2016). Furthermore, we identified the organization of both co-existing neuronal ensembles in the IL and found that both neuronal ensembles were highly overlapping, but each ensemble also had a reward-specific component. Thus, the IL seems to function as a general integration hub for reward-seeking behavior, but also contains distinct subsets of neurons, which encode cue-and reward-specific information.

4.6.2 Limitations of cFos-based *post-mortem* methods

In the above discussed studies permanent or *post-mortem* cFos based methods were used, with a limited temporal resolution. The Daun02 inactivation method, cFos immunohistochemistry (IHC) and cFos fluorescent in-situ hybridization (FISH) detect strongly activated cells throughout the whole behavioral test-session. The detected cells could be possibly activated by the exposure to the respective context of the operant chamber, by the presentation of cues, by the execution of lever pressing behavior, by the seeking for the reward or other actions. This is a clear limitation of these methods, as neuronal ensembles involved in e.g. the lever pressing event cannot be separated from cells encoding the other aspects of reward-seeking behavior. Furthermore, the Daun02 inactivation method is a permanent ablation method, as demonstrated in Study 1, which does not allow to test the inactivation effect of different neuronal ensembles in one animal. Detection of two different neuronal ensmebles and

quantification of the overlap between both was possible by using a double cFos FISH approach in Study 2. However, this method has to be performed *post-mortem*, and does not allow to study neuronal ensembles at different timepoints during a long-term behavior experiment.

4.6.3 Advantages of in-vivo calcium imaging

One possibility to overcome these limitations in temporal precision is *in-vivo* electrophysiology, which is reliably used to record the acitivity of mPFC neurons during behavior tasks (Hajos et al., 2003; Ji and Neugebauer, 2012). Although this method provides excellent temporal resolution, the spatial information of neuronal ensembles is clearly limited using this approach. A method with good temporal and spatial resolution is in-vivo calcium imaging. Although the temporal resolution of the calcium-indicator signal is slower compared to *in-vivo* electrophysiology signals, the temporal resolution enables separation of events during several aspects of the animal's behavior. *In-vivo* calcium can be performed in head-fixed preparations (Low et al., 2014; Kondo et al., 2017; Otis et al., 2017; Tian et al., 2018) or more advanced in freely moving animals (Ghosh et al., 2011; Resendez and Stuber, 2014; Jennings et al., 2015; Cai et al., 2016; Gulati et al., 2017). Advantages of head-fixed *in-vivo* calcium imaging experiments are stable recordings with only little movement artefacts. However, behavioral experiments are clearly limited in such an approach. *In-vivo* calcium imaging using the miniscope system enables live calcium imaging of deep brain regions in freely moving animals but so far, this method has been only successfully used in mice. In order to detect specific activity patterns during a certain behavioral response, e.g. responding at the active lever, we used the miniscope system for live calcium imaging in freely moving rats during an operant saccharin seeking task (Study 3). This method allowed us to detect a subgroup of neurons which decreased their activity and another subgroup of neurons that increased their activity around the lever pressing event, which is consistent with findings from in-vivo single neuron recordings in the mPFC during drug seeking behavior (Chang et al., 1997b; Chang et al., 1997a; Rebec and Sun, 2005; West et al., 2014). Compared to these single unit recording techniques, our calcium recording technique regularily detects more than hundred neurons simultanously and thus enables the analysis of specific activation patterns with single cell resolution.

4.6.4 Infralimbic mGluR2 deficit as a common molecular mechanism for excessive alcohol seeking behavior and impaired executive functioning

Both, loss of control over alcohol seeking behavior (Goldstein and Volkow, 2011) and impaired executive functions have been reported in human alcoholics (Loeber et al., 2009; Houston et al., 2014) and can be caused by impaired top-down control of the mPFC over behavior. Chronic alcohol exposure was found to cause damage in the prefrontal cortex in humans as well as in animals (Jernigan et al., 1991; Pfefferbaum et al., 1997; Zahr et al., 2011; Meinhardt et al., 2013; Meinhardt and Sommer, 2015). In rats chronic alcohol exposure was found to be especially damaging to the infralimbic (IL) subregion of the mPFC, as IL – NAc shell projection neurons exhibit deficits in the NR-2A subunit of the NMDA receptor, as well as significant reductions in egr-1 and mGluR2 gene expression (Meinhardt et al., 2013). This alcohol-induced mGluR2 deficit was found to be associated with loss of control over alcohol seeking behavior. Restoration of mGluR2 expression levels in the IL normalized the alcohol seeking behavior, which demonstrated that an IL mGluR2 deficit is necessary for this high alcohol seeking phenotype (Meinhardt et al., 2013).

In order to answer the question if an mGluR2 deficit in the IL is only necessary or even sufficient to induce this high alcohol seeking phenotype, we used viral knockdown strategies to reduce mGluR2 gene expression levels in the IL (Study 4). Interestingly a general, non-selective knockdown of mGluR2 in the IL had no effect on alcohol seeking. However, a CamKII- neuron targeted downregulation of mGluR2 in the IL induced the excessive alcohol seeking phenotype, comparable to the post dependent animals (Study 4) (Meinhardt et al., 2013). A similar finding was obtained from Study 5, where a CamKII- targeted, but not a general knockdown induced impairments in the EDS subtask of the ASST, similar to the ones after chronic intermittent alchol exposure in post dependent rats. Thus, a downregulation of mGluR2 in IL projection neurons seems to be a common molecular mechanism underlying both, excessive alcohol seeking and impaired executive functions. Interestingly, similar to Study 1, non-selective manipulation methods in the IL do not induce changes in alcohol seeking or ASST behavior. Similarly, mGluR2 knockout rats (Indiana P rat) were not impaired in ASST performance when compared to Indiana NP rats. These findings strengthen the hypothesis, that the IL area does not generally excert an inhibitory tone, but rather that different subsets or specific cell types are involved in the control of alcohol seeking and ASST behavior.

4.6.5 Validation of mGluR2 knockdown approach

Both, the general and the Cre-inducible mGluR2 shRNA AAV constructs contained the identical shRNA sequence. The knockdown efficiency of this shRNA sequence in comparison with a non-targeting shRNA was validated *in-vitro* using a dual luciferase assay. Using *post-mortem* FISH analysis for quantification of mRNA and western blot for quantification of protein levels, the knockdown efficiency of the shRNA was validated *in-vivo*. The downregulation of mGluR2 protein by our shRNA approach is comparable with a study in the PL using lentiviral shRNA vectors (Ding et al., 2017).

All knockdown data shown here were generated in comparison with a universal control shRNA (Mauceri et al., 2015), which has no known targets in the mouse or rat genome. The comparison with non-targeting shRNAs is important, because they also recruit the same enzymatic mRNA degradation machinery, including the Dicer enzyme and RNA-induced silencing complex (RISC) (Moore et al., 2010). The comparison with control shRNAs can prevent unspecific effects on behavior by the recruitment of the mRNA degradation machinery. Potential off-target knockdown effects of the mGluR2 shRNA cannot be completely ruled out (Jackson and Linsley, 2010) however, the shRNA sequence used in our studies to our knowledge does not have any other targets in the rat genome, so off-target knockdown effects are unlikely.

Summary and Outlook

By combining transgenic cFos-based neuronal ablation techniques with molecular and behavioral techniques, this PhD thesis provides important insights into the function and organization of neuronal ensembles in the infralimbic cortex, invovled in reward seeking behavior (Study 1 - 3). Furthermore this thesis identifies an IL mGluR2 deficit as a common molecular mechanism underlying excessive alcohol seeking behavior, as well as impared cognitive functioning (Study 4 + 5).

In order to further clarify the underlying neuronal activity patterns during reward seeking, further studies are necessary. Study 2 of this thesis identified largely overlapping neuronal

ensembles in the IL, involved in alcohol and saccharin seeking. In order to identify potential differences in neuronal activity patterns during alcohol and saccharin seeking behavior, *in-vivo* calcium imaging should be performed during this task, e.g. using the miniscope technique from Study 3.

To further analyze differences in the neurocircuitry involved in alcohol and saccharin seeking, activity-dependent anterograde tracing experiments should be performed. One possible experiment would be activity dependent labeling of IL projection neurons using e.g. Cal-Light (Lee et al., 2017), FLARE (Wang et al., 2017) or pRAM promoter (Sørensen et al., 2016) based viral fluorescence marker expression systems. In order to perform a brain-wide neurocuircuit analysis, the activated projection neurons can be recorded and traced by combining brain clearing techniques (Azaripour et al., 2016) and single plane illumination microscopy (Economo et al., 2016). After identifying key projections, GCaMP6f could be expressed specifically in these projections in order to study acitvity patterns of these specific subgroups of neurons. Projection specific expression could be achieved using e.g. the novel rAAV2-retro serotype (Tervo et al., 2016).

Study 4 and 5 revealed that a general loss or downregulation of mGluR2 in the IL does not influence alcohol seeking behavior or ASST performance. Excessive alcohol seeking behavior and imapaired ASST performance were only observed after restricting the IL mGluR2 knockdown to projection neurons. In order to further characterize the neurocircuitry involved in both behavioral phenotypes, a projection specific knockdown of mGluR2 could be performed. Together with the above described future experiments, these studies will help to further characterize the neurocircuitry invovled in the control of reward seeking behavior and cognitive functions.

Acknowledgements

This thesis was carried out at the Central Institute of Mental Health (CIMH), University of Heidelberg, Mannheim, Germany. All animal experiments were conducted within the Institute of Psychopharmacology at the CIMH. My PhD was financially supported by the collaborative research center SFB636 as well as the Deutsche Forschungsgemeinschaft Center Grants SFB1134 subproject B04.

Many people were involved and helped me at different phases of my PhD thesis and I would like to deeply thank all of them for their scientific and moral support:

First of all I would like to thank my supervisors Professor Wolfgang Sommer and Professor Rainer Spanagel for their excellent guidance through my PhD. Thank you for giving me the opportunity to participate in several important conferences and meetings, including the ISBRA conference in Berlin and the Gordon Research Conference in Galveston.

I want to thank Professor Stephan Frings and Dr. Kevin Allen for being part of my PhD committee.

A special thank goes to Dr. Anita Hansson, Dr. Kai Schönig, Dr. Thomas Enkel, Prof. Dusan Bartsch, Dr. Christoph Körber, Ivo Sonntag, Janine Reinert, Marion Schmitt and Prof. Thomas Kuner for their precious collaboration. This work would not have been possible without your help and scientific support.

My deep gratitude goes to all the Bachelor and Master students whom I was allowed to supervise during all these years. It has been a pleasure to work with you and I am truly grateful for your scientific and moral support. Jana Zell and Ana Gallego-Roman, thank you for your help with the mGluR2 Project, that was always ongoing from the beginning of my PhD until the very end. I would like to thank Sarah Meister, Daniel Gehrlach, Eva Ausbüttel, Eva Metzger, Laura Gey, Katja Lingelbach, Nicole Weigelt, Arian Hach and Valentina Neukel for their help with operant conditioning experiments and their enormous help in generating post-dependent animals. A special thank goes to Elisabeth Paul, Laura Schaaf and Rebecca Hoffmann for their excellent help with two really ambitious ongoing projects. All of you were fundamental for this thesis and I really enjoyed working with you and supervising you. It was a pleasure to spend time with you in and outside the lab.

Acknowledgements

I am grateful for my wonderful colleagues and friends Laura Broccoli, Elisabeth Paul, Tatiane Takahashi, Laura Schaaf, Rebecca Hoffmann and Janet Barroso-Flores. You made my life inside and outside the lab much easier.

A special thank goes to Elisabeth Röbel. Thank you for your patience, your everlasting support, your optimism and your encouragement. Without you, life in the lab would have been much harder.

I would like to thank all my laboratory and office colleagues, who helped me during all the good and harder times during my PhD. It was so good to work with you, to go to Retreats and Conferences together, or to have some Margaritas in the evening: Claudia Schäfer, Christine Roggenkamp, Stefanie Uhrig, Natalie Hirth, Sandra Dieter, Anastasia Olevska, Manuela Eisenhardt, Sarah Leixner, Catarina Luis, Valentina Vengeliene, Martin Roßmanith, Sabrina Koch, Ainhoa Bilbao, Maria Secci, Peggy Schneider, Elena Büchler, Anne Mallien, Alejandro Cosa-Linan, Hamid Noori, Oliver Stählin, Esi Domi, Peter Breunig, Marvin Pätz, Shoepeng Wei, Tianyang Ma, Georg Köhr and Thorsten Lau.

An enormous "Thank you!" goes to all my friends outside the lab! A special thank goes to Franziska, Jessica, Katrin, Lisa, Lisa-Marie and Luisa. Since our time at the Heinrich-Böll Gymnasium in Ludwigshafen I could always count on your friendship and support.

All this work would not have been possible without the constant support and help from my family. I thank you for all your help! Richard, I thank you for all your patience and never ending support. Together with my family, you gave me the necessary energy especially towards the end of this thesis.

There surely should be many more names mentioned here. I am truly grateful for everyone supporting me during the last years and joining me during all the good and harder times.

It was the best of times, it was the worst of times.

Charles Dickens
A Tale of Two Cities

References

Agell N, Bachs O, Rocamora N, Villalonga P (2002) Modulation of the Ras/Raf/MEK/ERK pathway by Ca(2+), and calmodulin. Cell Signal 14:649-654.

Akerboom J et al. (2012) Optimization of a GCaMP calcium indicator for neural activity imaging. J Neurosci 32:13819-13840.

American Psychiatric Association (2013) Diagnostic and Statistical Manual of Mental Disorders, 5th Edition. Washington, DC.

Angel P, Karin M (1991) The role of Jun, Fos and the AP-1 complex in cell-proliferation and transformation. Biochim Biophys Acta 1072:129-157.

Arias-Carrión O, Stamelou M, Murillo-Rodríguez E, Menéndez-González M, Pöppel E (2010) Dopaminergic reward system: a short integrative review. Int Arch Med 3:24.

Aronica E, van Vliet EA, Mayboroda OA, Troost D, da Silva FH, Gorter JA (2000) Upregulation of metabotropic glutamate receptor subtype mGluR3 and mGluR5 in reactive astrocytes in a rat model of mesial temporal lobe epilepsy. Eur J Neurosci 12:2333-2344.

Augier E, Dulman RS, Rauffenbart C, Augier G, Cross AJ, Heilig M (2016) The mGluR2 Positive Allosteric Modulator, AZD8529, and Cue-Induced Relapse to Alcohol Seeking in Rats. Neuropsychopharmacology 41:2932-2940.

Azaripour A, Lagerweij T, Scharfbillig C, Jadczak AE, Willershausen B, Van Noorden CJF (2016) A survey of clearing techniques for 3D imaging of tissues with special reference to connective tissue. Progress in Histochemistry and Cytochemistry 51:9-23.

Bäckström P, Hyytiä P (2005) Suppression of alcohol self-administration and cue-induced reinstatement of alcohol seeking by the mGlu2/3 receptor agonist LY379268 and the mGlu8 receptor agonist (S)-3,4-DCPG. Eur J Pharmacol 528:110-118.

Bading H, Hardingham GE, Johnson CM, Chawla S (1997) Gene regulation by nuclear and cytoplasmic calcium signals. Biochem Biophys Res Commun 236:541-543.

Bahrami S, Drablos F (2016) Gene regulation in the immediate-early response process. Adv Biol Regul 62:37-49.

Bashir ZI, Banks PJ (2017) Dead or alive? The manipulation of neuronal ensembles and pathways by daunorubicin. Brain and Neuroscience Advances 1:2398212817728229.

References

Beckmann AM, Wilce PA (1997) Egr transcription factors in the nervous system. Neurochem Int 31:477-510; discussion 517-476.

Bell RL, Rodd ZA, Sable HJ, Schultz JA, Hsu CC, Lumeng L, Murphy JM, McBride WJ (2006) Daily patterns of ethanol drinking in peri-adolescent and adult alcohol-preferring (P) rats. Pharmacol Biochem Behav 83:35-46.

Berg EA (1948) A simple objective technique for measuring flexibility in thinking. J Gen Psychol 39:15-22.

Berretta S, Pantazopoulos H, Caldera M, Pantazopoulos P, Paré D (2005) Infralimbic cortex activation increases c-fos expression in intercalated neurons of the amygdala. Neuroscience 132:943-953.

Berridge KC, Kringelbach ML (2008) Affective neuroscience of pleasure: reward in humans and animals. Psychopharmacology (Berl) 199:457-480.

Berridge KC, Robinson TE, Aldridge JW (2009) Dissecting components of reward: 'liking', 'wanting', and learning. Curr Opin Pharmacol 9:65-73.

Berridge MJ, Lipp P, Bootman MD (2000) The versatility and universality of calcium signalling. Nat Rev Mol Cell Biol 1:11-21.

Birrell JM, Brown VJ (2000) Medial frontal cortex mediates perceptual attentional set shifting in the rat. J Neurosci 20:4320-4324.

Blaha CD, Yang CR, Floresco SB, Barr AM, Phillips AG (1997) Stimulation of the ventral subiculum of the hippocampus evokes glutamate receptor-mediated changes in dopamine efflux in the rat nucleus accumbens. Eur J Neurosci 9:902-911.

Bonaccorso C, Micale N, Ettari R, Grasso S, Zappala M (2011) Glutamate binding-site ligands of NMDA receptors. Curr Med Chem 18:5483-5506.

Bossert JM, Marchant NJ, Calu DJ, Shaham Y (2013) The reinstatement model of drug relapse: recent neurobiological findings, emerging research topics, and translational research. Psychopharmacology (Berl) 229:453-476.

Bossert JM, Stern AL, Theberge FR, Cifani C, Koya E, Hope BT, Shaham Y (2011) Ventral medial prefrontal cortex neuronal ensembles mediate context-induced relapse to heroin. Nat Neurosci 14:420-422.

Brady AM, Floresco SB (2015) Operant procedures for assessing behavioral flexibility in rats. J Vis Exp:e52387.

Brion M, D'Hondt F, Pitel AL, Lecomte B, Ferauge M, de Timary P, Maurage P (2017) Executive functions in alcohol-dependence: A theoretically grounded and integrative exploration. Drug Alcohol Depend 177:39-47.

Brog JS, Salyapongse A, Deutch AY, Zahm DS (1993) The patterns of afferent innervation of the core and shell in the "accumbens" part of the rat ventral striatum: immunohistochemical detection of retrogradely transported fluoro-gold. J Comp Neurol 338:255-278.

Buisson A, Choi DW (1995) The inhibitory mGluR agonist, S-4-carboxy-3-hydroxy-phenylglycine selectively attenuates NMDA neurotoxicity and oxygen-glucose deprivation-induced neuronal death. Neuropharmacology 34:1081-1087.

Buschman TJ, Miller EK (2014) Goal-direction and top-down control. Philosophical Transactions of the Royal Society B: Biological Sciences 369.

Buzsáki G (2004) Large-scale recording of neuronal ensembles. Nature Neuroscience 7:446.

Cahill E, Salery M, Vanhoutte P, Caboche J (2014) Convergence of dopamine and glutamate signaling onto striatal ERK activation in response to drugs of abuse. Front Pharmacol 4:172.

Cai DJ et al. (2016) A shared neural ensemble links distinct contextual memories encoded close in time. Nature 534:115-118.

Cannella N, Economidou D, Kallupi M, Stopponi S, Heilig M, Massi M, Ciccocioppo R (2009) Persistent increase of alcohol-seeking evoked by neuropeptide S: an effect mediated by the hypothalamic hypocretin system. Neuropsychopharmacology 34:2125-2134.

Caprioli D, Justinova Z, Venniro M, Shaham Y (2018) Effect of Novel Allosteric Modulators of Metabotropic Glutamate Receptors on Drug Self-administration and Relapse: A Review of Preclinical Studies and Their Clinical Implications. Biol Psychiatry 84:180-192.

Carta M, Ariwodola OJ, Weiner JL, Valenzuela CF (2003) Alcohol potently inhibits the kainate receptor-dependent excitatory drive of hippocampal interneurons. Proc Natl Acad Sci U S A 100:6813-6818.

Casanova E, Fehsenfeld S, Mantamadiotis T, Lemberger T, Greiner E, Stewart AF, Schutz G (2001) A CamKIIalpha iCre BAC allows brain-specific gene inactivation. Genesis 31:37-42.

Chan RC, Chen EY, Cheung EF, Cheung HK (2004) Executive dysfunctions in schizophrenia. Relationships to clinical manifestation. Eur Arch Psychiatry Clin Neurosci 254:256-262.

Chang JY, Zhang L, Janak PH, Woodward DJ (1997a) Neuronal responses in prefrontal cortex and nucleus accumbens during heroin self-administration in freely moving rats. Brain Res 754:12-20.

Chang JY, Sawyer SF, Paris JM, Kirillov A, Woodward DJ (1997b) Single neuronal responses in medial prefrontal cortex during cocaine self-administration in freely moving rats. Synapse 26:22-35.

Chen D, Wu CF, Shi B, Xu YM (2002a) Tamoxifen and toremifene cause impairment of learning and memory function in mice. Pharmacol Biochem Behav 71:269-276.

Chen D, Wu CF, Shi B, Xu YM (2002b) Tamoxifen and toremifene impair retrieval, but not acquisition, of spatial information processing in mice. Pharmacol Biochem Behav 72:417-421.

Chen RH, Sarnecki C, Blenis J (1992) Nuclear localization and regulation of erk- and rsk-encoded protein kinases. Mol Cell Biol 12:915-927.

Chen TW, Wardill TJ, Sun Y, Pulver SR, Renninger SL, Baohan A, Schreiter ER, Kerr RA, Orger MB, Jayaraman V, Looger LL, Svoboda K, Kim DS (2013) Ultrasensitive fluorescent proteins for imaging neuronal activity. Nature 499:295-300.

Cho A, Haruyama N, Kulkarni AB (2009) Generation of transgenic mice. Curr Protoc Cell Biol Chapter 19:Unit 19 11.

Ciccocioppo R (2013) Genetically selected alcohol preferring rats to model human alcoholism. Curr Top Behav Neurosci 13:251-269.

Ciccocioppo R, Angeletti S, Weiss F (2001) Long-lasting resistance to extinction of response reinstatement induced by ethanol-related stimuli: role of genetic ethanol preference. Alcohol Clin Exp Res 25:1414-1419.

Ciccocioppo R, Martin-Fardon R, Weiss F (2002) Effect of selective blockade of mu(1) or delta opioid receptors on reinstatement of alcohol-seeking behavior by drug-associated stimuli in rats. Neuropsychopharmacology 27:391-399.

Ciccocioppo R, Lin D, Martin-Fardon R, Weiss F (2003) Reinstatement of ethanol-seeking behavior by drug cues following single versus multiple ethanol intoxication in the rat: effects of naltrexone. Psychopharmacology (Berl) 168:208-215.

Ciccocioppo R, Panocka I, Polidori C, Froldi R, Angeletti S, Massi M (1998) Mechanism of action for reduction of ethanol intake in rats by the tachykinin NK-3 receptor agonist aminosenktide. Pharmacol Biochem Behav 61:459-464.

Ciccocioppo R, Economidou D, Cippitelli A, Cucculelli M, Ubaldi M, Soverchia L, Lourdusamy A, Massi M (2006) Genetically selected Marchigian Sardinian alcohol-

preferring (msP) rats: an animal model to study the neurobiology of alcoholism. Addict Biol 11:339-355.

Cohen S, Greenberg ME (2008) Communication between the synapse and the nucleus in neuronal development, plasticity, and disease. Annu Rev Cell Dev Biol 24:183-209.

Cole AJ, Saffen DW, Baraban JM, Worley PF (1989) Rapid increase of an immediate early gene messenger RNA in hippocampal neurons by synaptic NMDA receptor activation. Nature 340:474-476.

Colombo G (1997) ESBRA-Nordmann 1996 Award Lecture: ethanol drinking behaviour in Sardinian alcohol-preferring rats. Alcohol Alcohol 32:443-453.

Conn PJ, Pin JP (1997) Pharmacology and functions of metabotropic glutamate receptors. Annu Rev Pharmacol Toxicol 37:205-237.

Courtney KE, Ghahremani DG, Ray LA (2013) Fronto-striatal functional connectivity during response inhibition in alcohol dependence. Addict Biol 18:593-604.

Crombag HS, Shaham Y (2002) Renewal of drug seeking by contextual cues after prolonged extinction in rats. Behav Neurosci 116:169-173.

Cruz FC, Javier Rubio F, Hope BT (2015) Using c-fos to study neuronal ensembles in corticostriatal circuitry of addiction. Brain Res 1628:157-173.

Cruz FC, Koya E, Guez-Barber DH, Bossert JM, Lupica CR, Shaham Y, Hope BT (2013) New technologies for examining the role of neuronal ensembles in drug addiction and fear. Nat Rev Neurosci 14:743-754.

Cruz FC, Babin KR, Leao RM, Goldart EM, Bossert JM, Shaham Y, Hope BT (2014) Role of nucleus accumbens shell neuronal ensembles in context-induced reinstatement of cocaine-seeking. J Neurosci 34:7437-7446.

Csaba G, Karabelyos C (2001) The effect of a single neonatal treatment (hormonal imprinting) with the antihormones, tamoxifen and mifepristone on the sexual behavior of adult rats. Pharmacol Res 43:531-534.

Cui G, Jun SB, Jin X, Pham MD, Vogel SS, Lovinger DM, Costa RM (2013) Concurrent activation of striatal direct and indirect pathways during action initiation. Nature 494:238-242.

D'Souza MS (2015) Glutamatergic transmission in drug reward: implications for drug addiction. Front Neurosci 9:404.

D'Antoni S, Berretta A, Bonaccorso CM, Bruno V, Aronica E, Nicoletti F, Catania MV (2008) Metabotropic Glutamate Receptors in Glial Cells. Neurochemical Research 33:2436-2443.

Dalley JW, Cardinal RN, Robbins TW (2004) Prefrontal executive and cognitive functions in rodents: neural and neurochemical substrates. Neurosci Biobehav Rev 28:771-784.

Datiche F, Cattarelli M (1996) Reciprocal and topographic connections between the piriform and prefrontal cortices in the rat: a tracing study using the B subunit of the cholera toxin. Brain Res Bull 41:391-398.

Dayas CV, Liu X, Simms JA, Weiss F (2007) Distinct patterns of neural activation associated with ethanol seeking: effects of naltrexone. Biol Psychiatry 61:979-989.

de Bruin JP, Sanchez-Santed F, Heinsbroek RP, Donker A, Postmes P (1994) A behavioural analysis of rats with damage to the medial prefrontal cortex using the Morris water maze: evidence for behavioural flexibility, but not for impaired spatial navigation. Brain Res 652:323-333.

De Filippis B, Lyon L, Taylor A, Lane T, Burnet PW, Harrison PJ, Bannerman DM (2015) The role of group II metabotropic glutamate receptors in cognition and anxiety: comparative studies in GRM2(-/-), GRM3(-/-) and GRM2/3(-/-) knockout mice. Neuropharmacology 89:19-32.

de Guglielmo G, Crawford E, Kim S, Vendruscolo LF, Hope BT, Brennan M, Cole M, Koob GF, George O (2016) Recruitment of a Neuronal Ensemble in the Central Nucleus of the Amygdala Is Required for Alcohol Dependence. J Neurosci 36:9446-9453.

de Wit H (1996) Priming effects with drugs and other reinforcers.

de Wit H, Stewart J (1981) Reinstatement of cocaine-reinforced responding in the rat. Psychopharmacology (Berl) 75:134-143.

DeNardo LA, Berns DS, DeLoach K, Luo L (2015) Connectivity of mouse somatosensory and prefrontal cortex examined with trans-synaptic tracing. Nat Neurosci 18:1687-1697.

Denayer T, Stöhr T, Van Roy M (2014) Animal models in translational medicine: Validation and prediction. New Horizons in Translational Medicine 2:5-11.

DePoy L, Daut R, Brigman JL, MacPherson K, Crowley N, Gunduz-Cinar O, Pickens CL, Cinar R, Saksida LM, Kunos G, Lovinger DM, Bussey TJ, Camp MC, Holmes A (2013) Chronic alcohol produces neuroadaptations to prime dorsal striatal learning. Proc Natl Acad Sci U S A 110:14783-14788.

DHS Jahrbuch Sucht (2018) Deutsche Hauptstelle für Suchtfragen (DHS) e.V.

Di Chiara G (1999) Drug addiction as dopamine-dependent associative learning disorder. Eur J Pharmacol 375:13-30.

Di Chiara G, Imperato A (1988) Drugs abused by humans preferentially increase synaptic dopamine concentrations in the mesolimbic system of freely moving rats. Proc Natl Acad Sci U S A 85:5274-5278.

Die Drogenbeauftragte der Bundesregierung Drogen- und Suchtbericht Juli 2017. Bundesministerium für Gesundheit: 11055 Berlin, Germany.

Ding ZM, Ingraham CM, Hauser SR, Lasek AW, Bell RL, McBride WJ (2017) Reduced Levels of mGlu2 Receptors within the Prelimbic Cortex Are Not Associated with Elevated Glutamate Transmission or High Alcohol Drinking. Alcohol Clin Exp Res 41:1896-1906.

Dobbing J, Smart JL (1974) Vulnerability of developing brain and behaviour. Br Med Bull 30:164-168.

Douglas RJ, Martin KAC (2004) NEURONAL CIRCUITS OF THE NEOCORTEX. Annual Review of Neuroscience 27:419-451.

Duclot F, Kabbaj M (2017) The Role of Early Growth Response 1 (EGR1) in Brain Plasticity and Neuropsychiatric Disorders. Front Behav Neurosci 11:35.

Dudek M, Abo-Ramadan U, Hermann D, Brown M, Canals S, Sommer WH, Hyytia P (2015) Brain activation induced by voluntary alcohol and saccharin drinking in rats assessed with manganese-enhanced magnetic resonance imaging. Addict Biol 20:1012-1021.

Dudley R (2000) Evolutionary origins of human alcoholism in primate frugivory. Q Rev Biol 75:3-15.

Economo MN, Clack NG, Lavis LD, Gerfen CR, Svoboda K, Myers EW, Chandrashekar J (2016) A platform for brain-wide imaging and reconstruction of individual neurons. eLife 5:e10566.

Eisener-Dorman AF, Lawrence DA, Bolivar VJ (2009) Cautionary insights on knockout mouse studies: the gene or not the gene? Brain Behav Immun 23:318-324.

Ellenbroek B, Youn J (2016) Rodent models in neuroscience research: is it a rat race? Dis Model Mech 9:1079-1087.

Engeln M, Bastide MF, Toulme E, Dehay B, Bourdenx M, Doudnikoff E, Li Q, Gross CE, Boue-Grabot E, Pisani A, Bezard E, Fernagut PO (2016) Selective Inactivation of Striatal FosB/DeltaFosB-Expressing Neurons Alleviates L-DOPA-Induced Dyskinesia. Biol Psychiatry 79:354-361.

Epstein DH, Preston KL, Stewart J, Shaham Y (2006) Toward a model of drug relapse: an assessment of the validity of the reinstatement procedure. Psychopharmacology (Berl) 189:1-16.

Eriksson K (1969) The estimation of heritability for the self-selection of alcohol in the albino rat. Ann Med Exp Biol Fenn 47:172-174.

Euston DR, Gruber AJ, McNaughton BL (2012) The role of medial prefrontal cortex in memory and decision making. Neuron 76:1057-1070.

Everitt BJ, Belin D, Economidou D, Pelloux Y, Dalley JW, Robbins TW (2008) Review. Neural mechanisms underlying the vulnerability to develop compulsive drug-seeking habits and addiction. Philos Trans R Soc Lond B Biol Sci 363:3125-3135.

Farquhar D, Pan BF, Sakurai M, Ghosh A, Mullen CA, Nelson JA (2002) Suicide gene therapy using E. coli beta-galactosidase. Cancer Chemother Pharmacol 50:65-70.

Feil R, Wagner J, Metzger D, Chambon P (1997) Regulation of Cre recombinase activity by mutated estrogen receptor ligand-binding domains. Biochem Biophys Res Commun 237:752-757.

Flagel SB, Akil H, Robinson TE (2009) Individual differences in the attribution of incentive salience to reward-related cues: Implications for addiction. Neuropharmacology 56 Suppl 1:139-148.

Flavell CR, Lee JL (2012) Post-training unilateral amygdala lesions selectively impair contextual fear memories. Learn Mem 19:256-263.

Fosque BF, Sun Y, Dana H, Yang C-T, Ohyama T, Tadross MR, Patel R, Zlatic M, Kim DS, Ahrens MB, Jayaraman V, Looger LL, Schreiter ER (2015) Labeling of active neural circuits in vivo with designed calcium integrators. Science 347:755-760.

Fowler T, Sen R, Roy AL (2011) Regulation of primary response genes. Mol Cell 44:348-360.

Fuchs RA, Evans KA, Ledford CC, Parker MP, Case JM, Mehta RH, See RE (2005) The role of the dorsomedial prefrontal cortex, basolateral amygdala, and dorsal hippocampus in contextual reinstatement of cocaine seeking in rats. Neuropsychopharmacology 30:296-309.

Funk D, Li Z, Coen K, Le AD (2008) Effects of pharmacological stressors on c-fos and CRF mRNA in mouse brain: relationship to alcohol seeking. Neurosci Lett 444:254-258.

Fuxe K (1965) Evidence for the existence of monoamine neurons in the central nervous system. Zeitschrift für Zellforschung und Mikroskopische Anatomie 65:573-596.

Gabbott PL, Warner TA, Jays PR, Bacon SJ (2003) Areal and synaptic interconnectivity of prelimbic (area 32), infralimbic (area 25) and insular cortices in the rat. Brain Res 993:59-71.

Gabbott PL, Warner TA, Jays PR, Salway P, Busby SJ (2005) Prefrontal cortex in the rat: projections to subcortical autonomic, motor, and limbic centers. J Comp Neurol 492:145-177.

Gallego-Roman A (2016) THE EFFECT OF AAV-MEDIATED INFRALIMBIC MGLUR2 KNOCKDOWN ON ALCOHOL-SEEKING BEHAVIOR IN RATS. Master Thesis, University of Skövde.

Gardner EL (2011) Introduction: Addiction and Brain Reward and Anti-Reward Pathways. Advances in psychosomatic medicine 30:22-60.

Garland EL, Carter K, Ropes K, Howard MO (2012) Thought suppression, impaired regulation of urges, and Addiction-Stroop predict affect-modulated cue-reactivity among alcohol dependent adults. Biological Psychology 89:87-93.

Gass JT, Olive MF (2008) Glutamatergic substrates of drug addiction and alcoholism. Biochem Pharmacol 75:218-265.

Gass JT, Chandler LJ (2013) The Plasticity of Extinction: Contribution of the Prefrontal Cortex in Treating Addiction through Inhibitory Learning. Front Psychiatry 4:46.

German DC, Manaye KF (1993) Midbrain dopaminergic neurons (nuclei A8, A9, and A10): three-dimensional reconstruction in the rat. J Comp Neurol 331:297-309.

Ghosh KK, Burns LD, Cocker ED, Nimmerjahn A, Ziv Y, Gamal AE, Schnitzer MJ (2011) Miniaturized integration of a fluorescence microscope. Nat Methods 8:871-878.

Gibson JJ (1941) A critical review of the concept of set in contemporary experimental psychology. Psychological Bulletin 38:781-817.

Gilpin NW, Smith AD, Cole M, Weiss F, Koob GF, Richardson HN (2009) Operant behavior and alcohol levels in blood and brain of alcohol-dependent rats. Alcohol Clin Exp Res 33:2113-2123.

Ginsburg N, Karpiuk P (1994) Random Generation: Analysis of the Responses. Perceptual and Motor Skills 79:1059-1067.

Goldstein RZ, Volkow ND (2011) Dysfunction of the prefrontal cortex in addiction: neuroimaging findings and clinical implications. Nat Rev Neurosci 12:652-669.

Gomperts SN, Kloosterman F, Wilson MA (2015) VTA neurons coordinate with the hippocampal reactivation of spatial experience. Elife 4.

Gonda X (2012) Basic pharmacology of NMDA receptors. Curr Pharm Des 18:1558-1567.

Goodwani S, Saternos H, Alasmari F, Sari Y (2017) Metabotropic and ionotropic glutamate receptors as potential targets for the treatment of alcohol use disorder. Neurosci Biobehav Rev 77:14-31.

Green J, Dykstra L, Carelli RM (2015) A preclinical model of natural reward devaluation in cocaine addiction: Effects of dose. Drug & Alcohol Dependence 146:e129.

Greenberg ME, Ziff EB (1984) Stimulation of 3T3 cells induces transcription of the c-fos proto-oncogene. Nature 311:433-438.

Greenough WT, Hwang HM, Gorman C (1985) Evidence for active synapse formation or altered postsynaptic metabolism in visual cortex of rats reared in complex environments. Proc Natl Acad Sci U S A 82:4549-4552.

Grewe BF, Grundemann J, Kitch LJ, Lecoq JA, Parker JG, Marshall JD, Larkin MC, Jercog PE, Grenier F, Li JZ, Luthi A, Schnitzer MJ (2017) Neural ensemble dynamics underlying a long-term associative memory. Nature 543:670-675.

Grienberger C, Konnerth A (2012) Imaging calcium in neurons. Neuron 73:862-885.

Grüsser SM, Wrase J, Klein S, Hermann D, Smolka MN, Ruf M, Weber-Fahr W, Flor H, Mann K, Braus DF, Heinz A (2004) Cue-induced activation of the striatum and medial prefrontal cortex is associated with subsequent relapse in abstinent alcoholics. Psychopharmacology (Berl) 175:296-302.

Gulati S, Cao VY, Otte S (2017) Multi-layer Cortical Ca2+ Imaging in Freely Moving Mice with Prism Probes and Miniaturized Fluorescence Microscopy. J Vis Exp.

Gunaydin LA, Grosenick L, Finkelstein JC, Kauvar IV, Fenno LE, Adhikari A, Lammel S, Mirzabekov JJ, Airan RD, Zalocusky KA, Tye KM, Anikeeva P, Malenka RC, Deisseroth K (2014) Natural neural projection dynamics underlying social behavior. Cell 157:1535-1551.

Guzowski JF, McNaughton BL, Barnes CA, Worley PF (1999) Environment-specific expression of the immediate-early gene Arc in hippocampal neuronal ensembles. Nat Neurosci 2:1120-1124.

Hagenston AM, Bading H (2011) Calcium signaling in synapse-to-nucleus communication. Cold Spring Harb Perspect Biol 3:a004564.

Hajos M, Gartside SE, Varga V, Sharp T (2003) In vivo inhibition of neuronal activity in the rat ventromedial prefrontal cortex by midbrain-raphe nuclei: role of 5-HT1A receptors. Neuropharmacology 45:72-81.

Hamilton DL, Abremski K (1984) Site-specific recombination by the bacteriophage P1 lox-Cre system. Cre-mediated synapsis of two lox sites. J Mol Biol 178:481-486.

Hansson AC, Rimondini R, Neznanova O, Sommer WH, Heilig M (2008) Neuroplasticity in brain reward circuitry following a history of ethanol dependence. Eur J Neurosci 27:1912-1922.

Hara H, Friedlander RM, Gagliardini V, Ayata C, Fink K, Huang Z, Shimizu-Sasamata M, Yuan J, Moskowitz MA (1997) Inhibition of interleukin 1beta converting enzyme family proteases reduces ischemic and excitotoxic neuronal damage. Proc Natl Acad Sci U S A 94:2007-2012.

Hardingham GE, Arnold FJ, Bading H (2001) Nuclear calcium signaling controls CREB-mediated gene expression triggered by synaptic activity. Nat Neurosci 4:261-267.

Hart EE, Izquierdo A (2017) Basolateral amygdala supports the maintenance of value and effortful choice of a preferred option. Eur J Neurosci 45:388-397.

Hauck B, Chen L, Xiao W (2003) Generation and characterization of chimeric recombinant AAV vectors. Mol Ther 7:419-425.

Hebb DO (1949) The organization of behavior: a neuropsychological theory: Wiley.

Heidbreder CA, Groenewegen HJ (2003) The medial prefrontal cortex in the rat: evidence for a dorso-ventral distinction based upon functional and anatomical characteristics. Neurosci Biobehav Rev 27:555-579.

Heilig M, Koob GF (2007) A key role for corticotropin-releasing factor in alcohol dependence. Trends Neurosci 30:399-406.

Hendricson AW, Sibbald JR, Morrisett RA (2004) Ethanol alters the frequency, amplitude, and decay kinetics of Sr2+-supported, asynchronous NMDAR mEPSCs in rat hippocampal slices. J Neurophysiol 91:2568-2577.

Hendricson AW, Thomas MP, Lippmann MJ, Morrisett RA (2003) Suppression of L-type voltage-gated calcium channel-dependent synaptic plasticity by ethanol: analysis of miniature synaptic currents and dendritic calcium transients. J Pharmacol Exp Ther 307:550-558.

Herdegen T, Leah JD (1998) Inducible and constitutive transcription factors in the mammalian nervous system: control of gene expression by Jun, Fos and Krox, and CREB/ATF proteins. Brain Res Brain Res Rev 28:370-490.

Hermann D, Weber-Fahr W, Sartorius A, Hoerst M, Frischknecht U, Tunc-Skarka N, Perreau-Lenz S, Hansson AC, Krumm B, Kiefer F, Spanagel R, Mann K, Ende G, Sommer WH (2012) Translational magnetic resonance spectroscopy reveals excessive central glutamate levels during alcohol withdrawal in humans and rats. Biol Psychiatry 71:1015-1021.

Hermans E, Challiss RA (2001) Structural, signalling and regulatory properties of the group I metabotropic glutamate receptors: prototypic family C G-protein-coupled receptors. Biochem J 359:465-484.

Hernandez CM, McQuail JA, Schwabe MR, Burke SN, Setlow B, Bizon JL (2018) Age-Related Declines in Prefrontal Cortical Expression of Metabotropic Glutamate Receptors that Support Working Memory. eneuro 5.

Herry C, Ciocchi S, Senn V, Demmou L, Müller C, Lüthi A (2008) Switching on and off fear by distinct neuronal circuits. Nature 454:600.

Hill EL (2004) Executive dysfunction in autism. Trends Cogn Sci 8:26-32.

Hodos W (1961) Progressive ratio as a measure of reward strength. Science 134:943-944.

Hoess R, Abremski K, Irwin S, Kendall M, Mack A (1990) DNA specificity of the Cre recombinase resides in the 25 kDa carboxyl domain of the protein. J Mol Biol 216:873-882.

Hoffmann R (2017) Infralimbic mGluR2 Deficit as a Common Pathological Mechanism for Excessive Alcohol Seeking and Impaired Behavioral Flexibility. Master Thesis, University of Heidelberg.

Holtmaat A, Caroni P (2016) Functional and structural underpinnings of neuronal assembly formation in learning. Nat Neurosci 19:1553-1562.

Houston RJ, Derrick JL, Leonard KE, Testa M, Quigley BM, Kubiak A (2014) Effects of heavy drinking on executive cognitive functioning in a community sample. Addict Behav 39:345-349.

Howland JG, Taepavarapruk P, Phillips AG (2002) Glutamate receptor-dependent modulation of dopamine efflux in the nucleus accumbens by basolateral, but not central, nucleus of the amygdala in rats. J Neurosci 22:1137-1145.

Hu X-J, Ticku MK (1995) Chronic ethanol treatment upregulates the NMDA receptor function and binding in mammalian cortical neurons. Molecular Brain Research 30:347-356.

Huber D, Gutnisky DA, Peron S, O'Connor DH, Wiegert JS, Tian L, Oertner TG, Looger LL, Svoboda K (2012) Multiple dynamic representations in the motor cortex during sensorimotor learning. Nature 484:473-478.

Hurley KM, Herbert H, Moga MM, Saper CB (1991) Efferent projections of the infralimbic cortex of the rat. J Comp Neurol 308:249-276.

Ikemoto S, Bonci A (2014) Neurocircuitry of drug reward. Neuropharmacology 76 Pt B:329-341.

Indra AK, Warot X, Brocard J, Bornert JM, Xiao JH, Chambon P, Metzger D (1999) Temporally-controlled site-specific mutagenesis in the basal layer of the epidermis: comparison of the recombinase activity of the tamoxifen-inducible Cre-ER(T) and Cre-ER(T2) recombinases. Nucleic Acids Res 27:4324-4327.

Ito R, Robbins TW, Everitt BJ (2004) Differential control over cocaine-seeking behavior by nucleus accumbens core and shell. Nat Neurosci 7:389-397.

Jackson AL, Linsley PS (2010) Recognizing and avoiding siRNA off-target effects for target identification and therapeutic application. Nature Reviews Drug Discovery 9:57.

Jantas D, Lason W (2009) Protective effect of memantine against Doxorubicin toxicity in primary neuronal cell cultures: influence a development stage. Neurotox Res 15:24-37.

Jares-Erijman EA, Jovin TM (2003) FRET imaging. Nat Biotechnol 21:1387-1395.

Jennings JH, Stuber GD (2014) Tools for resolving functional activity and connectivity within intact neural circuits. Curr Biol 24:R41-50.

Jennings JH, Ung RL, Resendez SL, Stamatakis AM, Taylor JG, Huang J, Veleta K, Kantak PA, Aita M, Shilling-Scrivo K, Ramakrishnan C, Deisseroth K, Otte S, Stuber GD (2015) Visualizing hypothalamic network dynamics for appetitive and consummatory behaviors. Cell 160:516-527.

Jernigan TL, Butters N, DiTraglia G, Schafer K, Smith T, Irwin M, Grant I, Schuckit M, Cermak LS (1991) Reduced cerebral grey matter observed in alcoholics using magnetic resonance imaging. Alcohol Clin Exp Res 15:418-427.

Ji G, Neugebauer V (2012) Modulation of medial prefrontal cortical activity using in vivo recordings and optogenetics. Mol Brain 5:36.

Jurado J, Fuentes-Almagro CA, Prieto-Alamo MJ, Pueyo C (2007) Alternative splicing of c-fos pre-mRNA: contribution of the rates of synthesis and degradation to the copy number of each transcript isoform and detection of a truncated c-Fos immunoreactive species. BMC Mol Biol 8:83.

Kaczmarek L (1993) Molecular biology of vertebrate learning: Is c-fos a new beginning? Journal of Neuroscience Research 34:377-381.

Kalivas PW (1993) Neurotransmitter regulation of dopamine neurons in the ventral tegmental area. Brain Res Brain Res Rev 18:75-113.

Kasof GM, Mandelzys A, Maika SD, Hammer RE, Curran T, Morgan JI (1995) Kainic acid-induced neuronal death is associated with DNA damage and a unique immediate-early gene response in c-fos-lacZ transgenic rats. J Neurosci 15:4238-4249.

Katner SN, Magalong JG, Weiss F (1999) Reinstatement of alcohol-seeking behavior by drug-associated discriminative stimuli after prolonged extinction in the rat. Neuropsychopharmacology 20:471-479.

Kelley AE, Berridge KC (2002) The neuroscience of natural rewards: relevance to addictive drugs. J Neurosci 22:3306-3311.

Killcross S, Coutureau E (2003) Coordination of actions and habits in the medial prefrontal cortex of rats. Cereb Cortex 13:400-408.

Klee ML (2014) Prefrontal cortex fragility in alcohol dependence: Insights from metabolic activity and executive behavior studies. Master Thesis, University of Heidelberg.

Klugmann M, Goepfrich A, Friemel CM, Schneider M (2011) AAV-Mediated Overexpression of the CB1 Receptor in the mPFC of Adult Rats Alters Cognitive Flexibility, Social Behavior, and Emotional Reactivity. Front Behav Neurosci 5:37.

Kohl RR, Katner JS, Chernet E, McBride WJ (1998) Ethanol and negative feedback regulation of mesolimbic dopamine release in rats. Psychopharmacology (Berl) 139:79-85.

Kondo M, Kobayashi K, Ohkura M, Nakai J, Matsuzaki M (2017) Two-photon calcium imaging of the medial prefrontal cortex and hippocampus without cortical invasion. Elife 6.

Koob GF, Volkow ND (2010) Neurocircuitry of addiction. Neuropsychopharmacology 35:217-238.

Koya E, Margetts-Smith G, Hope BT (2016) Daun02 Inactivation of Behaviorally Activated Fos-Expressing Neuronal Ensembles. Curr Protoc Neurosci 76:8 36 31-38 36 17.

Koya E, Golden SA, Harvey BK, Guez-Barber DH, Berkow A, Simmons DE, Bossert JM, Nair SG, Uejima JL, Marin MT, Mitchell TB, Farquhar D, Ghosh SC, Mattson BJ, Hope BT (2009) Targeted disruption of cocaine-activated nucleus accumbens neurons prevents context-specific sensitization. Nat Neurosci 12:1069-1073.

Kroener S, Mulholland PJ, New NN, Gass JT, Becker HC, Chandler LJ (2012) Chronic alcohol exposure alters behavioral and synaptic plasticity of the rodent prefrontal cortex. PLoS One 7:e37541.

Kufahl PR, Martin-Fardon R, Weiss F (2011) Enhanced sensitivity to attenuation of conditioned reinstatement by the mGluR 2/3 agonist LY379268 and increased functional activity of mGluR 2/3 in rats with a history of ethanol dependence. Neuropsychopharmacology 36:2762-2773.

Kunkel GR, Maser RL, Calvet JP, Pederson T (1986) U6 small nuclear RNA is transcribed by RNA polymerase III. Proc Natl Acad Sci U S A 83:8575-8579.

Kupferschmidt DA, Brown ZJ, Erb S (2011) A procedure for studying the footshock-induced reinstatement of cocaine seeking in laboratory rats. J Vis Exp.

LaLumiere RT, Kalivas PW (2008) Glutamate Release in the Nucleus Accumbens Core Is Necessary for Heroin Seeking. The Journal of Neuroscience 28:3170-3177.

LaLumiere RT, Niehoff KE, Kalivas PW (2010) The infralimbic cortex regulates the consolidation of extinction after cocaine self-administration. Learn Mem 17:168-175.

LaLumiere RT, Smith KC, Kalivas PW (2012) Neural circuit competition in cocaine-seeking: roles of the infralimbic cortex and nucleus accumbens shell. Eur J Neurosci 35:614-622.

Lasseter HC, Ramirez DR, Xie X, Fuchs RA (2009) Involvement of the lateral orbitofrontal cortex in drug context-induced reinstatement of cocaine-seeking behavior in rats. Eur J Neurosci 30:1370-1381.

Lau A, Tymianski M (2010) Glutamate receptors, neurotoxicity and neurodegeneration. Pflugers Arch 460:525-542.

Lê AD, Harding S, Juzytsch W, Funk D, Shaham Y (2005) Role of alpha-2 adrenoceptors in stress-induced reinstatement of alcohol seeking and alcohol self-administration in rats. Psychopharmacology (Berl) 179:366-373.

Lê AD, Quan B, Juzytch W, Fletcher PJ, Joharchi N, Shaham Y (1998) Reinstatement of alcohol-seeking by priming injections of alcohol and exposure to stress in rats. Psychopharmacology (Berl) 135:169-174.

Lee D, Hyun JH, Jung K, Hannan P, Kwon H-B (2017) A calcium- and light-gated switch to induce gene expression in activated neurons. Nature Biotechnology 35:858.

Lenoir M, Serre F, Cantin L, Ahmed SH (2007) Intense sweetness surpasses cocaine reward. PLoS One 2:e698.

Lerma J, Marques JM (2013) Kainate receptors in health and disease. Neuron 80:292-311.

Li L, Carter J, Gao X, Whitehead J, Tourtellotte WG (2005) The neuroplasticity-associated arc gene is a direct transcriptional target of early growth response (Egr) transcription factors. Mol Cell Biol 25:10286-10300.

Li TK, Lumeng L, Doolittle DP (1993) Selective breeding for alcohol preference and associated responses. Behav Genet 23:163-170.

Liberti WA, Perkins LN, Leman DP, Gardner TJ (2017) An open source, wireless capable miniature microscope system. J Neural Eng 14:045001.

Lin D, Boyle MP, Dollar P, Lee H, Lein ES, Perona P, Anderson DJ (2011) Functional identification of an aggression locus in the mouse hypothalamus. Nature 470:221-226.

Liu P, Jenkins NA, Copeland NG (2003) A highly efficient recombineering-based method for generating conditional knockout mutations. Genome Res 13:476-484.

Liu X-B, Murray Karl D (2012) Neuronal excitability and calcium/calmodulin-dependent protein kinase type II: Location, location, location. Epilepsia 53:45-52.

Liu X, Weiss F (2002) Additive effect of stress and drug cues on reinstatement of ethanol seeking: exacerbation by history of dependence and role of concurrent activation of corticotropin-releasing factor and opioid mechanisms. J Neurosci 22:7856-7861.

Livak KJ, Schmittgen TD (2001) Analysis of relative gene expression data using real-time quantitative PCR and the 2(-Delta Delta C(T)) Method. Methods 25:402-408.

Loeber S, Duka T, Welzel H, Nakovics H, Heinz A, Flor H, Mann K (2009) Impairment of Cognitive Abilities and Decision Making after Chronic Use of Alcohol: The Impact of Multiple Detoxifications. Alcohol and Alcoholism 44:372-381.

Logue SF, Gould TJ (2014) The neural and genetic basis of executive function: attention, cognitive flexibility, and response inhibition. Pharmacol Biochem Behav 123:45-54.

Lopes G, Bonacchi N, Frazao J, Neto JP, Atallah BV, Soares S, Moreira L, Matias S, Itskov PM, Correia PA, Medina RE, Calcaterra L, Dreosti E, Paton JJ, Kampff AR (2015) Bonsai: an event-based framework for processing and controlling data streams. Front Neuroinform 9:7.

Lovinger DM, White G, Weight FF (1989) Ethanol inhibits NMDA-activated ion current in hippocampal neurons. Science 243:1721-1724.

Low RJ, Gu Y, Tank DW (2014) Cellular resolution optical access to brain regions in fissures: imaging medial prefrontal cortex and grid cells in entorhinal cortex. Proc Natl Acad Sci U S A 111:18739-18744.

Lumeng L, Hawkins TD, Li TK (1977) NEW STRAINS OF RATS WITH ALCOHOL PREFERENCE AND NONPREFERENCE. In: Alcohol and Aldehyde Metabolizing Systems, pp 537-544: Academic Press.

Lüscher C, Ungless MA (2006) The mechanistic classification of addictive drugs. PLoS Med 3:e437.

Lyford GL, Yamagata K, Kaufmann WE, Barnes CA, Sanders LK, Copeland NG, Gilbert DJ, Jenkins NA, Lanahan AA, Worley PF (1995) Arc, a growth factor and activity-regulated gene, encodes a novel cytoskeleton-associated protein that is enriched in neuronal dendrites. Neuron 14:433-445.

Madsen HB, Ahmed SH (2015) Drug versus sweet reward: greater attraction to and preference for sweet versus drug cues. Addict Biol 20:433-444.

Mao T, O'Connor DH, Scheuss V, Nakai J, Svoboda K (2008) Characterization and subcellular targeting of GCaMP-type genetically-encoded calcium indicators. PLoS One 3:e1796.

Maragakis NJ, Rothstein JD (2001) Glutamate transporters in neurologic disease. Arch Neurol 58:365-370.

Marchant NJ, Kaganovsky K, Shaham Y, Bossert JM (2015) Role of corticostriatal circuits in context-induced reinstatement of drug seeking. Brain Res 1628:219-232.

Martin-Fardon R, Weiss F (2013) Modeling relapse in animals. Curr Top Behav Neurosci 13:403-432.

Mauceri D, Hagenston AM, Schramm K, Weiss U, Bading H (2015) Nuclear Calcium Buffering Capacity Shapes Neuronal Architecture. J Biol Chem 290:23039-23049.

Mayford M (2014) The search for a hippocampal engram. Philosophical Transactions of the Royal Society B: Biological Sciences 369:20130161.

McAlonan K, Brown VJ (2003) Orbital prefrontal cortex mediates reversal learning and not attentional set shifting in the rat. Behav Brain Res 146:97-103.

McClure SM, York MK, Montague PR (2004) The neural substrates of reward processing in humans: the modern role of FMRI. Neuroscientist 10:260-268.

McDonald AJ, Mascagni F, Guo L (1996) Projections of the medial and lateral prefrontal cortices to the amygdala: a Phaseolus vulgaris leucoagglutinin study in the rat. Neuroscience 71:55-75.

McEntee WJ, Crook TH (1993) Glutamate: its role in learning, memory, and the aging brain. Psychopharmacology (Berl) 111:391-401.

McFarland K, Kalivas PW (2001) The circuitry mediating cocaine-induced reinstatement of drug-seeking behavior. J Neurosci 21:8655-8663.

McFarland K, Lapish CC, Kalivas PW (2003) Prefrontal Glutamate Release into the Core of the Nucleus Accumbens Mediates Cocaine-Induced Reinstatement of Drug-Seeking Behavior. The Journal of Neuroscience 23:3531-3537.

McKinney WT, Jr., Bunney WE, Jr. (1969) Animal model of depression. I. Review of evidence: implications for research. Arch Gen Psychiatry 21:240-248.

McLaughlin J, See RE (2003) Selective inactivation of the dorsomedial prefrontal cortex and the basolateral amygdala attenuates conditioned-cued reinstatement of extinguished cocaine-seeking behavior in rats. Psychopharmacology (Berl) 168:57-65.

Meinhardt MW, Sommer WH (2015) Postdependent state in rats as a model for medication development in alcoholism. Addict Biol 20:1-21.

Meinhardt MW, Hansson AC, Perreau-Lenz S, Bauder-Wenz C, Stahlin O, Heilig M, Harper C, Drescher KU, Spanagel R, Sommer WH (2013) Rescue of infralimbic mGluR2 deficit restores control over drug-seeking behavior in alcohol dependence. J Neurosci 33:2794-2806.

Mietlicki-Baase EG, Ortinski PI, Rupprecht LE, Olivos DR, Alhadeff AL, Pierce RC, Hayes MR (2013) The food intake-suppressive effects of glucagon-like peptide-1 receptor signaling in the ventral tegmental area are mediated by AMPA/kainate receptors. Am J Physiol Endocrinol Metab 305:E1367-1374.

Miller EK, Cohen JD (2001) An integrative theory of prefrontal cortex function. Annu Rev Neurosci 24:167-202.

Miyake A, Friedman NP, Emerson MJ, Witzki AH, Howerter A, Wager TD (2000) The unity and diversity of executive functions and their contributions to complex "Frontal Lobe" tasks: a latent variable analysis. Cogn Psychol 41:49-100.

Molyneaux BJ, Arlotta P, Menezes JR, Macklis JD (2007) Neuronal subtype specification in the cerebral cortex. Nat Rev Neurosci 8:427-437.

Moore CB, Guthrie EH, Huang MT, Taxman DJ (2010) Short hairpin RNA (shRNA): design, delivery, and assessment of gene knockdown. Methods Mol Biol 629:141-158.

Moorman DE, Aston-Jones G (2015) Prefrontal neurons encode context-based response execution and inhibition in reward seeking and extinction. Proc Natl Acad Sci U S A 112:9472-9477.

Moorman DE, James MH, McGlinchey EM, Aston-Jones G (2015) Differential roles of medial prefrontal subregions in the regulation of drug seeking. Brain Res 1628:130-146.

Morgan JI, Curran T (1991) Stimulus-transcription coupling in the nervous system: involvement of the inducible proto-oncogenes fos and jun. Annu Rev Neurosci 14:421-451.

Morrow BA, Elsworth JD, Lee EJ, Roth RH (2000) Divergent effects of putative anxiolytics on stress-induced fos expression in the mesoprefrontal system of the rat. Synapse 36:143-154.

Mortensen ME, Cecalupo AJ, Lo WD, Egorin MJ, Batley R (1992) Inadvertent intrathecal injection of daunorubicin with fatal outcome. Med Pediatr Oncol 20:249-253.

Moussawi K, Kalivas PW (2010) Group II metabotropic glutamate receptors (mGlu2/3) in drug addiction. Eur J Pharmacol 639:115-122.

Murphy JM, Gatto GJ, Waller MB, McBride WJ, Lumeng L, Li TK (1986) Effects of scheduled access on ethanol intake by the alcohol-preferring (P) line of rats. Alcohol 3:331-336.

Nakai J, Ohkura M, Imoto K (2001) A high signal-to-noise Ca(2+) probe composed of a single green fluorescent protein. Nat Biotechnol 19:137-141.

Nesse RM, Berridge KC (1997) Psychoactive drug use in evolutionary perspective. Science 278:63-66.

Netzeband JG, Trotter C, Caguioa JN, Gruol DL (1999) Chronic ethanol exposure enhances AMPA-elicited Ca2+ signals in the somatic and dendritic regions of cerebellar Purkinje neurons. Neurochem Int 35:163-174.

Nicolelis MA, Fanselow EE, Ghazanfar AA (1997) Hebb's dream: the resurgence of cell assemblies. Neuron 19:219-221.

Nie Z, Yuan X, Madamba SG, Siggins GR (1993) Ethanol decreases glutamatergic synaptic transmission in rat nucleus accumbens in vitro: naloxone reversal. J Pharmacol Exp Ther 266:1705-1712.

Nikiforuk A, Popik P, Drescher KU, van Gaalen M, Relo AL, Mezler M, Marek G, Schoemaker H, Gross G, Bespalov A (2010) Effects of a positive allosteric modulator

of group II metabotropic glutamate receptors, LY487379, on cognitive flexibility and impulsive-like responding in rats. J Pharmacol Exp Ther 335:665-673.

Nimmerjahn A, Mukamel EA, Schnitzer MJ (2009) Motor behavior activates Bergmann glial networks. Neuron 62:400-412.

Niswender CM, Conn PJ (2010) Metabotropic glutamate receptors: physiology, pharmacology, and disease. Annu Rev Pharmacol Toxicol 50:295-322.

Noori HR, Cosa Linan A, Spanagel R (2016) Largely overlapping neuronal substrates of reactivity to drug, gambling, food and sexual cues: A comprehensive meta-analysis. Eur Neuropsychopharmacol 26:1419-1430.

Noori HR, Schottler J, Ercsey-Ravasz M, Cosa-Linan A, Varga M, Toroczkai Z, Spanagel R (2017) A multiscale cerebral neurochemical connectome of the rat brain. PLoS Biol 15:e2002612.

O'Brien CP, Childress AR, McLellan AT, Ehrman R (1992) Classical conditioning in drug-dependent humans. Ann N Y Acad Sci 654:400-415.

O'Donovan KJ, Tourtellotte WG, Millbrandt J, Baraban JM (1999) The EGR family of transcription-regulatory factors: progress at the interface of molecular and systems neuroscience. Trends Neurosci 22:167-173.

Olds J, Milner P (1954) Positive reinforcement produced by electrical stimulation of septal area and other regions of rat brain. J Comp Physiol Psychol 47:419-427.

Olive MF (2009) Metabotropic glutamate receptor ligands as potential therapeutics for addiction. Curr Drug Abuse Rev 2:83-98.

Omelchenko N, Sesack SR (2007) Glutamate synaptic inputs to ventral tegmental area neurons in the rat derive primarily from subcortical sources. Neuroscience 146:1259-1274.

Oscar-Berman M, Valmas MM, Sawyer KS, Kirkley SM, Gansler DA, Merritt D, Couture A (2009) Frontal brain dysfunction in alcoholism with and without antisocial personality disorder. Neuropsychiatr Dis Treat 5:309-326.

Otis JM, Namboodiri VM, Matan AM, Voets ES, Mohorn EP, Kosyk O, McHenry JA, Robinson JE, Resendez SL, Rossi MA, Stuber GD (2017) Prefrontal cortex output circuits guide reward seeking through divergent cue encoding. Nature 543:103-107.

Paredes RM, Etzler JC, Watts LT, Zheng W, Lechleiter JD (2008) Chemical calcium indicators. Methods 46:143-151.

Parsons MP, Li S, Kirouac GJ (2007) Functional and anatomical connection between the paraventricular nucleus of the thalamus and dopamine fibers of the nucleus accumbens. J Comp Neurol 500:1050-1063.

Patel TP, Man K, Firestein BL, Meaney DF (2015) Automated quantification of neuronal networks and single-cell calcium dynamics using calcium imaging. J Neurosci Methods 243:26-38.

Paxinos G, Watson C (1998) The rat brain in stereotaxic coordinates. Vol. Academic Press, San Diego.

Pennartz CM, Groenewegen HJ, Lopes da Silva FH (1994) The nucleus accumbens as a complex of functionally distinct neuronal ensembles: an integration of behavioural, electrophysiological and anatomical data. Prog Neurobiol 42:719-761.

Peters J, LaLumiere RT, Kalivas PW (2008a) Infralimbic prefrontal cortex is responsible for inhibiting cocaine seeking in extinguished rats. J Neurosci 28:6046-6053.

Peters J, Kalivas PW, Quirk GJ (2009) Extinction circuits for fear and addiction overlap in prefrontal cortex. Learn Mem 16:279-288.

Peters J, Vallone J, Laurendi K, Kalivas PW (2008b) Opposing roles for the ventral prefrontal cortex and the basolateral amygdala on the spontaneous recovery of cocaine-seeking in rats. Psychopharmacology (Berl) 197:319-326.

Petralia RS, Wang YX, Niedzielski AS, Wenthold RJ (1996) The metabotropic glutamate receptors, mGluR2 and mGluR3, show unique postsynaptic, presynaptic and glial localizations. Neuroscience 71:949-976.

Pfarr S (2013) The Role of the Infralimbic Cortex in Cue-Induced Reinstatement of Alcohol Seeking in Rats. Master Thesis, University of Heidelberg.

Pfarr S, Meinhardt MW, Klee ML, Hansson AC, Vengeliene V, Schönig K, Bartsch D, Hope BT, Spanagel R, Sommer WH (2015) Losing Control: Excessive Alcohol Seeking after Selective Inactivation of Cue-Responsive Neurons in the Infralimbic Cortex. J Neurosci 35:10750-10761.

Pfarr S, Schaaf L, Reinert JK, Paul E, Herrmannsdorfer F, Rossmanith M, Kuner T, Hansson AC, Spanagel R, Korber C, Sommer WH (2018) Choice for drug or natural reward engages largely overlapping neuronal ensembles in the infralimbic prefrontal cortex. J Neurosci.

Pfefferbaum A, Sullivan EV, Mathalon DH, Lim KO (1997) Frontal lobe volume loss observed with magnetic resonance imaging in older chronic alcoholics. Alcohol Clin Exp Res 21:521-529.

Pin JP, Duvoisin R (1995) The metabotropic glutamate receptors: structure and functions. Neuropharmacology 34:1-26.

Pinto L, Dan Y (2015) Cell-Type-Specific Activity in Prefrontal Cortex during Goal-Directed Behavior. Neuron 87:437-450.

Pitchers KK, Schmid S, Di Sebastiano AR, Wang X, Laviolette SR, Lehman MN, Coolen LM (2012) Natural reward experience alters AMPA and NMDA receptor distribution and function in the nucleus accumbens. PLoS One 7:e34700.

Plath N et al. (2006) Arc/Arg3.1 is essential for the consolidation of synaptic plasticity and memories. Neuron 52:437-444.

Quirk GJ, Beer JS (2006) Prefrontal involvement in the regulation of emotion: convergence of rat and human studies. Curr Opin Neurobiol 16:723-727.

Rebec GV, Sun W (2005) Neuronal substrates of relapse to cocaine-seeking behavior: role of prefrontal cortex. J Exp Anal Behav 84:653-666.

Resendez SL, Stuber GD (2014) In vivo Calcium Imaging to Illuminate Neurocircuit Activity Dynamics Underlying Naturalistic Behavior. Neuropsychopharmacology 40:238.

Richardson NR, Roberts DC (1996) Progressive ratio schedules in drug self-administration studies in rats: a method to evaluate reinforcing efficacy. J Neurosci Methods 66:1-11.

Riga D, Matos MR, Glas A, Smit AB, Spijker S, Van den Oever MC (2014) Optogenetic dissection of medial prefrontal cortex circuitry. Frontiers in Systems Neuroscience 8.

Rimondini R, Arlinde C, Sommer W, Heilig M (2002) Long-lasting increase in voluntary ethanol consumption and transcriptional regulation in the rat brain after intermittent exposure to alcohol. FASEB J 16:27-35.

Robinson TE, Berridge KC (1993) The neural basis of drug craving: an incentive-sensitization theory of addiction. Brain Res Brain Res Rev 18:247-291.

Rodd-Henricks ZA, Bell RL, Kuc KA, Murphy JM, McBride WJ, Lumeng L, Li TK (2001) Effects of concurrent access to multiple ethanol concentrations and repeated deprivations on alcohol intake of alcohol-preferring rats. Alcohol Clin Exp Res 25:1140-1150.

Rodd ZA, McKinzie DL, Bell RL, McQueen VK, Murphy JM, Schoepp DD, McBride WJ (2006) The metabotropic glutamate 2/3 receptor agonist LY404039 reduces alcohol-seeking but not alcohol self-administration in alcohol-preferring (P) rats. Behav Brain Res 171:207-215.

Rogawski MA (2013) AMPA receptors as a molecular target in epilepsy therapy. Acta Neurol Scand Suppl:9-18.

Room P, Russchen FT, Groenewegen HJ, Lohman AH (1985) Efferent connections of the prelimbic (area 32) and the infralimbic (area 25) cortices: an anterograde tracing study in the cat. J Comp Neurol 242:40-55.

Rubio FJ, Liu QR, Li X, Cruz FC, Leao RM, Warren BL, Kambhampati S, Babin KR, McPherson KB, Cimbro R, Bossert JM, Shaham Y, Hope BT (2015) Context-induced reinstatement of methamphetamine seeking is associated with unique molecular alterations in Fos-expressing dorsolateral striatum neurons. J Neurosci 35:5625-5639.

Russell JT (2011) Imaging calcium signals in vivo: a powerful tool in physiology and pharmacology. Br J Pharmacol 163:1605-1625.

Saksida LM, Bussey TJ, Buckmaster CA, Murray EA (2006) No effect of hippocampal lesions on perirhinal cortex-dependent feature-ambiguous visual discriminations. Hippocampus 16:421-430.

Sams-Dodd F (1999) Phencyclidine in the social interaction test: an animal model of schizophrenia with face and predictive validity. Rev Neurosci 10:59-90.

Sams-Dodd F (2006) Strategies to optimize the validity of disease models in the drug discovery process. Drug Discovery Today 11:355-363.

Sanchis-Segura C, Spanagel R (2006) Behavioural assessment of drug reinforcement and addictive features in rodents: an overview. Addict Biol 11:2-38.

Santone KS, Oakes SG, Taylor SR, Powis G (1986) Anthracycline-induced inhibition of a calcium action potential in differentiated murine neuroblastoma cells. Cancer Res 46:2659-2664.

Saraswat N, Ranjan S, Ram D (2006) Set-shifting and selective attentional impairment in alcoholism and its relation with drinking variables. Indian J Psychiatry 48:47-51.

Sauer B (1998) Inducible gene targeting in mice using the Cre/lox system. Methods 14:381-392.

Saunders A, Johnson CA, Sabatini BL (2012) Novel recombinant adeno-associated viruses for Cre activated and inactivated transgene expression in neurons. Front Neural Circuits 6:47.

Schaaf L (2017) Spatial Organization of Infralimbic Neuronal Ensembles Activated by Alcohol- and Saccharin-Predicting Cues. Master Thesis, University of Heidelberg.

Schacht JP, Anton RF, Myrick H (2013) Functional neuroimaging studies of alcohol cue reactivity: a quantitative meta-analysis and systematic review. Addict Biol 18:121-133.

Scheggia D, Papaleo F (2016) An Operant Intra-/Extra-dimensional Set-shift Task for Mice. J Vis Exp:e53503.

Schilling K, Luk D, Morgan JI, Curran T (1991) Regulation of a fos-lacZ fusion gene: a paradigm for quantitative analysis of stimulus-transcription coupling. Proc Natl Acad Sci U S A 88:5665-5669.

Schmued LC, Hopkins KJ (2000) Fluoro-Jade B: a high affinity fluorescent marker for the localization of neuronal degeneration. Brain Res 874:123-130.

Schnütgen F, Doerflinger N, Callèja C, Wendling O, Chambon P, Ghyselinck NB (2003) A directional strategy for monitoring Cre-mediated recombination at the cellular level in the mouse. Nat Biotechnol 21:562-565.

Schoepp DD (2001) Unveiling the functions of presynaptic metabotropic glutamate receptors in the central nervous system. J Pharmacol Exp Ther 299:12-20.

Schoepp DD, Conn PJ (1993) Metabotropic glutamate receptors in brain function and pathology. Trends Pharmacol Sci 14:13-20.

Schönig K, Weber T, Frommig A, Wendler L, Pesold B, Djandji D, Bujard H, Bartsch D (2012) Conditional gene expression systems in the transgenic rat brain. BMC Biol 10:77.

Schultz W (2007) Multiple Dopamine Functions at Different Time Courses. Annual Review of Neuroscience 30:259-288.

Schwindel CD, McNaughton BL (2011) Hippocampal-cortical interactions and the dynamics of memory trace reactivation. Prog Brain Res 193:163-177.

See RE (2002) Neural substrates of conditioned-cued relapse to drug-seeking behavior. Pharmacol Biochem Behav 71:517-529.

Sesack SR, Deutch AY, Roth RH, Bunney BS (1989) Topographical organization of the efferent projections of the medial prefrontal cortex in the rat: an anterograde tract-tracing study with Phaseolus vulgaris leucoagglutinin. J Comp Neurol 290:213-242.

Shaham Y, Shalev U, Lu L, de Wit H, Stewart J (2003) The reinstatement model of drug relapse: history, methodology and major findings. Psychopharmacology (Berl) 168:3-20.

Shallice T (1982) Specific impairments of planning. Philos Trans R Soc Lond B Biol Sci 298:199-209.

Sheng M, Greenberg ME (1990) The regulation and function of c-fos and other immediate early genes in the nervous system. Neuron 4:477-485.

Shepherd G (2009) Intracortical cartography in an agranular area. Frontiers in Neuroscience 3.

Shigemoto R, Kinoshita A, Wada E, Nomura S, Ohishi H, Takada M, Flor PJ, Neki A, Abe T, Nakanishi S, Mizuno N (1997) Differential presynaptic localization of metabotropic glutamate receptor subtypes in the rat hippocampus. J Neurosci 17:7503-7522.

Simon HA (1975) The functional equivalence of problem solving skills. Cognitive Psychology 7:268-288.

Sinha R, Shaham Y, Heilig M (2011) Translational and reverse translational research on the role of stress in drug craving and relapse. Psychopharmacology (Berl) 218:69-82.

Sommer WH, Rimondini R, Hansson AC, Hipskind PA, Gehlert DR, Barr CS, Heilig MA (2008) Upregulation of voluntary alcohol intake, behavioral sensitivity to stress, and amygdala crhr1 expression following a history of dependence. Biol Psychiatry 63:139-145.

Sompolinsky H (2014) Computational neuroscience: beyond the local circuit. Current Opinion in Neurobiology 25:xiii-xviii.

Sørensen AT, Cooper YA, Baratta MV, Weng F-J, Zhang Y, Ramamoorthi K, Fropf R, LaVerriere E, Xue J, Young A, Schneider C, Gøtzsche CR, Hemberg M, Yin JCP, Maier SF, Lin Y (2016) A robust activity marking system for exploring active neuronal ensembles. eLife 5:e13918.

Spanagel R (2000) Recent animal models of alcoholism. Alcohol Res Health 24:124-131.

Spanagel R (2003) Alcohol addiction research: from animal models to clinics. Best Pract Res Clin Gastroenterol 17:507-518.

Spanagel R (2009) Alcoholism: a systems approach from molecular physiology to addictive behavior. Physiol Rev 89:649-705.

Spanagel R, Zieglgänsberger W (1997) Anti-craving compounds for ethanol: new pharmacological tools to study addictive processes. Trends in Pharmacological Sciences 18:54-59.

Spanagel R, Weiss F (1999) The dopamine hypothesis of reward: past and current status. Trends Neurosci 22:521-527.

Spanagel R, Kiefer F (2008) Drugs for relapse prevention of alcoholism: ten years of progress. Trends in Pharmacological Sciences 29:109-115.

Spanagel R, Pendyala G, Abarca C, Zghoul T, Sanchis-Segura C, Magnone MC, Lascorz J, Depner M, Holzberg D, Soyka M, Schreiber S, Matsuda F, Lathrop M, Schumann G, Albrecht U (2004) The clock gene Per2 influences the glutamatergic system and modulates alcohol consumption. Nature Medicine 11:35.

Stefani MR, Groth K, Moghaddam B (2003) Glutamate receptors in the rat medial prefrontal cortex regulate set-shifting ability. Behav Neurosci 117:728-737.

Sternberg N, Sauer B, Hoess R, Abremski K (1986) Bacteriophage P1 cre gene and its regulatory region. Evidence for multiple promoters and for regulation by DNA methylation. J Mol Biol 187:197-212.

Sullivan EV, Mathalon DH, Zipursky RB, Kersteen-Tucker Z, Knight RT, Pfefferbaum A (1993) Factors of the Wisconsin Card Sorting Test as measures of frontal-lobe function in schizophrenia and in chronic alcoholism. Psychiatry Res 46:175-199.

Sullivan RJ, Hagen EH (2002) Psychotropic substance-seeking: evolutionary pathology or adaptation? Addiction 97:389-400.

Suto N, Laque A, De Ness GL, Wagner GE, Watry D, Kerr T, Koya E, Mayford MR, Hope BT, Weiss F (2016) Distinct memory engrams in the infralimbic cortex of rats control opposing environmental actions on a learned behavior. Elife 5.

Tabbara RI, Maddux JM, Beharry PF, Iannuzzi J, Chaudhri N (2016) Effects of sucrose concentration and water deprivation on Pavlovian conditioning and responding for conditioned reinforcement. Behav Neurosci 130:231-242.

Tait DS, Chase EA, Brown VJ (2014) Attentional set-shifting in rodents: a review of behavioural methods and pharmacological results. Curr Pharm Des 20:5046-5059.

Takahashi A, Camacho P, Lechleiter JD, Herman B (1999) Measurement of intracellular calcium. Physiol Rev 79:1089-1125.

Tamaru Y, Nomura S, Mizuno N, Shigemoto R (2001) Distribution of metabotropic glutamate receptor mGluR3 in the mouse CNS: differential location relative to pre- and postsynaptic sites. Neuroscience 106:481-503.

Tervo DG, Hwang BY, Viswanathan S, Gaj T, Lavzin M, Ritola KD, Lindo S, Michael S, Kuleshova E, Ojala D, Huang CC, Gerfen CR, Schiller J, Dudman JT, Hantman AW,

Looger LL, Schaffer DV, Karpova AY (2016) A Designer AAV Variant Permits Efficient Retrograde Access to Projection Neurons. Neuron 92:372-382.

Thomas KR, Capecchi MR (1987) Site-directed mutagenesis by gene targeting in mouse embryo-derived stem cells. Cell 51:503-512.

Tian L, Hires SA, Mao T, Huber D, Chiappe ME, Chalasani SH, Petreanu L, Akerboom J, McKinney SA, Schreiter ER, Bargmann CI, Jayaraman V, Svoboda K, Looger LL (2009) Imaging neural activity in worms, flies and mice with improved GCaMP calcium indicators. Nat Methods 6:875-881.

Tian Y et al. (2018) An Excitatory Neural Assembly Encodes Short-Term Memory in the Prefrontal Cortex. Cell Rep 22:1734-1744.

Tolliver GA, Sadeghi KG, Samson HH (1988) Ethanol preference following the sucrose-fading initiation procedure. Alcohol 5:9-13.

Tonegawa S, Liu X, Ramirez S, Redondo R (2015) Memory Engram Cells Have Come of Age. Neuron 87:918-931.

Trepel M (2017) Neuroanatomie, 7 Edition. München: Elsevier, Urban & Fischer.

Trick L, Kempton MJ, Williams SC, Duka T (2014) Impaired fear recognition and attentional set-shifting is associated with brain structural changes in alcoholic patients. Addict Biol 19:1041-1054.

Uylings HB, Groenewegen HJ, Kolb B (2003) Do rats have a prefrontal cortex? Behav Brain Res 146:3-17.

van Aerde KI, Feldmeyer D (2015) Morphological and Physiological Characterization of Pyramidal Neuron Subtypes in Rat Medial Prefrontal Cortex. Cerebral Cortex 25:788-805.

Van den Oever MC, Spijker S, Smit AB, De Vries TJ (2010) Prefrontal cortex plasticity mechanisms in drug seeking and relapse. Neurosci Biobehav Rev 35:276-284.

Van Eden CG, Lamme VA, Uylings HB (1992) Heterotopic Cortical Afferents to the Medial Prefrontal Cortex in the Rat. A Combined Retrograde and Anterograde Tracer Study. Eur J Neurosci 4:77-97.

Vengeliene V, Bilbao A, Spanagel R (2014) The alcohol deprivation effect model for studying relapse behavior: a comparison between rats and mice. Alcohol 48:313-320.

Ventura A, Meissner A, Dillon CP, McManus M, Sharp PA, Van Parijs L, Jaenisch R, Jacks T (2004) Cre-lox-regulated conditional RNA interference from transgenes. Proc Natl Acad Sci U S A 101:10380-10385.

Vertes RP (2004) Differential projections of the infralimbic and prelimbic cortex in the rat. Synapse 51:32-58.

Voorn P, Vanderschuren LJMJ, Groenewegen HJ, Robbins TW, Pennartz CMA (2004) Putting a spin on the dorsal–ventral divide of the striatum. Trends in Neurosciences 27:468-474.

Walker AG, Wenthur CJ, Xiang Z, Rook JM, Emmitte KA, Niswender CM, Lindsley CW, Conn PJ (2015) Metabotropic glutamate receptor 3 activation is required for long-term depression in medial prefrontal cortex and fear extinction. Proc Natl Acad Sci U S A 112:1196-1201.

Wallace CS, Lyford GL, Worley PF, Steward O (1998) Differential intracellular sorting of immediate early gene mRNAs depends on signals in the mRNA sequence. J Neurosci 18:26-35.

Wang F, Flanagan J, Su N, Wang LC, Bui S, Nielson A, Wu X, Vo HT, Ma XJ, Luo Y (2012) RNAscope: a novel in situ RNA analysis platform for formalin-fixed, paraffin-embedded tissues. J Mol Diagn 14:22-29.

Wang JQ, McGinty JF (1996) Acute methamphetamine-induced zif/268, preprodynorphin, and preproenkephalin mRNA expression in rat striatum depends on activation of NMDA and kainate/AMPA receptors. Brain Res Bull 39:349-357.

Wang W, Wildes CP, Pattarabanjird T, Sanchez MI, Glober GF, Matthews GA, Tye KM, Ting AY (2017) A light- and calcium-gated transcription factor for imaging and manipulating activated neurons. Nature Biotechnology 35:864.

Warren BL, Mendoza MP, Cruz FC, Leao RM, Caprioli D, Rubio FJ, Whitaker LR, McPherson KB, Bossert JM, Shaham Y, Hope BT (2016) Distinct Fos-Expressing Neuronal Ensembles in the Ventromedial Prefrontal Cortex Mediate Food Reward and Extinction Memories. J Neurosci 36:6691-6703.

Weber T, Schönig K, Tews B, Bartsch D (2011) Inducible gene manipulations in brain serotonergic neurons of transgenic rats. PLoS One 6:e28283.

West EA, Saddoris MP, Kerfoot EC, Carelli RM (2014) Prelimbic and infralimbic cortical regions differentially encode cocaine-associated stimuli and cocaine-seeking before and following abstinence. Eur J Neurosci 39:1891-1902.

Whitelaw RB, Markou A, Robbins TW, Everitt BJ (1996) Excitotoxic lesions of the basolateral amygdala impair the acquisition of cocaine-seeking behaviour under a second-order schedule of reinforcement. Psychopharmacology (Berl) 127:213-224.

Wicks S, Hammar J, Heilig M, Wisén O (2001) Factors Affecting the Short-Term Prognosis of Alcohol Dependent Patients Undergoing Inpatient Detoxification. Substance Abuse 22:235-245.

Willcocks AL, McNally GP (2013) The role of medial prefrontal cortex in extinction and reinstatement of alcohol-seeking in rats. Eur J Neurosci 37:259-268.

Willner P, Muscat R, Papp M (1992) Chronic mild stress-induced anhedonia: a realistic animal model of depression. Neurosci Biobehav Rev 16:525-534.

Wilson DE, Reeder DAM (2005) Mammal Species of the World: A Taxonomic and Geographic Reference: Johns Hopkins University Press.

Wise RA (1996) Neurobiology of addiction. Curr Opin Neurobiol 6:243-251.

Wise RA (2004) Dopamine, learning and motivation. Nat Rev Neurosci 5:483-494.

Wise RA, Rompre PP (1989) Brain dopamine and reward. Annu Rev Psychol 40:191-225.

Witten IB, Steinberg EE, Lee SY, Davidson TJ, Zalocusky KA, Brodsky M, Yizhar O, Cho SL, Gong S, Ramakrishnan C, Stuber GD, Tye KM, Janak PH, Deisseroth K (2011) Recombinase-driver rat lines: tools, techniques, and optogenetic application to dopamine-mediated reinforcement. Neuron 72:721-733.

Wood JN, Grafman J (2003) Human prefrontal cortex: processing and representational perspectives. Nat Rev Neurosci 4:139-147.

World Health Organization (2014) Global status report on alcohol and health. Geneva, Switzerland.

Xiao W, Chirmule N, Berta SC, McCullough B, Gao G, Wilson JM (1999) Gene therapy vectors based on adeno-associated virus type 1. J Virol 73:3994-4003.

Zahr NM, Kaufman KL, Harper CG (2011) Clinical and pathological features of alcohol-related brain damage. Nature Reviews Neurology 7:284.

Zariwala HA, Borghuis BG, Hoogland TM, Madisen L, Tian L, De Zeeuw CI, Zeng H, Looger LL, Svoboda K, Chen TW (2012) A Cre-dependent GCaMP3 reporter mouse for neuronal imaging in vivo. J Neurosci 32:3131-3141.

Zhao Y, Dayas CV, Aujla H, Baptista MA, Martin-Fardon R, Weiss F (2006) Activation of group II metabotropic glutamate receptors attenuates both stress and cue-induced ethanol-seeking and modulates c-fos expression in the hippocampus and amygdala. J Neurosci 26:9967-9974.

Zhou YD, N.C (2014) Glutamate as a neurotransmitter in the healthy brain. In. Journal of Neural Transmission: Berlin, Springer.

Zhou Z, Karlsson C, Liang T, Xiong W, Kimura M, Tapocik JD, Yuan Q, Barbier E, Feng A, Flanigan M, Augier E, Enoch MA, Hodgkinson CA, Shen PH, Lovinger DM, Edenberg HJ, Heilig M, Goldman D (2013) Loss of metabotropic glutamate receptor 2 escalates alcohol consumption. Proc Natl Acad Sci U S A 110:16963-16968.

Ziskind-Conhaim L, Gao BX, Hinckley C (2003) Ethanol dual modulatory actions on spontaneous postsynaptic currents in spinal motoneurons. J Neurophysiol 89:806-813.

Ziv Y, Burns LD, Cocker ED, Hamel EO, Ghosh KK, Kitch LJ, El Gamal A, Schnitzer MJ (2013) Long-term dynamics of CA1 hippocampal place codes. Nat Neurosci 16:264-266.

Zorumski CF, Mennerick S, Izumi Y (2014) Acute and chronic effects of ethanol on learning-related synaptic plasticity. Alcohol 48:1-17.

Supplementary Information

Supplementary Methods

Experimental design

Male Wistar rats underwent seven weeks of chronic intermittent ethanol (CIE) vapor exposure. After a prolonged abstinence phase of three weeks, the animals were tested on their ASST performance (Figure 57A). A second batch of Wistar rats also underwent CIE vapor exposure. After an abstinence period of 3 weeks, the animals either received bilateral mGluR2 overexpression or control lenti virus injections into the IL. After a recovery period of two weeks, the animals were also tested on their ASST performance (Figure 57B). Both experiments were performed by Manuela Klee as part of her Master Thesis (Klee, 2014), under the supervision of Marcus Meinhardt at the Central Institute of Mental Health, Mannheim.

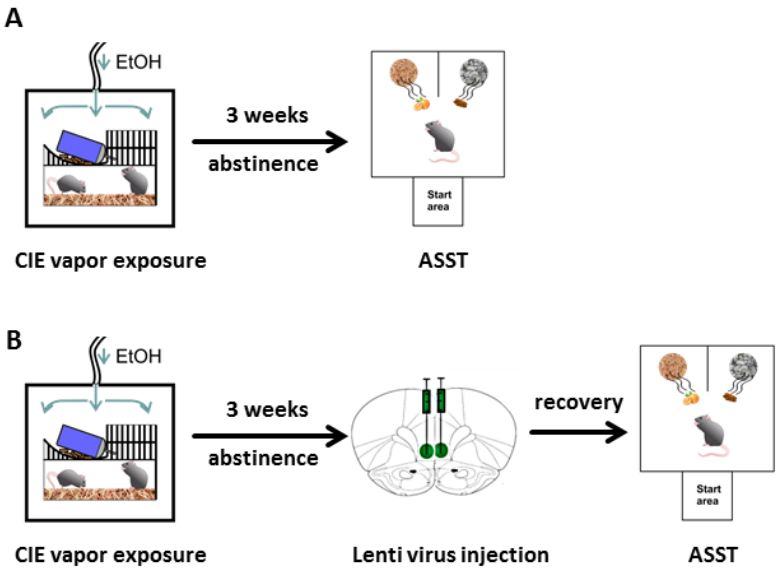

Figure 57: Experimental timelines for ASST in PD rats. A) One batch of Wistar rats underwent seven weeks of chronic intermittent ethanol (CIE) vapor exposure. After a prolonged abstinence period of three weeks, the animals were tested on their attentional set shifting task (ASST) performance. **B)** A second batch of Wistar rats also underwent seven weeks of CIE vapor exposure. After an abstinence period of three weeks the animals received either bilateral mGluR2 overexpression or control lenti virus injections into the IL. After a recovery period of two weeks, the animals were tested on their ASST performance.

Generation of PD rats

For ethanol vapor/ air exposure a protocol adapted from (Rimondini et al., 2002) was used. Briefly, pumps (Knauer) delivered alcohol into electrically heated stainless-steel coils (60°C) connected to an airflow of 18 L/min into glass and steel chambers (1 × 1 × 1 m). For the next 8 weeks rats were exposed to five cycles of 14 h of ethanol vapor per week (0:00 A.M. to 2:00 P.M.) separated by daily 10 h periods of withdrawal. Twice per week, blood (∼20 µl) was sampled from the lateral tail vein, and blood alcohol concentrations were determined using an AM1 Analox system (Analox Instruments). After the last exposure cycle the rats stayed abstinent for three weeks before further behavioral testing (Meinhardt et al., 2013; Meinhardt and Sommer, 2015). Etanol vapor exposure was performed by Manuela Klee as part of her Master Thesis under the supervision of Marcus Meinhardt (Klee, 2014).

Stereotaxic lenti virus injections

For lenti virus injections postdependent Wistar rats were anesthetized with isoflurane and placed in a Kopf stereotaxic frame. Bilateral injections of 1.2µl lenti virus into the IL (AP: +2.9, ML: +/- 0.5, DV -5.1) according to (Paxinos and Watson, 1998) were performed using a WPI microinjection pump through a 33 gauge beveled needle at a rate of 200 nl/min. Behavioral testing was started two weeks after lenti virus injection. Lenti virus injections were performed by Manuela Klee as part of her Master Thesis under the supervision of Marcus Meinhardt (Klee, 2014).

Supplementary Results

Effect of chronic intermittent alcohol exposure on ASST performance

In mice it was shown, that a history of chronic intermittent alcohol exposure leads to structural neuronal changes in the mPFC as well as impairments in an attentional set shifting task (ASST) (Kroener et al., 2012).

To investigate the effect of chronic intermittent alcohol exposure on ASST performance in rats, 16 alcohol exposed (post dependent) and 16 air exposed Wistar rats were used. Three weeks after alcohol/ air exposure, the animals were tested on their ASST performance (Figure 58A). Two post dependent (PD) and one control animal were excluded from the experiment, because they failed to learn the simple discrimination task. There was no significant difference between the groups in the simple discrimination (SD) task as confirmed by one-way ANOVA ($F_{(1,26)}$= 0.33, p = 0.57). There were also no significant differences between the groups in the compound discrimination (CD) ($F_{(1,26)}$= 0.36, p = 0.55), compound discrimination reversal (CDrev) ($F_{(1,26)}$= 2,72, p = 0.11) and compound discrimination repetition (CDrep) ($F_{(1,26)}$= 0.001, p = 0.98), confirmed by one-way ANOVA. There was no significant difference between the groups in the intradimensional shift 1 (IDS) ($F_{(1,26)}$= 1.91, p = 0.18), but there was a significant difference between the groups in the intradimensional shift 2 (IDS2) as confirmed by one-way ANOVA ($F_{(1,26)}$= 5.99, p = 0.02). There was also a significant difference between the groups in the extradimensional shift (EDS) as confirmed by one-way ANOVA ($F_{(1,26)}$= 7.4, p 0.011). Repeated ANOVA analysis revealed an overall significant difference between post-dependent and control animals for the ASST ($F_{(1,27)}$ =11.34, p = 0.002). Thus, ASST performance is not generally impaired after chronic intermittent alcohol exposure. However, significant impairments were observed when the rules of the task were changed (IDS2 and EDS). This inability to change their strategy indicates a reduced cognitive flexibility of the post dependent (PD) rats.

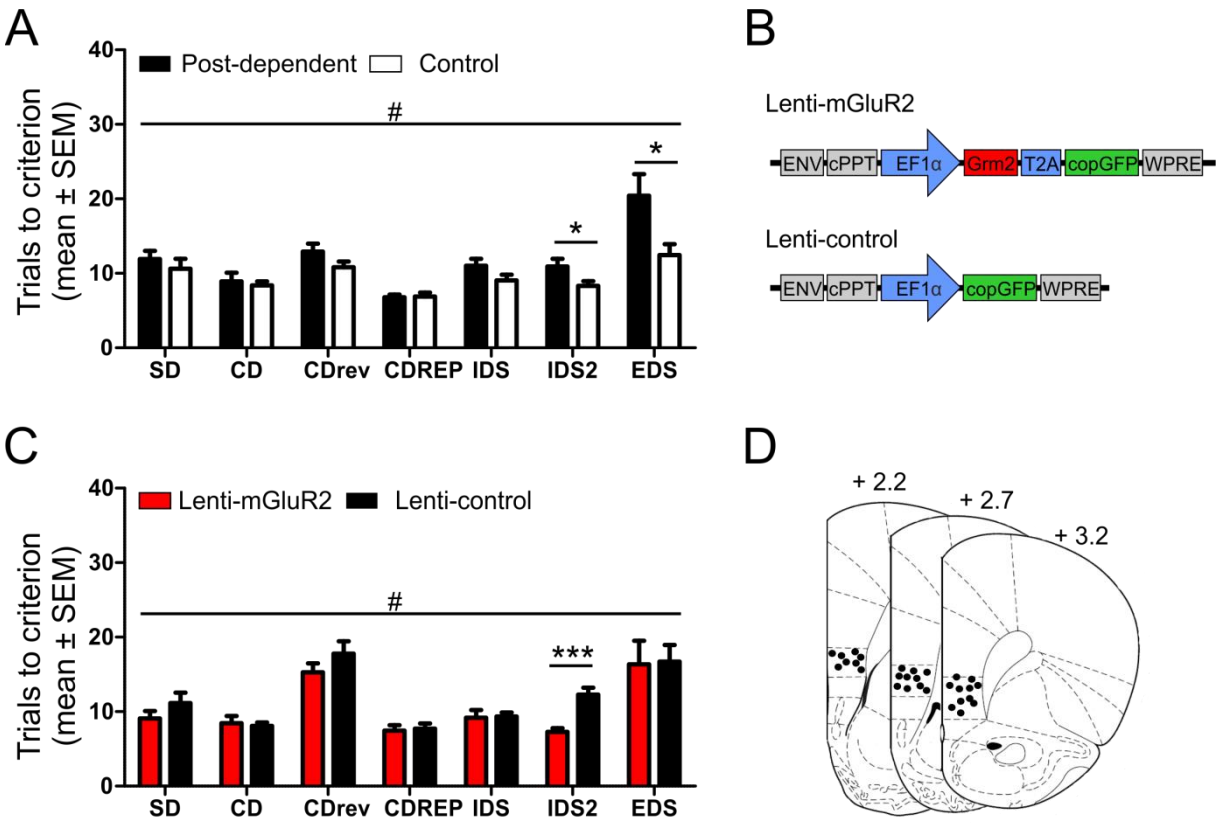

Figure 58: Alcohol-induced mGluR2 deficit leads to impaired ASST performance. A) ASST performance of post-dependent (PD) rats (n=14, black bars) and control rats (n=15, white bars). PD rats needed significantly more trials to criterion in the IDS2 and EDS subtasks. There was also an overall significant difference between PD and control rats. **B)** Schematic representation of lentiviral constructs. Lenti-mGluR2 expresses Grm2 and copGFP under control of EF1α promoter. Lenti-control only expresses copGFP under EF1α control. **C)** ASST performance of PD rats injected with either Lenti-mGluR2 (n=16, red bars) or Lenti-control (n=16, black bars) into the IL. Lenti-mGluR2 injected animals overall needed significantly less trials to criterion in the IDS2. **D)** Injection placements are represented by black circles. Injection sites were verified within the IL from +3.2 to +2.2mm anterior to bregma (Paxinos and Watson, 1998). SD=simple discrimination, CD=compound discrimination, CDrev=compound discrimination reversal, CDREP=repetition of CDrev, IDS=intradimensional shift, IDS2=intradimensional shift 2, EDS=extradimensional shift. ANOVA: *$p<0.05$, ***$p<0.001$. Repeated measures ANOVA: $^{\#\#}p<0.01$. These experiments were performed by Manuela Klee as part of her Master Thesis under the supervision of Marcus Meinhardt (Klee, 2014).

Partial rescue of ASST performance of PD rats after mGluR2 restoration in IL

In a previous study from our lab it was shown that chronic intermittent alcohol exposure leads to a significant reduction of mGluR2 in the infralimbic cortex (IL) (Meinhardt et al., 2013). Furthermore, restoration of IL mGluR2 using lentiviral overexpression also normalized the elevated alcohol seeking behavior of post-dependent rats to control level. In order to test the effect of mGluR2 restoration in the IL of post-dependent rats on ASST performance 32 post dependent male Wistar rats were used. After chronic intermittent vapor exposure the animals

received bilateral IL injections (Figure 58D) with the respective lenti vectors (lenti-mGluR2 n=16; lenti-control n=16, Figure 58B). The animals were allowed to recover for 2 weeks before the start of the ASST. As can be seen in Figure 58C, the impairment of PD rats in the IDS2 could be reversed by IL mGluR2 restoration. There was a significant reduction of the number of trials to criterion in the lenti-mGluR2 group, compared to lenti-control, as confirmed by one-way ANOVA ($F_{(1,23)}$ = 19.45, p = 0.0002). There were no significant differences in the other ASST subtasks as confirmed by one-way ANOVA (SD: $F_{(1,23)}$ = 1.27, p = 0.27; CD: $F_{(1,23)}$ = 0.14, p = 0.71; CDrev: $F_{(1,23)}$ = 1.35, p = 0.26; CDrep: $F_{(1,23)}$ = 0.06, p = 0.801; IDS: $F_{(1,23)}$ = 0.03, p = 0.87; EDS: $F_{(1,23)}$ = 0.008, p = 0.93). There was no overall significant difference between lenti-mGluR2 animals and lenti-control animals for the ASST as confirmed by repeated measures ANOVA ($F_{(1,23)}$ = 3,22; p=0,08). IL restoration of mGluR2 expression did not affect the other ASST subtasks, leading only to a partial rescue of cognitive flexibility.